POLITECNICO DI MILANO

Energy Department

PhD Thesis in Electrical Engineering

Conservative Functions: An Approach in Nonlinear and Switched Network Analysis

Candidate: Simone Barcellona

Tutor: Prof. Antonino Di Gerlando

Supervisor: Prof. Gabrio Superti Furga

Coordinator: Prof. Alberto Berizzi

XXVII cycle – 2011-2014

Abstract

Conservative functions or generalized powers in the electric network are those that satisfy the balance Tellegen's theorem, and they are powerful tools in different contests. The attention for these functions is still, at the present time, very animated. The main reason behind that is the wide diffusion and usefulness of the reactive power for practical and theoretical point of view for linear networks under sinusoidal steady state. It is significant to recognize two formal properties of reactive power under sinusoidal steady state conditions: the balance property and its invariance on resistors. The balance property states that the algebraic sum of reactive power on the single one-port elements in a network is equal to the corresponding term on the whole network. The invariance means that the reactive power is always nil on resistors.

However, important changes have occurred in the last 50 years. In the electric networks, the presence of power electronics equipment, arc and induction furnaces, in addition to clusters of personal computers, represent major nonlinear and parametric loads proliferating among industrial and commercial customers. The main problems emerge from the flow of nonactive power caused by harmonic currents and voltages. The efforts to extend the concept of reactive power also under distorted conditions provided significant results for the analysis and theoretical comprehension of the distorted steady state. The literature on this subject is very large; in the past many authors have proposed different definitions of nonactive power in distorted steady state.

In particular, when power converters are present in networks, as sources of distortion or as active filters to eliminate this distortion, these networks are considered as time-variant networks and called switched networks. They pose several challenges in the construction of efficient time domain simulators. Due to the wide range of applications, operating conditions, and phenomena to be studied, many different tools for computer analysis and simulation of switched networks have been developed.

The switch model plays an important role within the analysis and simulation of switched networks. The ideal switch model is the simplest possible one and has several advantages with respect to others. In the presence of switching, classical issues that rise up are related to network solution and inconsistent initial conditions. Network solution is fulfilled by several methods. The main one is the complementary approach, where commutations are basically the external constraints to a time-invariant multi-port. Meanwhile, inconsistent initial conditions, caused by switching, imply discontinuities on state variables and impulsive behavior on some voltages and/or currents. In fact, Dirac's delta impulses of voltage and/or current may occur at the switching transitions. Impulses redistribute charge and flux at the switching instants when capacitor voltages and inductor currents, respectively, are discontinuous. Nevertheless, as a whole it appears to lack general principles as well as applications of generalized powers in the field of switched networks.

In this work, according to the concept of "area" on the *v-i* plane, a new approach called Swept Area Theory, under both nonlinear continuous and discontinuous conditions, is developed. Novel conservative functions, as Area Velocity and Closed Area over Time, involved in this theory, are proposed. An analysis is carried out, by means of these functions, over nonlinear R, L, C elements and over the ideal switch and ideal diode. In addition, jump discontinuities are discussed in detail. The Closed Area over Time is related to the harmonic reactive powers and under sinusoidal steady state becomes proportional to the classical reactive power. A balance rule concerning harmonic reactive powers over nonlinear resistor under continuous conditions is obtained and discussed as a novel interesting result. This aspect impacts on a possible extended definition of reactive power under distorted conditions. Thanks to the Switching Power, a novel quantitative relation between hard switching commutations and Closed Area over Time is obtained, with both theoretical and applicative relevance. More explanation is presented through a demonstration that shows how ideal

switch and power converters can become sources of reactive power. Issues of principle regarding the ideal switch model with respect to the real one is another important result of this work.

Moreover, concepts of Ideal Switch Multi Port and multilevel voltage/current elements are proposed as a unified theory of power converters, whereby most of the power converters existing can be recognized in a general and modular way. Furthermore, the Swept Area Theory is extended to the Ideal Switch Multi Port in order to find relations between Switching Power and commutations of power converters. In this way, the possibility of a power converter to generate or absorb reactive power is proved. Hence, a contribution will be available to develop new control strategies of power converters based on the Swept Area Theory.

Another conservative function, called Jump Power, is proposed in order to address some properties and issues of principle regarding one-port elements, in particular ideal diodes and ideal switches, in the presence of jump discontinuities. Some theorems based on the Jump Power are stated. In particular, possible conditions in networks are addressed whereby soft switching, passive or active hard switching commutations occur.

Other conservative functions, called Inductive Impulsive Power and Capacitive Impulsive Power, are defined in order to analyze the switched networks in the presence of Dirac's delta impulses in the electric quantities. These impulses are due to inconsistent initial conditions caused by switching. Also in this case, some properties and issues of principle regarding one-port elements, in particular ideal switches and ideal diodes, are addressed. Moreover, some theorems based on Inductive Impulsive Power and Capacitive Impulsive Power are stated. These conservative functions, despite having similar properties to the Connection Energy that was presented in the past literature as a function regarding the whole network, are still more powerful and meaningful. In fact, through Inductive Impulsive Power and Capacitive Impulsive Power functions, it is possible to separate the effect of capacitors from inductors.

Furthermore, an interesting result is found: the ideal switch can absorb or generate electric energy when an impulse of current or voltage occurs meanwhile the ideal diode can only generate. These facts are important mathematical aspects regarding the ideal model of switches and diodes. In some cases these facts cannot have a physical meaning as it is shown in analytical examples. However, the total energy absorbed by switching has a clear physical significance, as it is related to the variation of energy stored in the set of reactive elements or generated by electric sources. On the other hand, in the presence of more than one element, the partition of this energy among the different switching elements still has no physical correspondence with the loss of energy into the single element.

Index

Introduction

Conservative functions play an important role in different fields. In electric network conservative functions are those that satisfy balance Tellegen's theorem [1], often called generalized powers [2], and they are powerful tools in different contests. The search for these functions is still, at the present time, very animated. The basic reason is the wide diffusion and usefulness of the reactive power under sinusoidal steady state. In fact, it is well known that two functions, namely active power P and reactive power Q, are very effective for linear networks under sinusoidal steady state in terms of practical and theoretical point of view.

It is worth to recognize two formal properties of P and Q under sinusoidal steady state conditions that are essential for their handling: namely the balance (or conservative) property and their invariance on some elements. The balance property states that the algebraic sum of P or Q on the single one-port elements in a network is equal to the corresponding term on the whole network. The invariance relative to one-port element means that P or Q is always nil on this element. The active power is invariant on inductors and capacitors. The reactive power is invariant on resistors. As a result, the reactive power has a great success under sinusoidal steady state also for these reasons: for sinusoidal single-phase power systems and sinusoidal balanced three-phase systems, it has proved to be very useful and efficient for characterizing the quality of power transmission, for designing the equipment, for billing purposes, and for compensation. Indeed, the reactive power absorbed by inductors and generated by capacitors is easy to compensate using properly capacitors or inductors. If the reactive power is completely compensated the RMS value of the current is minimized. This definition serves the industry well as long as the current and voltage waveforms remain nearly sinusoidal and balanced on the three phases. In the high and medium voltage systems, it is used in order to regulate the voltage.

However, important changes have occurred in the last 50 years. The new environment is conditioned by the following evolution: power electronics equipment, such as adjustable speed drives, controlled rectifiers, cycloconverters, electronically ballasted lamps, arc and induction furnaces, and clusters of personal computers, represent major nonlinear and parametric loads proliferating among industrial and commercial customers. Such loads have the potential to create a host of disturbances for the utility and the end user. The main problems stem from the flow of nonactive power caused by harmonic currents and voltages. Therefore, the concept of reactive power and the related concept of power factor have to be adapted to the new environment such that measurement algorithms and instrumentation can be designed which give guidance with respect to the quantities, that should be measured or monitored for revenue purposes and engineering economic decisions. For these reasons, power theories under nonsinusoidal conditions are mainly aimed to approach different class of problems, relating to metering, tariffs, and distorting load identification issues, harmonic and reactive power compensation issues. Several approaches have been developed, both in time and frequency domain, which are suitable to solve classes of problems under nonsinusoidal conditions, like design and optimization of passive compensation networks [3]–[8], design and control of active compensators [9]–[11], identification of distorting loads [12] and measuring techniques [13]. In addition, comprehensive theories have been developed [14], which offer the basis for a general analysis of networks behavior under nonsinusoidal conditions, some of them relate to the frequency domain [15]–[17] and some to the time domain [9]–[11], [18]. These latter give special emphasis to instantaneous quantities or average quantities, depending on the aim of the work. The efforts to extend the concept of reactive power under distorted conditions gave significant results for the analysis and theoretical comprehension of the distorted steady state. The literature on this subject is very large; in the past many authors have proposed different definitions of nonactive power in distorted steady state. Limited to single-phase systems, some general discussions and surveys have been presented some time ago [19]–[21]. The debate is still

alive [22]−[24]. Among others, systematic analysis on this subject is presented in [2], [25]. New approaches and tools have given substantial improvements, as the geometric algebra [24], [26], [27] and [28].

Another application field of generalized powers is regarding the network stability analysis and network dynamics. General integrals in *v-i* coordinates have been considered many decades ago in milestone papers [29]−[31], in order to study the stability of nonlinear networks. On this track, fundamental results have been achieved on dynamic modeling of nonlinear RLC networks [32]−[35].

In particular, when power converters are present in networks, as sources of distortion or as active filters to eliminate this distortion, these networks are considered as time-variant networks and called switched networks. This kind of networks poses several challenges in the construction of efficient time domain simulators. Due to the wide range of applications, operating conditions, and phenomena to be studied, many different tools for computer analysis and simulation of switched networks have been developed so far [36].

The switch model plays an important role within the analysis and simulation of switched networks. The ideal switch model is the simplest possible one and has several advantages with respect to others. Firstly, the parameters of a real switch must be chosen according to the kind of semiconductor device used. For the two values resistor model, arbitrary choices of very small and very large values for the ON and OFF resistances, respectively, may increase the computational time and decrease the accuracy of the simulation. Secondly, for long term simulations, the response of the circuit usually does not change significantly if ideal or real switches are used, however the simulation time can be considerably affected. The general problem and solution methods of switched networks are presented in [37]. In the presence of switching, classical issues that rise up are related to network solution and inconsistent initial conditions. Network solution (related to problems of uniqueness of solution and stability) is fulfilled by several methods. The main one is the complementary approach, where commutations are basically the external constraints to a time-invariant multi-port [38], [39]. Meanwhile, inconsistent initial conditions, caused by switching, imply discontinuities on state variables and impulsive behavior on some voltages and/or currents, as deeply dealt in [40]−[42]. In fact, Dirac's delta impulses of voltage and/or current may occur at the switching transitions. Impulses redistribute charge and flux at the switching instants when capacitor voltages and inductor currents, respectively, are discontinuous. Nevertheless, as a whole it appears to lack general principles as well as applications of generalized powers in the field of switched networks; notable exception is the "Connection Energy" [43].

Another important aspect, already appeared in the past literature, is the "area" on the *v-i* plane. Through this idea, in [44] a conservative function was proposed, called "Mean Generalized Content" (MGC) which is balanced over the whole network. In addition, under periodical continuous conditions is invariant on nonlinear resistors. Therefore, the MCG could be seen as a generalization of the reactive power in distorted conditions [45]. In [46] the MGC was extended to circuits with ideal switches where the definition of Switching Power (SP) was introduced and a relation between switching and reactive power had been outlined.

In this thesis, the main goal is the definition of some other new conservative functions in order to obtain some properties, theorems and issues of principle regarding nonlinear and time-variant elements and give a new approach in nonlinear and switched network analysis. In particular, the ideal switch is given more attention and treated as a one-port element with its own constitutive relations. Moreover, this works aims to give a possible extension of the reactive power concept under nonsinusoidal conditions, and state some theorems regarding the networks under both nonlinear continuous and discontinuous conditions. Another goal of this work is to propose an unified theory of power converters that is still missing in previous surveys.

The content of this thesis is presented as the following: chapter 1 shows the demonstration of Tellegen's theorem, and a brief of the most important reactive and nonactive power definitions in distorted conditions of the past literature.

Starting from the previously mentioned area approach, chapter 2 develops the Swept Area Theory (SAT), which widely uses the concepts of trajectory and area on the *v*-*i* plane under both nonlinear continuous and discontinuous conditions. Initially, a conservative function of time, called Area Velocity (AV), is proposed. By this function, it is possible to demonstrate, in a general way, the quantities already proposed in [44], [45]. Specifically, the mean value of AV under periodical steady state, here called Closed Area over Time (CAT), expands the concept of MCG [44]. In the presence of ideal switching, the AV leads to the SP [46]. The integral function CAT basically turns out to be a restriction to periodical condition of the content and co-content introduced by [29], [31] and the voltage/current potential by [30]. Further expressions similar to CAT have appeared many times in the literature, mainly in the contest confined to powers in distorted conditions. However, general properties and balance principle are not highlighted properly. Furthermore, the ideal switch is, as abovementioned, treated as a one-port element, without any formal difference with other network components. This position makes it possible to apply the generalized powers to the ideal switch and, the so-called, switched networks can be dealt with topographically unchanged when the switches change their state. The relation between swept area and commutations of ideal switches yields a remarkable result. A quantitative relation between reactive power and periodical commutations of ideal switches is found. Besides, the results can be extended to power converters in order to demonstrate their ability to generate or absorb reactive power.

Chapter 3 defines concepts of Ideal Switch Multi Port (ISMP) and multilevel voltage/current elements so that most of the power converters existing can be recognized in a general and modular way, this results in a new unified theory in power converters. Furthermore, the SAT theory is extended to the ISMP.

Chapter 4 validates the SAT theory through performing some simulations on some power converters.

Chapter 5 defines another conservative function, called Jump Power (JP), in order to address some properties and issues of principle regarding one-port elements, in particular ideal switches and ideal diode.

In Chapters 2−5, jump discontinuities are only considered. Impulses and other kinds of discontinuities in the electric quantities are excluded.

Finally, chapter 6 defines other conservative functions, called Inductive Impulsive Power (IIP), Capacitive Impulsive Power (CIP) and Connection Energy (CE) in order to analyze electric networks in the presence of first order Dirac's delta impulses in voltage and/or current quantities. By means of these functions, it is possible to address some other properties of ideal switches and ideal diodes in the presence of these impulses. The Connection Energy is a function already appeared in the past literature regarding the whole switched network [43]. Instead, in this work the Connection Energy is redefined as a generalized conservative function related to any electric element. Moreover, cases in which initial conditions are not congruent and present in networks containing ideal switches, are analyzed. This last chapter is so far separated from the others and aims to be an introduction of future works that will be carried out. It will includes the initial steps and preliminary results to be performed and continued.

1. Generalized Powers

1.1 Tellegen's Theorem

In this chapter a brief on Tellegen's theorem and on the past several definitions of reactive and nonactive powers are reported.

Tellegen's theorem states that if i_{A1}, i_{A2}, i_{Al} are the branch currents of a l-branch network A, and v_{B1}, v_{B2}, v_{Bl} are the branch voltages of another l-branch network B, where A and B have a common graph but may otherwise be different, then

$$\sum_{k=1}^{l} i_{Ak} v_{Bk} = 0 \tag{1.1}$$

where the summation is over all branches k of the network. The sign convention adopted for branch voltages and currents is such that, if A and B were identical, the product $i_{A1}v_{B1}$ would be the instantaneous power supplied to the branch. Tellegen's theorem is unusual in that only Kirchhoff's laws are invoked in its proof. The theorem therefore applies to all electrical networks that obey these laws, whether they be linear or nonlinear, time-invariant or time-variant, reciprocal or nonreciprocal, passive or active, hysteretic or nonhysteretic. The excitation is arbitrary, indeed it may be sinusoidal, exponential, periodic, transient, or random. The initial conditions are also arbitrary.

1.1.1 Proof

Consider two different networks A and B having the same topology with l branches, n nodes, and s separate parts. Kirchhoff's current law places $n - s$ constraints upon the currents, so that only $m = l - n + s$ currents may be specified independently. Thus all the branch currents of the network A may then be found by means of the linear relations

$$i_{Ak} = \sum_{h=1}^{m} B_{kh} j_{Ah} \tag{1.2}$$

where i_{Ak}, denotes the branch currents of network A, j_{Ah} denotes the m independent currents and B_{kh} is the kh-th element of the m x l loop matrix $\boldsymbol{B}$ of the both networks.
Kirchhoff's voltage law may also be expressed in terms of B_{kh}. For each arbitrary current there is one closed path within the remainder of the network that does not include any other branch whose current is independently specified. Thus there are m such loops, for each of which Kirchhoff's voltage law for the network B may be written as

$$\sum_{k=1}^{l} B_{hk} v_{Bk} = 0 \tag{1.3}$$

where the summation is over all branches in the loop. From Kirchhoff's laws, as expressed by (1.2) and (1.3) a simple power theorem can be proved. Multiplication of (1.2) by v_{Ak}, yields

$$i_{Ak} v_{Bk} = \sum_{h=1}^{m} j_{Ah} B_{kh} v_{Bk} = 0. \tag{1.4}$$

If this is summed over all k (that is, over all branches of the network), then, because of (1.3), the right-hand side of (1.4) vanishes so that

$$\sum_{k=1}^{l} i_{Ak} v_{Bk} = 0. \tag{1.5}$$

Equation (1.5) is the theorem originally presented by Tellegen [47], [48], and has since been known, deservedly, as Tellegen's theorem.
If A and B are identical the (1.5) becomes

$$\sum_{k=1}^{l} i_k v_k = 0. \tag{1.6}$$

The physical interpretation of (1.6) is, of course, the conservation of energy within a network.

1.1.2 Generalized Tellegen's Theorem

As reported in [49] the generalized form of Tellegen's theorem can be expressed in terms of "Kirchhoff operators." The purpose of these operators is to derive, from one set of currents (or voltages) that obeys Kirchhoff's current (or voltage) law, another set of quantities that obeys the law. For example, if the set of currents $\boldsymbol{i}$ obeys Kirchhoff's current law, then so do their time derivatives d$\boldsymbol{i}$/dt. Thus, one example of a Kirchhoff current operator is differentiation with respect to time. Another is the Fourier or Laplace transform. Similarly, an operator is called a Kirchhoff voltage operator if, when operating upon a set of voltages that obeys Kirchhoff's voltage law, it generates a set of branch "voltages" that also obeys this law. It is sufficient that the operator applies a linear transformation on the electric quantities.

Let Δ_1 be a Kirchhoff current operator whose effects upon the set of branch current i_k, of a l-branch network is the generation of a new set of l-branch "currents" $\Delta_1 i_k$, that obeys Kirchhoff's current law. Similarly, let Δ_2, a Kirchhoff voltage operator, operates upon the set of branch voltages v_k, to generate a new set of branch "voltages" $\Delta_2 v_k$, that obeys Kirchhoff's voltage law. For a network it then follows immediately from (1.6) that

$$\sum_{k=1}^{l} \Delta_1 i_{Ak} \Delta_2 v_{Bk} = 0. \tag{1.7}$$

This generalized form of Tellegen's theorem holds for any Kirchhoff operators Δ_1 and Δ_2 and, because it is derived solely from Kirchhoff's laws, is valid for any constitutive laws of the elements, for any form of excitation, and for any initial conditions. Either or both of the Kirchhoff operators may, in fact, consist of a sequence of Kirchhoff operators applied in any order that makes sense.

In many applications of the generalized form of Tellegen's theorem it is simpler to apply what is called the difference form of the theorem [1]. Its derivation is simple: if the roles of Δ_1 and Δ_2 in (1.7) are interchanged and the result is subtracted from (1.7), it becomes

$$\sum_{k=1}^{l} (\Delta_1 i_{Ak} \Delta_2 v_{Bk} - \Delta_2 i_{Ak} \Delta_1 v_{Bk}) = 0. \tag{1.8}$$

Clearly, the operators appearing in (1.8) must be both Kirchhoff current operators and Kirchhoff voltage operators.

1.1.3 Corollary

If some branches are, in fact, ports of the network, the products associated with the ports can conveniently be placed on the opposite side of the equality sign to yield

$$\sum_{k=1}^{l} i_{Ak} v_{Bk} = \sum_{g=1}^{p} i_{Bg} v_{Ag} \tag{1.9}$$

where k and g now denote internal branches and ports, respectively. In this way the (1.7) can be rewritten as

$$\sum_{k=1}^{l} \Delta_1 i_{Ak} \Delta_2 v_{Bk} = \sum_{g=1}^{p} \Delta_1 i_{Bg} \Delta_2 v_{Ag} \tag{1.10}$$

and the (1.8) becomes

$$\sum_{k=1}^{l} (\Delta_1 i_{Ak} \Delta_2 v_{Bk} - \Delta_2 i_{Ak} \Delta_1 v_{Bk}) = \sum_{g=1}^{p} (\Delta_1 i_{Ag} \Delta_2 v_{Bg} - \Delta_2 i_{Ag} \Delta_1 v_{Bg}). \tag{1.11}$$

1.2 Some Active, Reactive and Nonactive Power Definitions

For the general case the instantaneous electric power related to any port of the network is

$$p = vi \tag{1.12}$$

that is conservative according to Tellegen's theorem, and the active (mean) electrical power under periodical conditions is

$$P = \frac{1}{T} \int_T p dt \tag{1.13}$$

also conservative, where T is the period time.

Sinusoidal Conditions

Under sinusoidal conditions the voltage and current quantities can be written as follows

$$\begin{aligned} v(t) &= \sqrt{2} V \cos(\omega t + \alpha) \\ i(t) &= \sqrt{2} I \cos(\omega t + \alpha - \varphi) \end{aligned} \tag{1.14}$$

where $\omega = 2\pi/T$ and V and I are the RMS values of the electric quantities. In this chapter, lower case letter are used for instantaneous functions while upper case letter are used for the RMS and mean values.
In this case the instantaneous electric power is

$$p(t) = VI \cos\varphi - VI \cos(2\omega t + 2\alpha - \varphi). \tag{1.15}$$

If the cosine of the second term is expanded becomes

$$\begin{aligned} p(t) &= VI\cos\varphi\left[1-\cos(2\omega t+2\alpha)\right]-VI\sin\varphi\sin(2\omega t+2\alpha)= \\ &= P\left[1-\cos(2\omega t+2\alpha)\right]-Q\sin(2\omega t+2\alpha) \end{aligned} \tag{1.16}$$

where

$$P = VI\cos\varphi \tag{1.17}$$

is the active power equal to (1.13) and

$$Q = VI\sin\varphi \tag{1.18}$$

is the classic reactive power under sinusoidal conditions. Q is conservative according to the well-known Boucherot's theorem.
The apparent power is defined as

$$S = VI \tag{1.19}$$

and under sinusoidal conditions the well-known power triangle is satisfied

$$S = \sqrt{P^2+Q^2}\,. \tag{1.20}$$

Nonsinusoidal conditions

If the voltage and current both are nonsinusoidal but periodic functions of time with the same period T, the voltage and current can be expressed as Fourier series

$$\begin{aligned} v(t) &= \sqrt{2}\sum_{n=1}^{\infty} V_n\cos(n\omega t+\alpha_n) \\ i(t) &= \sqrt{2}\sum_{n=1}^{\infty} I_n\cos(n\omega t+\beta_n) \end{aligned} \tag{1.21}$$

and the active power can be defined as

$$P = \sum_{n=1}^{\infty} P_n = \sum_{n=1}^{\infty} V_n I_n\cos\varphi_n \tag{1.22}$$

where $\varphi_n = \alpha_n - \beta_n$ is the phase shift angle between V_n and I_n.

Definitions (1.12), (1.13), (1.15), (1.18) and (1.22) are based on the physical phenomena of electrical power and energy; this electric power, for instance, can be transferred and turned into thermal, mechanical or other kinds of power. Therefore, there are no controversies about equations neither in the general case nor in the special cases of sinusoidal signals and nonsinusoidal periodic signals. Apparent and reactive powers, on the other hand, are not based on a single, well defined, physical phenomenon as the active power is. They are conventionally defined quantities that are useful in sinusoidal situations. Under nonsinusoidal conditions the reactive power (1.18) is still

valid only for harmonic by harmonic and the apparent power definitions (1.19) is usually used where V and I are the RMS values of the distorted waveforms.

There are quite a few proposals on how to extend the definition of reactive power to cover nonsinusoidal situations. The definition that is most widely spread, and is also approved of by ANSI/IEEE as standard [50], has been given by Budeanu [50]. However, the definition according to Budeanu is not considered useful for any practical applications [19], [20]. Furthermore, as stated earlier, reactive power is not a quantity defined by any single physical phenomenon but a mathematically defined quantity that has some very useful characteristics and physical interpretations at sinusoidal conditions.

1.2.1 Budeanu's Definition

Budeanu [50] proposed to define the reactive power in the nonsinusoidal case by

$$Q_B = \sum_n Q_n = \sum_n V_n I_n \sin\varphi_n \tag{1.23}$$

in analogy with the expression for the active power (1.22). The active and reactive power do not satisfy the triangle equality with the apparent power as in the sinusoidal case, indeed

$$S^2 > P^2 + Q_B^2 \tag{1.24}$$

and therefore, Budeanu had to introduce an additional power quantity called deformation power D_B,

$$D_B^2 = S^2 - P^2 - Q_B^2. \tag{1.25}$$

The distortion power mainly consists of cross-products of voltage and current harmonics of different orders and will be reduced to zero if the harmonics are reduced to zero, i.e. at sinusoidal conditions.

Note that the Budeanu reactive power is a conservative quantity. Indeed, the currents and voltages at each harmonic frequency separately satisfy Kirchhoff's laws, and hence, the reactive powers at each frequency satisfy Tellegen's theorem. Thus, the sum of the reactive powers also satisfies the conservation property. The main disadvantages are that it is not sure that the power factor will be unity if the reactive power by this definition is reduced to zero and that the reactive power can be totally compensated by inserting inductive or capacitive components. Further, designing an analogue meter that measures Q_B is virtually impossible since it requires a filter that utilizes a phase angle displacement of 90 degrees for all frequencies and at the same time has an amplification factor of unity for all frequencies.

1.2.2 Fryze's Definition

The reactive power definition proposed by [52] is based on a time domain analysis. The current is divided into two parts. The first part, i_a, is a current of the same wave-shape and phase angle as the voltage, and has an amplitude such that $I_a V$ is equal to the active power. The second part of the current is just a residual term called i_r. The two currents will then be determined by the equations

$$i_a = \frac{P}{V^2} v \tag{1.26}$$

and

$$i_r = i - i_a. \tag{1.27}$$

The reason for this division is that the current i_a is the current of a purely resistive load that, for the same voltage, would develop the same power as the load measured on. That is, if i_r can be compensated, the source will see a purely resistive load and the power factor will be equal to unity. It can easily be shown that i_a and i_r are orthogonal and then the RMS values can be determined by

$$I^2 = I_a^2 + I_r^2. \tag{1.28}$$

In fact, (1.26) gives the only possible amplitude of i_a if it should be orthogonal to the residual term i_r and have the same wave-shape as v. The apparent power can then be obtained as the product of the RMS current and the RMS voltage

$$S^2 = V(I_a^2 + I_r^2) = P^2 + Q_F^2. \tag{1.29}$$

An unquestionable advantage of Fryze's theory is elimination, form initial Budeanu theory, of fourier series and third power component (deformation power).

1.2.3 Kusters and Moore's Definition

This definition of reactive power [4], is again a time domain definition. It expands the definition according to Fryze by a further split of the residual current into two orthogonal components. How this split is made depends on whether the load is predominantly a capacitive or an inductive load. The three currents achieved by this split are then called active current, inductive or capacitive reactive current and the residual reactive current, which results in an apparent power sum:

$$S^2 = P^2 + Q_c^2 + Q_{cr}^2 = P^2 + Q_l^2 + Q_{lr}^2. \tag{1.30}$$

The active current is, as by Fryze, defined by

$$i_p = \frac{P}{V^2} v \tag{1.31}$$

the capacitive reactive current is similarly defined as

$$i_{qc}(t) = v_{der} \frac{\frac{1}{T}\int_T v_{der} i dt}{V_{der}^2} \tag{1.32}$$

and the inductive reactive current as

$$i_{ql}(t) = v_{\text{int}} \frac{\frac{1}{T}\int_T v_{\text{int}} i dt}{V_{\text{int}}^2} \tag{1.33}$$

where v_{der} and v_{int} are the periodic part of the derivative and integral of the instantaneous voltage, respectively, and V_{der} and V_{int} the corresponding RMS values. Both these currents can then be

shown orthogonal to the residual current in the same way as i_p. Because of the orthogonality P, Q_c and Q_l can now be determined by the equations:

$$\begin{aligned} P &= VI_p \\ Q_c &= VI_{qc} \\ Q_l &= VI_{ql} \end{aligned} \tag{1.34}$$

where I_{qc} and I_{ql} are the RMS value of the i_{qc} and i_{ql}. The reactive powers Q_c and Q_l will then be signed quantities that can be compensated by capacitors or inductors if they are negative. That is, Q_c follows the sign convention of the reactive power in sinusoidal situations while Q_l will have an opposite sign. The rest terms will be determined by

$$\begin{aligned} i_{qcr} &= i - i_p - i_{qc} \\ i_{qlr} &= i - i_p - i_{ql} \end{aligned} \tag{1.35}$$

and

$$\begin{aligned} Q_{cr} &= \sqrt{S^2 - P^2 - Q_c^2} \\ Q_{lr} &= \sqrt{S^2 - P^2 - Q_l^2}\,. \end{aligned} \tag{1.36}$$

Q_l and Q_c are not equal to the reactive power according to Budeanu, but for sinusoidal signals they will be equal to Q (apart from the sign of Q_l). The rest term will be zero for sinusoidal signals.

Compared with the Fryze decomposition, the definition by Kusters and Moore has the advantage that it identifies the part of the current that can be compensated with a shunt capacitor or inductor. The value of the reactive compensating component can easily be calculated. This is, however, only valid if the source impedance is negligible, i.e. the voltage change when the compensation is applied must be negligible.

1.2.4 W. Shepherd and P. Zakikhani's Definition

This definition of reactive power [3] is based on a frequency domain analysis. A nonlinear load connected to an ideal source will result in current harmonics that do not have any corresponding voltage harmonics. In order to handle such nonlinear loads, the current and voltage harmonics are divided into "common" and "noncommon" harmonics. For the common harmonic of n order both V_n and I_n are nonzero, while for the noncommon harmonic of order n only one of V_n and I_n is nonzero. Then the apparent power can be expressed as

$$S^2 = \left(\sum_{n \in N} V_n^2 + \sum_{m \in M} V_m^2 \right) \left(\sum_{n \in N} I_n^2 + \sum_{f \in F} I_f^2 \right) \tag{1.37}$$

where N is the set of all common harmonic orders and M and F contain all noncommon, nonzero, harmonic orders of the voltage and the current respectively (that is, M is the set of orders for which the voltage harmonics are nonzero while the corresponding current harmonics, due to nonlinearity, are zero). The active power is still of course defined by

$$P = P_n = \sum_n V_n I_n \cos\varphi_n. \tag{1.38}$$

Shepherd then suggested a spilt of apparent power according to

$$\begin{aligned} S_R^2 &= \sum_{n\in N} V_n^2 \sum_{n\in N} I_n^2 \cos^2\varphi_n \\ S_X^2 &= \sum_{n\in N} V_n^2 \sum_{n\in N} I_n^2 \sin^2\varphi_n \end{aligned} \tag{1.39}$$

and the remaining terms

$$S_D^2 = \sum_{n\in N} V_n^2 \sum_{f\in F} I_f^2 + \sum_{m\in M} V_m^2 \left(\sum_{n\in N} I_n^2 + \sum_{f\in F} I_f^2 \right) \tag{1.40}$$

which yields

$$S^2 = S_R^2 + S_X^2 + S_D^2. \tag{1.41}$$

As all apparent power components are defined by RMS values, none of them has a sign. Shepherd et al consider their definition to be closer to the physical reality, especially for compensation of reactive power for a maximum power factor (with passive components). This is only achieved if S_X is minimized, according to Shepherd et al, since S_D only contains noncommon harmonics that cannot be compensated by passive components.

One major disadvantage of this scheme is that S_R is not equal to P, even if it contain P, which follows directly if the Cauchy-Schwarz inequality is applied on S_R and P. If the voltage (or the current) is purely sinusoidal then

$$\begin{aligned} S_R &= VI_1 \cos\varphi_1 = P \\ S_X &= VI_1 \sin\varphi_1 = Q_B \\ S_D &= D. \end{aligned} \tag{1.42}$$

For linear systems $S_D = 0$ since there are no noncommon harmonics.

1.2.5 Sharon's Definition

This definition of reactive power [53] is also based on a frequency domain analysis. It starts with the same division into common and noncommon harmonic components like Shepherd and Zakikhani. Sharon suggested an apparent power component according to

$$S_Q^2 = V^2 \sum_{n\in N} I_n^2 \sin^2\varphi_n \tag{1.43}$$

and the rest term

$$S_C^2 = \sum_{m\in M} V_m^2 \sum_{n\in N} I_n^2 \cos^2\varphi_n + V^2 \sum_{f\in F} I_f^2 + \frac{1}{2} \sum_{\beta\in N} \sum_{\gamma\in N} \left(V_\beta I_\gamma \cos\varphi_\gamma - V_\gamma I_\beta \cos\varphi_\beta \right) \tag{1.44}$$

which yields

$$S^2 = P^2 + S_Q^2 + S_C^2. \tag{1.45}$$

There are two important differences between this definition and the definition according to Shepherd and Zakikhani. The first is that in the definition by Sharon, P is one of the power components and not separately defined. The second is less obvious and is that S_Q is derived by a multiplication by the total RMS voltage and not only the RMS voltage of the common harmonic orders. This may seem a minor change but it removes some of the ambiguities due to the difficulty of sorting the noncommon orders from the common in a measurement situation. The active power is of course not affected by such a sorting. S_Q is not affected by any voltage harmonic sorting problem because all voltage harmonics is already used for the calculation of it.

1.2.6 L. S. Czarnecki's Definition

This is a frequency domain definition [19]. According to Czarnecki, since the idea of reactive power Q_F introduced by Fryze is defined without the use of Fourier series, it can be easily measured and can be similarly defined in nonlinear networks with variable parameters. Unfortunately, it is not related directly to the load properties and parameters, therefore, it does not provide any information about the reasons for which this power is greater than zero. Thus the Q_F power does not possess these properties for which the reactive power Q in sinusoidal systems is such an important quantity. It remains only a measure of the power system utilization and nothing else; but this property does not seem to be sufficient for the claim that Q_F power has physical interpretation. In particular, the Q_F power does not provide any information relevant to the possibility of the power factor improvement by means of a passive circuit. The reactive power S_X defined in the frequency domain by Shepherd and Zakikhani is able to solve the problem of the source power factor maximization by means of a single-shunt capacitor. Nonetheless, the nature of the remaining quantity S_R is vague and does not provide any information about the possibilities of its minimization. The results obtained by particular authors using frequency domain and time domain approaches, when compared from the viewpoint of power properties of nonsinusoidal systems interpretation and power factor improvement show that Shepherd's equation is more promising for the power factor improvement problems, whereas Fryze's equation is more useful for the power transmission efficiency description. Unfortunately, the nature of powers Q_F, S_R and the corresponding currents are vague and they do not elucidate the power properties of the systems. Therefore, according to Czarnecki it is advisable to combine these two approaches in a way which preserves their advantages, but removes their vague points like made by Sharon. Unfortunately, Sharon did not manage to explain the physical meaning of introduced quantities. They can be joined together, providing basic answers relevant to both power transmission interpretation and methods of power factor improvement, on the ground of the source current orthogonal decomposition in the frequency domain. For linear nonsinusoidal systems this idea can be explained as follows. The instantaneous value of a periodic voltage can be expressed as a complex Fourier series

$$v(t) = \sqrt{2}\,\mathrm{Re}\sum_{n\in N} V_n e^{jn\omega_1 t} \tag{1.46}$$

where ω_1 is the fundamental angular frequency, and n is a harmonic order for which V_n is nonzero. In a power system this voltage may be connected to a linear load with the admittance

$$Y_n = G_n + jB_n \tag{1.47}$$

that is, both G_n and B_n can be dependent on the frequency. The current will then be

$$i(t) = \sqrt{2}\,\mathrm{Re}\sum_{n\in N} V_n(G_n + jB_n)e^{jn\omega_1 t}. \tag{1.48}$$

Assuming that all power is absorbed by a (frequency invariant) conductance G_e, as in the power definition according to Fryze, this conductance can be determined by

$$G_e = \frac{P}{V^2}. \tag{1.49}$$

When exposed to the voltage V, the current through this conductance will be equal to the active current i_a according to [52] and (1.26). The residual current can then be calculated by

$$i(t) - i_a(t) = \sqrt{2}\,\mathrm{Re}\sum_{n\in N} V_n(G_n - G_e + jB_n)e^{jn\omega_1 t}. \tag{1.50}$$

This current can further be divided into

$$i_s(t) = \sqrt{2}\,\mathrm{Re}\sum_{n\in N} V_n(G_n - G_e)e^{jn\omega_1 t} \tag{1.51}$$

which is called scatter current and

$$i_r(t) = \sqrt{2}\,\mathrm{Re}\sum_{n\in N} jB_n V_n e^{jn\omega_1 t}$$

which is denoted reactive current. All these currents are orthogonal and therefore the RMS values of the currents can be expressed by

$$I^2 = I_a^2 + I_s^2 + I_r^2. \tag{1.52}$$

If this expression is multiplied by V^2 the apparent power is obtained

$$S^2 = P_a^2 + D_s^2 + Q_r^2. \tag{1.53}$$

The meaning of the current component i_a, is rather clear. It is the current of a resistive load which at voltage v is equivalent to the considered load with respect to its active power P. It has to be present in the source current if the source is loaded with the power P. Therefore, it seems to be quite justified to call it an "active current." Since i_s appears if $(G_n - G_e)$ and it is a measure at the voltage v of the source current increase due to a scattering of conductance G_n around the equivalent conductance G_e, so, it might be called a "scattered current." From the viewpoint of power factor improvement it is important that the value of terms $(G_n - G_e)$ may be positive as well as negative, hence, there does not exist any passive one-port which, connected at the load terminals, could compensate the i_s current. The i_r current appears if there is a phase-shift between voltage and current harmonics, i.e., if the source is loaded uselessly by the harmonic reactive powers Q_n. However, it is not the algebraic sum of Q_n powers, as was suggested by Budeanu, that is the measure of the apparent power increase caused by powers Q_n, but the product $|v||i_r|$, where $|i_r|$ is related to harmonic reactive powers Q_n by the formula

$$\|i_r\| = \sqrt{\sum_n B_n^2 V_n^2} = \sqrt{\sum_n \left(\frac{Q_n}{V_n}\right)^2}. \tag{1.54}$$

From the viewpoint of the power factor improvement it is important that Q_r power and i_r current can be wholly compensated by a shunt reactance one-port. Due to the properties of the i_r current, it seems to be justified to call it a "reactive current." According to Czarnecki currents i_a, i_s, i_r are directly related to three different phenomena, namely, to the active power transmission, to the load conductance scattering, and to the source loading with harmonics reactive power Q_n. Therefore, it seems that these three parts of the source current have quite clear physical meaning. But the nature of D_s and Q_r powers is quite the same as the nature of the source apparent power S. They are only the formal products of voltage and currents RMS value. However, the Q_r represents this part of the source apparent power which can be wholly compensated by a shunt reactance one-port, whereas the D_s represents this part of apparent power which cannot be compensated by any passive one-port.

1.2.7 Tenti's Definition

Tenti et al [54] introduced a new approach to reactive power and current in distorted, also three-phase, situations. Their approach starts from a quantity, which they call reactive energy, which is the scalar product of the current and the integral of the voltage, the reactive energy is given by

$$W_T = \sum_n \frac{1}{n\omega} V_n I_n \sin\varphi_n. \tag{1.55}$$

The corresponding reactive current is defined as the minimal current needed to convey this reactive energy to the load. Explicitly, this current is

$$i_T(t) = \frac{\sum_n \frac{1}{n} V_n I_n \sin\varphi_n}{\sum_n \left(\frac{1}{n} V_n\right)^2} \sum_n \frac{1}{n} \sqrt{2} V_n \sin(n\omega t + \alpha_n). \tag{1.56}$$

If a parallel element delivers this current to the load, then the losses in the supply are reduced and the supply conveys zero reactive energy W_T. All reactive energy of the load is conveyed by the parallel compensator.

1.2.8 M. Iliovici's Definition

M. Iliovici has presented a reactive power interpretation as loop area which is made by current and voltage coordinates [55]

$$Q_I = -\frac{1}{2\pi} \oint i dv. \tag{1.57}$$

Iliovici's reactive power is associated with electric and magnetic energy accumulated in circuits. Characteristics in *v-i* coordinates of nonlinear objects are usually complex and create multiple loops and furthermore their shape changes strongly under the influence of voltage change. Areas inside loops are circulated clockwise or counterclockwise. Therefore, the energy of electric or magnetic

field is sometimes drawn and sometimes returned. If energy is not mentioned, the object characteristic in *v-i* coordinates is reduced to a line segment.

1.2.9 Emanuel's Definitions

The idea of Emanuel's proposal is based on separation of fundamental active and reactive powers from the remaining apparent power components [56], [57]. In [56] Emanuel explained why he proposes this: "The power frequency apparent, active and reactive powers are the essential components among all the components of the apparent power. The electric energy is generated with nearly pure sinusoidal voltage and currents and the end-users, who buy the electric energy, expect a high quality product, i.e. the provider of electric energy is expected to deliver reasonable sinusoidal voltage waveforms that support the useful energy $P_1 t$. The harmonic powers P_h are often considered electromagnetic pollution − a by− product of the energy conversion process that takes place within the nonlinear loads. Thus, it makes good sense to separate P_1 and Q_1 from the rest of the powers." Emanuel's proposal is based on the Fourier series as follows: the current is separated into fundamental and total harmonic current

$$\begin{aligned} I^2 &= I_1^2 + I_H^2 \\ I_H &= \sum_{h\neq 1} I_h^2 \end{aligned} \tag{1.58}$$

and in the same way the voltage

$$\begin{aligned} V^2 &= V_1^2 + V_H^2 \\ V_H &= \sum_{h\neq 1} V_h^2 . \end{aligned} \tag{1.59}$$

The apparent power has four terms

$$S^2 = V^2 I^2 = \left(V_1^2 + V_H^2\right)\left(I_1^2 + I_H^2\right) = \left(V_1^2 I_1^2\right) + \left(V_1^2 I_H^2\right) + \left(V_H^2 I_1^2\right) + \left(V_H^2 I_H^2\right) = S_1^2 + D_I^2 + D_V^2 + S_H^2 \tag{1.60}$$

where S_1 is the fundamental apparent power, D_I is the current distortion power, D_U is the voltage distortion power, S_H is the harmonic apparent power.

1.3 Electric Quantities in Generalized Functions Domain

Since in this work networks working under both nonlinear continuous and discontinuous conditions are taking into account, the instantaneous electric quantities voltage and current can be decomposed in the generalized functions domain as follows

$$\begin{aligned} v(t) &= \tilde{v} + \sum_k \lambda_{\phi k}\delta(t - t_k) \\ i(t) &= \tilde{i} + \sum_k \lambda_{qk}\delta(t - t_k) \end{aligned} \tag{1.61}$$

where ~ denotes the bounded part including jump discontinuities of the electric quantity, δ denotes the first order Dirac's delta impulse which can be present in the electric quantities. $\lambda_{\phi k}$ and λ_{qk} are, respectively, the amplitudes of the voltage and current impulses. In this work impulses of higher

order and other kinds of discontinuities are excluded. However, in case of jump discontinuity the electric quantities are defined as

$$\begin{aligned}\tilde{v}(t) &= \frac{1}{2}(v(t_+) + v(t_-)) \\ \tilde{i}(t) &= \frac{1}{2}(i(t_+) + i(t_-)).\end{aligned} \tag{1.62}$$

It is possible to address the jump discontinuities as follows

$$\begin{aligned}\tilde{v}(t) &= v_{cont} + \sum_k V_{\mu k}\mu(t - t_k) \\ \tilde{i}(t) &= i_{cont} + \sum_k I_{\mu k}\mu(t - t_k)\end{aligned} \tag{1.63}$$

where $V_{\mu k} = V_{k+} - V_{k-}$ and $I_{\mu k} = I_{k+} - I_{k-}$ are the amplitudes of the jump discontinuities.

Now, let us define other functions which obey to the Kirchhoff laws:

1) *Jump functions*

$$\begin{aligned}J(v(t)) &= v(t_+) - v(t_-) \\ J(i(t)) &= i(t_+) - i(t_-).\end{aligned} \tag{1.64}$$

This functions are nil everywhere except in discrete points in which the left and right limits of the function are different. In these discontinuity instants the jump functions are equal to the step (with sign).

$$\begin{aligned}J(v(t_k)) &= V_{k+} - V_{k-} \\ J(i(t_k)) &= I_{k+} - I_{k-}\end{aligned} \tag{1.65}$$

2) *Impulsive functions*

$$\begin{aligned}Y(v(t)) &= \int_{t_-}^{t_+} v dt \\ Y(i(t)) &= \int_{t_-}^{t_+} i dt\end{aligned} \tag{1.66}$$

This functions are nil everywhere except in discrete points in which a first order Dirac's delta impulse is present. In these discontinuity instants the impulsive functions are equal to the amplitude of the impulse (with sign).

$$\begin{aligned}Y(v(t_k)) &= \lambda_{\phi k} \\ Y(i(t_k)) &= \lambda_{qk}\end{aligned} \tag{1.67}$$

3) *Derivatives in the generalized functions domain*

$$\frac{dv(t)}{dt} \qquad \frac{di(t)}{dt} \tag{1.68}$$

4) *Integrals*

$$\Delta\phi = \int_{t_0}^{t} v(t)dt \qquad \Delta q = \int_{t_0}^{t} i(t)dt \tag{1.69}$$

This finite integrals are to be referred to a common initial time t_0. In this way Kirchhoff laws are met.

By means of this functions it is possible to define several generalized functions which are developed in next chapters.

Systems with finite energy

In order to avoid infinite energy in the system, impulses of voltage and current at the same time and on the same electric port are excluded. Indeed

$$E = \int_{-\infty}^{+\infty} \lambda_{\phi k}\delta(t-t_k)\lambda_{qk}\delta(t-t_k)dt = \lambda_{\phi k}\lambda_{qk}\delta(t_k) \tag{1.70}$$

is infinite.

2. Swept Area Theory

2.1 Introduction

In this chapter novel conservative functions are proposed. In particular, starting from the area approach mentioned in the introduction and similarly to the Iliovici approach, the Swept Area Theory (SAT), which widely uses the concepts of trajectory and area on the *v*-*i* plane under both nonlinear continuous and discontinuous conditions, is developed. Impulses on voltages and/or currents are not covered in this chapter and in the followings 3−5.

2.2 Area Velocity

Let us consider a lumped-parameter circuit formed by connection of electrical ports. Voltages and currents are continuous functions with possible jump discontinuities. In order to handle discontinuities, all subsequent differential relations must be considered in the domain of generalized functions, as stated in chapter 1.

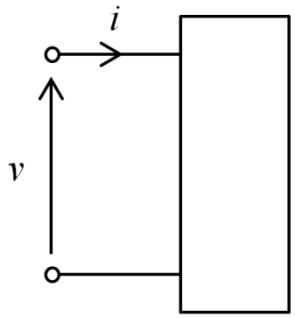

Fig. 2.1 Reference directions for voltage and current on a one-port element

For a two-terminals component, with the reference directions for voltage and current reported in Fig. 2.1, let us define the *Area Velocity* (AV), here indicated with *h*, as

$$h(t)=\frac{1}{2}\left(v\frac{di}{dt}-i\frac{dv}{dt}\right). \tag{2.1}$$

The AV (2.1) is a generalized power in the sense of [2]. The sign of AV depends on the product of the signs of *v* and *i* like the usual power. Therefore, it is possible to assume for AV the same terminology, absorbed or generated, with the same sign rules as power. Expression (2.1) is not the differential of a function. In order to evidence a derivative of a function, namely the instantaneous power *vi*, (2.1) can be rewritten in the equivalent forms

$$h(t)=v\frac{di}{dt}-\frac{1}{2}\frac{d}{dt}(vi)=\frac{1}{2}\frac{d}{dt}(vi)-i\frac{dv}{dt}. \tag{2.2}$$

2.2.1 Continuous Conditions

The AV has a significant graphic correspondence on the *v*-*i* plane, which makes reason of its name. Under the condition that $v(t)$ and $i(t)$ are continuous functions, it is possible to get a graphical interpretation as follows: let dv and di be the increments of voltage and current on the *v*-*i* plane. Let us evidence the incremental area dA swept on the *v*-*i* plane respect to the origin of the axes, as depicted in Fig. 2.2. From graphical analysis it is possible to write the following expression

$$dA = \frac{1}{2}(vdi - idv). \tag{2.3}$$

The ratio of the incremental swept area dA and the incremental time dt gives rise to (2.1).

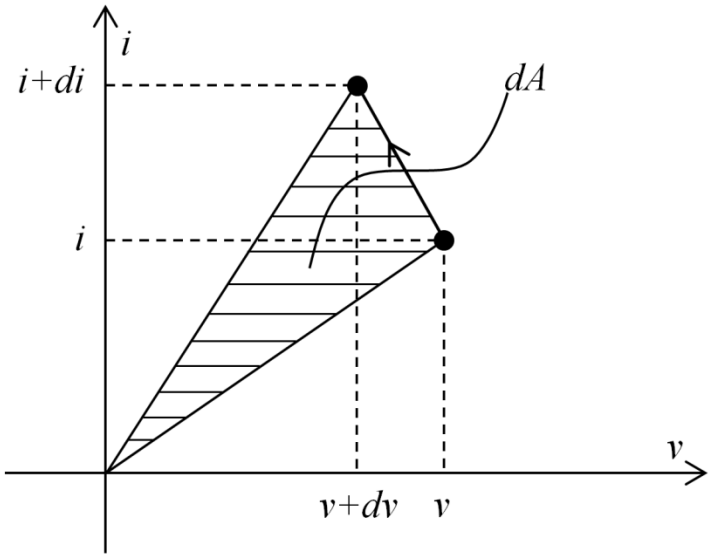

Fig. 2.2. Infinitesimal swept area

2.2.2 Discontinuous Conditions

In case the voltage and/or current present a jump discontinuity, let us introduce the unitary step $u(t)$ and its generalized derivative, the unitary impulse $\delta(t)$. Let us suppose a discontinuity both on $v(t)$ and $i(t)$ at time t^*. Around a small neighborhood of the discontinuity, $v(t)$ and $i(t)$ can be assumed as constant, as shown in Fig. 2.3, and it is possible to write

$$\begin{aligned} v(t) &= v_A + (v_B - v_A)u(t - t^*) \\ i(t) &= i_A + (i_B - i_A)u(t - t^*). \end{aligned} \tag{2.4}$$

Taking into account (2.4) in (2.1) and the generalized derivative, the following expression involving an impulse is obtained.

$$h_\delta(t) = \frac{1}{2}(v_A i_B - v_B i_A)\delta(t - t^*) \tag{2.5}$$

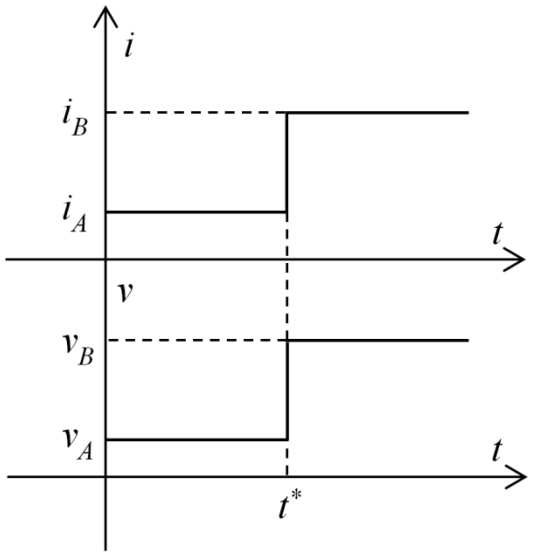

Fig. 2.3. Voltage and current jump discontinuities

Also in this case a simple graphical interpretation can be given to (2.5). Indeed, the amplitude of the impulse of AV is the triangle of finite swept area of Fig. 2.4. Hence, in case of discontinuity, the two points A and B have to be joint by a straight line yielding a finite area. As a particular case, (2.5) is valid for a discontinuity present only in the current ($v_A = v_B$) or in the voltage ($i_A = i_B$).

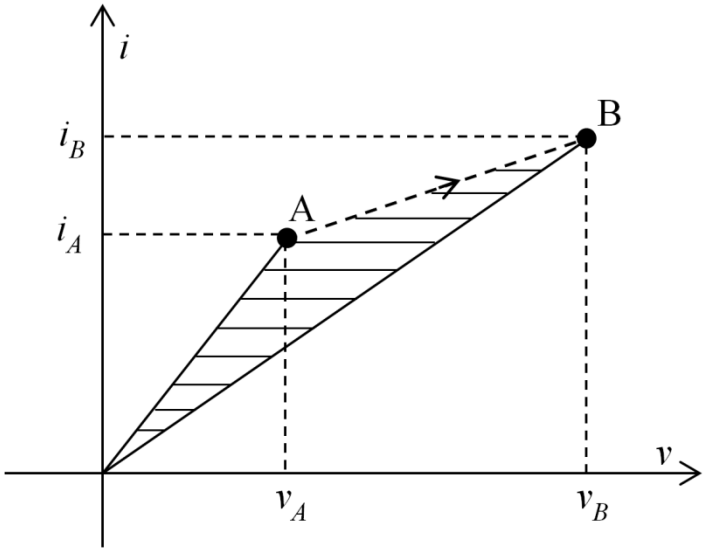

Fig. 2.4. Jump discontinuity on the *v*-*i* plane

From the given hypotheses on functions $v(t)$ and $i(t)$, and the graphical interpretations sketched in Fig. 2.2 and Fig. 2.4, it is possible to recognize that the trajectory on the *v*-*i* plane is a continuous piecewise regular curve.

2.2.3 Switching Power

As reported in [46] it is possible to define the Switching Power (SP) as the area on the *v*-*i* plane generated in case of discontinuity. The name "Switching" refers to the fact that, usually, a discontinuity is generated by an ideal switch but, in principle, it can be due to a generator with discontinuity, as a square wave voltage source. Mathematically, taking into account (2.5) and Fig. 2.4, the Switching Power can be define as

$$A_\delta(t^*) = \int_{t_-^*}^{t_+^*} h dt = \frac{1}{2}(v_A i_B - v_B i_A). \tag{2.6}$$

In this way the (2.6) is always valid but gives a result different from zero only when in the Area Velocity is present an impulse due to a discontinuity on the *v-i* plane.

2.2.4 Balance Theorem over Area Velocity

In electrical network satisfying the voltage and current Kirchhoff laws, Tellegen's theorem [1] states that the product *vi* is balanced, i.e. the sum over the whole network is nil. Hence, also the generalized derivatives of those quantities satisfy the Kirchhoff laws. In other words, according to the generalized form of Tellegen's theorem (1.8), it is possible to recognize the Kirchhoff's operators as

$$\Delta_1 = \frac{1}{2}\frac{di}{dt} \quad \Delta_2 = \frac{1}{2}\frac{dv}{dt}$$

and the following theorem can be stated.

Theorem 2.I. Given a network constituted by a connection of "p" electric ports and chosen the same reference directions for all ports, the sum of Area Velocity extended to the whole network is nil, namely the sum of Area Velocity generated is equal to the sum of Area Velocity absorbed.

$$\sum_{k=1}^{p} h(t) = \frac{1}{2}\left(v\frac{di}{dt} - i\frac{dv}{dt} \right) = 0$$

2.3 Closed Area over Time

Let us consider an electric port under periodical steady state of period *T*. Hence, it is possible to define the *Closed Area over Time* (CAT) as the mean value of AV over the period, as follows

$$H = \frac{1}{T}\int_T h(t)dt. \tag{2.7}$$

For the periodicity *T* on the *v-i* plane the trajectory forms a closed curve. Graphically, (2.7) is the swept area enclosed on the *v-i* plane averaged over the period *T*, as shown in Fig. 2.5. According to the positive direction in Fig. 2.2, the CAT is positive when its contour is oriented in counterclockwise direction.

In case of jump discontinuities, (2.7) is still valid in domain of generalized functions. Specifically, the impulse (2.5) gives a finite contribution equal of the impulse amplitude in the integral (2.7) and the graphical result of Fig. 2.4 is extended: the trajectory on the *v-i* plane is to be closed by a straight line between the points of discontinuity (for example the A-B segment in Fig. 2.5). In this case the (2.7) can be written as follow

$$H = \frac{1}{T}\left(\sum_j \int_C h dt + \sum_k A_{\delta k} \right) \tag{2.8}$$

where *C* are the intervals in which $h(t)$ is a continuous function.

In general the trajectory is a closed piecewise regular curve. It may not contain the axis origin and may be a nonsimple curve (some points of the trajectory may be covered more than once). Therefore, the graphical approach is a general and very useful support for the evaluation of the CAT in every circumstance.

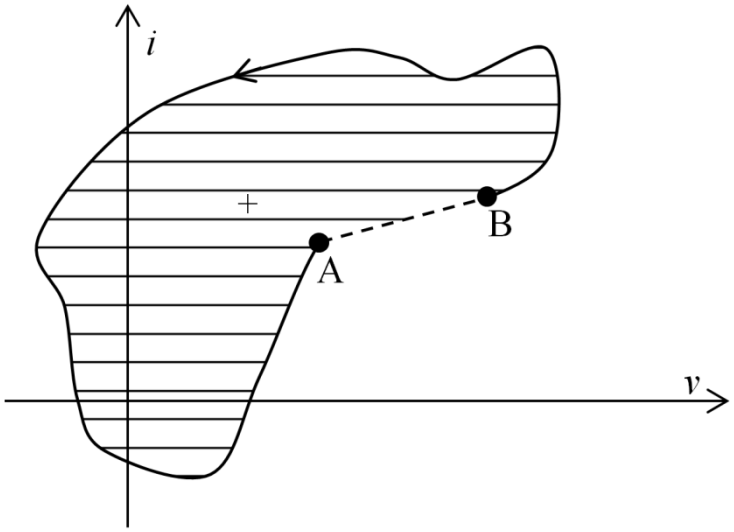

Fig. 2.5. Closed swept area under periodical steady state

From (2.2) and taking into account the periodicity, two equivalent explicit forms of (2.7) are obtained:

$$H = \frac{1}{T}\int_T v\frac{di}{dt}dt = -\frac{1}{T}\int_T i\frac{dv}{dt}dt. \tag{2.9}$$

2.3.1 Balance Theorem over Closed Area over Time

It is worth noting that, according to the definition (2.7), the swept area is divided by the local period T. Hence, this definition is independent of the common period of the network, if exists, whereas only the periodicity of the quantities of the considered port is required. If all network ports are periodic and such periods are in rational ratio each other, then a common period (least common multiple) exists. Referring the CAT to this common period, since AV is balanced also its mean value is balanced too, hence:

Theorem 2.II. Given a network under periodical steady state constituted by a connection of electric ports and chosen the same reference directions for all ports, the sum of Close Area over Time (referred to common period) extended to the whole network is nil, namely the sum of Closed Area over Time generated is equal to the sum of Closed Area over Time absorbed.

2.3.2 Relation between CAT and Harmonic Reactive Powers

Let us consider the two terminal component of Fig. 2.1under periodical steady state of period T. The Fourier series expansions of the voltage and current are ($\omega = 2\pi/T$)

$$\begin{aligned} v(t) &= \sum_{k_1=-\infty}^{+\infty} \boldsymbol{V}_{k_1} e^{jk_1\omega t}, \quad \boldsymbol{V}_{-k_1} = \boldsymbol{V}_{k_1}^* \\ i(t) &= \sum_{k_2=-\infty}^{+\infty} \boldsymbol{I}_{k_2} e^{jk_2\omega t}, \quad \boldsymbol{I}_{-k_2} = \boldsymbol{I}_{k_2}^* \end{aligned} \tag{2.10}$$

in which $\boldsymbol{V}_{k1}$ and $\boldsymbol{I}_{k2}$ are complex number and * marks conjugate components. Furthermore

$$\begin{aligned} \frac{dv(t)}{dt} &= \sum_{k_1=-\infty}^{+\infty} jk_1\omega \boldsymbol{V}_{k_1} e^{jk_1\omega t} \\ \frac{di(t)}{dt} &= \sum_{k_2=-\infty}^{+\infty} jk_2\omega \boldsymbol{I}_{k_2} e^{jk_2\omega t}. \end{aligned} \tag{2.11}$$

Taking into account (2.10) and (2.11) in (2.1), the Fourier expansion of AV is obtained:

$$h(t) = \frac{1}{2} \sum_{k_1=-\infty}^{+\infty} \sum_{k_1=-\infty}^{+\infty} j(k_2 - k_1)\omega \boldsymbol{V}_{k_1} \boldsymbol{I}_{k_2} e^{j(k_1+k_2)\omega t}. \tag{2.12}$$

Averaging over a period T only terms with $k_1 + k_2 = 0$ contribute to the CAT quantity (2.7):

$$H = -\sum_{k=-\infty}^{+\infty} jk\omega \boldsymbol{V}_k \boldsymbol{I}_k^* = \sum_{k=1}^{+\infty} jk\omega(\boldsymbol{V}_k^* \boldsymbol{I}_k - \boldsymbol{V}_k \boldsymbol{I}_k^*). \tag{2.13}$$

Since the reactive power associated to the k-th sinusoidal component of voltage and current is by definition

$$Q_k = 2\,\mathrm{Im}(\boldsymbol{V}_k \boldsymbol{I}_k^*) = j(\boldsymbol{V}_k^* \boldsymbol{I}_k - \boldsymbol{V}_k \boldsymbol{I}_k^*) \tag{2.14}$$

it follows

$$H = \sum_{k=1}^{+\infty} k\omega Q_k. \tag{2.15}$$

Equation (2.15) gives the CAT versus the Fourier components of the reactive power, in which each contribution is weighted on its own angular frequency. Relation (2.15) is valid provided the series is convergent. It is possible that (2.15) converges even if one or both terms of series (2.11) are not convergent. A significant case is given by the square waveform of both current and voltage. Series (2.10) exist, the derivatives are series of impulses and (2.11) do not converge. However (2.15) converges to the expected value.

2.3.3 Elementary Cases

As a particular case, under dc steady state both $h = 0$ and $H = 0$. Whether only v or i is constant, then h is not zero but $H = 0$.

Instead, under sinusoidal steady state conditions, by elementary passages, it can be proved that AV is constant and equal to $h(t) = \omega Q$ and consequently the CAT is

$$H = \omega Q. \tag{2.16}$$

Whether only $v(t)$ or $i(t)$ is sinusoidal, (2.16) still holds.

2.4 AV and CAT on Electric Components

2.4.1 Resistive one-port

Let us consider a time-invariant nonlinear resistive one-port, with a continuous characteristic on the *v-i* plane, as shown in Fig. 2.6. Let us define the resistor in parametric form as

$$v = v(x); i = i(x) \tag{2.17}$$

with $x(t)$ the curvilinear abscissa. The parametric form makes it possible to include resistors not voltage-controllable, not current-controllable or neither.

Area Velocity

Taking into account (2.17) in (2.1), the AV on the resistor is obtained:

$$h_R(t) = \frac{1}{2}\left(v\frac{di}{dx} - i\frac{dv}{dx}\right)\frac{dx}{dt}. \tag{2.18}$$

Across a jump discontinuity at time t^* taking into account (2.5), the (2.18) becomes

$$h_{R\delta}(t) = \frac{1}{2}\left[v(x(t_-^*))i(x(t_+^*)) - v(x(t_+^*))i(x(t_-^*))\right]\delta(t-t^*). \tag{2.19}$$

If the current-voltage characteristic is linear, i.e. $v = Ri$ or $i = Gv$, it is straightforward to recognize that in (2.18) and (2.19)

$$h_R(t) = 0. \tag{2.20}$$

Closed Area over Time

Under periodical steady state, from (2.7) and (2.18) the CAT on the resistor is

$$H_R = \frac{1}{2T}\int_{t_0}^{t_0+T}\left(v\frac{di}{dx} - i\frac{dv}{dx}\right)\frac{dx}{dt}dt. \tag{2.21}$$

Under the condition that $x(t)$ is a continuous function of time, changing of integration variable is allowed in (2.21), becoming the line integral

$$H_R = \frac{1}{2T}\int_{x(t_0)}^{x(t_0+T)}\left(v\frac{di}{dx} - i\frac{dv}{dx}\right)dx. \tag{2.22}$$

Because of periodicity, $x(t_0) = x(t_0+T)$ and hence

$$H_R = 0. \tag{2.23}$$

The graphical interpretation is straightforward: *v(x)* and *i(x)* are constrained over the characteristic and the periodic trajectory on the *v-i* plane has always a null swept area.

Different result applies in case of jump discontinuity. In this case some jumps may appear among couples of points on the characteristic, $x(t)$ is not yet continuous, so (2.22) is not yet valid on the whole trajectory. Let be n jumps in the period at times t_j (j=1,…,n). Each jump j identifies a couple of points $x(t_{j(-)}) = x_{j(-)}, x(t_{j(+)}) = x_{j(+)}$. The time integral (2.21) is now decomposed in a number of continuous intervals $]t_j{-}t_{j+1}[$ between the discontinuities. Since in the continuous curve portions $]x(t_j){-}x(t_{j+1})[$, $x(t)$ is continuous, the variable substitution (2.22) applies on each continuous interval. Moreover, the contributions of the discontinuities must be added according to (2.19). Hence, (2.21) turns into

$$H_R = \frac{1}{2T}\left\{\sum_{j=0}^{n}\int_{x_{j(+)}}^{x_{j+1(-)}}\left(v\frac{di}{dx} - i\frac{dv}{dx}\right)dx + \sum_{j=1}^{n}\left[v(x_{j-})i(x_{j+}) - v(x_{j+})i(x_{j-})\right]\right\} \tag{2.24}$$

with $x_{0(+)} = x(t_0)$ and $x_{n+1(-)} = x(t_0{+}T)$.

In the integral (2.24) the portions of the characteristic tracked twice have nil sum, but because of the presence of some portions involved in a jump, (2.24) may be not nil. A graphical interpretation of (2.24) is exemplified in Fig. 2.6 for a single jump. The line is tracked periodically from A to D. The first term in (2.24) has two factors, the first ABCDC over the characteristic (after reaching the point D, the abscissa comes back to point C), the second BA over the characteristic. The second term in (2.24) is a straight line CB representing the jump. According to swept areas in Fig. 2.2 (continuous) and Fig. 2.4 (jump), the remaining net area is the shadowed area between the lines. Therefore, the value of the CAT can be evaluated by the sketch on the *v-i* plane.

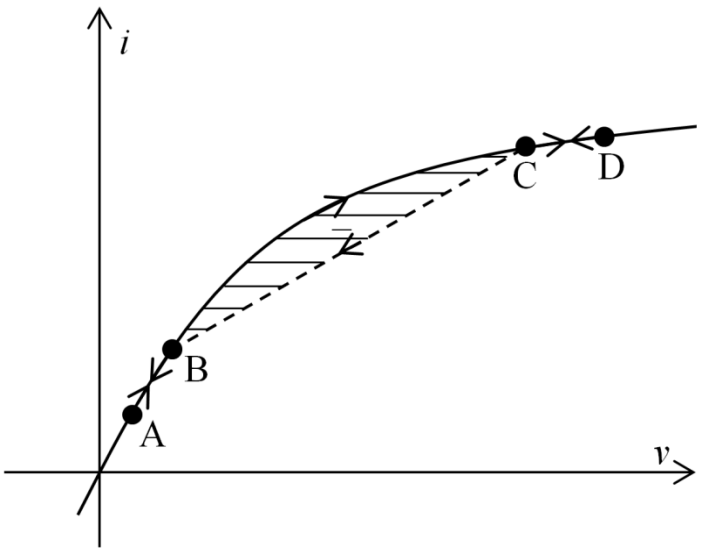

Fig. 2.6. Nonlinear resistor characteristic on the *v-i* plane with jump discontinuity

On a linear resistor, according to (2.20) all terms in (2.24) are nil. Therefore, the outstanding result applies that only on a nonlinear resistor under jump discontinuities, the CAT may be not nil, otherwise CAT is nil on resistors.

2.4.2 Inductive one-port

Let us consider a time-invariant nonlinear inductive one-port. Assuming a flux-controlled continuous characteristic, as shown in Fig. 2.7, at its terminal it holds:

$$v(t) = \frac{d\psi}{dt} \tag{2.25}$$

$$i = i(\psi). \tag{2.26}$$

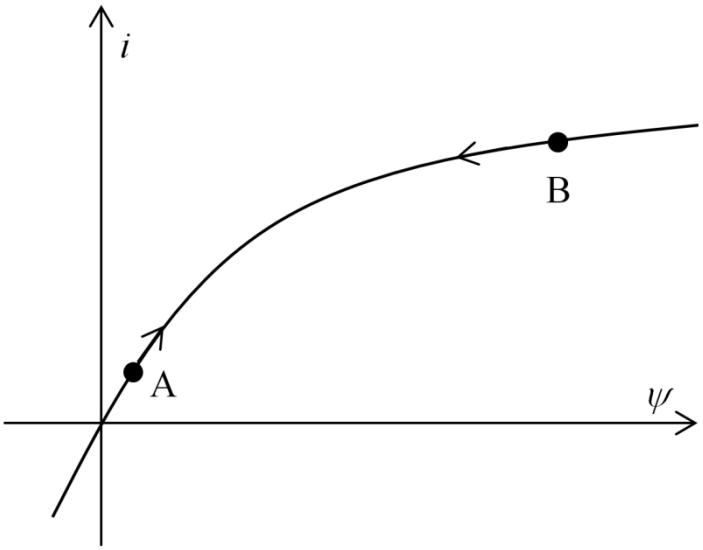

Fig. 2.7. Nonlinear inductor characteristic on the ψ-i plane

Area Velocity

Taking into account (2.25) and by deriving the characteristic (2.26) in the first of (2.2), the AV h_L is obtained

$$h_L(t) = \frac{di}{d\psi} v^2 - \frac{1}{2}\frac{d}{dt}(vi). \tag{2.27}$$

Closed Area over Time

Under periodical steady state according to (2.27), H_L is

$$H_L = \frac{1}{T}\int_T \frac{di}{d\psi} v^2 dt. \tag{2.28}$$

If the current-flux characteristic is monotone and nondecreasing

$$\frac{di}{d\psi} \geq 0 \quad \forall \psi$$

then the integrand in (2.28) is nonnegative and consequently

$$H_L \geq 0 \tag{2.29}$$

showing a close trajectory enclosing a positive area on the *v*-*i* plane (Fig. 2.8).

If the current-flux characteristic is linear time-invariant, it is possible to write

$$i = \frac{\psi}{L} \tag{2.30}$$

and taking into account (2.30) in (2.28), H_L becomes

$$H_L = \frac{1}{T}\int_T \frac{v^2}{L}\,dt = \frac{V^2}{L} \tag{2.31}$$

where V is RMS value.

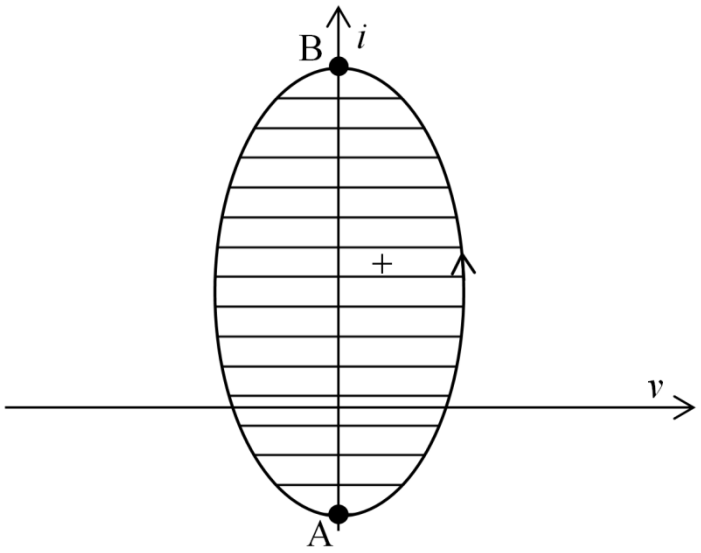

Fig. 2.8. CAT on the *v*-*i* plane of the inductor

Equations (2.27), (2.28), and (2.31) are valid also under jump discontinuities on the voltage. Discontinuity on the current is not allowed, otherwise according to (2.25), (2.26), an impulse on the voltage could arise.

2.4.3 Capacitive one-port

Let us consider a time-invariant nonlinear capacitive one-port. Assuming a charge-controlled continuous characteristic, as shown in Fig. 2.9, at its terminal it holds:

$$i(t) = \frac{dq}{dt} \tag{2.32}$$

$$v = v(q). \tag{2.33}$$

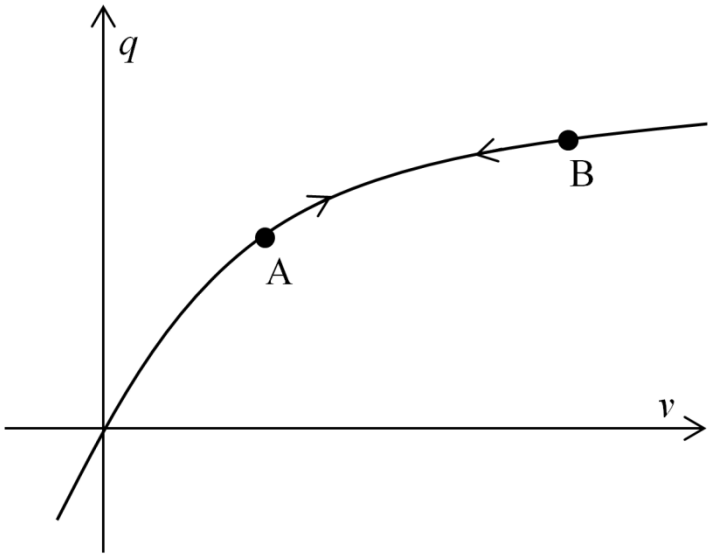

Fig. 2.9. Nonlinear inductor characteristic on the *v*-*q* plane

Area Velocity

Taking into account (2.32) and by deriving the characteristic (2.33) in the second of (2.2), the AV h_C is obtained

$$h_C(t) = \frac{1}{2}\frac{d}{dt}(vi) - \frac{dv}{dq}i^2. \tag{2.34}$$

Closed Area over Time

Under periodical steady state according to (2.34), H_C is

$$H_C = -\frac{1}{T}\int_T \frac{dv}{dq}i^2 dt. \tag{2.35}$$

If the voltage-charge characteristic is monotone and nondecreasing

$$\frac{dv}{dq} \geq 0 \quad \forall q$$

then the integrand in (2.35) is nonnegative and consequently

$$H_C \leq 0 \tag{2.36}$$

showing a close trajectory enclosing a negative area on the *v*-*i* plane (Fig. 2.10).

If the voltage-charge characteristic is linear time-invariant, it is possible to write

$$v = \frac{q}{C} \tag{2.37}$$

and taking into account (2.37) in (2.35), H_C becomes

$$H_C = -\frac{1}{T}\int_T \frac{i^2}{C}dt = -\frac{I^2}{C} \tag{2.38}$$

where I is RMS value.

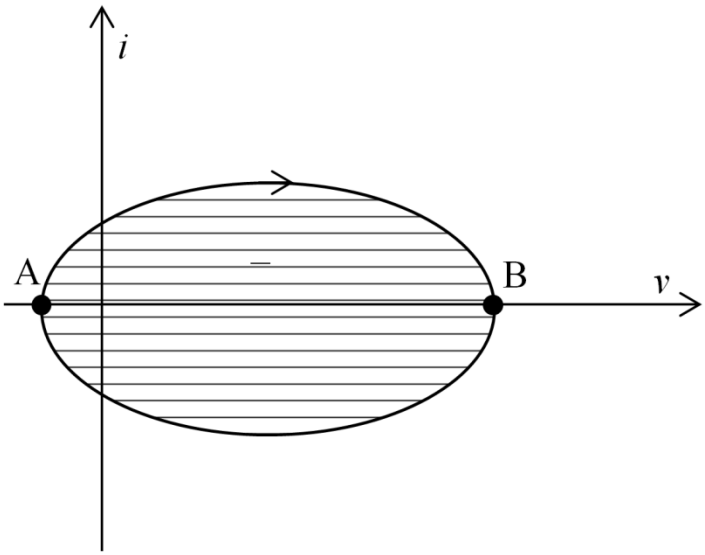

Fig. 2.10. CAT on the *v-i* plane of the capacitor

Regarding jump discontinuities, a discontinuity on the voltage is not allowed, otherwise, according to (2.32) and (2.33) an impulse on the current could arise. A discontinuity on the current is allowed without any change in results.

2.4.4 Ideal Switch one-port

Let us consider an ideal switch as depicted in Fig. 2.11. The ideal switch is a time-variant two-state element represented by the switch variable s with the convention

$$\begin{aligned} &i(t) = 0,\ s = 0\ \forall v \quad open \\ &v(t) = 0,\ s = 1\ \forall i \quad close \end{aligned} \tag{2.39}$$

with instantaneous transition between states. The s variable is also called *Switching Function* (SF).

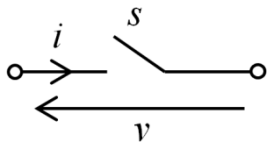

Fig. 2.11. Ideal switch one-port

Area Velocity

When the ideal switch opens at time t^*, the current $I_{SW} = i(t^*_-)$ that was flowing is interrupted and the voltage that was nil becomes $V_{SW} = v(t^*_+)$. Hence, a discontinuity in both quantities appears as shown in Fig. 2.12 and according to (2.5) it is possible to write

$$h_{SWopen}(t) = -\frac{1}{2} I_{SW} V_{SW} \delta(t - t^*). \tag{2.40}$$

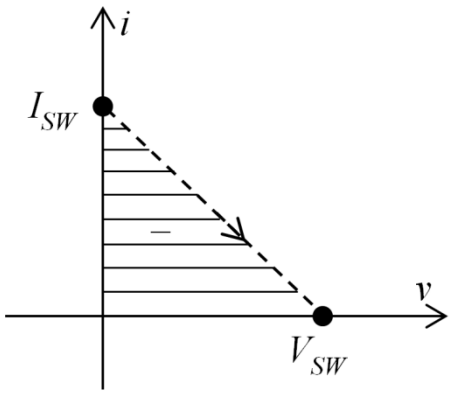

Fig. 2.12. Switching Power in the opening transition

On the *v-i* plane the trajectory is a linear segment moving from I_{SW} to V_{SW}, and hence, a triangle area is created as shown in Fig. 2.12 (negative area if $V_{SW}I_{SW} > 0$).

When the ideal switch closes at time t^*, the voltage $V_{SW} = v(t^*_-)$ that was applied on the switch becomes nil and the current that was nil becomes $I_{SW} = i(t^*_+)$. Hence, a discontinuity in both quantities appears as shown in Fig. 2.13 and according to (2.5) it is possible to write

$$h_{SWclosed}(t) = \frac{1}{2} I_{SW} V_{SW} \delta(t - t^*). \tag{2.41}$$

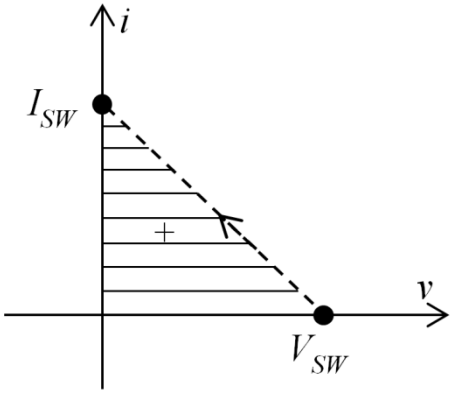

Fig. 2.13. Switching Power in the closing transition

On the *v-i* plane the trajectory is a linear segment moving from V_{SW} to I_{SW}, and hence, a triangle area is created as shown in Fig. 2.13 (positive area if $V_{SW}I_{SW} > 0$).

Switching Power

It was shown that a switching produces an impulse in the AV corresponding to a finite area on the *v-i* plane. According to (2.6) in the opening transition the SP is

$$A_{SWopen} = -\frac{1}{2} I_{SW} V_{SW} \tag{2.42}$$

while, in the closing transition the SP is

$$A_{SWclosed} = \frac{1}{2} I_{SW} V_{SW}. \tag{2.43}$$

According to the definitions of *hard switching* when $V_{SW}I_{SW} \neq 0$ and *soft switching* when $V_{SW}I_{SW} = 0$, it is possible to state that only when an *hard switching* commutation occurs the SP is not nil. It is important to note that the SP has the same dimension of a power [VA] and it can be useful in order to identify the switching.

Closed Area over Time

Let us calculate the average value (2.7) of the ideal switch. Commutations (2.40), (2.41) are the only contributions to the CAT and then (2.7) becomes the sum of the SP (2.42) and (2.43) extended to all k commutations over the period T.

$$H_{SW} = \frac{1}{T} \sum_k A_{SWk}. \tag{2.44}$$

It is worth to note that under periodical steady state the number of both closing and opening commutations of the switch must be the same.

Note that, in case of ideal switching, the calculation of the CAT is very simple because the integral (2.7) becomes a discrete summation (2.44) of finite terms in the period T.

2.4.5 Ideal Diode one-port

Let us consider an ideal diode, with its characteristic on the *v-i* plane, as reported in Fig. 2.14. It is a particular nonlinear resistor.

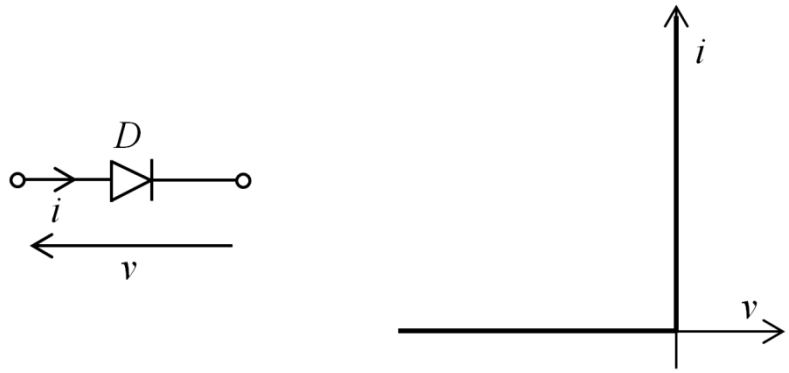

Fig. 2.14. Ideal diode and its characteristic on the *v-i* plane

When the ideal diode, due to the remaining part of the network, jumps at time t^* from the point B to the point A (Fig. 2.15) on its characteristic (opening transition), the current $I_D = i(t^*_-) \geq 0$ that was flowing is interrupted and the voltage that was nil becomes $V_D = v(t^*_+) \leq 0$. Hence, a discontinuity in both quantities appears as shown in Fig. 2.15 and according to (2.5) the AV absorbed by the ideal diode is

$$h_{Dopen}(t) = -\frac{1}{2} I_D V_D \delta(t - t^*) \geq 0 \quad (V_D I_D \geq 0) \tag{2.45}$$

and, according to (2.6) the SP absorbed is

$$A_{Dopen} = -\frac{1}{2} V_D I_D \geq 0 \quad (V_D I_D \leq 0). \tag{2.46}$$

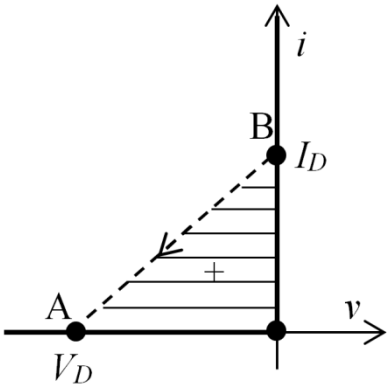

Fig. 2.15. Switching Power in the transition from the point B to the point A (opening transition)

When the ideal diode, due to the remaining part of the network, jumps at time t^* from the point A to the point B on its characteristic (closing transition), the voltage $V_D = v(t^*_-) \leq 0$ that was applied on the diode becomes nil and the current that was nil becomes $I_D = i(t^*_+) \geq 0$. Hence, a discontinuity in both quantities appears as shown in Fig. 2.16 and according to (2.5) the AV absorbed by the ideal diode is

$$h_{Dclosed}(t) = \frac{1}{2} I_D V_D \delta(t - t^*) \leq 0 \quad (V_D I_D \leq 0) \tag{2.47}$$

and, according to (2.6) the SP absorbed is

$$A_{Dclosed} = \frac{1}{2} V_D I_D \leq 0 \quad (V_D I_D \leq 0). \tag{2.48}$$

By (2.46) and (2.48) it is possible to recognize that the ideal diode always absorbs SP in opening commutations and always generates SP in closing commutations.

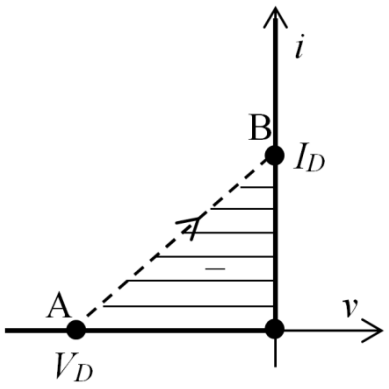

Fig. 2.16. Switching Power in the transition from the point A to the point B (closing transition)

2.5 Active and Passive Hard Switching

In order to get more stringent results, let us define *active hard switching* the ideal switch commutations (2.40), (2.41) so that the following strict inequality is valid

$$V_{SW} I_{SW} > 0. \tag{2.49}$$

Let us define *passive hard switching* the opposite case

$$V_{SW} I_{SW} < 0. \tag{2.50}$$

Let us consider a network constituted by continuous generators, which impose voltages or currents as continuous functions of time, resistors, inductors, capacitors, ideal switches and ideal diodes under the hypothesis that there are no impulses. Let us suppose that only one ideal switch commutes at time. In this way, it is possible to make the Thèvenin's equivalent circuit of the network respect to the ideal switch that commutes, where inductors and capacitors are substituted by equivalent current and voltage generators in the switching instant, as reported in Fig. 2.17.

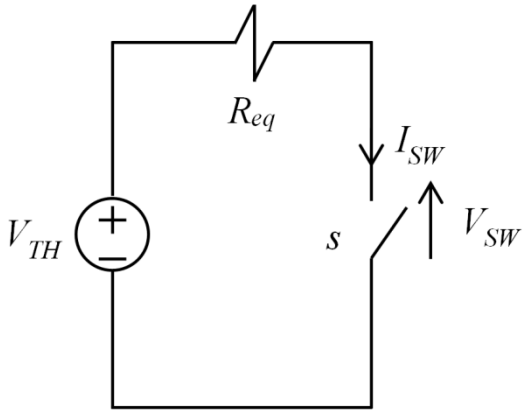

Fig. 2.17. Thèvenin's equivalent circuit

When the ideal switch closes, the voltage that was applied on the switch before the commutation is

$$V_{SW} = V_{TH} \tag{2.51}$$

while the current flowing through the ideal switch after the commutation is

$$I_{SW} = \frac{V_{TH}}{R_{eq}}. \tag{2.52}$$

When the ideal switch opens the current flowing through the ideal switch before the commutation is

$$I_{SW} = \frac{V_{TH}}{R_{eq}} \tag{2.53}$$

while the voltage that was applied on the switch after the commutation is

$$V_{SW} = V_{TH}. \tag{2.54}$$

In both cases, with $R_{eq} > 0$, if the voltage V_{TH} and the equivalent resistance R_{eq} do not change during the commutation, the product $V_{SW}I_{SW} > 0$, and hence, an active hard switching applies. This is the expected case when a controlled valve device is fired as alone. Instead, a passive hard switching could apply if the voltage V_{TH} or the equivalent resistance R_{eq} change during the commutation, in order to have the product $V_{SW}I_{SW} < 0$. This situation can apply when two, or more, devices switch at the same time, such way the Thevenin equivalent, as seen by a device, before and after the switching is not the same.

In addition, it will be demonstrated that a passive hard switching always matches with a contemporary active hard switching.

According to the definitions of *active* and *passive hard switching*, and based on (2.46), (2.48), it is possible for the ideal diode to state the following:

the ideal diode is a nonlinear resistor which can be seen as an ideal switch that can commute in soft switching and only in passive hard switching. It works only in the II quadrant of the v-i plane.

2.6 CAT under Continuous and Discontinuous Conditions

Provided that impulses or and other kinds of discontinuities are out of the scope of this chapter, a deeper discussion and insight of CAT features requires distinction between continuous and discontinuous conditions.

2.6.1 Continuous Conditions

Sinusoidal conditions

Under sinusoidal conditions the only harmonic component presents in the electric quantities is the fundamental one. Indeed, according to (2.16) the relation between H and Q is proportional by means the angular frequency ω. In this case H and Q give the same information on the R, L and C components. Table 2.1 shows the P, Q and H conditions on passive elements.

Table 2.1. P, Q, H relations under sinusoidal conditions

	R	L	C
Active Power	$P \geq 0$	$P = 0$	$P = 0$
Reactive Power	$Q = 0$	$Q \geq 0$	$Q \leq 0$
CAT	$H = 0$	$H \geq 0$	$H \leq 0$

Nonsinusoidal conditions

Under periodical nonsinusoidal conditions, by Fourier series on each port variable, network under distorted steady state can be decomposed in (possibly infinite) sinusoidal harmonic networks. For each k harmonic, it is well-known that active power P_k and reactive power Q_k are balance inside its own harmonic network. In general, the nonsinusoidal conditions can be due to the present of distorted sources and/or nonlinear elements. Nonlinear elements give rise of power exchange between harmonic frequencies. Typically, in nonlinear network supplied by sinusoidal source, nonlinear components absorb active power at fundamental source frequency and become sources at harmonic frequencies.

Let's define CAT at harmonic k as $H_k = \omega_k Q_k$. Under assumption of continuous voltages and currents, Table 2.2 and Table 2.3 show the P and H conditions on passive elements.

Table 2.2. *P*, *H* relations under nonsinusoidal conditions with nonlinear elements with monotone nondecreasing characteristics

	R	*L*	*C*
Active Power	$P=\sum_k P_k \geq 0$	$P=\sum_k P_k = 0$	$P=\sum_k P_k = 0$
CAT	$H=\sum_k H_k = 0$	$H=\sum_k H_k \geq 0$	$H=\sum_k H_k \leq 0$

Table 2.3. *P*, *H* relations under nonsinusoidal conditions with linear elements

	R	*L*	*C*
Active Power	$P_k \geq 0 \quad \forall k$	$P_k = 0 \quad \forall k$	$P_k = 0 \quad \forall k$
CAT	$H_k = 0 \quad \forall k$	$H_k \geq 0 \quad \forall k$	$H_k \leq 0 \quad \forall k$

The linear condition involving P_k and Q_k are well-known, from which linear condition involving H_k are straightforward. The general relations concerning *P* are imposed by conservation of energy. The general relations concerning *H* are novelty of this work; they are obtained by (2.15), (2.23), (2.29). In Table 2.2 and Table 2.3 the CAT shows a conservation property complementary in respect to active power, as *P* and *Q* do in linear sinusoidal environment. CAT states the balance rule of reactive powers across nonlinear elements with monotone nondecreasing characteristics, in this aspect fulfilling a lack in network theory. As main result, the CAT represents the constraint of exchange of reactive powers between different harmonics trough a nonlinear resistor under continuous conditions. In explicit form, from (2.15), (2.23)

$$\sum_{k=1}^{+\infty} kQ_k = 0. \tag{2.55}$$

At this purpose, the result (2.55) on nonlinear resistor is peculiar of the SAT approach. Other linear combinations of reactive powers give of course different results. In particular, Budeanu's popular definition of reactive power (1.23) [20], [23] is not zero on nonlinear resistor.

2.6.2 Discontinuous Conditions

Under discontinuous conditions, i.e. jump discontinuities occur on voltages or currents, the CAT is not exclusive of reactive elements. It is involved also by time-variant components and nonlinear resistors under discontinuities. Therefore, the above discussions about nonlinear resistors not yet apply.

A conceptual distinction must be done between time-variant elements and nonlinear elements. Nevertheless, the ideal diode, typical nonlinear resistor, can be conveniently considered an internally controlled switch [37] and as stated in section 2.5. The fact remains that the working point of the diode follows, time to time, from the circuit environment. In detail, hard switching diode transition is by rule imposed by an externally controlled switch or a discontinuous voltage or current sources. An example will be discussed in case study 6 and 7. From theoretical point of view, the SAT explains the equivalence, in this aspect, between a nonlinear resistor and a time-variant device.

The results in section 2.4.4 have a significant impact on operation principles and design of power converters, the core of which is based on connection of static switches. Under periodical steady state the CAT involved by a power converter is equal to the sum of all SPs involved by the switches of the converter in the whole period *T*, as stated by (2.44). Furthermore, under sinusoidal condition (at least) of $v(t)$ or $i(t)$, CAT reduces to (2.16). Therefore, (2.16) and (2.44) state a quantitative link between hard switching and classical reactive power in a period

$$Q = \frac{1}{2\pi} \sum_k A_{SWk} . \tag{2.56}$$

Equation (2.56) takes relevance in case a port, in which at least $v(t)$ or $i(t)$ can be regarded as sinusoidal, is connected with a switching converter, and clarifies what is experimentally known for a long time, namely that power converters are able to generate or absorb reactive power without reactive elements.

In practical applications usually passive linear reactive components are also present for filtering purpose. In such cases the CAT balance is completed by expressions (2.31). Usually, the power factor correction requests to generate a reactive power, and hence, in an active filter the total net SP should be negative (generated).

2.7 CAT as Generalized Reactive Power

Some of the features of the CAT lead to the issue of reactive powers under distorted conditions, namely

- it shows balance property;
- it reduces to reactive power in sinusoidal conditions;
- under continuous and nonlinear conditions, it is nil on resistors, nonnegative on inductors and nonpositive on capacitors;
- beside conventional compensation by reactive components, a criterion exists to compensate it by means of switching devices.

The third feature is the most stringent. This allows us to state that the CAT reproduces and extends to nonsinusoidal conditions the fundamental property of reactive power of being nil on resistors, adsorbed by inductors, and generated by capacitors. More specifically, bonds are established between harmonic reactive powers, as detailed in Table 2.2. Discussion and examples presented in the pioneering paper [45] may be translated to CAT.

Another salient result of the theory is the compensation criterion of CAT by switching devices. Nevertheless, it must be noticed that full zeroing of CAT o even the instantaneous AV, is not sufficient to achieve unity power factor.

Even if it must be recognized that no generalized power function seems to combine in itself all the properties that could useful and meaningful, as long as it is involved in reactive elements, it is a reasonable assumption to consider the CAT as a generalization of the reactive power in this sense.

As more general discussion, a recurrent features of reactive power concepts and definitions are associated with time-shift of (distorted) current waveform in respect to (distorted) voltage waveform. This phenomenon is well represented by the area on the *v*-*i* plane. Therefore, in author's opinion should be fruitful to associate to the reactive power, both in sinusoidal and distorted conditions, the idea of area on the *v*-*i* plane. Such way the CAT could become meaningful in distorted conditions with the above feature.

2.8 Matching with Some Results Presented in the Literature

The function "$p_{react,2}$" proposed in [58] as one of possible definitions of instantaneous reactive power, is the same as AV (2.1), except 1/2 coefficient. Such definition is recalled in [2], [33]. Some results presented in [58] shortly and without demonstration, are retrieved in this work, namely statements (2.16), (2.20), (2.23), and (2.29). This work demonstrates in detail and extends such results to the discontinuous case.

The AV looks also similar to the *differential reactive power* proposed in [59] with the aim of instantaneous compensation of the nonactive current.

The integral function CAT in either form of (2.9) is related to [29]−[31] and followings, as previously mentioned in the introduction.

The CAT matches an old and recurrent definition of reactive power. Firstly, [55] introduced a function similar to the second of (2.9) for the sinusoidal steady state, saying that this quantity has not a physical meaning but it is balance and easy to measure. By [60] it has been recognized as applicable to distorted conditions.

The *capacitive reactive power* proposed in [4] looks like CAT too.

Recently, the idea in [55] has been discussed and proposed again by [61], [62]. In particular, the form proposed in [61], appears as (2.21). In addition, both [60], [61] recognize the representativeness on the *v*-*i* plane.

The above authors were mainly interested in particular aspects and applications, as quantify the distortion and compensate the distorting loads. Conversely, general properties of such functions have been poorly discussed, are also remained questionable interpretations and misunderstandings in respect to nonlinear resistive elements and time-variant elements.

It is worth noting that (2.55) matches with a classical result in [63] over nonlinear resistor.

2.9 Discontinuity and Model

According to the SAT, the presence or absence of jump discontinuities leads to qualitatively different results, as different swept areas are generated. On the other hand, the discontinuities are a convenient modeling of continuous and fast patterns; though some difficulties, from a practical point of view and for measuring, can arise. However, the SAT is consistent with the discontinuities and the assumptions made in this work. The answer to this contradiction is that the SAT is applicable to the model, not to the real system. In the model the ambiguity between ideal, or not ideal discontinuity, disappears. Indeed any circuital theory is applied to a model and not to the real system. Different models can represent a given real system, on each model results may be qualitatively different, but always congruent with SAT. Provided that the modeling is correct, the overall properties are preserved.

In order to clarify this aspect, let us consider a switch. The ideal switching is a schematization of the detailed behavior in which the ubiquitous parasitic reactive elements deny the ideal jump transition. Let us compare the behavior of the ideal switch with the real one. First, let us consider the circuit shown in Fig. 2.18.

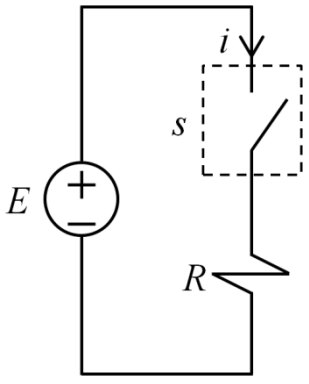

Fig. 2.18. Circuit with ideal switch and constant voltage source

Each commutation of the ideal switch produces a SP, both in opening (2.42) and closing transient (2.43), as follows

$$A_{SWopen} = -\frac{1}{2}\frac{E^2}{R} \tag{2.57}$$

$$A_{SWclosed} = \frac{1}{2}\frac{E^2}{R}. \tag{2.58}$$

The real switch would require a distributed parameter circuit, but for simplicity let us use two separate simple circuits, one for the opening commutation and the other for the closing commutation, with the only dominant stray element.

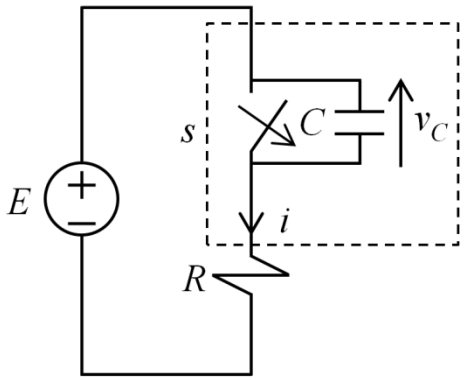

Fig. 2.19. Circuit with switch opening and stray capacitance

In Fig. 2.19 the circuit regarding the opening of the switch is shown. The transients caused by the switching are:

$$\begin{aligned} v_C(t) &= E(1-e^{-\frac{t}{RC}}) \\ i(t) &= \frac{E}{R}e^{-\frac{t}{RC}}. \end{aligned} \tag{2.59}$$

Taking into account (2.59) in (2.1), the h_C of the capacitance is obtained

$$h_C(t) = -\frac{1}{2}\frac{E^2}{R^2C}e^{-\frac{t}{RC}}.$$

Now in order to obtain the swept area, the integration of the whole opening transient is needed.

$$A_C = \int_0^\infty h_C(t)dt = -\frac{1}{2}\frac{E^2}{R} \tag{2.60}$$

Eq. (2.60) is equal to (2.57). Hence, it is possible to claim that the SP is in this case nil, as a soft switching is performed, but an area equivalent to the missing SP is generated by the capacitor. Moreover, (2.60) does not depend by the value of the capacitance, congruent with the fact that the parasitic element may be very small and unknown.

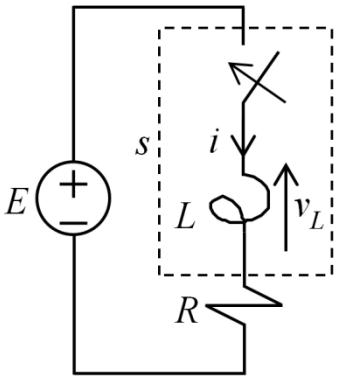

Fig. 2.20. Circuit with switch closing and stray inductance

In Fig. 2.20 the circuit regarding the closing of the switch is shown. The transients caused by the switching are:

$$\begin{aligned} i(t) &= \frac{E}{R}(1-e^{-\frac{R}{L}t}) \\ v_L(t) &= Ee^{-\frac{R}{L}t}. \end{aligned} \tag{2.61}$$

Taking into account (2.61) in (2.1), the h_L of the inductance is obtained

$$h_L(t) = \frac{1}{2}\frac{E^2}{L}e^{-\frac{R}{L}t}. \tag{2.62}$$

Now in order to obtain the swept area, the integration of the closing transient is needed.

$$A_L = \int_0^\infty h_L(t)dt = \frac{1}{2}\frac{E^2}{R} \tag{2.63}$$

Eq. (2.63) is equal to (2.58). Hence, also in this case the SP is nil, as a soft switching is performed, but an equivalent area is absorbed by the inductor, irrespective of the value of the inductance.

These cases show the equivalence between the ideal circuit and the real one with parasitic elements regarding the swept area at the external terminals of the switch. It is possible to state that the area involved by the ideal switch under hard switching is a simple schematization of the area involved by parasitic elements or by snubber circuits. The equivalence of the swept areas at external terminals also assures the equivalence of CAT in periodic conditions.

2.10 Analytical Examples

In order to validate the proposed theory and, in particular to test the balance principle and the series (2.15), some case studies will be discussed by analytical way. Meanwhile some simple applications of the theory are exposed.

2.10.1 Case 1

Let be considered the network in Fig. 2.21, composed of a sinusoidal voltage source, a nonlinear resistor and a linear inductor.

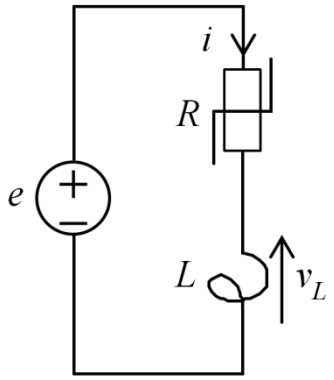

Fig. 2.21. Case1. Electric Circuit

The nonlinear resistor distorts the current, and the reactive powers at the harmonic frequencies are generated by the nonlinear resistor and absorbed by the inductor. Indeed, at the harmonic frequencies ($k > 1$), the linear inductor always absorbs reactive power, while the sinusoidal voltage generator does not give any contribution, hence the nonlinear resistor, for the balance theorem for each harmonic component, must generate harmonic reactive powers. Since the CAT absorbed by the nonlinear resistor, without discontinuity, is nil ($H_R = 0$) and according to (2.55) the following equations applies

$$\sum_{k=1}^{\infty} kQ_{Rk} = 0. \tag{2.64}$$

This way, it is possible to state that the nonlinear resistor absorbs reactive power Q_{R1} at the fundamental frequency and generates harmonic reactive powers at the harmonic frequencies ($k > 1$).

$$Q_{R1} = -\sum_{k=2}^{\infty} kQ_{Rk}. \tag{2.65}$$

The balance theorem over CAT states:

$$H_e = H_L \tag{2.66}$$

and from (2.31) it result

$$H_e = \frac{V_L^2}{L} \tag{2.67}$$

where V_L is the RMS value of the inductor voltage. The voltage source is sinusoidal, and hence, the only reactive power generated is the fundamental one and according to (2.16) it is possible to write

$$Q_e = \frac{V_L^2}{\omega L}. \tag{2.68}$$

This way, the reactive power involved by the forcing sinusoidal source is linked to the RMS value of the distorted voltage on the inductor. Then, if the balance theorem over reactive powers at the first harmonic is considered, it must be taken into account the reactive power absorbed by the nonlinear resistor, so that

$$Q_e = \frac{V_{L1}^2}{\omega L} + Q_{R1} \tag{2.69}$$

where V_{L1} is the RMS value of the first harmonic of the inductor voltage. At this frequency the forcing voltage source supplies reactive power to the inductor and to the resistor. The comparison between (2.68) and (2.69) makes evident that the increasing of the generated reactive power is linked to the distortion of voltage at the terminal of the inductor by

$$Q_{R1} = \frac{V_L^2 - V_{L1}^2}{\omega L}. \tag{2.70}$$

2.10.2 Case 2

Let be considered the network in Fig. 2.22, composed of a sinusoidal voltage source, a nonlinear resistor and a linear capacitor.

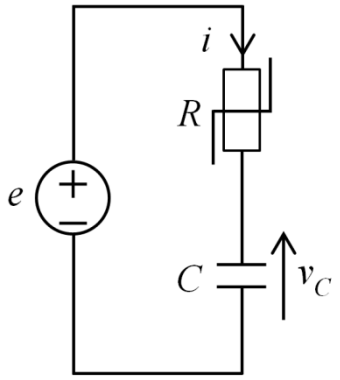

Fig. 2.22. Case 2. Electric Circuit

The nonlinear resistor distorts the current, and the reactive powers at the harmonic frequencies are absorbed by the nonlinear resistor and generated by the capacitor. Indeed, at the harmonic frequencies ($k > 1$), the linear capacitor always generates reactive power, while the sinusoidal voltage generator does not give any contribution, hence the nonlinear resistor, for the balance theorem on each harmonic component, must absorb harmonic reactive powers. Since the CAT absorbed by the nonlinear resistor, without discontinuity, is nil ($H_R = 0$), according to (2.64) it is possible to state that the nonlinear resistor generates reactive power Q_{R1} at the fundamental frequency and absorbs harmonic reactive powers at the harmonic frequencies ($k > 1$). The balance theorem over CAT states:

$$H_e = H_C \tag{2.71}$$

and from (2.31) it result

$$H_e = -\frac{I_C^2}{C} \tag{2.72}$$

where I_C is the RMS value of the capacitor current. The voltage source is sinusoidal, and hence, the only reactive power generated is the fundamental one and according to (2.16) it is possible to write

$$Q_e = -\frac{I_C^2}{\omega C}. \tag{2.73}$$

This way, the reactive power involved by the forcing sinusoidal source is linked to the RMS value of the distorted current in the capacitor. Then, if the balance theorem over reactive powers at the first harmonic is considered, it must be taken into account the reactive power absorbed by the nonlinear resistor, so that

$$Q_e = -\frac{I_{C1}^2}{\omega C} + Q_{R1} \tag{2.74}$$

where I_{C1} is the RMS value of the first harmonic of the capacitor current. At this frequency the forcing voltage source absorbs reactive power from the capacitor and supplies to the resistor. The comparison between (2.73) and (2.74) makes evident that the increasing of the generated reactive power is linked to the distortion of current in the capacitor by

$$Q_{R1} = -\frac{I_C^2 - I_{C1}^2}{\omega C}. \tag{2.75}$$

2.10.3 Case 3

This case shows how the ideal switch can absorb/generate reactive power. The circuit depicted in Fig. 2.23 is fed by a sinusoidal voltage source $e(t) = E\sin(\omega t)$, ($\omega = 2\pi/T$).

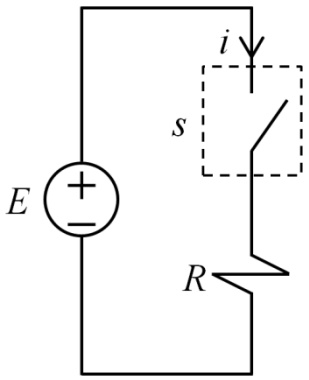

Fig. 2.23. Case 3. Switched resistor

The ideal switch s commutates periodically in each semi period as depicted in Fig. 2.24, where α and β are, respectively, the closing and opening switching angles. According to (2.42), (2.43) the CAT absorbed by the switch is

$$H_{SW} = \frac{1}{T}\left(\frac{E^2\sin^2(\alpha)}{R} - \frac{E^2\sin^2(\beta)}{R}\right). \tag{2.76}$$

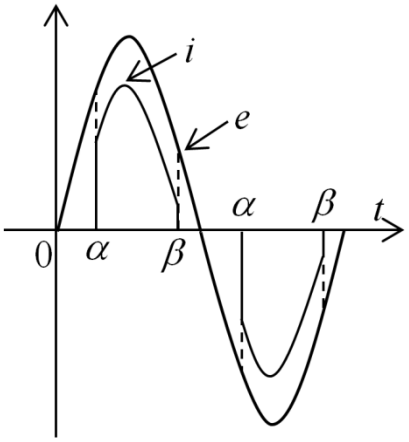

Fig. 2.24. Case 3. Sinusoidal voltage source

Since the CAT of the linear resistor is nil, the CAT H_e generated by e is equal to the CAT absorbed by the ideal switch. Moreover, as e is sinusoidal, only the first component of reactive power is generated by e, yielding

$$Q_e = \frac{H_e}{\omega} = \frac{H_{SW}}{\omega} = \frac{E^2}{2\pi R}\left(\sin^2(\alpha) - \sin^2(\beta)\right). \tag{2.77}$$

By equation (2.77) it is possible to obtain in a simple analytical way the relation between commutation instants α, β and the reactive power. Note that the result is not limited to $\alpha < \beta$. Furthermore, the (2.77) could also be deduced in a standard way by a Fourier analysis of the current waveform. Indeed, according to (2.10) the fundamental harmonic component of voltage source e is

$$\boldsymbol{E}_1 = -j\frac{E}{2} \tag{2.78}$$

and the fundamental harmonic component of current i is

$$\boldsymbol{I}_1 = \frac{E}{2R\pi}\left[\sin^2(\beta) - \sin^2(\alpha) - j(\sin(2\alpha) - \sin(2\beta) + \beta - \alpha)\right]. \tag{2.79}$$

Taking into account (2.78) and (2.79) in (2.14), the reactive power is as follows

$$Q_e = 2\,\mathrm{Im}(\boldsymbol{E}_1\boldsymbol{I}_1^*) = \frac{E^2}{2\pi R}\left(\sin^2(\alpha) - \sin^2(\beta)\right). \tag{2.80}$$

Equation (2.80) gives the same result of (2.77). Meanwhile SAT gets the (2.77) in a straightforward and concise mode.

Relation (2.77) reveals a meaningful result. As particular case in which α or β are zero, when only forced closing commutation takes place, the sign of reactive power is necessary positive and vice versa. It means that in order to generate reactive power, a switching device with hard opening capability is mandatory.

2.10.4 Case 4

The purpose of this example is to verify the relationship between switching and series (2.15) in very simplified conditions. The theory also leads to predict a surprising piecewise constant behavior of the series (2.15) in function of switching timing. Let us consider the circuit depicted in Fig. 2.25 under periodical steady state of period T.

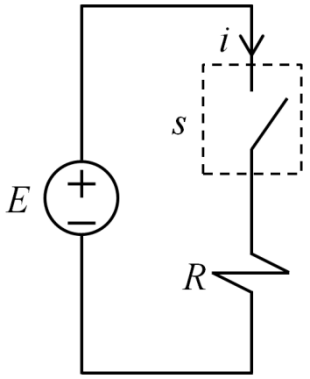

Fig. 2.25. Case 4. Circuit with ideal switch and square waveform voltage source

Let $e(t)$ be a two level square waveform with a generic duty-cycle as shown in Fig. 2.26. For the sake of simplicity the transitions occur at the time $-t_A$ and $+t_A$. Let us assume that the ideal switch periodically commutes twice inside the period T, one switch-on at time t_{ON} and one switch-off at time t_{OFF} ($t_{ON} < t_{OFF}$). Since R is a linear resistor, just the ideal switch can be exchange CAT with the voltage source.

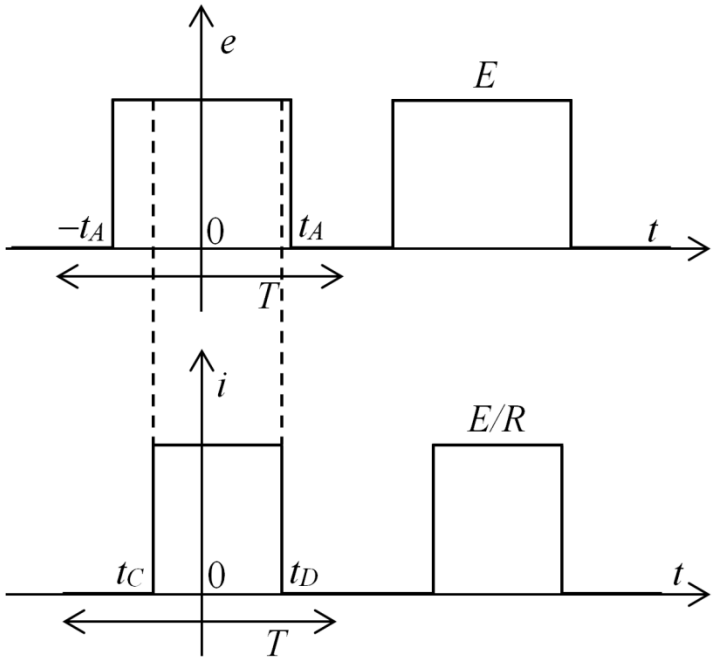

Fig. 2.26. Case 4. Square waveform of voltage and current sources

Let us analyze these cases:

1) if $t_{ON} < -t_A$ and $t_{OFF} > -t_A$ the current presents a jump at the time $-t_A$ simultaneously to the voltage. The linear segment 1 of Fig. 2.27 is tracked. There is a soft switching commutation of the switch $A_{SWclosed} = 0$.

2) if $-t_A < t_{ON} < +t_A$ the current presents a jump at the time t_{ON}. The linear segment 2 of Fig. 2.27 is tracked. There is an hard switching commutation of the switch and according to (2.43) it has $A_{SWclosed} = E^2/(2R)$;

3) if $-t_A < t_{OFF} < +t_A$ the current presents a jump at the time t_{OFF}. The linear segment 3 of Fig. 2.27 is tracked. There is an hard switching commutation of the switch and according to (2.42) it has $A_{SWopen} = E^2/(2R)$;

4) if $t_{OFF} > t_A$ and $t_{ON} < t_A$ the current presents a jump at the time t_A simultaneously to the voltage. The linear segment 4 of Fig. 2.27 is tracked. There is a soft switching commutation of the switch $A_{SWopen} = 0$.

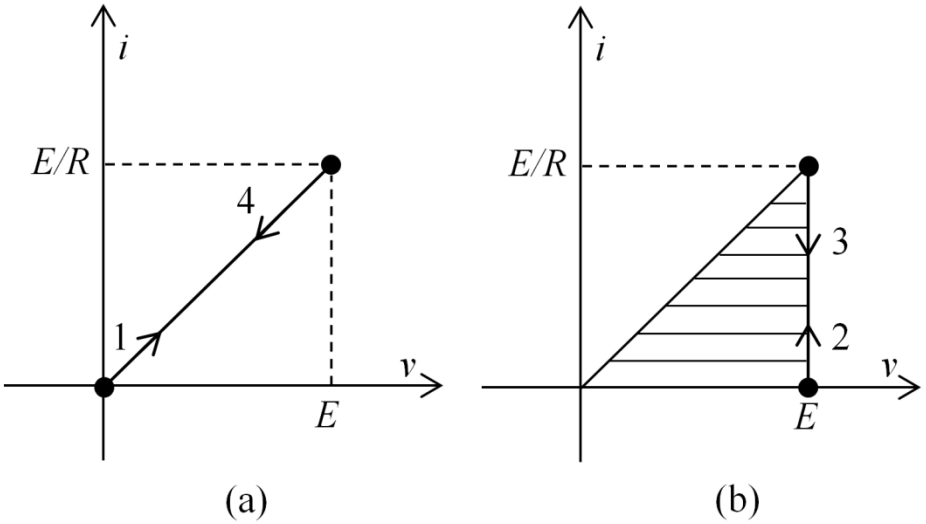

Fig. 2.27. Case 4. Voltage source swept areas

On the period T four meaningful combinations are possible, as in Table 2.4, first column. The further cases $t_{ON} < t_{OFF} < -t_A$ and $t_A < t_{ON} < t_{OFF}$ imply a nil current waveform and are trivial. The current is a square waveform as depicted in Fig. 2.26 with the constrains: $t_C \geq -t_A$ and $t_D \leq t_A$. The resulting CAT of voltage source is

$$H_e = \frac{A_{SWclosed} + A_{SWopen}}{T}.$$

The four cases are reported in Table 2.4, columns two and three. The same results should be found from the Fourier series expansions of the voltage and current sources (Fig. 2.26):

$$v(t) = E\left[\frac{\alpha}{\pi} + \frac{2}{\pi}\sum_{k=1}^{\infty}\frac{\sin(k\alpha)\cos(k\omega t)}{k}\right], \alpha = \pi\frac{2t_A}{T} \tag{2.81}$$

$$i(t) = \frac{E}{R}\left[\frac{\beta}{\pi} + \frac{2}{\pi}\sum_{k=1}^{\infty}\frac{\sin(k\beta)\cos(k\omega t - k\varphi)}{k}\right],$$
$$\beta = \pi\frac{t_D - t_C}{T}, \quad \varphi = \pi\frac{t_D + t_C}{T}. \tag{2.82}$$

According to (2.14) and taking into account (2.15)

$$H_e = \frac{E^2}{R}\frac{4}{\pi T}\sum_{k=1}^{\infty}\frac{\sin(k\alpha)\sin(k\beta)\sin(k\varphi)}{k}. \tag{2.83}$$

Substituting into (2.83) the value of β and φ (2.82) and according to trigonometric formulas, the (2.83) becomes (2.84).

$$H_e = \frac{E^2}{R}\frac{2}{\pi T}\sum_{k=1}^{\infty}\frac{\sin(k\alpha)\left[\cos(k\omega t_C)-\cos(k\omega t_D)\right]}{k} \tag{2.84}$$

In order to demonstrate analytically the convergence, it is possible to rewrite (2.84) in this way

$$H_e = \frac{E^2}{RT}(a-b) \tag{2.85}$$

where

$$\begin{aligned} a &= \frac{\alpha}{\pi}+\frac{2}{\pi}\sum_{k=1}^{\infty}\frac{1}{k}\sin(k\alpha)\cos(k\omega t_C) \\ b &= \frac{\alpha}{\pi}+\frac{2}{\pi}\sum_{k=1}^{\infty}\frac{1}{k}\sin(k\alpha)\cos(k\omega t_D). \end{aligned} \tag{2.86}$$

Now it is possible to recognize that the two series (2.86) are the Fourier expansions of the square waveform of Fig. 2.26 of unitary amplitude and evaluated at times t_C and t_D. The values of a and b related to the four combination depicted in Table 2.4, second column, are provided by Fig. 2.26 and reported in the fourth column. Taking into account (2.85) it is straightforward to recognize that the values of column three are retrieved. Such way the equivalence between the series (2.83) and the CAT evaluated form Fig. 2.27 is confirmed.

Table 2.4. Case 4. Switching Combinations

Switching $t_{ON} < t_{OFF}$	Current	CAT	a, b
$-t_A < t_{ON} < +t_A$ $-t_A < t_{OFF} < +t_A$	$-t_A < t_C < +t_A$ $-t_A < t_D < +t_A$	$H = 0$	$a = 1$ $b = 1$
$-t_A < t_{ON} < +t_A$ $t_{OFF} \geq +t_A$	$-t_A < t_C < +t_A$ $t_D = +t_A$	$H=E^2/(2RT)$	$a = 1$ $b = 1/2$
$t_{ON} \leq -t_A$ $-t_A < t_{OFF} < +t_A$	$t_C = -t_A$ $-t_A < t_D < +t_A$	$H=-E^2/(2RT)$	$a = 1/2$ $b = 1$
$t_{ON} \leq -t_A$ $t_{OFF} \geq +t_A$	$t_C = -t_A$ $t_D = +t_A$	$H = 0$	$a = 1/2$ $b = 1/2$

Note the unusual result. The series (2.83) is obtained by the Fourier series of square waves of Fig. 2.26. Due to the particular relationship between the square waves, the limit of the series is constituted by constant values separated by jump discontinuities; inside the constant intervals the limit is independent from the $v(t)$ and $i(t)$ wave shapes.

2.10.5 Case 5

This case considers standard single-phase Thyristor-Controlled Reactor for reactive power regulation. The circuit depicted in Fig. 2.28 is composed of a sinusoidal voltage source $e(t) = E\cos(\omega t)$, ($\omega = 2\pi/T$), a linear inductor L and an ideal switch s, which in industrial application models two antiparallel thyristors.

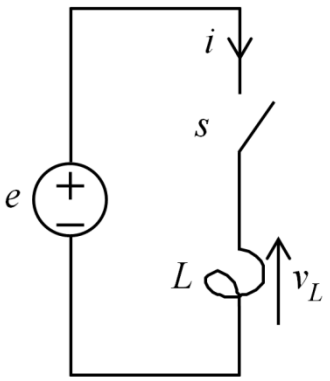

Fig. 2.28. Case 5. Tyristor-controlled reactor

α is the control angle as depicted in Fig. 2.29.

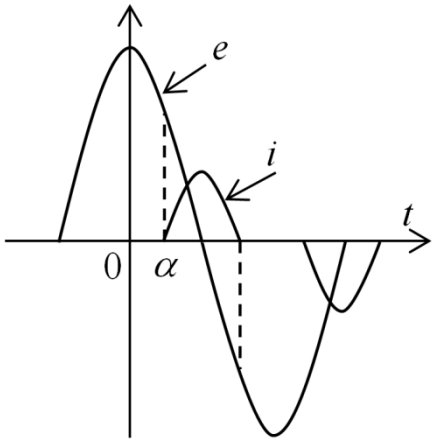

Fig. 2.29. Case 5. Voltage and current sources

As the switch opens and closes when the current is nil, only soft switching commutations occur. In this way the CAT absorbed by the switch is nil and the CAT absorbed by the inductor is equal to the CAT generated by e. According to (2.31) and Fig. 2.29, the CAT on reactor is:

$$H_L = \frac{1}{\pi L}\left(\int_{\alpha}^{\pi-\alpha} (E\cos(\omega t))^2 d(\omega t)\right) = \frac{E^2}{2L}(1-\alpha\frac{2}{\pi}-\frac{1}{\pi}\sin(2\alpha)) \tag{2.87}$$

and according to (2.16) Q_e is

$$Q_e = \frac{H_e}{\omega} = \frac{H_L}{\omega} = \frac{E^2}{2\omega L}(1-\alpha\frac{2}{\pi}-\frac{1}{\pi}\sin(2\alpha)). \tag{2.88}$$

Also in this case, (2.88) could be obtained from standard Fourier analysis of the current [64]. Indeed, according to [64] the amplitude of the fundamental current *i* can be expressed as a function of angle α

$$I_1 = \frac{E}{\omega L}(1 - \alpha\frac{2}{\pi} - \frac{1}{\pi}\sin(2\alpha)). \tag{2.89}$$

The fundamental current lags the voltage source by 90 degree. Consequently, the reactive power at the fundamental harmonic component generated by *e* can be calculated as

$$Q_e = \frac{1}{2}EI = \frac{E^2}{2\omega L}(1 - \alpha\frac{2}{\pi} - \frac{1}{\pi}\sin(2\alpha)) \tag{2.90}$$

giving the same result of (2.88). Hence, the SAT yields (2.88) in a simpler way without the need of explicit current waveform.

2.10.6 Case 6

This is an another example analyzed in order to verify the relationship between switching and series (2.15) in conditions similar to the Case 4 but with a general sawtooth waveform. The circuit is depicted in Fig. 2.30 and shows a sawtooth voltage source in series to an ideal diode and a linear resistor.

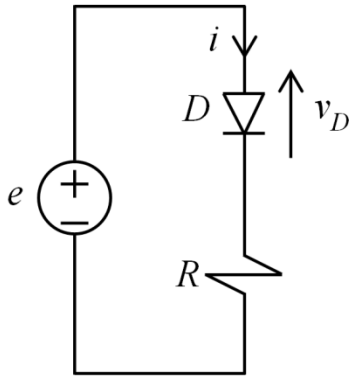

Fig. 2.30. Case 6. Circuit with a series of ideal diode, linear resistor, and a sawtooth voltage source

There are two cases: 1) no discontinuity in the waveform; 2) presence of discontinuities in the waveform when one of the two ramps becomes of infinite slope. In both cases the CAT absorbed by the linear resistor is nil according to (2.23).

1) No discontinuity

Let us start to suppose the waveform depicted in Fig. 2.31 where there is no discontinuity.

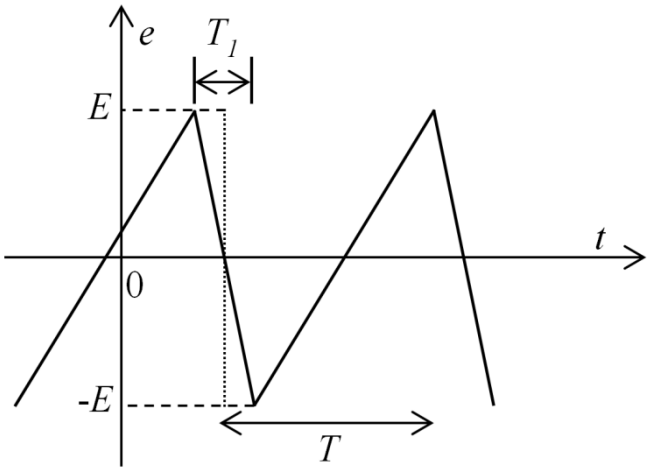

Fig. 2.31. Case 6. Sawtooth waveform without discontinuity

Being defined $\gamma = T_1/T$ the following complex Fourier expansion hold:

$$e(t) = \sum_{k=-\infty}^{\infty} \boldsymbol{E}_k e^{jk\omega t} \qquad \boldsymbol{E}_k = (-1)^k \frac{jE}{\pi^2 k^2} \frac{sin(k\pi\gamma)}{\gamma(1-\gamma)} \tag{2.91}$$

$$v_R(t) = \sum_{k=-\infty}^{\infty} \boldsymbol{V}_{Rk} e^{jk\omega t} \qquad \boldsymbol{V}_{Rk} = \frac{E}{2\pi^2 k^2} \frac{(-1)^k e^{jk\pi\gamma} - \gamma - (-1)^k (1-\gamma)}{\gamma(1-\gamma)} \tag{2.92}$$

$$v_D(t) = \sum_{k=-\infty}^{\infty} \boldsymbol{V}_{Dk} e^{jk\omega t} \qquad \boldsymbol{V}_{Dk} = \frac{E}{2\pi^2 k^2} \frac{\gamma + (-1)^k (1-\gamma) - (-1)^k e^{-jk\pi\gamma}}{\gamma(1-\gamma)} \tag{2.93}$$

$$i(t) = \frac{v_R(t)}{R} = \sum_{k=-\infty}^{\infty} \boldsymbol{I}_k e^{jk\omega t} \qquad \boldsymbol{I}_k = \frac{E}{2R\pi^2 k^2} \frac{\gamma + (-1)^k (1-\gamma) - (-1)^k e^{-jk\pi\gamma}}{\gamma(1-\gamma)}. \tag{2.94}$$

According to (2.14) the reactive power for each harmonic frequency of the voltage source is

$$Q_{ek} = 2\,\mathrm{Im}(\boldsymbol{E}_k \boldsymbol{I}_k^*) = \frac{E^2}{2R\pi^4 \gamma^2 (1-\gamma)^2 k^4} \mathrm{Im}\left\{\left[\gamma + (-1)^k (1-\gamma) - (-1)^k e^{-jk\pi\gamma}\right]^2\right\}. \tag{2.95}$$

According to (2.15) the CAT generated by the source is

$$\begin{aligned} H_e &= \sum_{k=1}^{\infty} k\omega Q_k = \frac{\omega E^2}{2R\pi^4 \gamma^2 (1-\gamma)^2} \sum_{k=1}^{\infty} \frac{1}{k^3} \left\{sin(2k\pi\gamma) - 2\left[1 - \gamma(1-(-1)^k)\right] sin(k\pi\gamma)\right\} = \\ &= \frac{\omega E^2}{2R\pi^4 \gamma^2 (1-\gamma)^2} \left(\sum_{k=1}^{\infty} \frac{1}{k^3} \left\{sin(2k\pi\gamma) - 2sin(k\pi\gamma)\right\} + 4\gamma \sum_{\substack{k=1 \\ ODD}}^{\infty} \frac{sin(k\pi\gamma)}{k^3} \right). \end{aligned} \tag{2.96}$$

For the linear resistor the CAT is nil $H_R = 0$, indeed

$$Q_{Rk} = 2\,\mathrm{Im}(\boldsymbol{V}_{Rk} \boldsymbol{I}_k^*) = 2\,\mathrm{Im}(\boldsymbol{V}_{Rk} \frac{\boldsymbol{V}_{Rk}^*}{R}) = 0. \tag{2.97}$$

Hence, the reactive power absorbed by the ideal diode is equal to the one generated by the voltage source

$$Q_{Dk} = 2\,\mathrm{Im}(\boldsymbol{V}_{Dk}\boldsymbol{I}_k^*) = Q_{ek}. \tag{2.98}$$

Therefore, also the CAT absorbed by the ideal diode is equal to the one generated by the source

$$H_D = H_e. \tag{2.99}$$

Now, it is possible to rewritten the (2.96) as

$$H_e = \frac{\omega E^2}{2R\pi^4\gamma^2(1-\gamma)^2}\left[\sum_{k=1}^{\infty}\frac{sin(2k\pi\gamma)}{k^3} - 2\sum_{k=1}^{\infty}\frac{sin(k\pi\gamma)}{k^3} + 4\gamma\sum_{\substack{k=1\\odd}}^{\infty}\frac{sin(k\pi\gamma)}{k^3}\right]. \tag{2.100}$$

According to [65]

$$\sum_{k=1}^{\infty}\frac{sin(kx)}{k^3} = \frac{x}{12}(x-\pi)(x-2\pi)$$

the first two terms of (2.100) converge to

$$\begin{aligned}\sum_{k=1}^{\infty}\frac{sin(k\pi\gamma)}{k^3} &= \frac{\pi\gamma}{12}(\pi\gamma-\pi)(\pi\gamma-2\pi) = \frac{\pi^3\gamma}{12}(\gamma-1)(\gamma-2)\\ \sum_{k=1}^{\infty}\frac{sin(2k\pi\gamma)}{k^3} &= \frac{2\pi\gamma}{12}(2\pi\gamma-\pi)(2\pi\gamma-2\pi) = \frac{\pi^3\gamma}{3}(2\gamma-1)(\gamma-1).\end{aligned} \tag{2.101}$$

According to [66]

$$\sum_{\substack{k=1\\odd}}^{\infty}\frac{sin(kx)}{k^3} = \frac{\pi}{8}x(\pi-x)$$

the last term of (2.100) converges to

$$\sum_{\substack{k=1\\odd}}^{\infty}\frac{sin(k\pi\gamma)}{k^3} = \frac{\pi}{8}\pi\gamma(\pi-\pi\gamma) = -\frac{\pi^3}{8}\gamma(\gamma-1). \tag{2.102}$$

Finally, taking into account (2.101) and (2.102), the (2.100) converges to zero, indeed

$$H_e = \frac{\omega E^2}{2R\pi^4\gamma^2(1-\gamma)^2}\frac{\pi^3\gamma}{6}(\gamma-1)\left[(\gamma-2)-2(2\gamma-1)+3\gamma\right] = 0.$$

This example shows that if there are no discontinuity in the waveform ($\gamma \neq 0$) the CAT involved in the circuit is nil.

2) Presence of discontinuities

Let us tend γ to zero. In this way a discontinuity appears in the waveform, as depicted in Fig. 2.32.

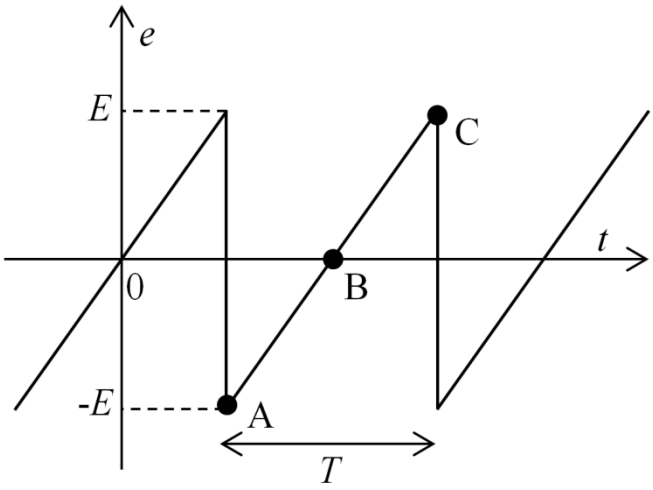

Fig. 2.32. Case 6. Sawtooth waveform with discontinuity

Equations (2.91)–(2.94) become

$$e(t)=\sum_{k=-\infty}^{\infty}\boldsymbol{E}_k e^{jk\omega t}\qquad \boldsymbol{E}_k=E\frac{j(-1)^k}{\pi k} \tag{2.103}$$

$$v_R(t)=\sum_{k=-\infty}^{\infty}\boldsymbol{V}_{Rk} e^{jk\omega t}\qquad \boldsymbol{V}_{Rk}=E\frac{1}{2\pi^2k^2}\left[(-1)^k(1+j\pi k)-1\right] \tag{2.104}$$

$$v_D(t)=\sum_{k=-\infty}^{\infty}\boldsymbol{V}_{Dk} e^{jk\omega t}\qquad \boldsymbol{V}_{Dk}=E\frac{1}{2\pi^2k^2}\left[1-(-1)^k(1-j\pi k)\right] \tag{2.105}$$

$$i(t)=\frac{v_R(t)}{R}=\sum_{k=-\infty}^{\infty}\boldsymbol{I}_k e^{jk\omega t}\qquad \boldsymbol{I}_k=\frac{E}{R}\frac{1}{2\pi^2k^2}\left[(-1)^k(1+j\pi k)-1\right]. \tag{2.106}$$

From the above expressions the reactive power generated by the source is

$$Q_{ek}=2\,\mathrm{Im}(\boldsymbol{E}_k\boldsymbol{I}_k^*)=\frac{E^2}{R}\frac{1-(-1)^k}{\pi^3k^3} \tag{2.107}$$

and the CAT of the voltage source is

$$H_e=\frac{E^2}{R}\frac{\omega}{\pi^3}\sum_{k=1}^{\infty}\frac{1-(-1)^k}{k^2}. \tag{2.108}$$

The CAT absorbed by the resistor is nil and then the following expression can be written

$$Q_{Dk}=2\,\mathrm{Im}(\boldsymbol{V}_{Dk}\boldsymbol{I}_k^*)=Q_{ek} \tag{2.109}$$

$$H_D = H_e. \tag{2.110}$$

The following series converges to

$$\sum_{k=1}^{\infty} \frac{1-(-1)^k}{k^2} = \frac{\pi^2}{4}$$

from which a not zero value of CAT generated by the voltage source and adsorbed by the ideal diode appears

$$H_D = H_e = \frac{E^2}{R}\frac{\omega}{4\pi} = \frac{1}{2}\frac{E^2}{RT}. \tag{2.111}$$

From (2.111) it is possible to recognize

$$A_D = A_e = \frac{1}{2}\frac{E^2}{R} \tag{2.112}$$

where A_D and A_e are the SPs depicted in Fig. 2.33. Therefore, the (2.111) is equal to the ratio of the swept area A_e (2.112) on the period T. This example shows that if a discontinuity appears in the waveform ($\gamma = 0$) the CAT involved in the circuit is no longer zero. Moreover, the balance property of the CAT in a nonlinear resistor under discontinuous conditions and the equivalence between the area on the *v-i* plane and the series (2.15) are shown.

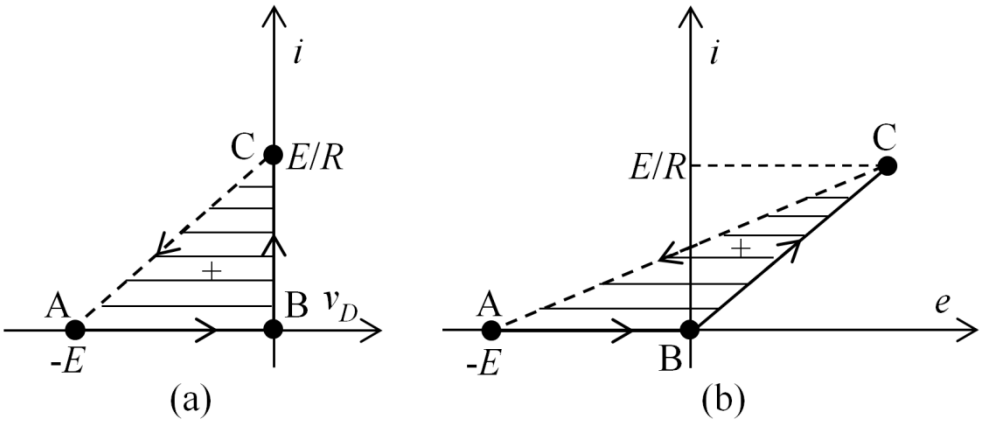

Fig. 2.33. Case 6. (a) Ideal diode; (b) Voltage source

2.10.7 Case 7

The buck converter in Fig. 2.34 is composed of an on-off controlled valve (GTO or IGBT) and a diode. This case is discussed in detail in order to examine the behavior of the diode and to recognize the balance property of CAT. Moreover, the series (2.15) is evaluated.

In order to achieve results in simpler analytical form, all parasitic resistances are neglected and both the voltage source E and the output voltage V_o are assumed as constant.

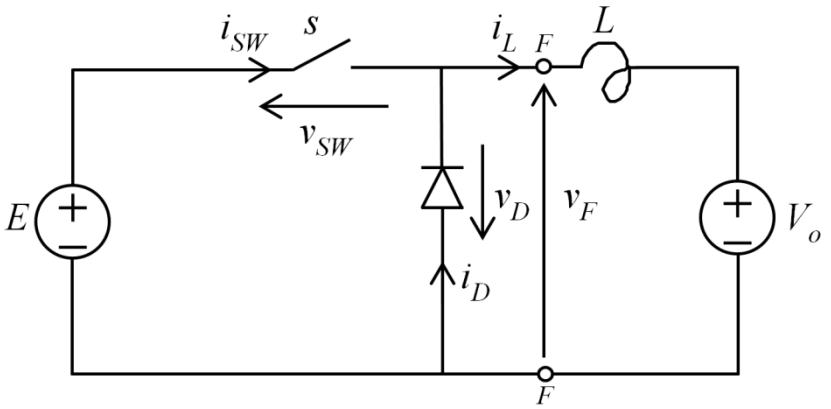

Fig. 2.34. Case 7. Buck converter

Continuous conduction mode

Provided that $E > V_o$, in steady state continuous conduction mode the current and the voltage are depicted in Fig. 2.35. At time t_A the controlled valve is switched off. According to (2.42) and Fig. 2.12, a SP appears on controlled valve

$$A_{SWopen} = -\frac{1}{2} E I_A. \tag{2.113}$$

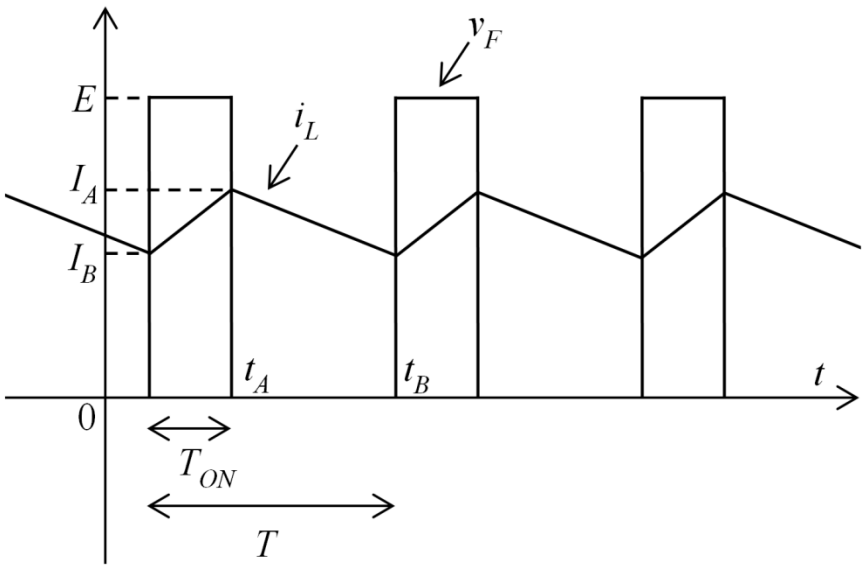

Fig. 2.35. Case 7. Continuous conduction mode

Because of continuity of inductance current, the diode turns from off to on condition. Such transition involves discontinuities both in the voltage and in the current. Therefore, the diode gives rise to a SP of the same sign (counterclockwise) and equal to (2.113), $A_{Dclose} = A_{SWopen}$.

Similarly, on transition at time t_B, the controlled valve is fired and the diode is forced off. The (2.43) and Fig. 2.13 apply on controlled valve, whereas on the diode an equal SP takes place

$$A_{SWclose} = A_{Dopen} = \frac{1}{2} E I_B. \tag{2.114}$$

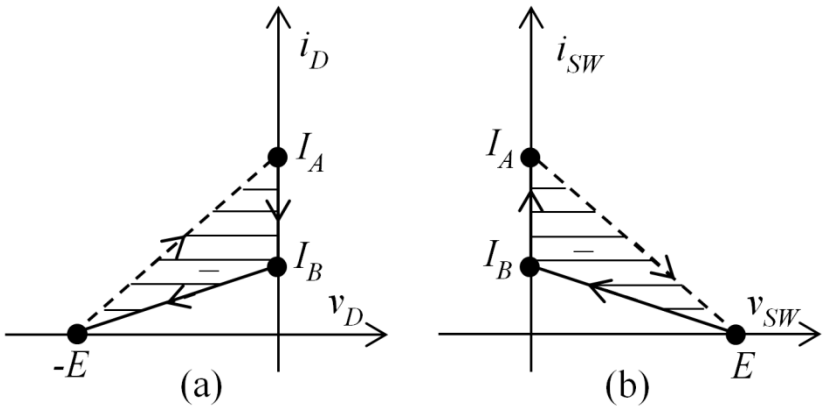

Fig. 2.36. Case 7. Swept areas (a) on diode and (b) controlled valve

Transitions in one switching period and the swept areas generated by the diode and the controlled valve are depicted in Fig. 2.36. Note that in either transition, the diode presents a jump across its nonlinear characteristic, therefore, as previously stated in section 2.5, it looks like a switch in hard switching giving a contribution on SP. Nevertheless, the diode hard switching is caused by an external device, in this case the controlled valve.

From (2.44), the total CAT in one period T caused by switching is

$$H_{SWtot} = \frac{A_{SWDclose} + A_{SWIopen} + A_{SWIclose} + A_{SWDopen}}{T} = \frac{E\left(I_B - I_A\right)}{T}. \tag{2.115}$$

The (2.115) is negative, therefore generated.

It is possible now to verify the balance property of CAT. The CAT is nil on the dc generator and load terminal, because of constant voltages. The only significant CAT are on the switch, diode and on inductance. The swept area at FF terminals in a period T, depicted in Fig. 2.37, can be deduced graphically from Fig. 2.35. As first balance result, the area in Fig. 2.37 is the sum of areas in Fig. 2.36 (taking into account reference directions). It represents the swept area generated by the buck converter and corresponds to CAT (2.115). According to (2.31) the CAT on the inductance depends on voltage RMS V_L. By condition that the voltage across the inductance is of zero average on steady state, it results

$$H_L = \frac{E\left(E - V_o\right)}{L}\frac{T_{ON}}{T}. \tag{2.116}$$

Finally, the current ripple is imposed by the voltage levels

$$I_A - I_B = \frac{T_{ON}}{L}\left(E - V_o\right). \tag{2.117}$$

From (2.115), (2.116), (2.117), the overall balance property of CAT is verify

$$H_{SWtot} + H_L = 0. \tag{2.118}$$

The equivalence (2.15) is now addressed.

Let us calculate the CAT at buck terminals FF. The Fourier series of voltage and current at these terminals are

$$v_F(t) = V_o + E\frac{2}{\pi}\sum_{k=1}^{\infty}\frac{\sin(k\pi\delta)\cos(k\omega t)}{k} \tag{2.119}$$

$$i(t) = \frac{I_A + I_B}{2} + \frac{I_A - I_B}{\pi^2\delta(1-\delta)}\sum_{k=1}^{\infty}\frac{\sin(k\pi\delta)\sin(k\omega t)}{k^2} \tag{2.120}$$

where $\delta = T_{ON}/T$ is the duty-cycle. From (2.15) and (2.119), (2.120) the CAT at FF terminals is obtained.

$$H_{FF} = \omega E\frac{I_A - I_B}{\pi^3\delta(1-\delta)}\sum_{k=1}^{\infty}\frac{\sin^2(k\pi\delta)}{k^2} \tag{2.121}$$

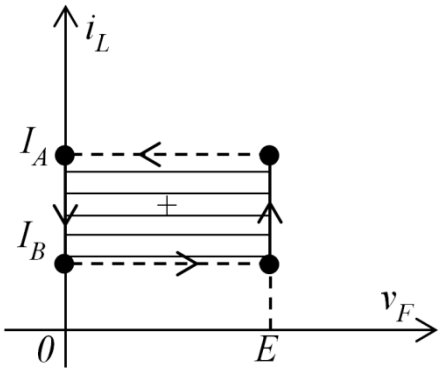

Fig. 2.37. Case 7. Swept area at FF terminals

In order to evaluate the series (2.121), the known Fourier expansion of the function $f(x) = x(\pi - x)$ $0 \le x \le \pi$ is considered

$$f(x) = \frac{\pi^2}{6} - \sum_{k=1}^{\infty}\frac{\cos(2kx)}{k^2}. \tag{2.122}$$

Taking into account (2.122), from (2.121) it follows

$$\sum_{k=1}^{\infty}\frac{\sin^2(k\pi\delta)}{k^2} = \frac{1}{2}\sum_{k=1}^{\infty}\frac{1-\cos(2k\pi\delta)}{k^2} = \frac{1}{2}\left[-f(0) + f(\pi\delta)\right] = \frac{\pi^2}{2}\delta(1-\delta) \tag{2.123}$$

Finally, replacing (2.123) in (2.121), the opposite of (2.115) is obtained. Therefore, the equivalence (2.15) is verified.

Discontinuous conduction mode

The current and the voltage are depicted in Fig. 2.38. As long as the switching is concerned, only switching at time t_A is an hard switching. Consequently the CAT is given by (2.115) with $I_B = 0$. Also (2.116), (2.117) are still valid under $I_B = 0$ and T_{ON} referred to Fig. 2.38. Therefore, the balance relation (2.118) is confirmed.

The graphical approach is of great aid to recognize the relation between continuous and discontinuous mode. From Fig. 2.38 plots similar to Fig. 2.36 and Fig. 2.37 are deduced, with the only difference $I_B = 0$. The time interval in which the current i_L stay at zero in discontinuous mode,

gives rise to a point of stop on the abscissas in Fig. 2.36 and Fig. 2.37, with no impact on swept areas and values of CATs.

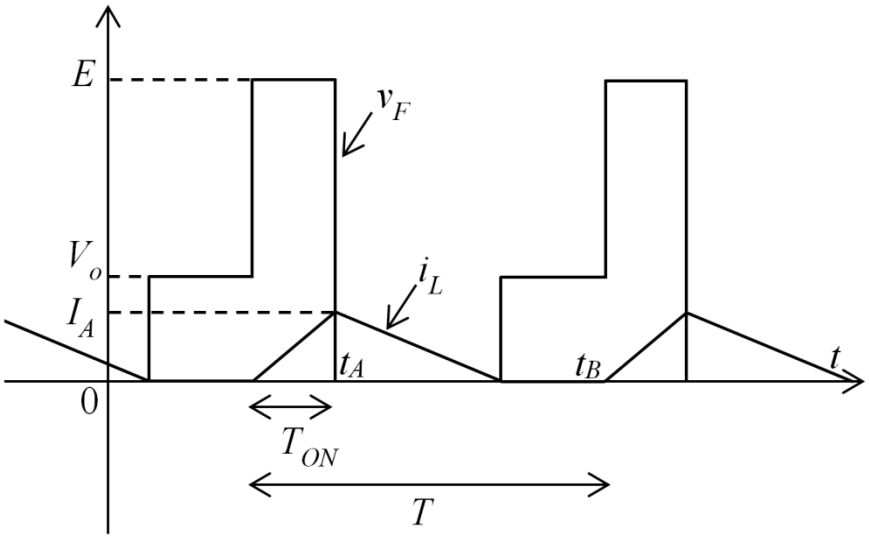

Fig. 2.38. Case 7. Discontinuous conduction mode

As concluding discussion, the buck converter has shown the balance property of the CAT and the equivalence between the CAT and the series (2.15). Moreover, this example shows that the contribution of SP by the diode is necessary for the correct CAT balance. More generally, it confirms the assumption that a jump discontinuity over a nonlinear resistor gives rise to an impulsive area on AV and the related contribution on CAT, as in Fig. 2.6.

2.10.8 Case 8

The goal of this case is to verify the relation between the reactive power at the ac terminals and the hard switching commutations in a typical industrial application. Let us consider a well-known basic topology, called Power Electronic Building Block (PEBB) [67], [68] as shown in Fig. 2.39. This scheme generalizes the valve layout of the buck converter to fully bidirectional switches. PEBBs are constituent, e.g., of bridge single-phase converter or three-phase voltage source converter.

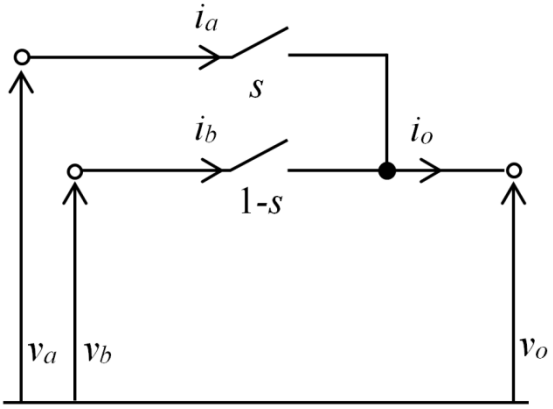

Fig. 2.39. Case 8. Electric circuit of PEBB

The two switching functions are forced in complementary state. Therefore, the state of the switches can be identified by a single switch variable $s(t) = 0,1$. The constitutive relations are the following

$$\begin{aligned} v_o &= v_b + s(v_a - v_b) \\ i_a &= s i_o \\ i_b &= (1-s) i_o. \end{aligned} \tag{2.124}$$

However, it is possible to find the expression of the total SP absorbed by PEBB in two ways: 1) applying the balance principle and summing the contributions of each ideal switch; 2) considering the whole system as a three-port component. The latter will be deeply dealt with in chapter 3. Let us follow both paths and verify the balance principle.

1) Considering each contribution of the switches

On transition $s = 0 \rightarrow 1$ (switch *a* closes, switch *b* opens) at generic time t^*, it is convenient to define a collective Switching Power as $A_{SW1} = A_{SWclosed(a)} + A_{SWopen(b)}$. Similarly, on transition $s = 1 \rightarrow 0$ (switch *a* opens, switch *b* closes) the collective Switching Power is $A_{SW0} = A_{SWopen(a)} + A_{SWclosed(b)}$. From (2.42), (2.43) and taking into account the scheme in Fig. 2.39, it results

$$\begin{aligned} A_{SW1} &= i_o(t^*)[v_a(t^*) - v_b(t^*)] \quad transition\ 0 \rightarrow 1 \\ A_{SW0} &= i_o(t^*)[v_b(t^*) - v_a(t^*)] \quad transition\ 1 \rightarrow 0. \end{aligned} \tag{2.125}$$

2) Considering the whole system as a three-port element

The (2.1) can be extended to *n* port component as the sum of *h(t)* relatives to each port. In this case, according to (2.1) the $h_{SW}(t)$ absorbed by the PEBB is

$$h_{SW}(t) = \frac{1}{2}\left(-v_o \frac{di_o}{dt} + i_o \frac{dv_o}{dt} + v_a \frac{di_a}{dt} - i_a \frac{dv_a}{dt} + v_b \frac{di_b}{dt} - i_b \frac{dv_b}{dt} \right). \tag{2.126}$$

Taking into account (2.124) into (2.126), it yields

$$h_{SW}(t) = (v_a - v_b) i_o \delta(t). \tag{2.127}$$

According to the kind of transition ($0 \rightarrow 1$, $1 \rightarrow 0$), the (2.127) yields the same result of (2.125), and hence, the balance theorem over AV is verified. Furthermore, being the PEBB a three-port element, for each port it is possible to draw the trajectories followed by the voltage and current. In Fig. 2.40 on the *v-i* planes are depicted the trajectories and the swept areas when *s* switches from 0 to 1. Note that the trajectory of the port *o* of Fig. 2.40 has the reference directions opposed to the other ports. In this case the sum of the three swept areas is equal to the A_{SW1}. In the opposite case, when *s* switches from 1 to 0, the trajectories are reversed and the sum of the areas is equal to A_{SW0}. In either switching the balance property is recognized.

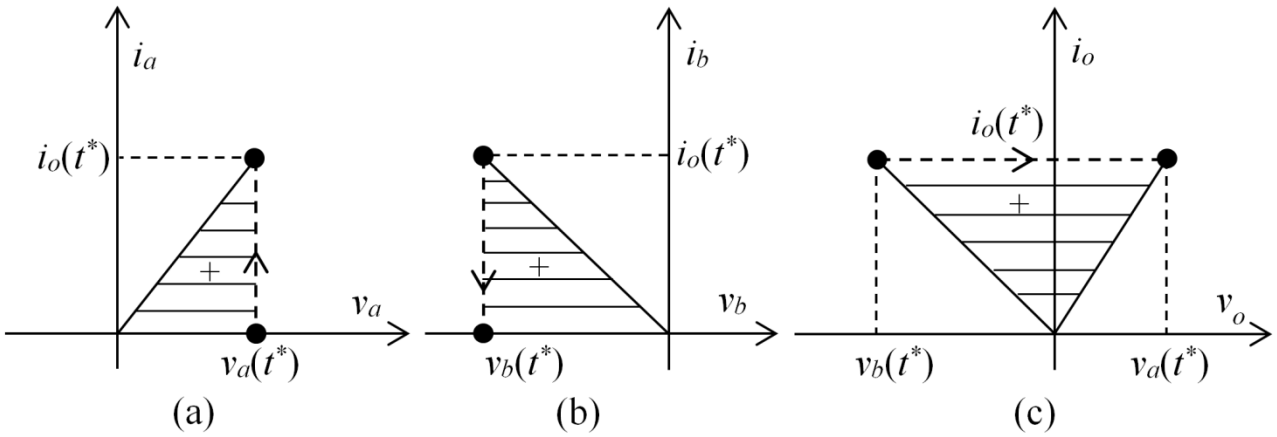

Fig. 2.40. Case 8. Swept areas: (a) port *a*; (b) port *b*; (c) port *o*

Now, let us consider the PEBB depicted in Fig. 2.41 under periodical steady state of period T, with a constant dc voltage V_D and controlled by a PWM strategy.

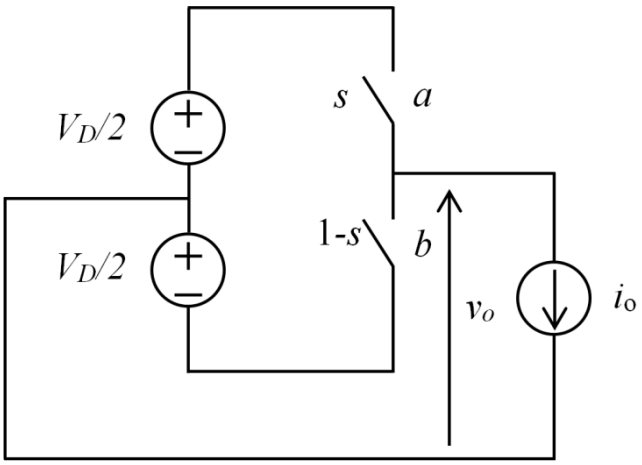

Fig. 2.41. Case 8. Electric circuit of PEBB

Let the output current be sinusoidal as follows.

$$i_o(t) = I\cos(\omega t + \psi_I) \qquad \omega = 2\pi / T \tag{2.128}$$

The Fig. 2.42 shows a detail of the PWM output voltage $v_o(t)$ and the sinusoidal output current $i_o(t)$. The periodic PWM can be analyzed by superposition of elementary pulses. Such way, the PWM voltage is decomposed in n waves periodic in T, each of them composed of one positive pulse in the period, as in bold highlighted in Fig. 2.42, with its own width and displacement. In each pulse wave n, two commutations occur in the period T, at the time t_{An} and t_{Bn}. In view of Fourier expansion, each of these pulse waves has been arbitrary translated to have nil mean value. This fact is allowed as the mean value does not affect the CAT. The Fourier series of the n-th pulse wave is consequently

$$v_{on}(t) = \frac{2}{\pi} V_D \sum_{k=1}^{\infty} \frac{\sin(k\alpha_n)\cos(k\omega t + k\psi_{Vn})}{k} \tag{2.129}$$

where

$$\alpha_n = \pi \frac{t_{Bn} - t_{An}}{T}; \psi_{Vn} = -\pi \frac{t_{An} + t_{Bn}}{T}. \tag{2.130}$$

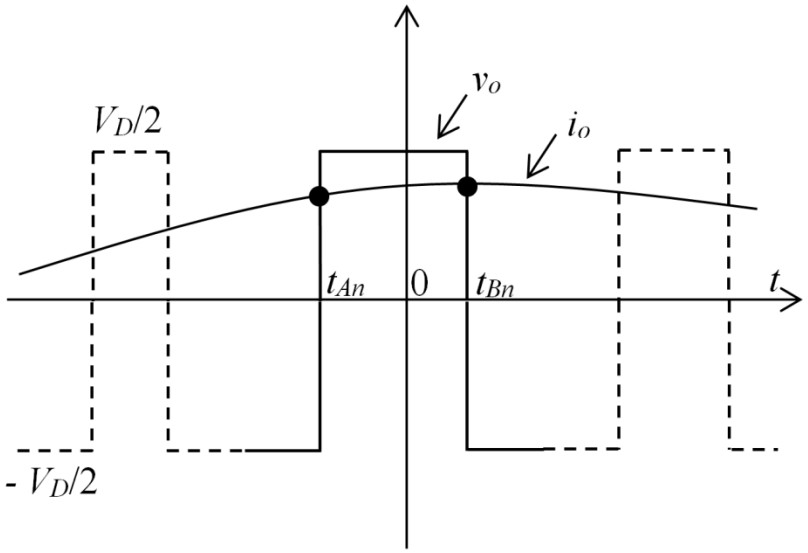

Fig. 2.42. Case 8. PWM output voltage and sinusoidal current

Since the output current is sinusoidal, only the first component Q_{1n} of reactive power at the ac terminal is present. From the current (2.128) and the term $k = 1$ in (2.129), it results

$$Q_{1n} = \frac{1}{\pi} V_D I \sin\alpha_n \sin(\psi_{Vn} - \psi_I). \tag{2.131}$$

From (2.42), (2.43), (2.128) and taken into account (2.125) and the scheme in Fig. 2.41, the collective SPs are respectively

$$\begin{aligned} A_{SW1n} &= V_D i_o(t_{An}) = V_D I \cos(\omega t_{An} + \psi_I) \\ A_{SW0n} &= -V_D i_o(t_{Bn}) = -V_D I \cos(\omega t_{Bn} + \psi_I). \end{aligned} \tag{2.132}$$

Taking into account (2.130), (2.132) and trigonometric formulas, the total SP in the period for a single pulse is

$$A_{SWn} = A_{SW1n} + A_{SW0n} = 2V_D I \sin\alpha_n \sin(\psi_I - \psi_{Vn}). \tag{2.133}$$

According to (2.44) and comparing (2.133) with (2.131), the relation between commutations, CAT and reactive power are verified for the n-th impulse. Indeed:

$$H_n = \frac{A_{SWn}}{T} = -\omega Q_{1n}. \tag{2.134}$$

The minus sign originates because the reference direction of the CAT is absorbed, whereas the reactive power is referred as outgoing at port o. For the whole PWM the total CAT is the sum of each finite voltage impulse:

$$H = \sum_n H_n. \tag{2.135}$$

The first component of the total output voltage is the sum of the first components in (2.129). So even the total reactive power at output terminals is the sum and by (2.131), it results

$$Q_1 = \sum_n Q_{1n} = \frac{1}{\pi} V_D I \sum_n \sin\alpha_n \sin(\psi_{Vn} - \psi_I). \tag{2.136}$$

Therefore, by superposition, (2.134) is valid also for the whole PWM. It is possible to find (2.56) applied to the SPs (2.133). Additional insights in the result and taking into account the intermediate terms in (2.132), it leads to

$$Q_1 = \frac{1}{2\pi} V_D \sum_n \left[i(t_{Bn}) - i(t_{An}) \right]. \tag{2.137}$$

The reactive power (2.137) appears to depend on the current sampled at the instants of switching. In detail, it can be noted that the reactive power is proportional to the difference between the values of current at commutations times t_{An} and t_{Bn}. If $i(t_{Bn}) > i(t_{An})$ the contribution of the n-th pulse to the reactive power is positive (outgoing), otherwise is negative.

This example had shown in detail the quantitative relation between PEBB switching and the reactive power at output terminals.

3. Electronic Power Converters

3.1 Introduction

For several years, many kinds of electronic power converters, are emerging in various topologies. They are based on the use of semiconductor controlled/not controlled devices in opening and/or in closing commutations.

Based on the kind of converter, a certain type of switching device can be used. Among which, it is possible to mention: diode, thyristor, GTO, IGBT or a composition of these ones. In any case, these switching devices can be theoretically considered clones of controlled switch, and the corresponding ideal circuit element is the ideal switch as reported in section 2.4.4.

In the following, regardless the kind of real switching device used into a certain kind of power converter, the ideal switch will be taken into account. In addition, power converters can be divided into different categories according to the type of electric transformation involved, the number of phases, the kind of electric quantities imposed, the number of level supported: dc-dc, dc-ac, ac-dc, ac-ac, three-phase or single-phase, voltage source converter (VSC) or current source converter (CSC), two, three or *n* level supported. Often, all these different subdivisions may suggest that these converters are very different both in topology and their control. Actually, principles are the same so theory and control strategies can be unified.

In the first instance, it is possible to state that the division due to the type of electric transformation is often formal only; for example, the so-called bridge chopper and the single-phase inverter have the same H-bridge topology with the same kind of real switches, but what changes is just the kind of tracking of the output quantities to control.

Regarding the division based on the electric quantities imposed, it is interesting to highlight that the so-called current source converter is not, as one might expect, the dual of the voltage source converter. In fact, while the VSC can, independently, impose different voltage levels to each output phase, the CSC cannot dually impose different current levels to each output phase. Anyway, both kinds of converter can be seen as the composition of more elementary structures. The VSC is composed of elementary structures with two voltage levels and one current level meanwhile the CSC includes three voltage levels and one current level. In the literature, this kind of elementary structure is called Power Electronic Building Block (PEBB), as reported in section 2.10.8. It represents the elementary structure of converters with two voltage levels and one current level, while nothing is stated about its dual structure with two current levels and one voltage level.

Actually, current or voltage source terms mean what electric quantity is imposed by an electric source that feeds the converter itself. In general, both electric quantities can be imposed at the same time.

Furthermore, many apparent different converters have the same topology and can be seen as a variation of more general structures. Also the control strategies, in some cases, are very similar and what changes is only the kind of waveform to tracking.

Therefore, the goal of this chapter is a trial to shed light on these subdivisions and search for other more general elementary structures which are common to the most of these converters. Also, they can allow, in some cases, a modular control of very complex converters. For this reason, concepts of Ideal Switch Multi Port (ISMP) and multilevel elements are introduced in order to deal with converters as multi-port elements with their constitutive relations. Moreover, the SAT theory is extend to the ISMP in order to find relations between commutations and reactive power involved by converters.

3.2 Ideal Switch

The ideal switch is treated as a one-port element with its own constitutive relations. AV and CAT functions of the ideal switch were calculated and the SP defined as the area on the *v*-*i* plane associated to the switching was reported in the previous chapter. The ideal switch is a linear time-variant resistive one-port element with two possible states, open and closed.

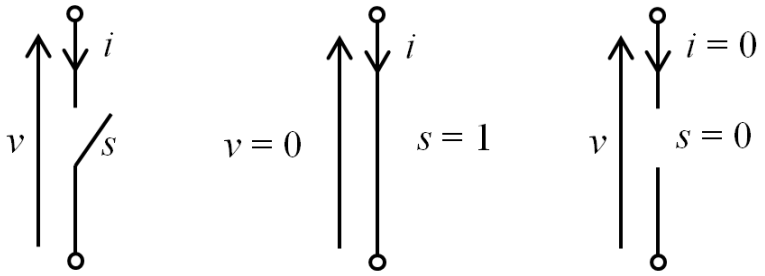

Fig. 3.1. Ideal switch closed and open

When it is closed the voltage *v* is nil while the current *i* depends on the remaining network, instead, when it is open the current *i* is nil while the voltage *v* depends on the remaining network. As previously stated in chapter 2, it is possible to represent the state of the ideal switch by means of a function of time *s*(*t*) called switching function. In general, this function can have different discrete values, but in the particular case of ideal switch, it has only two values. This values are 0 and 1. Conventionally, 0 corresponds to open state while 1 corresponds to closed state. Under normal conditions, in which impulses in the electric quantities are not present, the instantaneous electric power absorbed by the ideal switch is always nil. In fact, one of the two electric quantities is always nil.

The ideal switch is an element which is not always uniquely voltage or current controllable, and this fact depends on its state, open or closed. The ideal switch, however, can control an element that is complementary to it, i.e. an element that is both voltage and current controllable. For example, it can control the voltage or the current in a resistor or in a real voltage or current source.

Chopped conductance

The series of ideal switch and a conductance leads to a one-port element always voltage controllable.

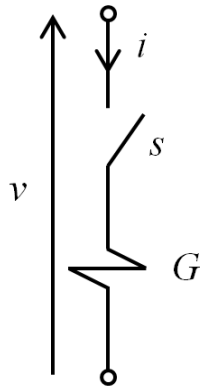

Fig. 3.2. Chopped conductance

Indeed, when the ideal switch is closed $i = Gv$ instead when the ideal switch is open $i = 0$. Hence, it is possible to write the following relation

$$i = sGv. \tag{3.1}$$

Note that the relation is not invertible, i.e. the one-port element is not current controllable, in fact

$$v = \frac{i}{hG} \tag{3.2}$$

that is not possible for $s = 0$.

Chopped Resistance

Dually, the parallel constituted by an ideal switch and a resistor leads to a one-port element always current controllable.

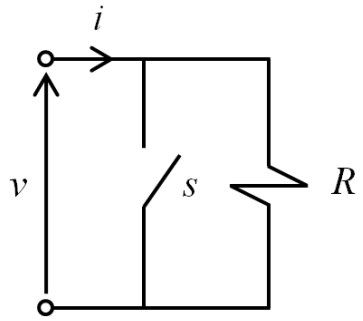

Fig. 3.3. Chopped resistance

Indeed, when the ideal switch is open $v = Ri$ instead when the ideal switch is closed $v = 0$. Hence, it is possible to write the following relation

$$v = (1-s)Ri. \tag{3.3}$$

Note that the relation is not invertible, i.e. the one-port element is not voltage controllable, in fact

$$i = \frac{v}{(1-s)R} \tag{3.4}$$

that is not possible for $s = 1$.

3.3 Ideal Switch Multi Port

Now, let us introduce the concept of Ideal Switch Multi Port namely a generic switching system composed of several ideal switch one-ports, by means of a matrix structure, in order to obtain a unified theory on power converters and extend the calculation of the AV and CAT to the ISMP.

In particular, let us consider structures of ISMP which always present invariant voltage and/or current controls. According to this hypothesis, it is interesting to note that the ideal switch alone does not correspond to the particular case of ISMP one-port element for the abovementioned reason.

Under this hypothesis, any generic ISMP must be a switching system consisting of n voltage controlled ports and m current controlled ports, as reported in Fig. 3.4. In this way, it is constituted by at least two ports.

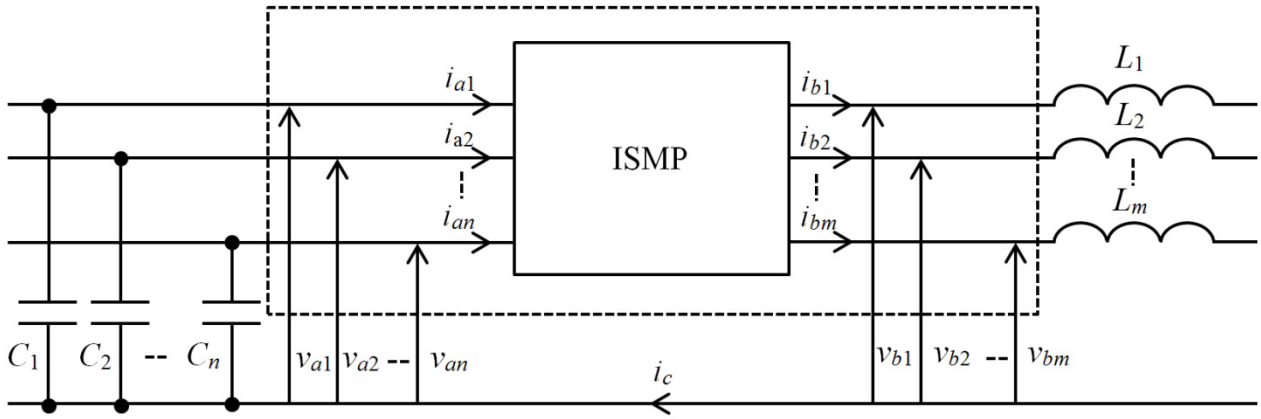

Fig. 3.4. Ideal Switch Multi Port

Let us assume, for convenience, the reference directions reported in Fig. 3.4 and according to which the instantaneous electric power flows from the n voltage controlled ports, of which $\boldsymbol{v}_a$ and $\boldsymbol{i}_a$ are the vectors of the associated electric quantities, to the m current controlled ports, of which $\boldsymbol{v}_b$ and $\boldsymbol{i}_b$ are the vectors of the associated electric quantities.

The controlled quantities $\boldsymbol{v}_b$ and $\boldsymbol{i}_a$ are in general discontinuous because of the switching, instead the control variables $\boldsymbol{v}_a$ and $\boldsymbol{i}_b$ can be continuous or discontinuous. In most of the system conversions, in order to allow to the system itself to work, it is essential that the control quantities are continuous. For this reason the voltage controlled ports are typically connected to capacitors or ideal voltage sources while current controlled ports are connected to inductors or ideal current sources. The constitutive relations of ISMP are the following

$$\begin{aligned} \boldsymbol{i}_a &= \boldsymbol{S}\boldsymbol{i}_b \\ \boldsymbol{v}_b &= \boldsymbol{S}^t\boldsymbol{v}_a \end{aligned} \tag{3.5}$$

where

$$\boldsymbol{v}_a = \begin{bmatrix} v_{a1} \\ v_{a2} \\ \vdots \\ v_{an} \end{bmatrix}; \quad \boldsymbol{v}_b = \begin{bmatrix} v_{b1} \\ v_{b2} \\ \vdots \\ v_{bm} \end{bmatrix}; \quad \boldsymbol{i}_a = \begin{bmatrix} i_{a1} \\ i_{a2} \\ \vdots \\ i_{an} \end{bmatrix}; \quad \boldsymbol{i}_b = \begin{bmatrix} i_{b1} \\ i_{b2} \\ \vdots \\ i_{bm} \end{bmatrix}$$

$$\boldsymbol{S} = \begin{bmatrix} s_{11} & s_{12} & \cdots & s_{1m} \\ \vdots & \vdots & \vdots & \vdots \\ s_{n1} & s_{n2} & \cdots & s_{nm} \end{bmatrix}.$$

$\boldsymbol{S}$ is the time-variant matrix characterized by a finite number of *switching functions* or *switching states* and transitions between instantaneous states (*switching transitions*). Each s_{ij} is a variable with different discrete states. In particular, the s_{ij} can be defined as elementary variable, if it corresponds to the single ideal switch with only two different state, 0 and 1; it can be defined as derivative

variable, if it is a combination of elementary variables. Moreover, there are often constraints on row or column. In any case, equations (3.5) can be rewritten in a matrix form as follows

$$\begin{bmatrix} \boldsymbol{i}_a \\ \boldsymbol{v}_b \end{bmatrix} = \begin{bmatrix} 0 & \boldsymbol{S} \\ \boldsymbol{S}^t & 0 \end{bmatrix} \begin{bmatrix} \boldsymbol{v}_a \\ \boldsymbol{i}_b \end{bmatrix}. \tag{3.6}$$

The (3.6) shows that ISMP is a time-variant reciprocal resistive multi-port.

Instantaneous electric power

According to the reference direction reported in Fig. 3.4, the total instantaneous electric power absorbed by the *n* voltage controlled ports is equal to the total instantaneous electric power generated by the *m* current controlled ports. From (3.5) the following expression applies

$$p = p_a = p_b = \boldsymbol{v}_a{}^t \boldsymbol{i}_a = \boldsymbol{v}_b{}^t \boldsymbol{i}_b. \tag{3.7}$$

Taking into account (3.5) in (3.7), it is possible to write

$$p = p_1 = \boldsymbol{v}_a{}^t \boldsymbol{i}_a = \boldsymbol{v}_a{}^t \boldsymbol{S} \boldsymbol{i}_b. \tag{3.8}$$

3.3.1 Area Velocity

The AV absorbed by the ISMP is equal to the sum of all AVs of each port as

$$\begin{aligned} h_w(t) &= \sum_{j=1}^{n} h_{aj} - \sum_{k=1}^{m} h_{bk} = \frac{1}{2}\left(\boldsymbol{v}_a^t \frac{d\boldsymbol{i}_a}{dt} - \boldsymbol{i}_a^t \frac{d\boldsymbol{v}_a}{dt} - \boldsymbol{v}_b^t \frac{d\boldsymbol{i}_b}{dt} + \boldsymbol{i}_b^t \frac{d\boldsymbol{v}_b}{dt} \right) = \\ &= \frac{1}{2}\left(\boldsymbol{v}_a^t \frac{d(\boldsymbol{S}\boldsymbol{i}_b)}{dt} - \boldsymbol{i}_b^t \boldsymbol{S}^t \frac{d\boldsymbol{v}_a}{dt} - \boldsymbol{v}_a^t \boldsymbol{S} \frac{d\boldsymbol{i}_b}{dt} + \boldsymbol{i}_b^t \frac{d(\boldsymbol{S}^t \boldsymbol{v}_a)}{dt} \right) = \\ &= \frac{1}{2}\left(\boldsymbol{v}_a^t \frac{d\boldsymbol{S}}{dt} \boldsymbol{i}_b + \boldsymbol{v}_a^t \boldsymbol{S} \frac{d\boldsymbol{i}_b}{dt} - \boldsymbol{i}_b^t \boldsymbol{S}^t \frac{d\boldsymbol{v}_a}{dt} - \boldsymbol{v}_a^t \boldsymbol{S} \frac{d\boldsymbol{i}_b}{dt} + \boldsymbol{i}_b^t \frac{d\boldsymbol{S}^t}{dt} \boldsymbol{v}_a + \boldsymbol{i}_b^t \boldsymbol{S}^t \frac{d\boldsymbol{v}_a}{dt} \right) = \boldsymbol{v}_a{}^t \frac{d\boldsymbol{S}}{dt} \boldsymbol{i}_b = \boldsymbol{v}_a{}^t \boldsymbol{W}_\delta \boldsymbol{i}_b. \end{aligned} \tag{3.9}$$

The $\boldsymbol{W}_\delta$ is a matrix of pulses. The h_w function is constituted by a sequence of pulses corresponding to the switching, and nil else. Out of the commutations, the (3.9) is a linear time-invariant reciprocal resistive multi-port. At the pulse corresponding to the transition from the state *j* to the state *k* at time t_{jk} the matrix $\boldsymbol{W}_\delta$ is

$$\boldsymbol{W}_\delta = \left(\boldsymbol{S}_k - \boldsymbol{S}_j \right) \delta(t - t_{jk}) = \boldsymbol{S}_{jk} \delta(t - t_{jk}) \tag{3.10}$$

where $\boldsymbol{S}_{jk}$ is defined as *Switching Transition Matrix*.

3.3.2 Switching Power

The SP absorbed by the ISMP associated to the transition from the state *j* to the state *k* in the switching instant t_{jk} according to (2.6) is

$$A_{jk} = \int_{jk-}^{jk+} h_w dt = \int_{t_{jk-}}^{t_{jk+}} \boldsymbol{v}_a{}^t \boldsymbol{W}_\delta \boldsymbol{i}_b dt = \boldsymbol{v}_a{}^t \left(\int_{t_{jk-}}^{t_{jk+}} \boldsymbol{W}_\delta dt \right) \boldsymbol{i}_b = \boldsymbol{v}_a{}^t \left(\boldsymbol{S}_k - \boldsymbol{S}_j \right) \boldsymbol{i}_b = \boldsymbol{v}_a{}^t \boldsymbol{S}_{jk} \boldsymbol{i}_b. \tag{3.11}$$

The (3.11) can be seen as generalization of (2.42), (2.43). In (3.11) $\boldsymbol{v}_a$ and $\boldsymbol{i}_b$, under the hypothesis that they are continuous quantities, can be brought out of the integral. Moreover, from (3.8) and (3.9) it is possible to obtain

$$h_w(t) = \left(p_k - p_j \right) \delta(t - t_{jk}) = \left[p(t_{jk+}) - p(t_{jk-}) \right] \delta(t - t_{jk}). \tag{3.12}$$

By integration of (3.12), the (3.11) becomes

$$A_{kj} = p_k - p_j = p(t_{jk+}) - p(t_{jk-}). \tag{3.13}$$

Equation (3.13) is a remarkable achievement. The SP (absorbed) by the ISMP is equal to the difference between the instantaneous electric power before and after the switching. In other words, it is the variation of the instantaneous electric power flowing through the ISMP caused by the switching. From (3.13), under the hypothesis of power flowing from voltage controlled ports to current controlled ports, it is possible to state the following:

Theorem 3.I. Given an Ideal Switch Multi Port, switching gives a positive contribution of Switching Power, if and only if, the instantaneous electric power flowing from the voltage controlled ports to the current controlled ports increases, while switching gives a negative contribution of Switching Power, if and only if, the instantaneous electric power flowing from the voltage controlled ports to the current controlled ports decreases. Vice versa for the opposite flow of power.

Since any ISMP can be seen as constituted by several ideal switches, the AV can be calculated even as the sum of the all AVs of each ideal switch. This fact is proved by the balance theorem over AV.

3.3.3 Closed Area over Time

The total CAT absorbed by the ISMP is

$$H_w = H_a - H_b = \frac{1}{T} \int_T \boldsymbol{v}_a{}^t \boldsymbol{W}_\delta \boldsymbol{i}_b dt. \tag{3.14}$$

The derivative of $\boldsymbol{W}_\delta$ over the period T is not nil and it is impulsive for a certain number of switching instants. For this reason the CAT is

$$H_w = \frac{1}{T} \sum_r A_{jk(r)}. \tag{3.15}$$

Equation (3.15) is the generalization of (2.44). An important result about converters: the CAT is the sum of a finite number of terms determined by switching and evaluated in the instants of commutation, rather than integral of continuous functions, much easier. Furthermore, the (3.15) also shows a sampling phenomenon: by means of the SP, which depends only on the values at the switching instants, it is possible to calculate the value of the CAT.

Taking into account (3.13) and (3.15), the relation between CAT and the sum of the variations of instantaneous electric power is

$$H_w = \omega \sum_k kQ_k = \frac{1}{T} \sum_r (p_{k(r)} - p_{j(r)}). \tag{3.16}$$

Equation (3.16) shows a link between the CAT and the instantaneous electric power. It is possible to state that an ISMP converts an instantaneous electric power jump into a generalized reactive power. In this way, the ISMP generates or absorbs CAT by the commutations in which only the values of the electric quantities in the switching instants are taking into account.

Let us state that each commutation produces SP and let us call inductive contribution of SP when this is positive absorbed and capacitive contribution when the SP is negative absorbed (i.e. generated).

Under sinusoidal control variables the (3.16) becomes

$$\begin{aligned} H &= \omega Q = \frac{1}{T} \sum_r (p_{k(r)} - p_{j(r)}) \\ Q &= \frac{1}{2\pi} \sum_r (p_{k(r)} - p_{j(r)}). \end{aligned} \tag{3.17}$$

Finally, it is also possible to calculate the total CAT involved by the ISMP as sum of each CAT absorbed by the ideal switches constituting the ISMP. This fact is proved by the balance theorem over CAT.

3.4 Multilevel Elements

It has been seen that a generic switching system, i.e. a power converter, can be treated as an ideal switch multi-port with *n* voltage controlled ports and *m* current controlled ports. Moreover, it is possible to reduce most of the ISMPs, which are used, as a composition of more general and modular elements that can be called multilevel elements. Nevertheless, these multilevel elements are particular sub-cases of ISMPs by means of which, it is possible to construct other many kinds of more complex ISMPs in a modular manner. Hence, it is possible to reduce most of the existing converters as a composition of these elementary structures. These elementary structures, that will be analyzed below, are composed of a certain number of ideal switches and dynamic elements such as inductors and capacitors. In general, it is possible to have ports as many as dynamic elements. Theoretically, these dynamic elements may be replaced by voltage and current ideal sources, otherwise they will be fed by real sources or even by other elementary structures. In any case, it is possible to define some electric quantities as imposed quantities at the ports when they are fed by ideal or real sources. Any converter to be able to work must have at least one port fed. Let us divide these multilevel elements into two main sub-categories:

1) *multilevel voltage element* is constituted by *n* voltage controlled ports (input) and one current controlled port (output). In this case the *n* voltage controlled ports correspond to *n* possible voltage levels (Fig. 3.5).

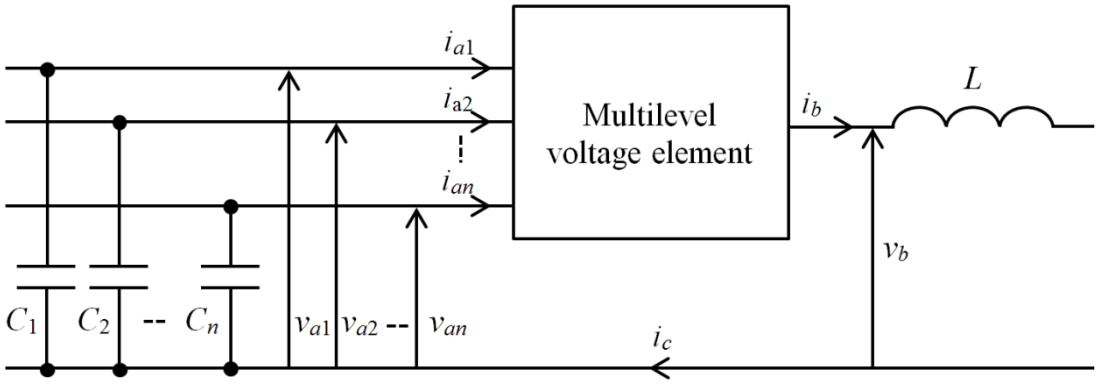

Fig. 3.5. Multilevel voltage element

2) *multilevel current element* is constituted by *n* current controlled ports (input) and one voltage controlled port (output). In this case the *n* current controlled ports correspond to *n* possible current levels (Fig. 3.6).

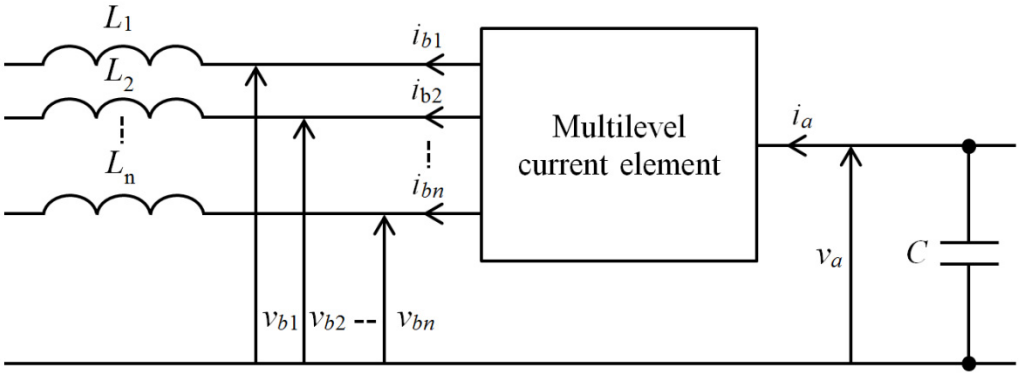

Fig. 3.6. Multilevel current element

Taking the term PEBB used in the literature, let us call as N-level Voltage PEBB (VPEEB) the multilevel voltage element with *n* voltage levels and, the dual, as N-level Current PEBB (CPEEB) with *n* current levels.

3.5 Multilevel Voltage Element

The multilevel voltage element is composed of *n* voltage controlled ports and one current controlled port. A scheme of principle is reported in Fig. 3.7. A particular structure of multilevel voltage element can be constructed by using *n* ideal switches, as reported in Fig. 3.7, where only one switch is closed in turn. In this way, the output voltage v_b can be chosen among *n* different voltage levels. Conversely, the output current i_b can be injected in one of the input ports. This levels of voltage and current can be constant or variable in function of time. In this way, it is possible to reproduce different kinds of ac-dc, dc-dc, dc-ac, and ac-ac converters. In fact, many power converters have the same topological structure but what changes are the kind of electrical quantities applied and the control strategy used.

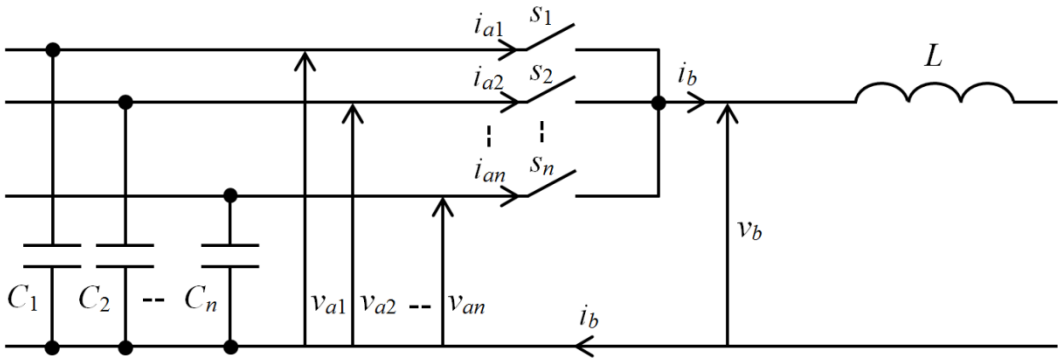

Fig. 3.7. Multilevel voltage element with ideal switches. Only one switch closed

The constitutive relations of this element in matrix form are as the following

$$\begin{bmatrix} \boldsymbol{i}_a \\ v_b \end{bmatrix} = \begin{bmatrix} 0 & \boldsymbol{S} \\ \boldsymbol{S}^t & 0 \end{bmatrix} \begin{bmatrix} \boldsymbol{v}_a \\ i_b \end{bmatrix} \tag{3.18}$$

where

$$\boldsymbol{v}_a = \begin{bmatrix} v_{a1} \\ v_{a2} \\ \vdots \\ v_{an} \end{bmatrix}; \boldsymbol{i}_a = \begin{bmatrix} i_{a1} \\ i_{a2} \\ \vdots \\ i_{an} \end{bmatrix}; \boldsymbol{S} = \begin{bmatrix} s_1 \\ s_2 \\ \vdots \\ s_n \end{bmatrix}. \tag{3.19}$$

s_j can assume only two values (0 = open, 1 = closed) with the constrains

$$\sum s_i = 1. \tag{3.20}$$

The (3.20) means that only one ideal switch at time must be closed. This kind of structure is equivalent to a switch with n states (selector switch) as reported in Fig. 3.8

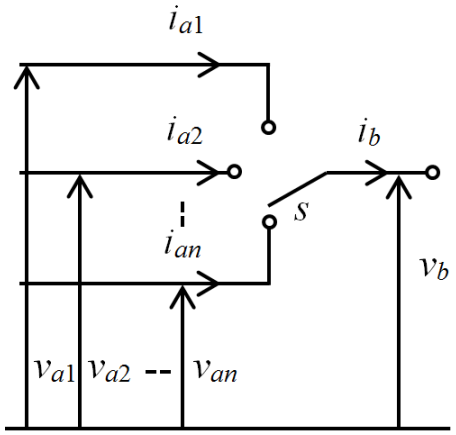

Fig. 3.8. Selector switch

The AV absorbed by the multilevel voltage element is

$$h_W(t) = \sum_{j=1}^{n} h_{aj} - h_b = \frac{1}{2}\left(\boldsymbol{v}_a^t \frac{d\boldsymbol{i}_a}{dt} - \boldsymbol{i}_a^t \frac{d\boldsymbol{v}_a}{dt} - v_b \frac{di_b}{dt} + i_b \frac{dv_b}{dt} \right) = \boldsymbol{v}_a{}^t \frac{d\boldsymbol{S}}{dt} i_b = \boldsymbol{v}_a{}^t \boldsymbol{W}_\delta i_b \tag{3.21}$$

and according to (3.11) the SP associated to the transition from the state j to the state k in the switching instant t_{jk} is

$$A_{jk} = \boldsymbol{v}_a{}^t \left(\boldsymbol{S}_k - \boldsymbol{S}_j \right) i_b = \boldsymbol{v}_a{}^t \boldsymbol{S}_{jk} i_b. \tag{3.22}$$

Taking into account (3.18), (3.19) and the constrains (3.20), the (3.22) becomes

$$A_{kj} = (v_k - v_j) i_b \tag{3.23}$$

where v_j and v_k are the voltage levels related to the states. The SP is proportional to the voltage jump due to the switching transition.

It is possible to recognize that when a generic ISMP has the $\boldsymbol{S}$ matrix composed of columns in which one and only one 1 is present at time, it is possible to reconstruct that ISMP by different VPEEBs.

3.5.1 Single 2–levels VPEBB

By means of this elementary structure with two voltage levels it is possible to derive power converters. The electric circuit is shown in Fig. 3.9. This structure is constituted by two voltage controlled ports and one current controlled port.

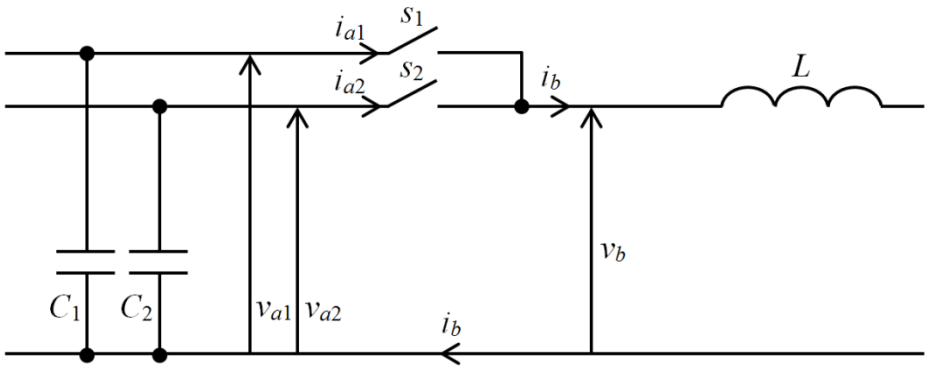

Fig. 3.9. Single 2 – levels VPEBB

The constitutive relations are the following

$$\begin{aligned} v_b &= s_1 v_{a1} + s_2 v_{a2} \\ i_{a1} &= s_1 i_b \\ i_{a2} &= s_2 i_b. \end{aligned} \tag{3.24}$$

In matrix form (3.24) becomes

$$\begin{bmatrix} i_{a1} \\ i_{a2} \\ v_b \end{bmatrix} = \begin{bmatrix} 0 & 0 & s_1 \\ 0 & 0 & s_2 \\ s_1 & s_2 & 0 \end{bmatrix} \begin{bmatrix} v_{a1} \\ v_{a2} \\ i_b \end{bmatrix}. \tag{3.25}$$

In this case, since $s_1 + s_2 = 1$, it is possible to express the two SFs as complementary of each other as follows

$$\begin{aligned} s_1 &= s \\ s_2 &= 1 - s. \end{aligned} \tag{3.26}$$

Taking into account (3.26) the (3.24) can be rewrite as

$$\begin{aligned} v_b &= v_{a2} + s(v_{a1} - v_{a2}) \\ i_{a1} &= s i_b \\ i_{a2} &= (1-s) i_b. \end{aligned} \tag{3.27}$$

In matrix form (3.27) becomes

$$\begin{bmatrix} i_{a1} \\ i_{a2} \\ v_b \end{bmatrix} = \begin{bmatrix} 0 & 0 & s \\ 0 & 0 & 1-s \\ s & 1-s & 0 \end{bmatrix} \begin{bmatrix} v_{a1} \\ v_{a2} \\ i_b \end{bmatrix}. \tag{3.28}$$

The AV absorbed is

$$\begin{aligned} h_W(t) &= h_{a1} + h_{a2} - h_b = \frac{1}{2}\left(v_{a1}\frac{di_{a1}}{dt} - i_{a1}\frac{dv_{a1}}{dt} + v_{a2}\frac{di_{a2}}{dt} - i_{a2}\frac{dv_{a2}}{dt} - v_b\frac{di_b}{dt} + i_b\frac{dv_b}{dt} \right) = \\ &= v_{a1}\frac{ds}{dt} i_b + v_{a2}\frac{d(1-s)}{dt} i_b = v_{a1}\frac{ds}{dt} i_b - v_{a2}\frac{ds}{dt} i_b = (v_{a1} - v_{a2})\frac{ds}{dt} i_b = (v_{a1} - v_{a2}) w_S i_b \end{aligned} \tag{3.29}$$

while according to (3.11) the SP associated to the transition from the state j to the state k in the switching instant t_{jk} is

$$A_{jk} = (v_{a1} - v_{a2}) s_{jk} i_b = (v_{a1} - v_{a2})(s_k - s_j) i_b. \tag{3.30}$$

It is possible to graphically represent the only allowable states of the converter as depicted in Fig. 3.10.

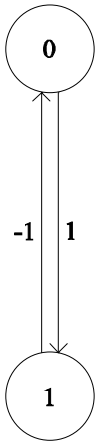

Fig. 3.10. Switching Functions and Switching Transitions

Related Converters

Chopper

If the voltages applied to the voltage controlled ports (capacitors), v_{a1} and v_{a2}, and the current flowing in the current controlled port (inductor), i_b, are constant is the bidirectional chopper. In fact, chopper has a single capacitor as one of the two voltage levels is nil and classic chopper shown in Fig. 3.11 is obtained. In this way, one voltage controlled port is eliminated. Usually, the voltage controlled port v_a is fed by a network and the output voltage v_b or current i_b are piloted.

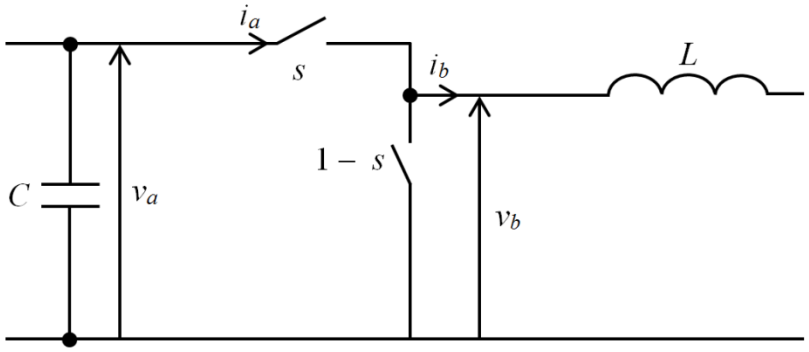

Fig. 3.11. Bidirectional chopper

The relations (3.27) becomes

$$\begin{aligned} v_b &= s v_a \\ i_a &= s i_b . \end{aligned} \tag{3.31}$$

In matrix form it has

$$\begin{bmatrix} i_a \\ v_b \end{bmatrix} = \begin{bmatrix} 0 & s \\ s & 0 \end{bmatrix} \begin{bmatrix} v_a \\ i_b \end{bmatrix}. \tag{3.32}$$

The AV absorbed by the chopper is

$$h_W(t) = h_a - h_b = \frac{1}{2}\left(v_a \frac{di_a}{dt} - i_a \frac{dv_a}{dt} - v_b \frac{di_b}{dt} + i_b \frac{dv_b}{dt} \right) = v_a \frac{ds}{dt} i_b = v_a w_\delta i_b \tag{3.33}$$

and the SP associated to the transition from state the j to the state k in the switching instant t_{jk} is

$$A_{jk} = v_a s_{jk} i_b = v_a (s_k - s_j) i_b . \tag{3.34}$$

When a transition from 0 to 1 occurs the SP is

$$A_{01} = v_a i_b \tag{3.35}$$

and conversely, when a transition from 1 to 0 occurs the SP is

$$A_{10} = -v_a i_b . \tag{3.36}$$

In this case, it is possible to take into account the switching period in order to calculate the CAT as follows

$$H_w = \frac{A_{W01} + A_{W10}}{T_s} = \frac{v_a i_b(t_1) - v_a i_b(t_2)}{T_s}. \tag{3.37}$$

If the electric quantities v_a and i_b applied to the electric ports were constant, $H_w = 0$. Otherwise H_w can be not nil and depending on the ripples. Note that $v_a i_b$ is the instantaneous electric power flowing from port a to port b when $s = 1$. Indeed, let us suppose $v_a = V_D$ = constant. The output voltage v_b and current i_b, are depicted in Fig. 3.12.

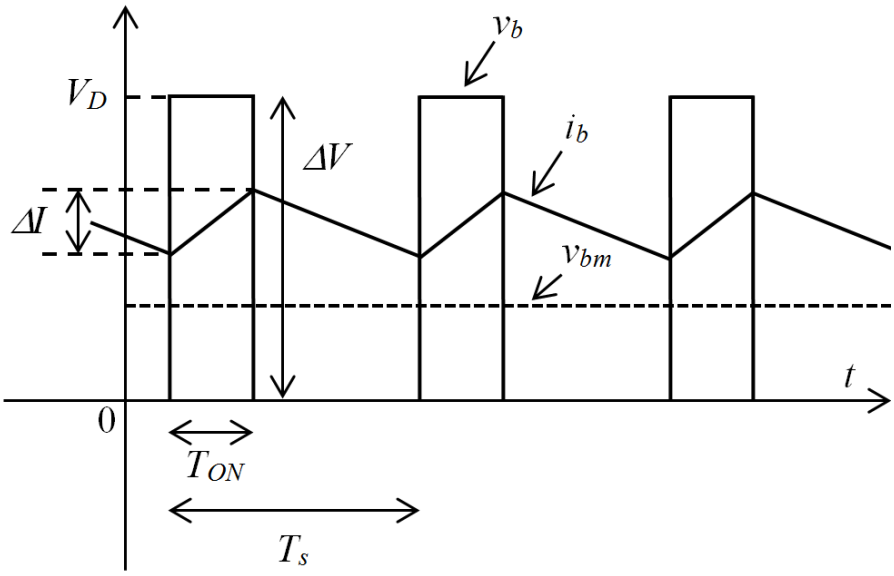

Fig. 3.12. Output voltage and current

Since v_a is constant the CAT absorbed by the voltage controlled port is nil. Instead, the CAT generated by the current controlled port, depicted in Fig. 3.13, is

$$H_w = \frac{\Delta V \Delta I}{T_s} \tag{3.38}$$

which is equal and opposed to (3.37).

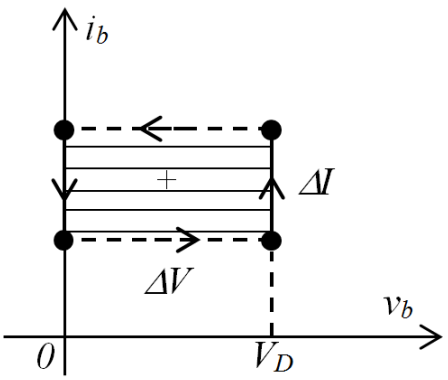

Fig. 3.13. Swept area at the port b

According to Fig. 3.12 the current ripple is

$$\Delta I = \frac{T_s \delta (1-\delta) \Delta V}{L} \tag{3.39}$$

where the duty cycle is defined as

$$\delta = \frac{T_{ON}}{T_s}. \tag{3.40}$$

Taking into account (3.39), (3.40) the (3.38) can be expressed as

$$H_w = \frac{\delta (1-\delta) \Delta V^2}{L} \tag{3.41}$$

or

$$H_w = \frac{L \Delta I^2}{\delta (1-\delta) T_s^2}. \tag{3.42}$$

The relations between ripple current, duty cycle, inductance, switching period and CAT is obtained.

Single-phase inverter

By means of the same topology, if the voltages applied to the voltage controlled ports (capacitors), v_{a1} and v_{a2}, are constant while the voltage v_b and/or the current i_b related to the current controlled port (inductor) are imposed as sinusoidal, the single-phase inverter with a single leg is obtained. What changes is just the control strategy and the kind of the electric quantities applied to the electric ports. Fig. 3.14 shows the classic scheme of the single-phase inverter with a single leg of which topology is the same of Fig. 3.9 unless a different arrangement of the elements. Usually, the two voltage controlled ports are fed by only one voltage source.

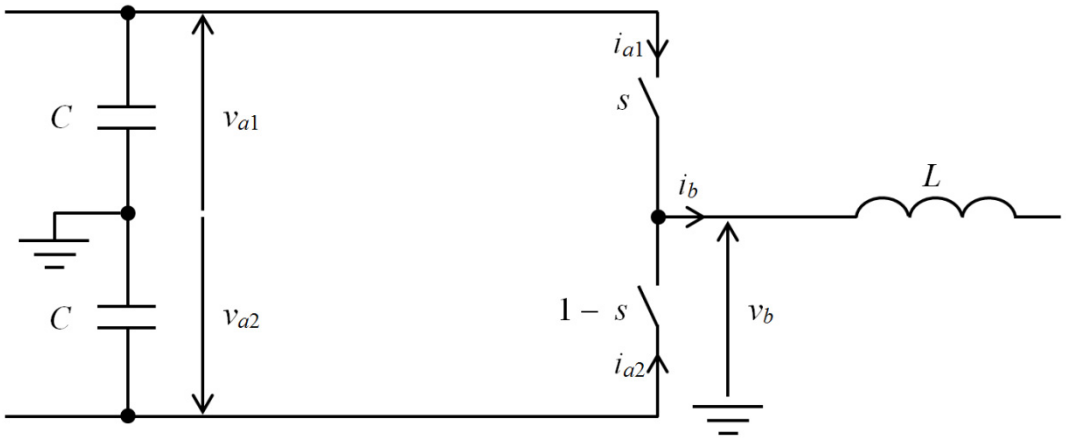

Fig. 3.14. Single-phase inverter

Buck-Boost

If one of the two voltage controlled ports is fed while the voltage in the other voltage controlled port is piloted with the controlled current port grounded the buck-boost converter, as shown in Fig. 3.15, is obtained.

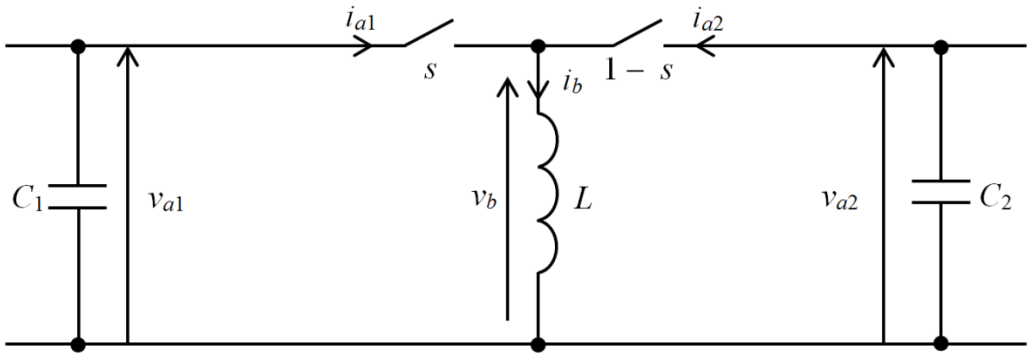

Fig. 3.15. Buck-Boost

3.5.2 Dual 2−levels VPEBB

This topology consists, in its most general form, in two 2-levels VPEEB of which the voltage controlled ports are shared, as shown in Fig. 3.16. This kind of converter has two voltage controlled ports and two current controlled ports.

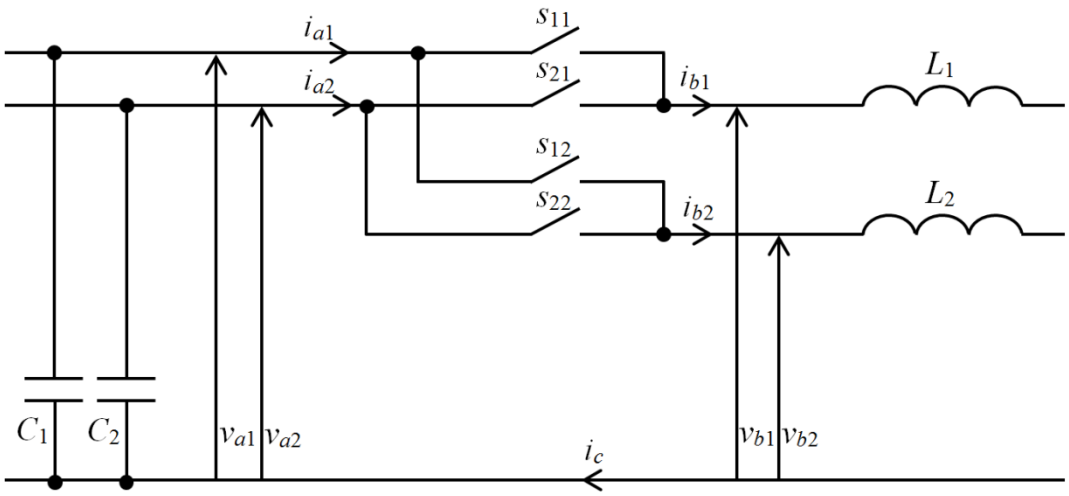

Fig. 3.16. Dual 2 − levels VPEBB

The constitutive relations in matrix form are as the following

$$\begin{bmatrix} i_{a1} \\ i_{a2} \\ v_{b1} \\ v_{b2} \end{bmatrix} = \begin{bmatrix} 0 & 0 & s_{11} & s_{12} \\ 0 & 0 & s_{21} & s_{22} \\ s_{11} & s_{21} & 0 & 0 \\ s_{12} & s_{22} & 0 & 0 \end{bmatrix} \begin{bmatrix} v_{a1} \\ v_{a2} \\ i_{b1} \\ i_{b2} \end{bmatrix}. \tag{3.43}$$

In this case, since $s_{11} + s_{21} = 1$ and $s_{12} + s_{22} = 1$, it is possible to express for each VPEBB the two SFs as complementary of each other as follows

$$\begin{aligned} s_{11} &= s_1 \\ s_{21} &= 1 - s_1 \\ s_{12} &= s_2 \\ s_{22} &= 1 - s_2. \end{aligned} \tag{3.44}$$

Taking into account the constrains (3.44), the (3.43) becomes

$$\begin{bmatrix} i_{a1} \\ i_{a2} \\ v_{b1} \\ v_{b2} \end{bmatrix} = \begin{bmatrix} 0 & 0 & s_1 & s_2 \\ 0 & 0 & 1-s_1 & 1-s_2 \\ s_1 & s_2 & 0 & 0 \\ 1-s_1 & 1-s_2 & 0 & 0 \end{bmatrix} \begin{bmatrix} v_{a1} \\ v_{a2} \\ i_{b1} \\ i_{b2} \end{bmatrix}. \tag{3.45}$$

The common current i_c is

$$i_c = i_{b1} + i_{b2}. \tag{3.46}$$

The AV absorbed is

$$\begin{aligned} h_W(t) &= h_{a1} + h_{a2} - h_{b1} - h_{b2} = v_{a1}\frac{ds_1}{dt} i_{b1} + v_{a2}\frac{d(1-s_1)}{dt} i_{b1} + v_{a2}\frac{ds_2}{dt} i_{b2} + v_{a2}\frac{d(1-s_2)}{dt} i_{b2} \\ &= (v_{a1} - v_{a2})\left(\frac{ds_1}{dt} i_{b1} + \frac{ds_2}{dt} i_{b2}\right) = (v_{a1} - v_{a2})(w_{\delta 1} i_{b1} + w_{\delta 2} i_{b2}) \end{aligned} \tag{3.47}$$

while according to (3.11) the SP associated to the transition from the state j to the state k in the switching instant t_{jk} is

$$A_{jk} = (v_{a1} - v_{a2})(s_{1jk} i_{b1} + s_{2jk} i_{b2}) = (v_{a1} - v_{a2})\left[(s_{1k} - s_{1j}) i_{b1} + (s_{2k} - s_{2j}) i_{b2}\right]. \tag{3.48}$$

It is possible to graphically represent the only allowable states and commutations obtained by switching only one switch at a time of the converter, as depicted in Fig. 3.17.

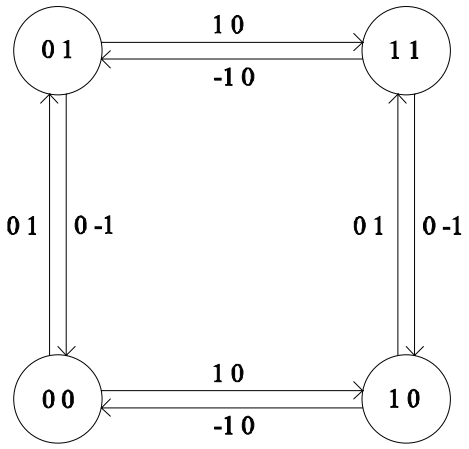

Fig. 3.17. Switching Functions and Switching Transitions

Related Converters

If the current controlled ports are independent each other, i.e. the third wire is used, topologies viewed as extensions of those obtained by Single 2 − levels VPEEB with two levels of voltage can be obtained. In particular, once voltages v_{a1} and v_{a2} are imposed as constants, the two current i_{b1} and i_{b2} can be separately controlled. If these currents are also imposed as constants the two-phase chopper is obtained. Instead, if the two currents are imposed as sinusoidal the two-phase inverter is obtained.

If the two current controlled ports are dependent each other, considering as only one current controlled port that one constituted by the difference between the two current controlled ports referred to ground, the H-bridge structure depicted in Fig. 3.18 is obtained and the current in the common wire i_c is constrained to be zero. This leads to

$$\begin{aligned} i_{b1} &= -i_{b2} = i_b \\ i_{a1} &= -i_{a2} = i_a \\ v_b &= v_{b1} - v_{b2}. \end{aligned} \tag{3.49}$$

H-Bridge Converter

As shown in Fig. 3.18 there is no longer the connection between the common point of the voltage controlled ports and one of the current controlled ports. In this way only one voltage controlled port can be considered with voltage v_a. This variation of topology allows to obtain three levels of voltages in the current controlled port and three levels of current in the voltage controlled port. This is possible because closing both the switches, which are connected at the same point, the output voltage v_b is nil.

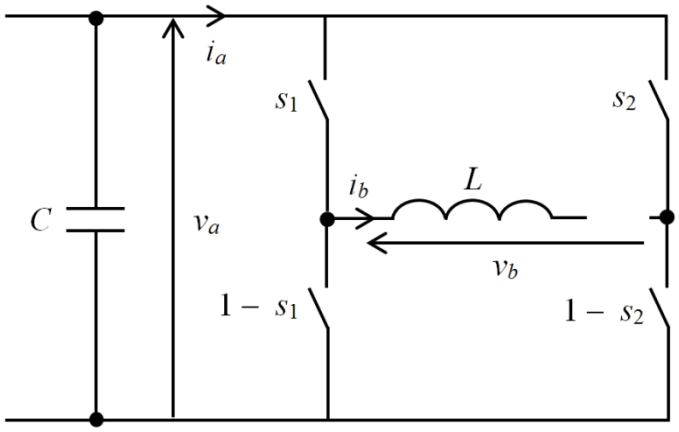

Fig. 3.18. H-bridge converter

According to Fig. 3.18 the constitutive relations (3.49) becomes

$$\begin{aligned} v_b &= (s_1 - s_2)v_a \\ i_a &= (s_1 - s_2)i_b. \end{aligned} \tag{3.50}$$

In matrix form, the (3.50) becomes

$$\begin{bmatrix} i_a \\ v_b \end{bmatrix} = \begin{bmatrix} 0 & s_1 - s_2 \\ s_1 - s_2 & 0 \end{bmatrix} \begin{bmatrix} v_a \\ i_b \end{bmatrix}. \tag{3.51}$$

According to (3.11) the SP associated to the transition from the state j to the state k in the switching instant t_{jk} is

$$A_{jk} = v_a(s_{1jk} - s_{2jk})i_b = v_a(s_{1k} - s_{1j} - s_{2k} + s_{2j})i_b \tag{3.52}$$

In the particular case in which the voltage imposed at the voltage controlled port is constant, the H-bridge chopper and the H-bridge single-phase voltage source inverter are obtained according to the electric quantities v_b and i_b are, respectively, constant or variable.

Instead, in the case the voltage imposed at the voltage controlled port is variable in function of the time, in particular sinusoidal, the single-phase controlled rectifiers, the 4Q converter and the single-phase cycloconverter can be obtained.

In the case the electric quantity to be controlled was the voltage or the current of the voltage controlled port, the chopper with imposed current and the single-phase current source inverter can be obtained.

3.5.3 Triple 2–levels VPEBB

This topology consists, in its most general form, in three 2-levels VPEEB of which the voltage controlled ports are shared, as shown in Fig. 3.19.

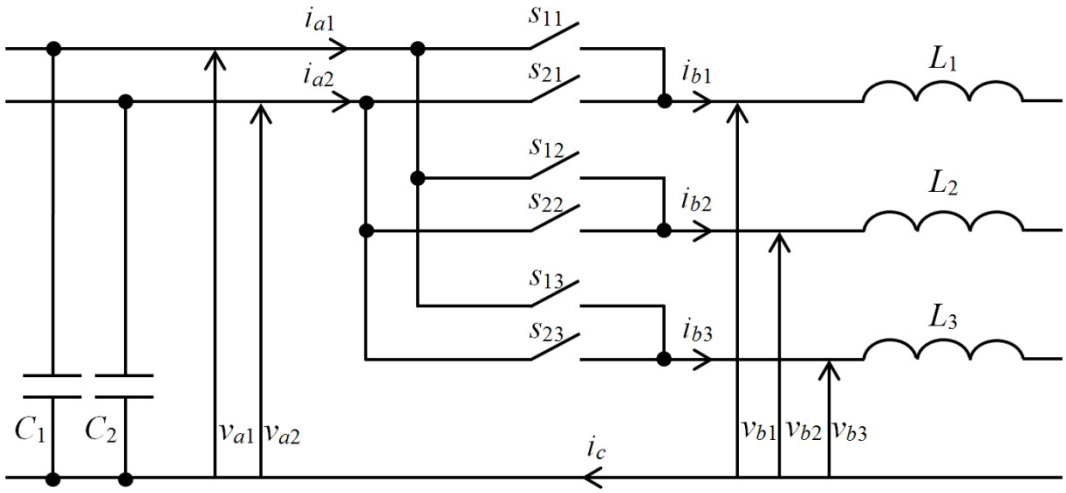

Fig. 3.19. Triple 2 – levels VPEBB

The constitutive relations in matrix form are as the following

$$\begin{bmatrix} i_{a1} \\ i_{a2} \\ v_{b1} \\ v_{b2} \\ v_{b3} \end{bmatrix} = \begin{bmatrix} 0 & 0 & s_{11} & s_{12} & s_{13} \\ 0 & 0 & s_{21} & s_{22} & s_{23} \\ s_{11} & s_{21} & 0 & 0 & 0 \\ s_{12} & s_{22} & 0 & 0 & 0 \\ s_{13} & s_{23} & 0 & 0 & 0 \end{bmatrix} \begin{bmatrix} v_{a1} \\ v_{a2} \\ i_{b1} \\ i_{b2} \\ i_{b3} \end{bmatrix}. \tag{3.53}$$

In this case, since $s_{11}+s_{21}=1$ e $s_{12}+s_{22}=1$ $s_{13}+s_{23}=1$, it is possible to express for each VPEBB the two SFs as complementary of each other as follows

$$\begin{aligned} s_{11} &= s_1 \\ s_{21} &= 1-s_1 \\ s_{12} &= s_2 \\ s_{22} &= 1-s_2 \\ s_{13} &= s_3 \\ s_{23} &= 1-s_3. \end{aligned} \tag{3.54}$$

Taking into account the constrains (3.54), the (3.53) becomes

$$\begin{bmatrix} i_{a1} \\ i_{a2} \\ v_{b1} \\ v_{b2} \\ v_{b3} \end{bmatrix} = \begin{bmatrix} 0 & 0 & s_1 & s_2 & s_3 \\ 0 & 0 & 1-s_1 & 1-s_2 & 1-s_3 \\ s_1 & 1-s_1 & 0 & 0 & 0 \\ s_2 & 1-s_2 & 0 & 0 & 0 \\ s_3 & 1-s_3 & 0 & 0 & 0 \end{bmatrix} \begin{bmatrix} v_{a1} \\ v_{a2} \\ i_{b1} \\ i_{b2} \\ i_{b3} \end{bmatrix}. \tag{3.55}$$

The common current i_c is

$$i_c = i_{b1} + i_{b2} + i_{b3}. \tag{3.56}$$

The AV absorbed is

$$\begin{aligned} &h_W(t) = h_{a1} + h_{a2} - h_{b1} - h_{b2} - h_{b3} = \\ &= v_{a1}\frac{ds_1}{dt}i_{b1} + v_{a2}\frac{d(1-s_1)}{dt}i_{b1} + v_{a1}\frac{ds_2}{dt}i_{b2} + v_{a2}\frac{d(1-s_2)}{dt}i_{b2} + v_{a1}\frac{ds_3}{dt}i_{b3} + v_{a2}\frac{d(1-s_3)}{dt}i_{b3} = \\ &= (v_{a1}-v_{a2})\left(\frac{ds_1}{dt}i_{b1} + \frac{ds_2}{dt}i_{b2} + \frac{ds_3}{dt}i_{b3}\right) = (v_{a1}-v_{a2})(w_{\delta 1}i_{b1} + w_{\delta 2}i_{b2} + w_{\delta 3}i_{b3}) \end{aligned} \tag{3.57}$$

and according to (3.11) the SP associated to the transition from the state j to the state k in the switching instant t_{jk} is

$$A_{jk} = (v_{a1}-v_{a2})(s_{1jk}i_{b1} + s_{2jk}i_{b2} + s_{3jk}i_{b3}) = (v_{a1}-v_{a2})\left[(s_{1k}-s_{1j})i_{b1} + (s_{2k}-s_{2j})i_{b2} + (s_{3k}-s_{3j})i_{b3}\right]. \tag{3.58}$$

It is possible to graphically represent the only allowable states and commutations obtained by switching only one switch at a time of the converter as depicted in Fig. 3.20.

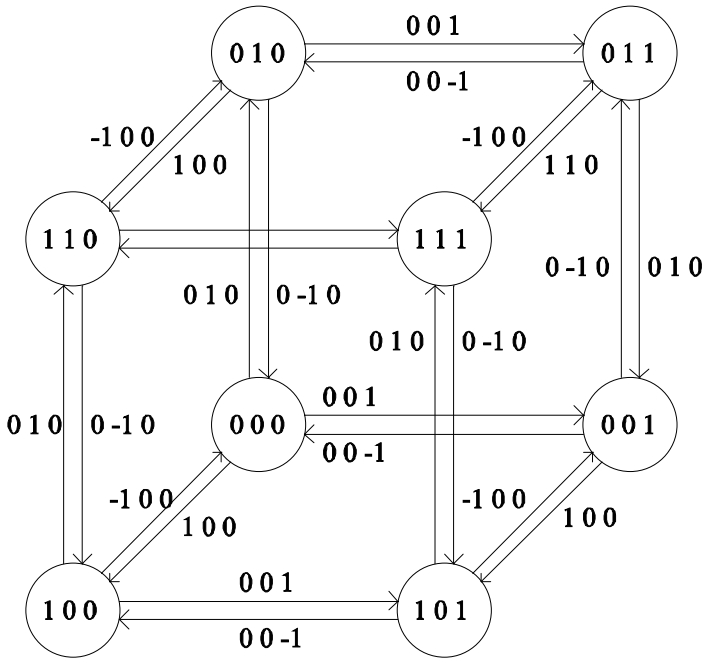

Fig. 3.20. Switching Functions and Switching Transitions

Related Converters

Four wires three-phase inverter

As reported in Fig. 3.19, if the current controlled ports are independent each other, i.e. the fourth wire is used, topologies viewed as extensions of those obtained by Single VPEEB with two levels of voltage can be obtained. In particular, once voltages v_{a1} and v_{a2} are imposed as constants, the three current, i_{b1}, i_{b2} and i_{b3}, can be separately controlled. If these currents are also imposed as constants the three-phase chopper is obtained. If instead, the three currents are imposed as sinusoidal the three-phase inverter with four wires is obtained.

Three-phase inverter

By elimination of the fourth wire, the topology shown in Fig. 3.21 is obtained, i.e. the classic three-wire three-phase inverter, where the sum of the three currents of the current controlled ports are constrained to be zero. This leads to

$$\begin{aligned} i_{b3} &= -i_{b1} - i_{b2} = i_b \\ i_{a1} &= -i_{a2} = i_a \\ v_{b13} &= v_{b1} - v_{b3} \\ v_{b23} &= v_{b2} - v_{b3}. \end{aligned} \tag{3.59}$$

In this way, it is possible to consider only one voltage controlled port and two current controlled ports. Taking into account (3.59) the (3.55) becomes

$$\begin{bmatrix} i_a \\ v_{b13} \\ v_{b23} \end{bmatrix} = \begin{bmatrix} 0 & s_1 - s_3 & s_2 - s_3 \\ s_1 - s_3 & 0 & 0 \\ s_2 - s_3 & 0 & 0 \end{bmatrix} \begin{bmatrix} v_a \\ i_{b1} \\ i_{b2} \end{bmatrix}. \tag{3.60}$$

The AV absorbed is

$$h_W(t) = h_a - h_{b13} - h_{b23} = v_a \left[\frac{d(s_1 - s_3)}{dt} i_{b1} + \frac{d(s_2 - s_3)}{dt} i_{b2} \right] = v_a \left[(w_{\delta 1} - w_{\delta 3}) i_{b1} + (w_{\delta 2} - w_{\delta 3}) i_{b2} \right] \quad (3.61)$$

and according to (3.11) the SP associated to the transition from the state j to the state k in the switching instant t_{jk} is

$$A_{jk} = v_a \left[(s_{1jk} - s_{3jk}) i_{b1} + (s_{2jk} - s_{3jk}) i_{b2} \right] = v_a \left[(s_{1k} - s_{1j} - s_{3k} + s_{3j}) i_{b1} + (s_{2k} - s_{2j} - s_{3k} + s_{3j}) i_{b2} \right]. \quad (3.62)$$

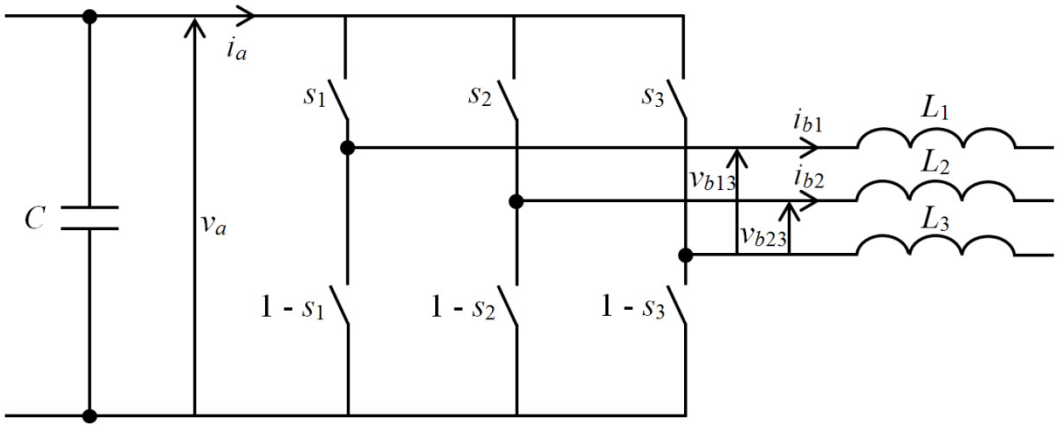

Fig. 3.21. Three-phase inverter

3.5.4 Dual 3−levels VPEBB

This topology consists, in its most general form, in two 3-levels VPEEB of which the voltage controlled ports are shared, as shown in Fig. 3.22.

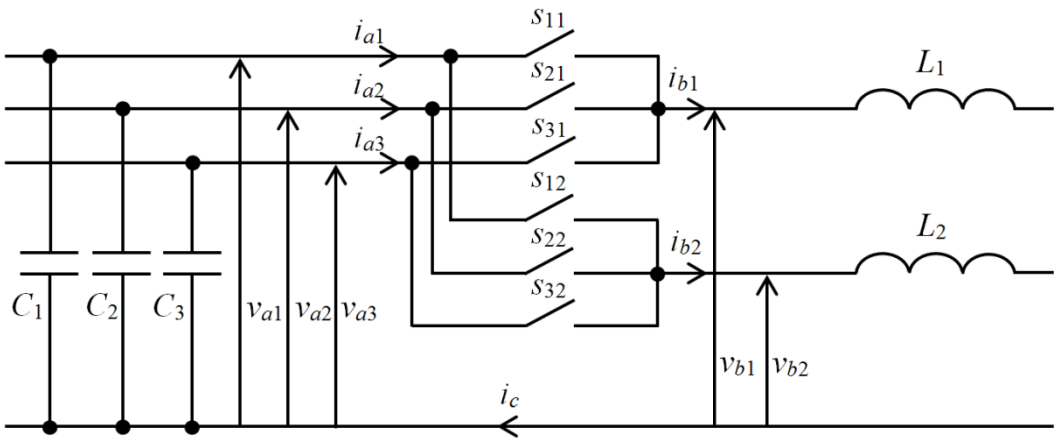

Fig. 3.22. Dual 3 − levels VPEBB

The constitutive relations are as the following

$$\begin{bmatrix} i_{a1} \\ i_{a2} \\ i_{a3} \\ v_{b1} \\ v_{b2} \end{bmatrix} = \begin{bmatrix} 0 & 0 & 0 & s_{11} & s_{12} \\ 0 & 0 & 0 & s_{21} & s_{22} \\ 0 & 0 & 0 & s_{31} & s_{32} \\ s_{11} & s_{21} & s_{31} & 0 & 0 \\ s_{12} & s_{22} & s_{32} & 0 & 0 \end{bmatrix} \begin{bmatrix} v_{a1} \\ v_{a2} \\ v_{a3} \\ i_{b1} \\ i_{b2} \end{bmatrix} \tag{3.63}$$

with the constrains

$$\begin{aligned} &s_{11} + s_{21} + s_{31} = 1 \\ &s_{12} + s_{22} + s_{32} = 1. \end{aligned} \tag{3.64}$$

The common current i_c is

$$i_c = i_{b1} + i_{b2}. \tag{3.65}$$

The AV absorbed is

$$\begin{aligned} &h_W(t) = h_{a1} + h_{a2} + h_{a3} - h_{b1} - h_{b2} = \\ &= v_{a1} \frac{ds_{11}}{dt} i_{b1} + v_{a2} \frac{ds_{21}}{dt} i_{b1} + v_{a3} \frac{ds_{31}}{dt} i_{b1} + v_{a1} \frac{ds_{12}}{dt} i_{b2} + v_{a2} \frac{ds_{22}}{dt} i_{b2} + v_{a3} \frac{ds_{32}}{dt} i_{b2} = \\ &= (v_{a1} - v_{a3})(\frac{ds_{11}}{dt} i_{b1} + \frac{ds_{12}}{dt} i_{b2}) + (v_{a2} - v_{a3})(\frac{ds_{21}}{dt} i_{b1} + \frac{ds_{22}}{dt} i_{b2}) = \\ &= (v_{a1} - v_{a3})(w_{\delta 11} i_{b1} + w_{\delta 12} i_{b2}) + (v_{a2} - v_{a3})(w_{\delta 21} i_{b1} + w_{\delta 22} i_{b2}) \end{aligned} \tag{3.66}$$

and according to (3.11) the SP associated to the transition from the state j to the state k in the switching instant t_{jk} is

$$\begin{aligned} &A_{jk} = (v_{a1} - v_{a3})(s_{11jk} i_{b1} + s_{12jk} i_{b2}) + (v_{a2} - v_{a3})(s_{21jk} i_{b1} + s_{22jk} i_{b2}) = \\ &= (v_{a1} - v_{a3})\left[(s_{11k} - s_{11j}) i_{b1} + (s_{12k} - s_{12j}) i_{b2}\right] + (v_{a2} - v_{a3})\left[(s_{21k} - s_{21j}) i_{b1} + (s_{22k} - s_{22j}) i_{b2}\right]. \end{aligned} \tag{3.67}$$

Usually, the topology with the current controlled ports dependent, without the third wire, is used. In this way, the common current i_c is forced to be zero and only one current controlled port and two voltage controlled port can be considered as reported in Fig. 3.23. According to Fig. 3.23 the constitutive relations (3.63) become

$$\begin{bmatrix} i_{a1} \\ i_{a2} \\ v_b \end{bmatrix} = \begin{bmatrix} 0 & 0 & s_{11} - s_{12} \\ 0 & 0 & s_{21} - s_{22} \\ s_{11} - s_{12} & s_{21} - s_{22} & 0 \end{bmatrix} \begin{bmatrix} v_{a13} \\ v_{a23} \\ i_b \end{bmatrix}. \tag{3.68}$$

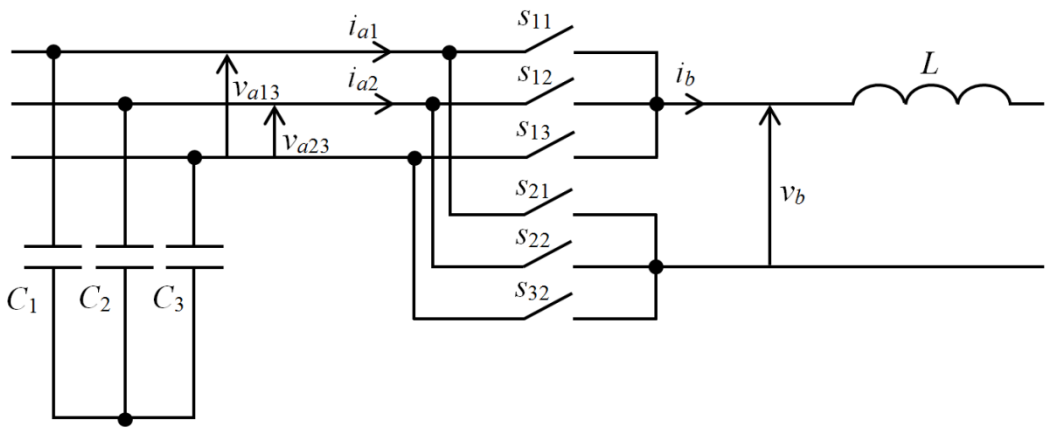

Fig. 3.23. Single 2 − levels VPEBB without the third wire

The AV absorbed is

$$\begin{aligned} &h_W(t) = h_{a13} + h_{a23} - h_b = \\ &= (v_{a1} - v_{a3})(\frac{ds_{11}}{dt} - \frac{ds_{12}}{dt})i_b + (v_{a2} - v_{a3})(\frac{ds_{21}}{dt} - \frac{ds_{22}}{dt})i_b = \\ &= (v_{a1} - v_{a3})(w_{\delta 11} - w_{\delta 12})i_b + (v_{a2} - v_{a3})(w_{\delta 21} - w_{\delta 22})i_b \\ &= \left[(v_{a1} - v_{a3})(w_{\delta 11} - w_{\delta 12}) + (v_{a2} - v_{a3})(w_{\delta 21} - w_{\delta 22})\right]i_b \end{aligned} \tag{3.69}$$

and according to (3.11) the SP associated to the transition from the state j to the state k in the switching instant t_{jk} is

$$\begin{aligned} &A_{jk} = (v_{a1} - v_{a3})(s_{11jk} - s_{12jk})i_b + (v_{a2} - v_{a3})(s_{21jk} - s_{22jk})i_b = \\ &= \left[(v_{a1} - v_{a3})(s_{11k} - s_{11j} - s_{12k} + s_{12j}) + (v_{a2} - v_{a3})(s_{21k} - s_{21j} - s_{22k} + s_{22j})\right]i_b. \end{aligned} \tag{3.70}$$

Related Converters

Many kinds of converters can be obtained by the topology of Fig. 3.23. If the voltage controlled ports are fed by sinusoidal voltages and the current i_b is piloted to be constant, it is the three-phase controlled rectifier; if the current controlled port is fed by a constant current and the voltage v_{a1}, v_{a2} and v_{a3} are piloted to be sinusoidal, it is the three-phase current source inverter; if the voltage controlled ports are fed by constant voltages and the voltage v_b or current i_b are piloted to be sinusoidal, it is the single-phase voltage source inverter with 3 levels of voltages; if the voltage controlled ports are fed by sinusoidal voltages and the voltage v_b or current i_b are piloted to be sinusoidal, it is the three-phase to single-phase matrix converter.

3.5.5 Triple 3−levels VPEBB

This topology consists, in its most general form, in three three-levels VPEEB of which the voltage controlled ports are shared, as shown in Fig. 3.24.

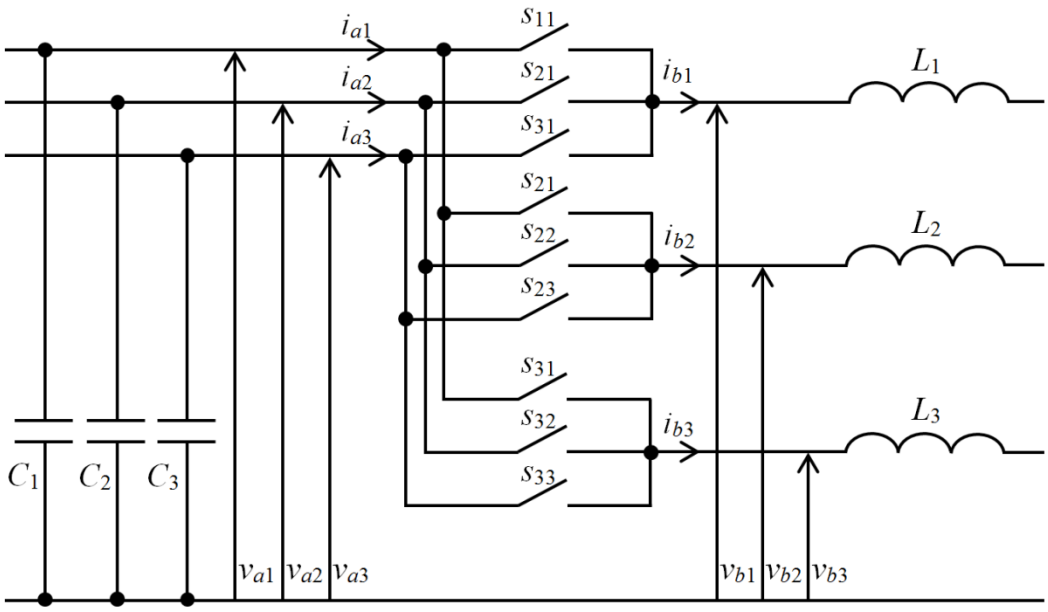

Fig. 3.24. Triple 3 − levels VPEBB

The constitutive relations are as the following

$$\begin{bmatrix} i_{a1} \\ i_{a2} \\ i_{a3} \\ v_{b1} \\ v_{b2} \\ v_{b3} \end{bmatrix} = \begin{bmatrix} 0 & 0 & 0 & s_{11} & s_{12} & s_{13} \\ 0 & 0 & 0 & s_{21} & s_{22} & s_{23} \\ 0 & 0 & 0 & s_{31} & s_{32} & s_{33} \\ s_{11} & s_{21} & s_{31} & 0 & 0 & 0 \\ s_{12} & s_{22} & s_{32} & 0 & 0 & 0 \\ s_{13} & s_{23} & s_{33} & 0 & 0 & 0 \end{bmatrix} \begin{bmatrix} v_{a1} \\ v_{a2} \\ v_{a3} \\ i_{b1} \\ i_{b2} \\ i_{b3} \end{bmatrix} \tag{3.71}$$

with the constrains

$$\begin{aligned} &s_{11} + s_{21} + s_{31} = 1 \\ &s_{12} + s_{22} + s_{32} = 1 \\ &s_{13} + s_{23} + s_{33} = 1. \end{aligned} \tag{3.72}$$

The common current i_c is

$$i_c = i_{b1} + i_{b2} + i_{b3}. \tag{3.73}$$

The AV absorbed is

$$
\begin{aligned}
&h_W(t) = h_{a1} + h_{a2} + h_{a3} - h_{b1} - h_{b2} - h_{b3} = \\
&= v_{a1}\frac{ds_{11}}{dt}i_{b1} + v_{a2}\frac{ds_{21}}{dt}i_{b1} + v_{a3}\frac{ds_{31}}{dt}i_{b1} + v_{a1}\frac{ds_{12}}{dt}i_{b2} + v_{a2}\frac{ds_{22}}{dt}i_{b2} + \\
&+v_{a3}\frac{ds_{32}}{dt}i_{b2} + v_{a1}\frac{ds_{13}}{dt}i_{b3} + v_{a2}\frac{ds_{23}}{dt}i_{b3} + v_{a3}\frac{ds_{33}}{dt}i_{b3} = \\
&= (v_{a1} - v_{a3})(\frac{ds_{11}}{dt}i_{b1} + \frac{ds_{12}}{dt}i_{b2} + \frac{ds_{13}}{dt}i_{b3}) + (v_{a2} - v_{a3})(\frac{ds_{21}}{dt}i_{b1} + \frac{ds_{22}}{dt}i_{b2} + \frac{ds_{23}}{dt}i_{b3}) = \\
&= (v_{a1} - v_{a3})(w_{\delta 11}i_{b1} + w_{\delta 12}i_{b2} + w_{\delta 13}i_{b3}) + (v_{a2} - v_{a3})(w_{\delta 21}i_{b1} + w_{\delta 22}i_{b2} + w_{\delta 23}i_{b3})
\end{aligned}
\tag{3.74}
$$

and according to (3.11) the SP associated to the transition from the state j to the state k in the switching instant t_{jk} is

$$
\begin{aligned}
&A_{jk} = (v_{a1} - v_{a3})(s_{11jk}i_{b1} + s_{12jk}i_{b2} + s_{13jk}i_{b3}) + (v_{a2} - v_{a3})(s_{21jk}i_{b1} + s_{22jk}i_{b2} + s_{23jk}i_{b3}) = \\
&= (v_{a1} - v_{a3})\left[(s_{11k} - s_{11j})i_{b1} + (s_{12k} - s_{12j})i_{b2} + (s_{13k} - s_{13j})i_{b3}\right] + \\
&+(v_{a2} - v_{a3})\left[(s_{21k} - s_{21j})i_{b1} + (s_{22k} - s_{22j})i_{b2} + (s_{23k} - s_{23j})i_{b3}\right].
\end{aligned}
\tag{3.75}
$$

Usually, the fourth wire is not used. In this way the common current i_c is forced to be zero.

Related Converters

If the voltage controlled ports are fed by constant voltages and the currents i_{b1}, i_{b2} and i_{b3} or the voltages v_{b1}, v_{b2} and v_{b3} are piloted to be sinusoidal, it is the three-phase voltage source three-level inverter; if the voltage controlled ports are fed by sinusoidal voltages and the currents i_{b1}, i_{b2} and i_{b3} or the voltages v_{b1}, v_{b2} and v_{b3} are piloted to be also sinusoidal but with different amplitude and frequency, it is three-phase matrix converter. In particular, for the so called nine-switch three-level inverter [69], which has a nil voltage level, the topology reported in Fig. 3.25 is obtained.

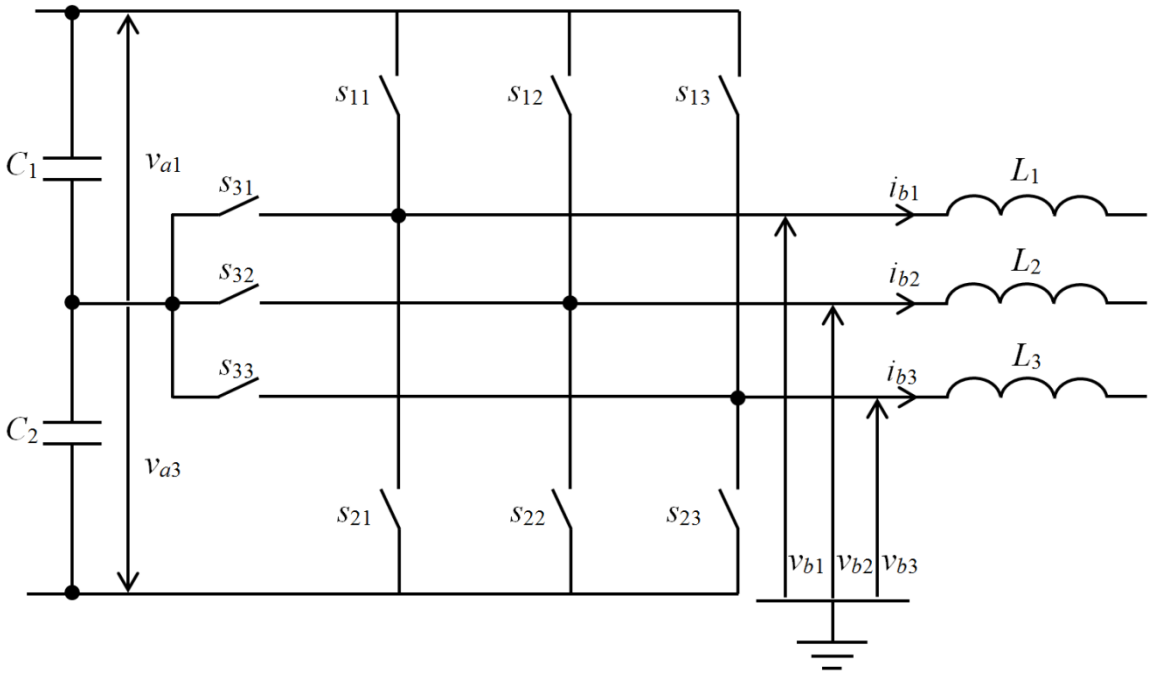

Fig. 3.25. Nine-switch three-level inverter

3.6 Multilevel Current Element

The multilevel current element is composed of n current controlled ports and one voltage controlled port. A scheme of principle is reported in Fig. 3.6. In this way, the output current i_b can be chosen among n different current levels. Conversely, the output voltage v_b can be imposed in one of the input ports.
The constitutive relations in matrix form are as the following

$$\begin{bmatrix} i_a \\ \boldsymbol{v}_b \end{bmatrix} = \begin{bmatrix} 0 & \boldsymbol{S} \\ \boldsymbol{S}^t & 0 \end{bmatrix} \begin{bmatrix} v_a \\ \boldsymbol{i}_b \end{bmatrix} \tag{3.76}$$

where

$$\boldsymbol{v}_b = \begin{bmatrix} v_{b1} \\ v_{b2} \\ \vdots \\ v_{bn} \end{bmatrix}; \quad \boldsymbol{i}_b = \begin{bmatrix} i_{b1} \\ i_{b2} \\ \vdots \\ i_{bn} \end{bmatrix}; \quad \boldsymbol{S} = \begin{bmatrix} s_1 & s_2 \cdots & s_n \end{bmatrix}. \tag{3.77}$$

s_j can assume only two values (0, 1) with the constrains

$$\sum s_i = 1. \tag{3.78}$$

The AV absorbed by the multilevel current element is

$$h_W(t) = h_a - \sum_{j=1}^{n} h_{bj} = \frac{1}{2}\left(v_a \frac{di_a}{dt} - i_a \frac{dv_a}{dt} - \boldsymbol{v}_b^t \frac{d\boldsymbol{i}_b}{dt} + \boldsymbol{i}_b \frac{d\boldsymbol{v}_b}{dt} \right) = v_a \frac{d\boldsymbol{S}}{dt} \boldsymbol{i}_b = v_a \boldsymbol{W}_{\delta} \boldsymbol{i}_b \tag{3.79}$$

and according to (3.11) the SP associated to the transition from the state j to the state k in the switching instant t_{jk} is

$$A_{jk} = v_a \left(\boldsymbol{S}_k - \boldsymbol{S}_j \right) \boldsymbol{i}_b = v_a \boldsymbol{S}_{jk} \boldsymbol{i}_b. \tag{3.80}$$

Taking into account (3.76), (3.77) and the constrains (3.78), the (3.80) becomes

$$A_{jk} = (i_k - i_j) v_a \tag{3.81}$$

where i_k and i_j are the current levels related to the states. The SP is proportional to the current jump due to the switching transition.

It is possible to recognize that when a generic ISMP has the $\boldsymbol{S}$ matrix composed of rows in which one and only one 1 is present at time, it is possible to reconstruct that ISMP by different CPEEBs.

Anyway, the multilevel current element, in order to be the dual of the multilevel voltage element reported in Fig. 3.7, can be made, from a theoretical point of view, as reported in Fig. 3.26. Only one of the switches is open in turn, the others are closed. If a system is constituted by only one of these multilevel current elements, it is possible to not use the ideal transformers. Instead, if a system is constituted by more than one of these multilevel current elements, in order to avoid short circuits among more capacitors, the ideal transformers are needed.

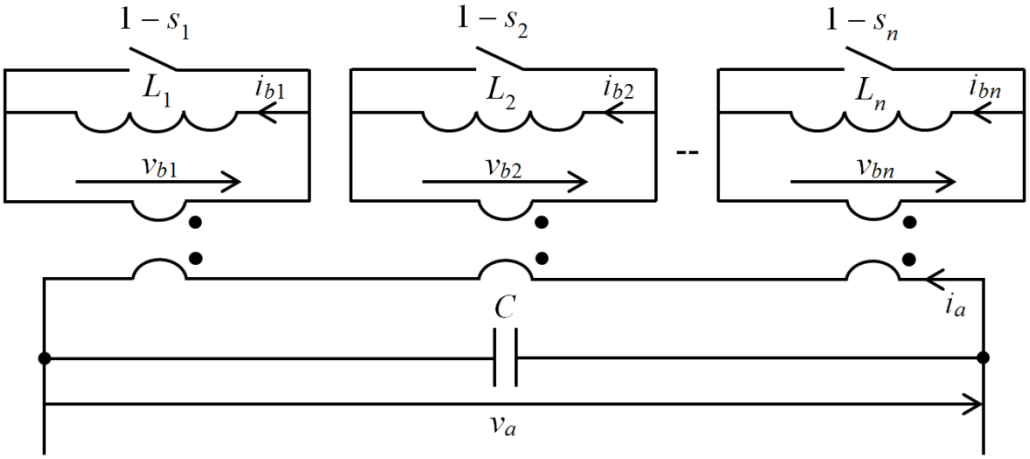

Fig. 3.26. Multilevel current element. Only one switch open

Another possible topology is that reported in Fig. 3.27.

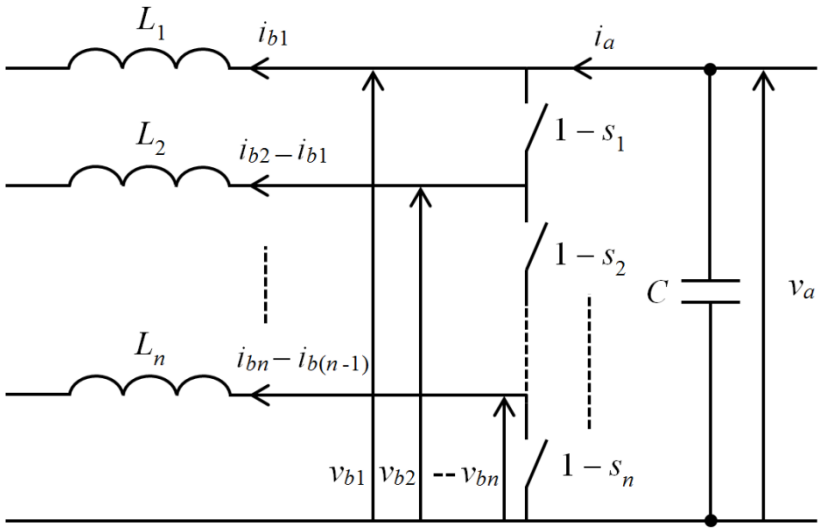

Fig. 3.27. Another possible topology of multilevel current element. Only one switch open

4. Simulation Results

4.1 Introduction

In order to test the theory developed in this work, some power converters were simulated by using Matlab/Simulink. In particular, three cases are threated:

1) chopper;
2) three-phase voltage source inverter;
3) three-phase matrix converter.

The aims of these simulation test are the followings: to verify the balance property of the CAT; the (2.44) applied to the converters (ISMP); the (2.15) applied at the input and output sides of the ISMP; the (2.31), (2.38) applied, respectively, to the inductors and capacitors.

4.2 Chopper

The electric circuit is depicted in Fig. 4.1 and it is composed of one capacitor fed by a constant voltage source E_a in the input side and another constant voltage source E_b in the output side which can represent an electric motor or a dc grid. The output voltage v_b is generated by using the standard PWM modulation with triangular carrier.

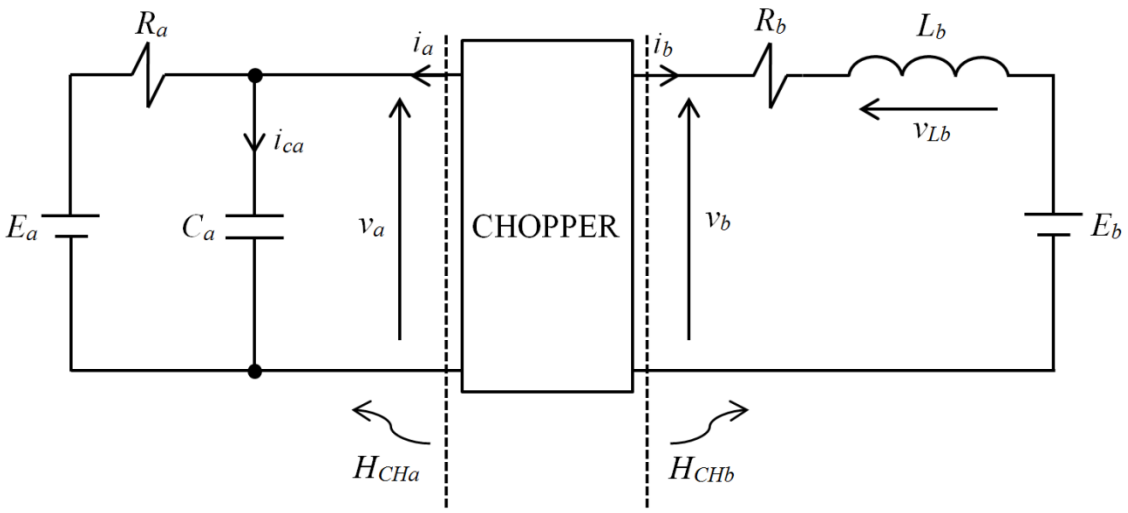

Fig. 4.1. Electric circuit with chopper

The parameters are reported in the Table 4.1.

Table 4.1. Electric circuit parameters

E_a	1000 V
Modulation index	0.7
E_b	600 V
R_d	0.5 Ω
C_d	0.1 mF
R_o	0.5 Ω
L_o	1 mH
switching frequency f_s	5 kHz

The input voltage v_a and the output current i_b absorbed by the load are depicted in Fig. 4.2. and Fig. 4.4.

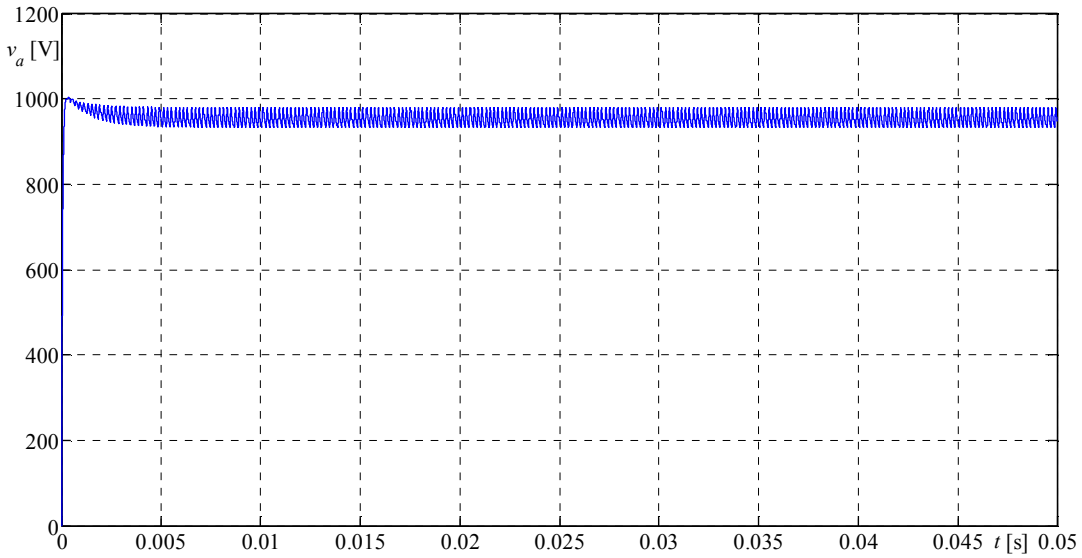

Fig. 4.2. Input voltage v_a

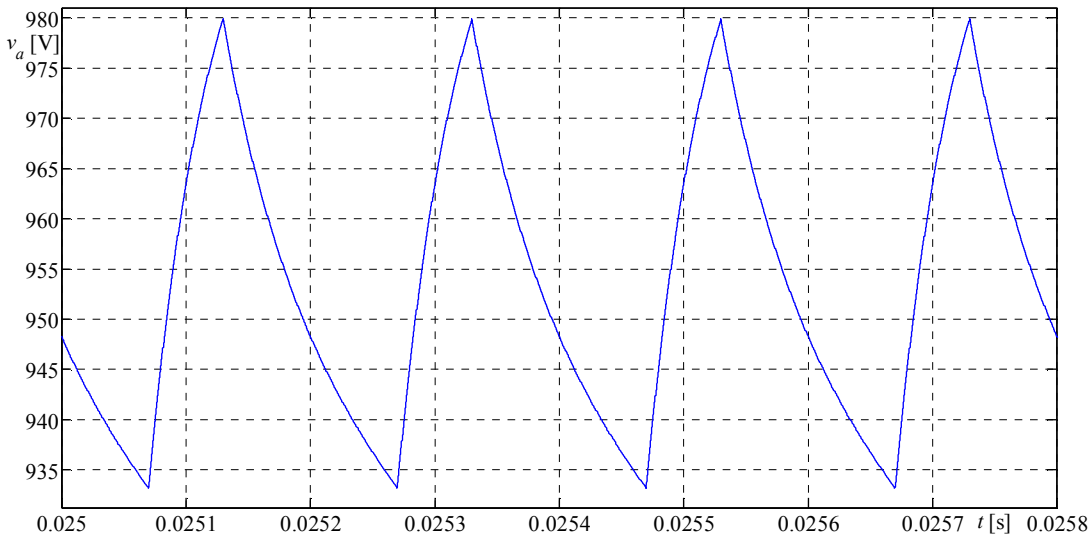

Fig. 4.3. Input voltage v_a (Zoom)

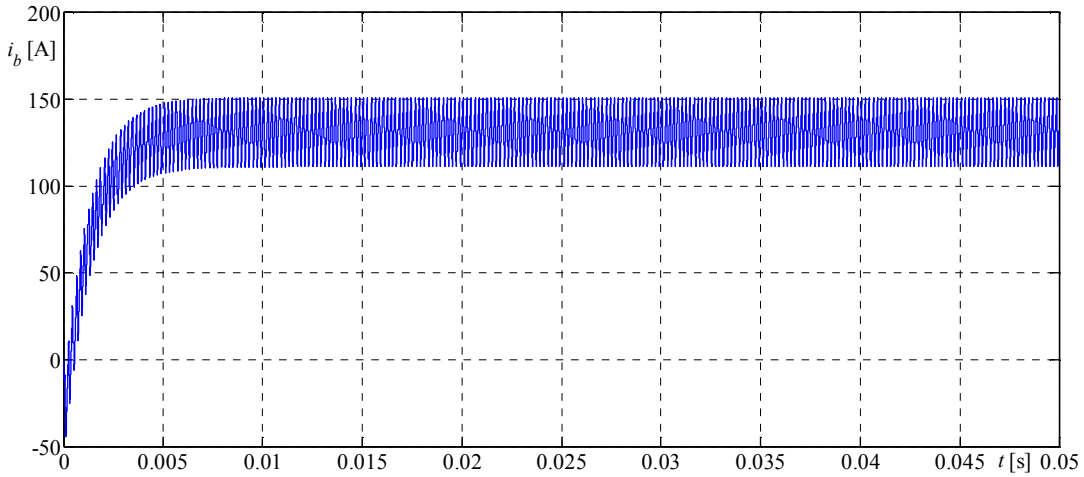

Fig. 4.4. Output current i_b

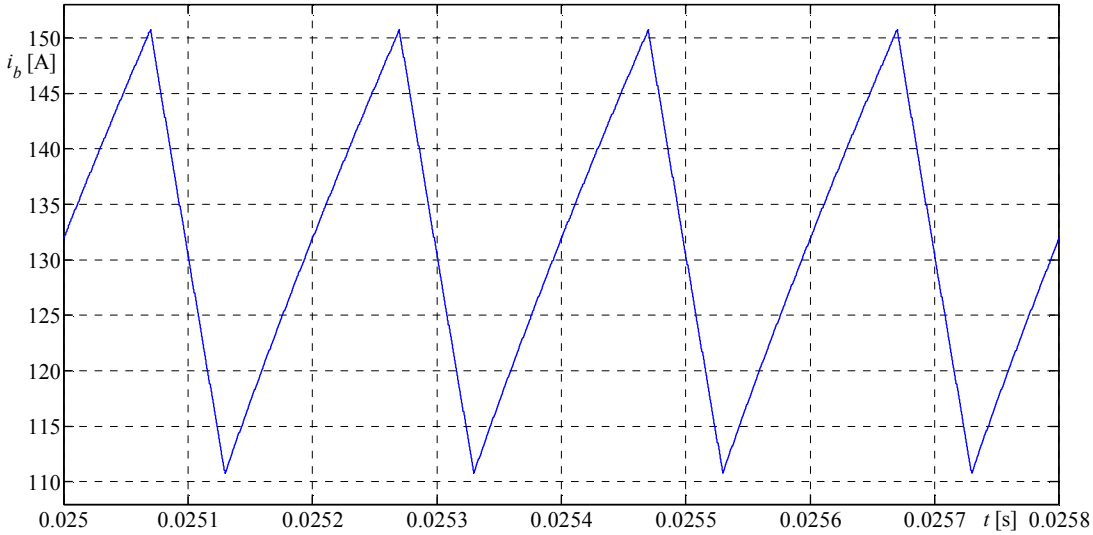

Fig. 4.5. Output current i_b (Zoom)

In order to meet the requests mentioned in the introduction the following electric quantities were measured: v_a, i_a, i_{ca}, v_b, i_b, v_{Lb} with a resolution of 2^{18} samples. All CAT values of the simulation are reported in Table 4.2.

Table 4.2. Values of the CAT

CAT	[MVA/s]
H_{CH}	160.39
H_{Cha}	-29.558
H_{CHb}	189.88
H_{Lb}	189.97
H_{Ca}	-29.575
H_{Ea}	0
H_{Eb}	0

As it can be seen from Table 4.2, the CAT generated by the chopper H_{CH} calculated by using the (2.44) and (3.34) is about equal to the CAT obtained by summing the two contributions H_{CHa} and H_{CHb} calculated by (2.15) doing FFT of voltage and current i_a, v_a, i_b, v_b. The same value H_{CH} is also

obtained by summing the CAT absorbed by the inductor H_{Lb} according to (2.31), capacitor H_{Ca} according to (2.38) and the voltage generators H_{Ea}, H_{Eb} which, in this case, are nil because they are constant dc voltage sources.

It is worth to note that the CAT obtained by the (2.44) and (3.34) is not an approximated value whereas the CATs obtained by (2.15), (2.31) and (2.38) are approximated values according to the resolution of the FFT of the voltage and current related to the input and output sides. In fact, in order to obtain the same values, the resolution of the FFT would be, theoretically, infinite for the exactly convergence of the series.

The following are figures of the closed areas on the *v-i* plane related to CATs generated by the chopper and absorbed by the capacitor and inductor. The observation period is, in this case, equal to the switching period.

Fig. 4.6 shows the closed area on the *v-i* plane related to H_{Cha} which is generated in the input side. From point A to point B the SF $s = 0$, and hence, $i_a = 0$ and v_a increases because the capacitor is charging by means of the voltage generator E_a. From point B to point C a commutation from $s = 0$ to $s = 1$ applies and the current i_a jumps from zero to i_b. From point C to point D the current i_a increases together with i_b which charges the inductor in the output side meanwhile the voltage v_a decreases because the capacitor is discharging.

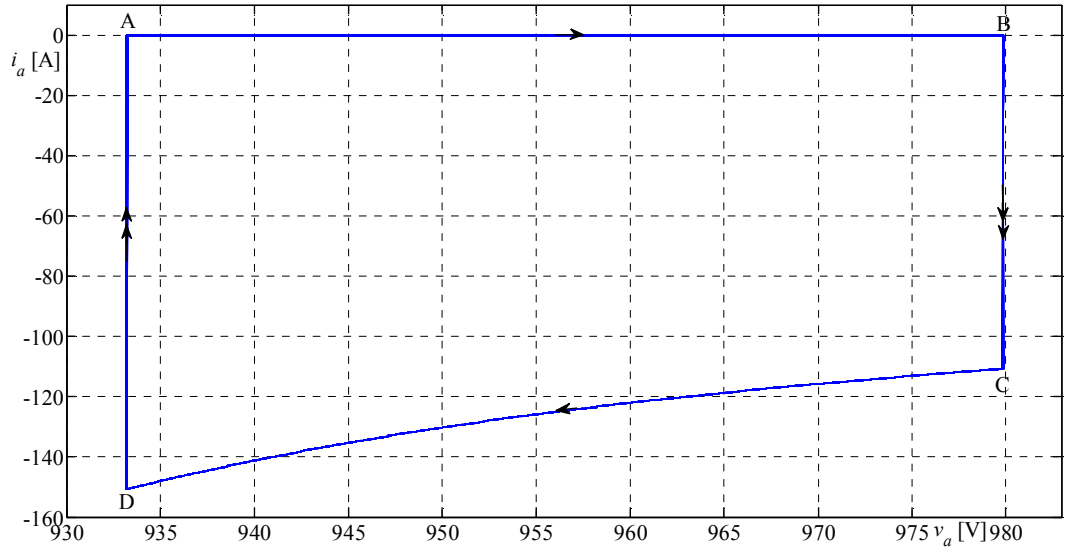

Fig. 4.6. Closed area on the *v-i* plane generated by the chopper in the input side. Single arrow stays for continuous part; double arrow stays for jump discontinuity

Fig. 4.7shows the closed area on the *v-i* plane related to H_{Chb} which is generated in the output side. From point A to point B the SF $s = 0$, and hence, $v_b = 0$ and i_b decreases because the inductor is discharging over the resistor R_b and over the voltage generator E_b. From point B to point C a commutation from $s = 0$ to $s = 1$ applies and the voltage v_b jumps from zero to v_a. From point C to point D the current i_b increases together with i_a which discharges the capacitor in the input side, indeed the voltage v_a decreases because the capacitor is discharging.

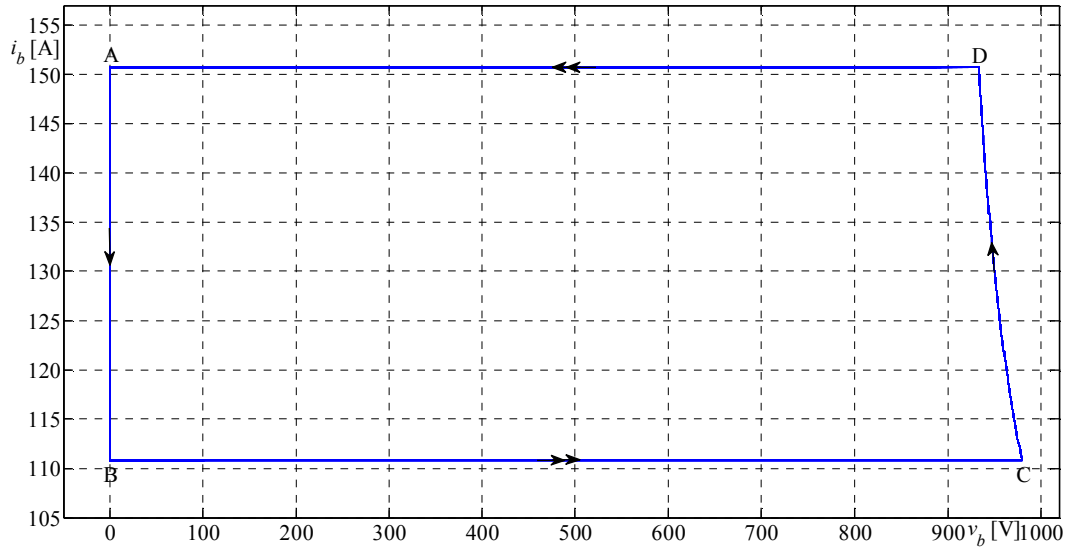

Fig. 4.7. Closed area on the *v-i* plane generated by the chopper in the output side. Single arrow stays for continuous part; double arrow stays for jump discontinuity

Fig. 4.8 shows the closed area on the *v-i* plane related to H_{Ca} which is absorbed by the capacitor in the input side. From point A to point B the SF $s = 0$, the capacitor is charging by the voltage generator E_a, and hence, v_a increases and i_{ca} decreases. From point B to point C a commutation from $s = 0$ to $s = 1$ applies and the current of the capacitor i_{ca} jumps from a positive value to a negative one. From point C to point D the current i_{ca} increases meanwhile the voltage v_a decreases because the capacitor is discharging. As it is possible to see by the Table 4.2, the CAT absorbed by the capacitor is equal to the CAT generated by the chopper in the input side. The two related closed areas of Fig. 4.6 and Fig. 4.8 are, indeed, the same.

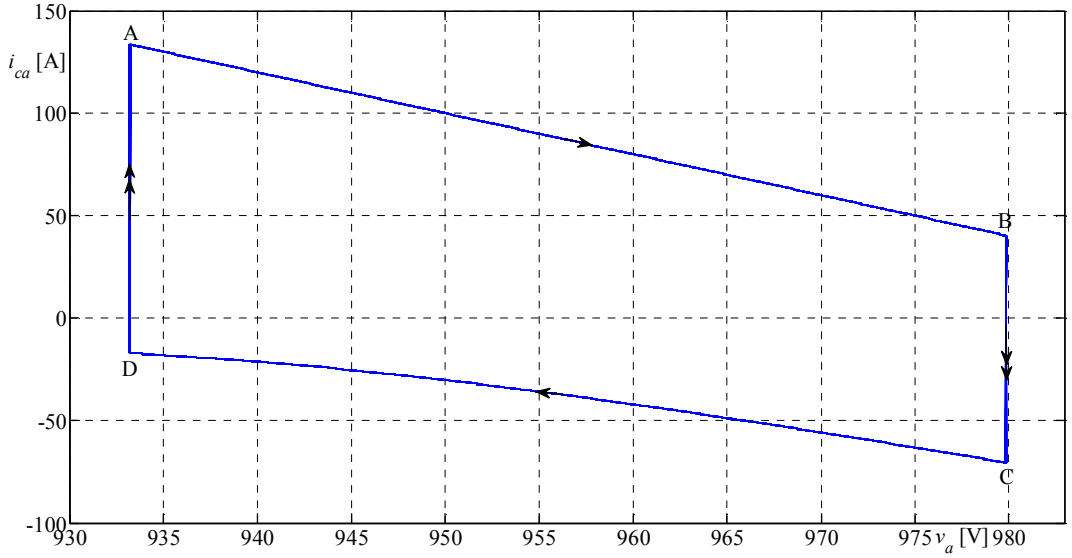

Fig. 4.8. Closed area on the *v-i* plane of the capacitor. Single arrow stays for continuous part; double arrow stays for jump discontinuity

Fig. 4.9 shows the closed area on the *v-i* plane related to H_{Lb} which is absorbed by the inductor in the output side. From point A to point B the SF $s = 0$, the inductor is discharging over the resistor R_b and over the voltage generator E_b, and hence, i_b decreases and v_{Lb} increases. From point B to point

C a commutation from $s = 0$ to $s = 1$ applies and the voltage on the inductor v_{Lb} jumps from a negative value to a positive one. From point C to point D the voltage v_{Lb} decreases meanwhile the current i_b increases because the inductor is charging. As it is possible to see by the Table 4.2, the CAT absorbed by the inductor is equal to the CAT generated by the chopper in the output side. The two related closed areas of Fig. 4.6, Fig. 4.8 and Fig. 4.7, Fig. 4.9 are, indeed, the same.

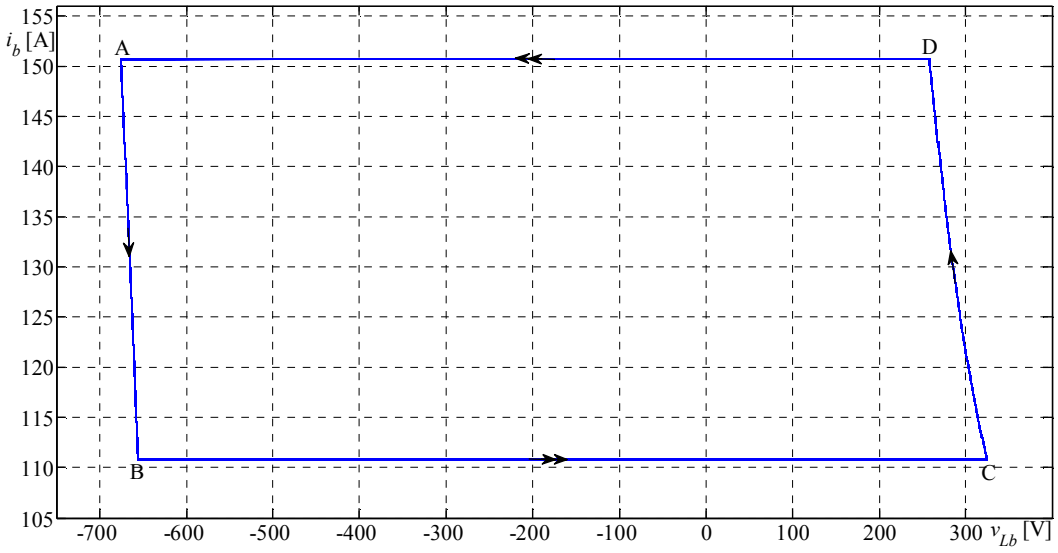

Fig. 4.9. Closed area on the *v-i* plane of the inductor. Single arrow stays for continuous part; double arrow stays for jump discontinuity

Under ideal conditions if the voltage on the capacitor v_a and the output current i_b were constant without ripple, the total area generated by the chopper would be nil because in the input side only vertical jumps between zero and i_b value of current would take place, and in the output side only horizontal jumps between zero and v_a value of voltage would take place.

Fig. 4.10 shows the SP generated by the chopper in a bar diagram. As it can be seen, the SP after two commutations is repeated at the same way. Indeed, into the switching period only two different commutations occur.

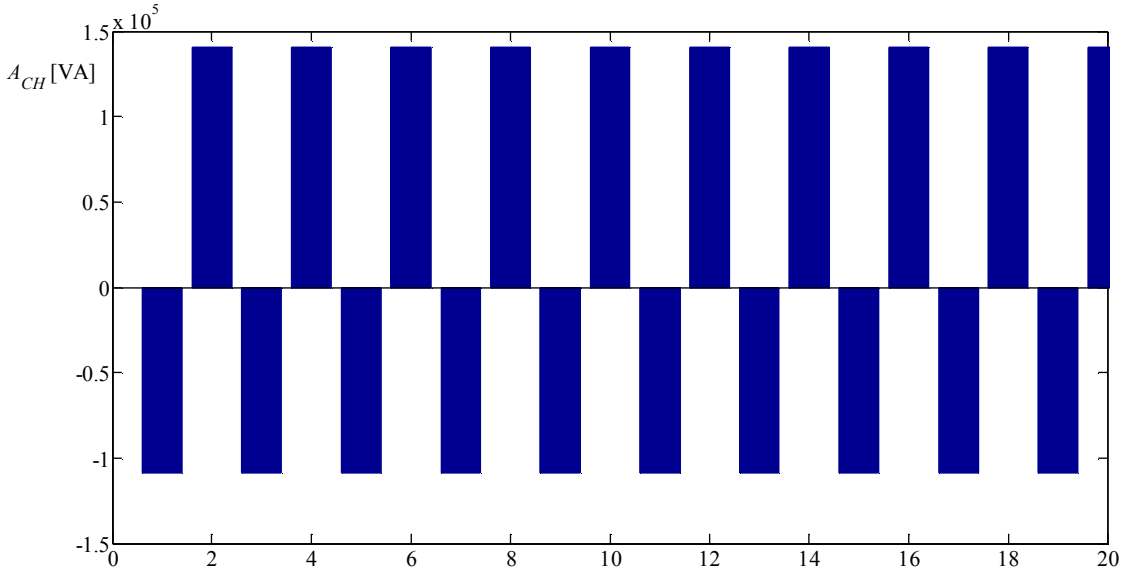

Fig. 4.10. Switching Power generated by the chopper

4.3 Three-Phase Voltage Source Inverter

The electric circuit is depicted in Fig. 4.11 and it is composed of two capacitors fed by a constant voltage source E_a in the dc side and a balanced active three-phase load in the ac side. In the ac side a sinusoidal balanced voltage tern $v_{b1,b2,b3}$ is generated by using the standard PWM modulation with a triangular carrier.

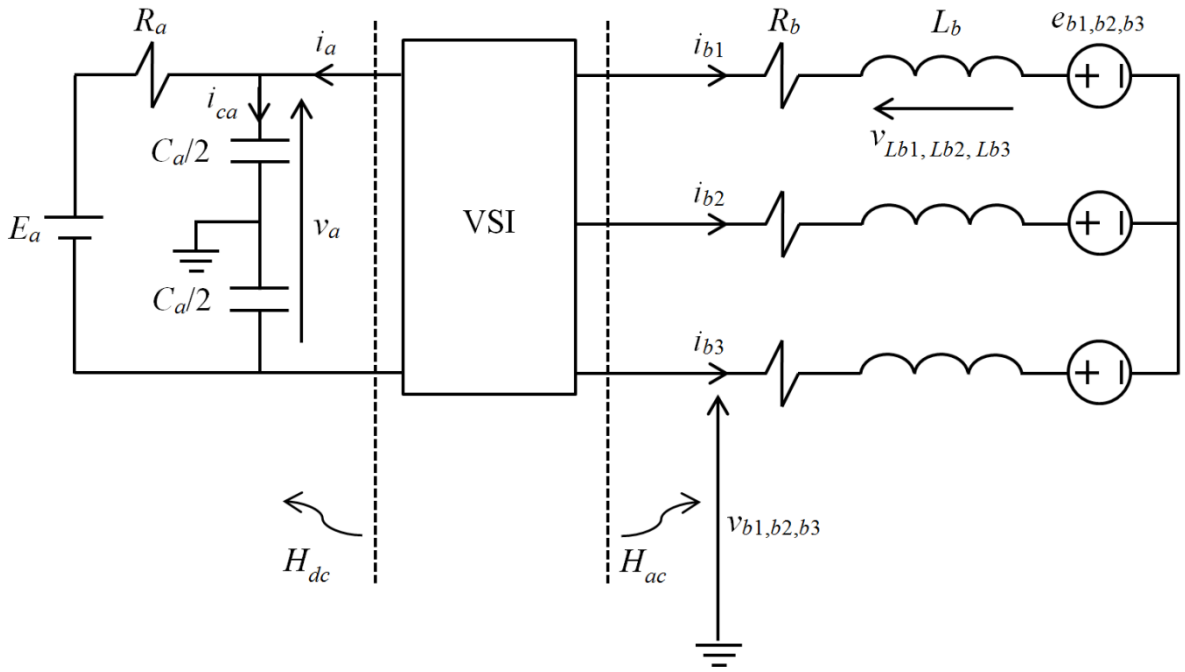

Fig. 4.11. Electric circuit with three-phase voltage source inverter

The parameters are reported in the Table 4.3.

Table 4.3. Electric circuit parameters

E_a	1000 V
AC voltage - mod. index	230 V (RMS) − 0.68
$e_{b1,b2,b3}$	173 V (RMS) − 5° lag.
R_a	0.5 Ω
C_a	0.1 mF
R_b	0.5 Ω
L_b	1 mH
output frequency f_o	50 Hz
switching frequency f_s	5 kHz

The input voltage v_a and the output currents $i_{b1,b2,b3}$ absorbed by the load are depicted in Fig. 4.12 and Fig. 4.13.

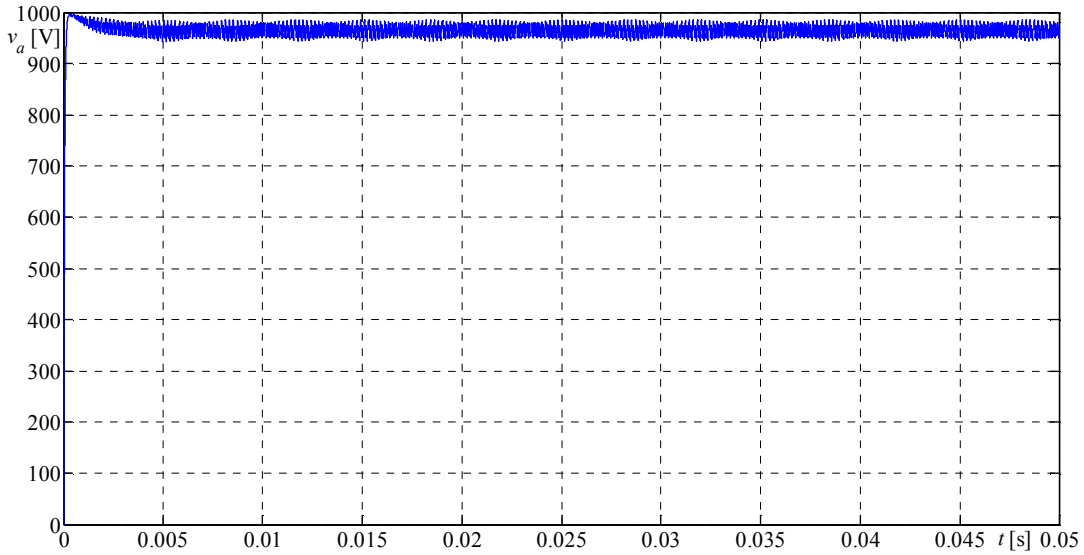

Fig. 4.12. Input voltage v_a

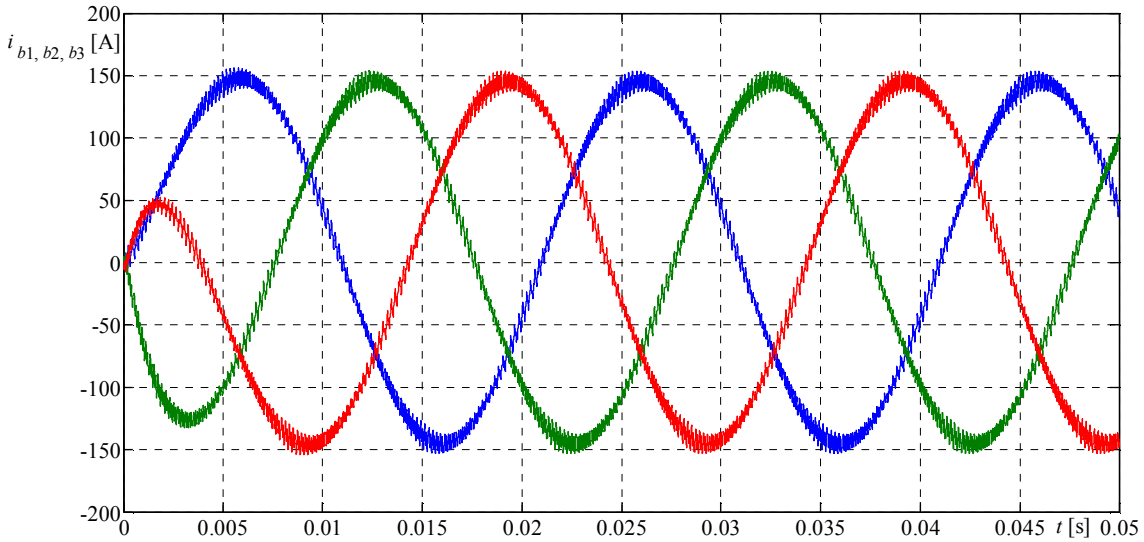

Fig. 4.13. Output currents $i_{b1,b2,b3}$

In order to meet the requests mentioned in the introduction the following electric quantities were measured: v_a, i_a, i_{ca}, $v_{b1,b2,b3}$, $i_{b1,b2,b3}$, $v_{Lb1,Lb2,Lb3}$, $e_{b1,b2,b3}$ with a resolution of 2^{18} samples. All CAT values of the simulation are reported in Table 4.4.

Table 4.4. Values of the CAT

CAT	[MVA/s]
H_{VSI}	155.19
H_{ac}	193.35
H_{dc}	-38.310
H_{Lb}	189.86
H_{Ca}	-38.341
H_{Ea}	0
H_e	3.6867

As it can be seen from Table 4.4, the CAT generated by the converter H_{VSI} calculated by using the (2.44) and (3.58) is about equal to the CAT obtained by summing the two contributions H_{ac} and H_{dc} calculated by (2.15) doing FFT of voltage and current i_a, v_a, $v_{b1,b2,b3}$, $i_{b1,b2,b3}$,. The same value H_{VSI} is also obtained by summing the CATs absorbed by inductors H_{Lb} according to (2.31), capacitor H_{Ca} according to (2.38), and voltage generators H_e, H_{Ea}.

The following are figures of the closed areas on the *v-i* plane related to CATs generated by the chopper and absorbed by the capacitor and inductor. The observation period is, in this case, equal to the fundamental period of the sinusoidal output, i.e. 20 ms.

Fig. 4.14 shows the closed area on the *v-i* plane related to H_{dc} which is generated by the inverter in the dc side. In this case the area is more complex respect to the previous case because the area involved depends by the three output currents. Considering the state diagram of the inverter reported in Fig. 3.20, the transition from one of the points A to one of the points B applies when all SFs are 1 or 0 and they are called nil configurations. Indeed, in this case the current i_a is nil because the sum of the three output currents is constrained to be zero. Hence, the voltage v_a on the capacitor increases because is charging by means of the voltage source E_a. The transition from one of the points C to one of the points D applies when the SFs are in a not nil configuration, i.e. SFs are not all 1 or 0 and they are called active configurations. The jump discontinuity from one of the points B to one of the points C occurs when a commutation between one nil configuration and one active configuration takes place. Vice versa the jump discontinuity from one of the points D to one of the points A occurs when a commutation between one active configuration and one nil configuration takes place. In the other cases, when a commutation between two different active configurations takes place, a jump discontinuity between one of the points C or D and one of the points E occurs.

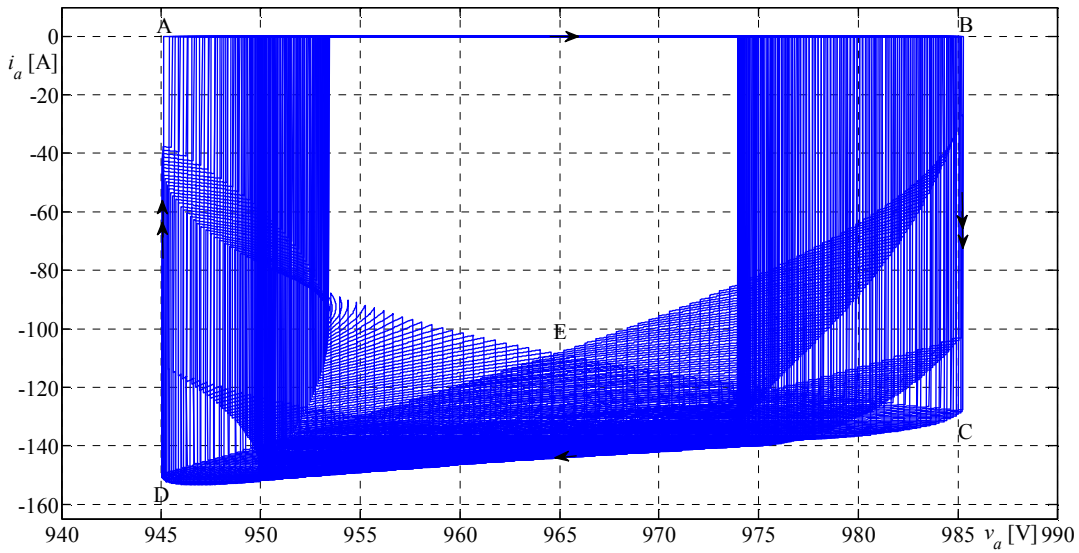

Fig. 4.14. Closed area on the *v-i* plane generated by the inverter in the dc side. Single arrow stays for continuous part; double arrow stays for jump discontinuity

Fig. 4.15, Fig. 4.16 and Fig. 4.17 show the closed areas on the *v-i* plane related to H_{ac} which is generated in the ac side. As it is possible to note the three figures are very similar each other because the three output voltages and the three output currents are balance. These areas are composed of several little rectangular subareas due to the switching. These rectangular subareas are distorted because of the ripple at the switching frequency. Indeed, under ideal conditions if the voltage on the capacitors v_a were constant and the three output currents were sinusoidal without ripple, then the area generated by the inverter in the dc side would be nil because only vertical jumps between different values of currents would take place. Instead, in the output side, the voltage v_{b1}, v_{b2} and v_{b3} would jump between $-v_a/2$ and $v_a/2$ and the sinusoidal currents i_{b1}, i_{b2} and i_{b3} would

track perfect rectangular areas. The total resulting area in the ac side would be related only to the fundamental reactive power.

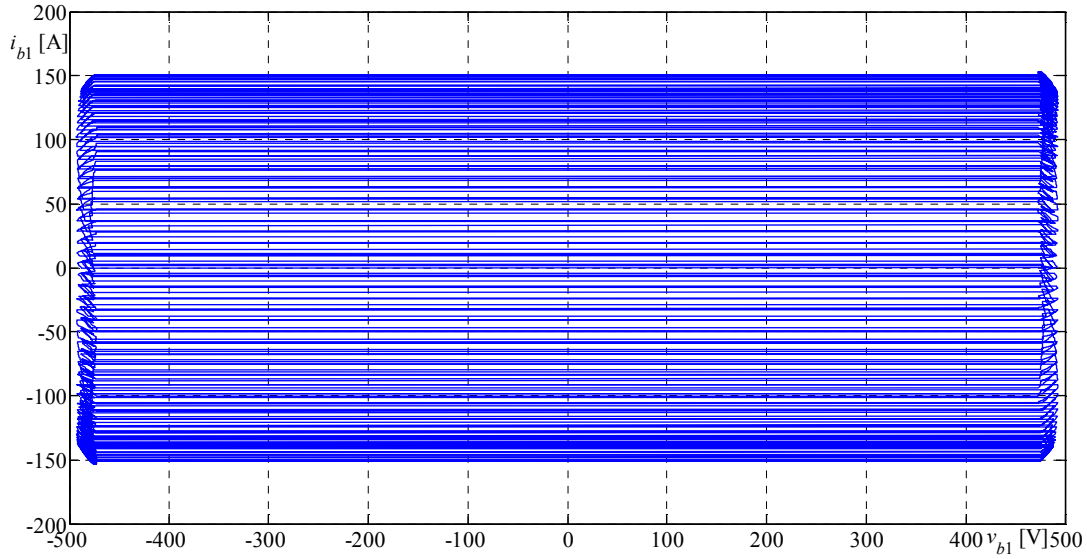

Fig. 4.15. Closed area on the *v*-*i* plane generated by the inverter in the ac side − phase 1.

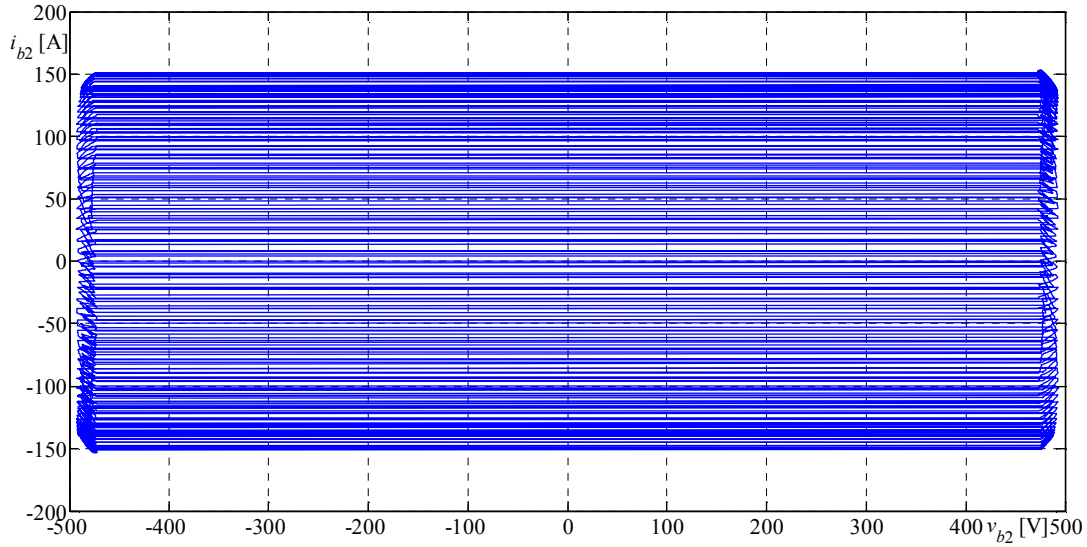

Fig. 4.16. Closed area on the *v*-*i* plane generated by the inverter in the ac side − phase 2.

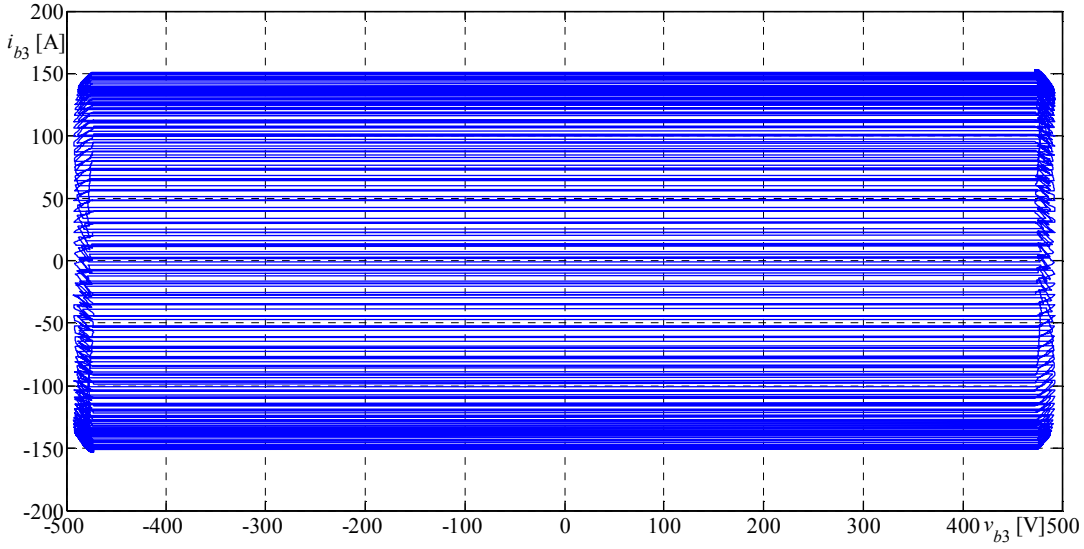

Fig. 4.17. Closed area on the *v*-*i* plane generated by the inverter in the ac side − phase 3.

Fig. 4.18, Fig. 4.19 and Fig. 4.20 show the SP generated by the inverter related to each phase. As it can be seen, into the fundamental period of the sinusoidal output, 200 different SPs are generated because 200 different commutations occur.

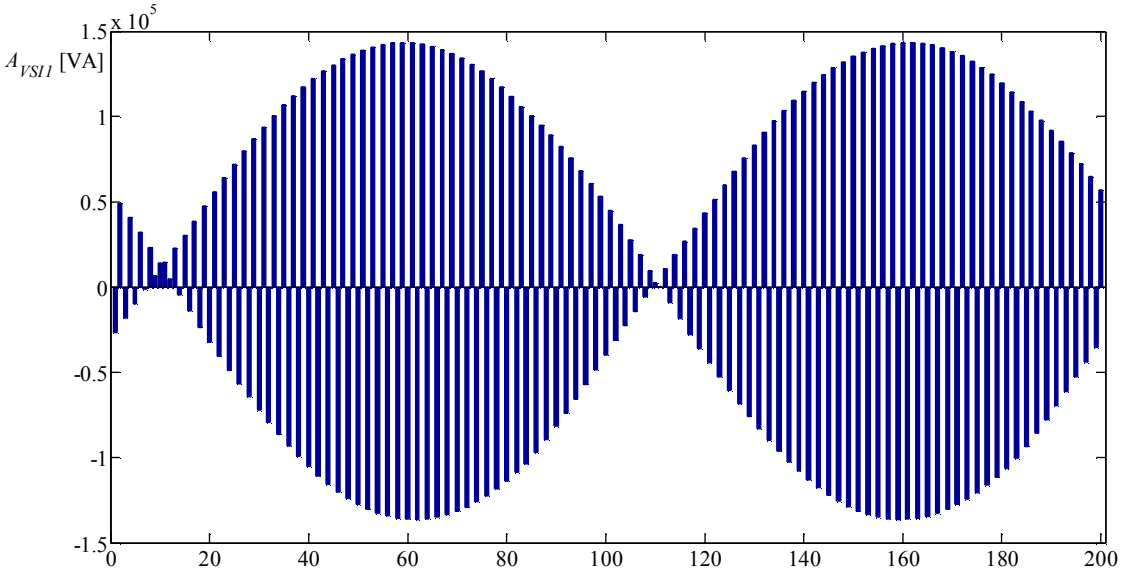

Fig. 4.18. Switching Power generated by the inverter − phase 1

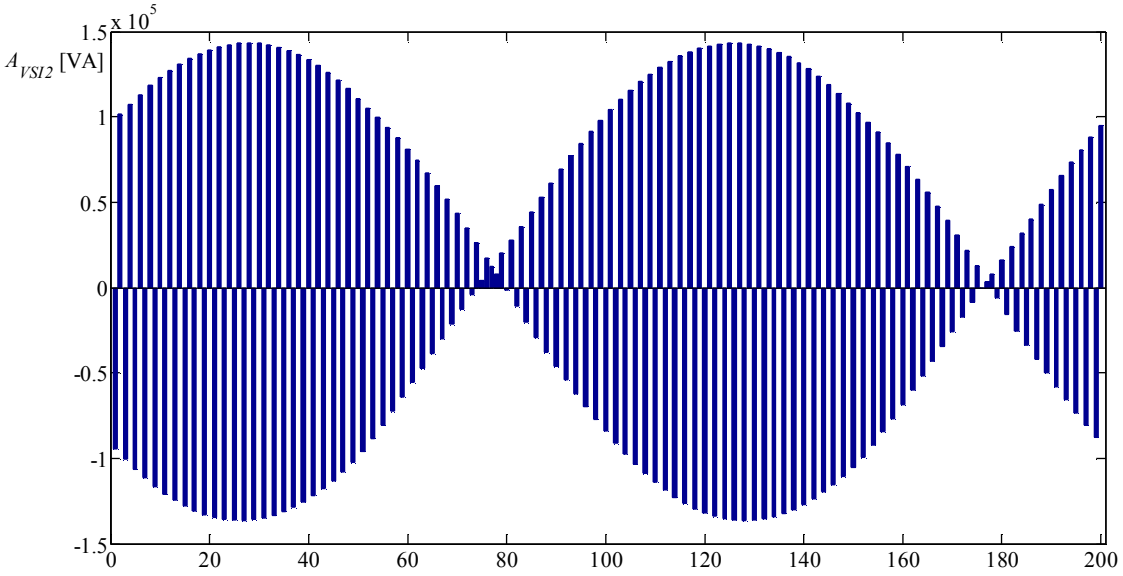

Fig. 4.19. Switching Power generated by the inverter − phase 2

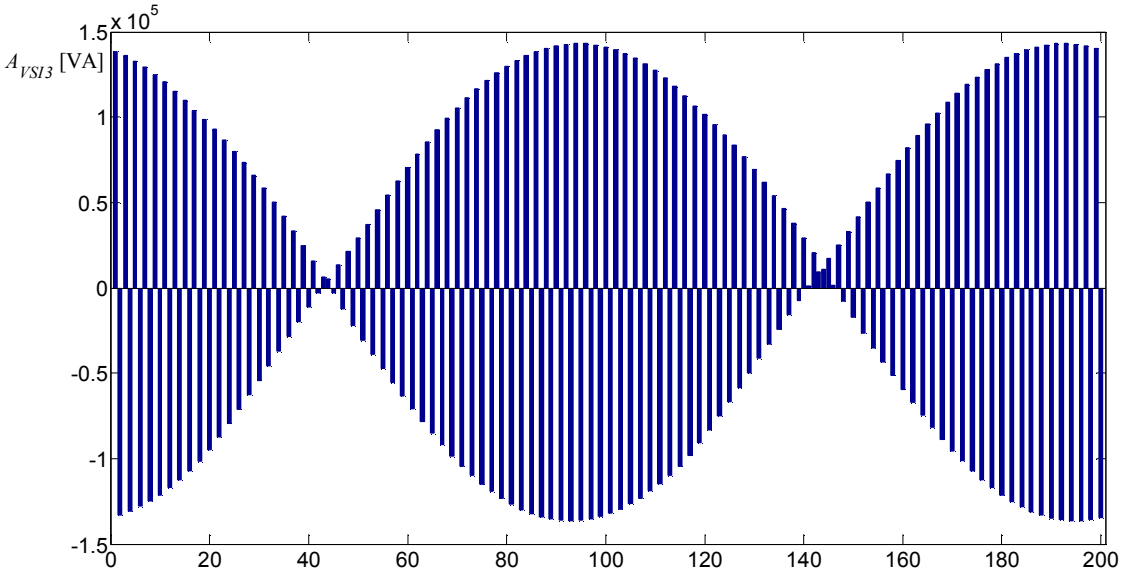

Fig. 4.20. Switching Power generated by the inverter − phase 3

4.4 Three-Phase Matrix Converter

The electric circuit is depicted in Fig. 4.21 and it is composed of three capacitors fed by a three-phase balanced voltage source $v_{s1,s2,s3}$ in the input side and a balanced active three-phase load (current load) in the ac side. Capacitors C_b are used in order to support a three-phase voltage supplying the load. Indeed, in this case the input voltage sources have a certain amplitude and frequency while the output voltages $v_{Cb1,Cb2,Cb3}$ have a different amplitude and frequency. The control strategy used in this converter is a current control modulation which tracks a rate voltage on the capacitors C_b and gives a unitary input power factor in the input side of the matrix converter.

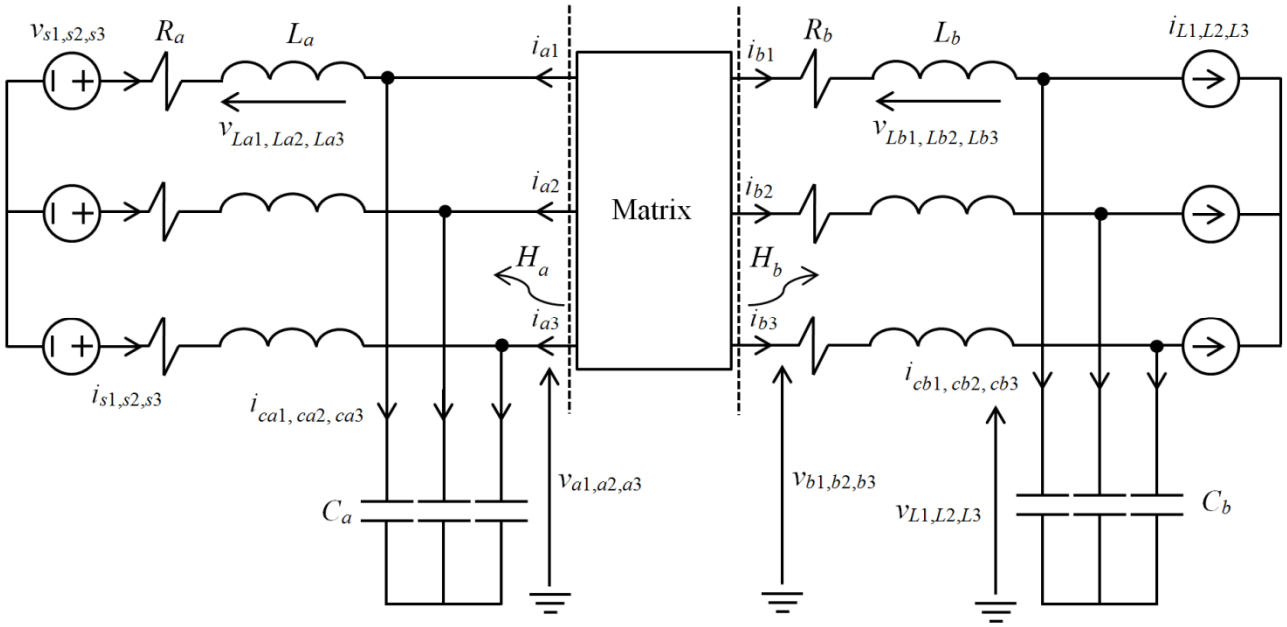

Fig. 4.21. Electric circuit with matrix converter

The parameters are reported in the Table 4.5.

Table 4.5. Electric circuit parameters

$v_{s1,s2,s3}$	306 V (RMS)
$v_{L1,L2,L3}$	220 V (RMS)
$i_{L1,L2,L3}$	49.5 A (RMS) − 20° lag.
R_a	0.02 Ω
L_a	5.6 μF
C_a	0.5 mF
R_b	0.001 Ω
L_b	0.3 mH
C_b	0.5 mF
input frequency f_i	50 Hz
output frequency f_o	100 Hz
average switching frequency	20 kHz

The input voltage $v_{a1,a2,a3}$, the output currents $i_{b1,b2,b3}$ and the voltage on the load are depicted in Fig. 4.22, Fig. 4.23 and Fig. 4.24.

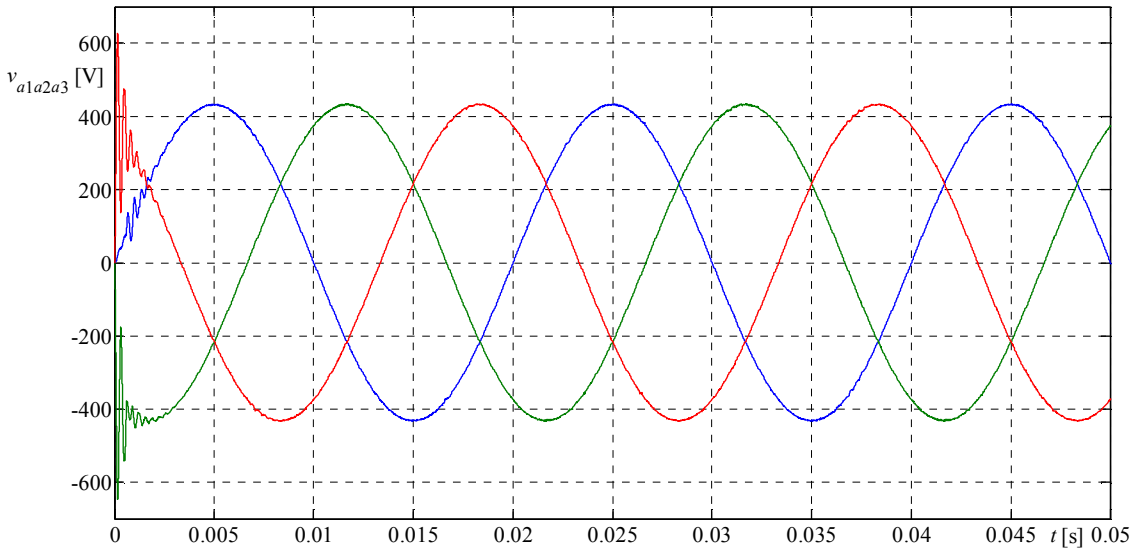

Fig. 4.22. Input voltages $v_{a1,a2,a3}$

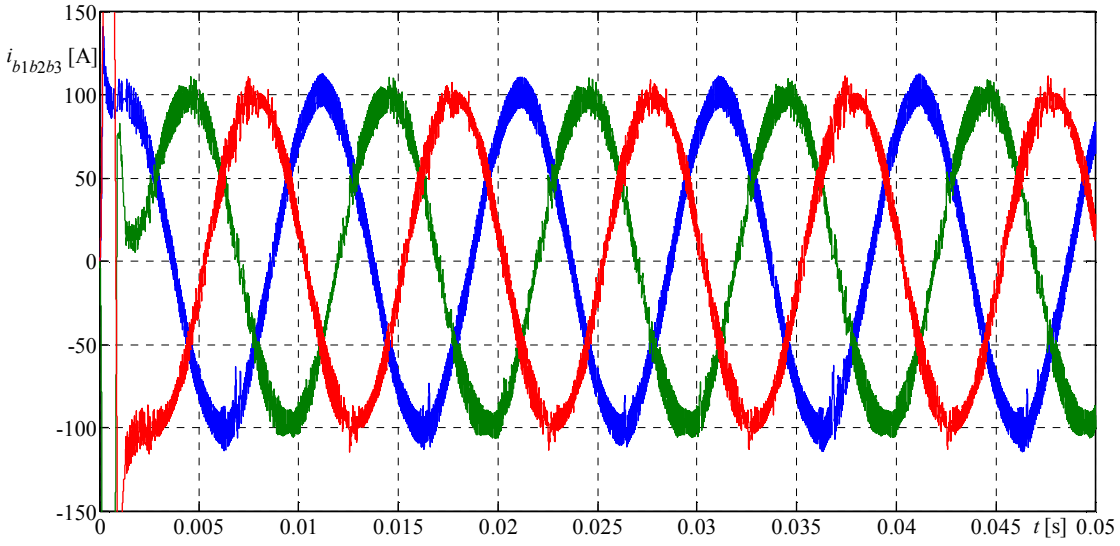

Fig. 4.23. Output currents $i_{b1,b2,b3}$

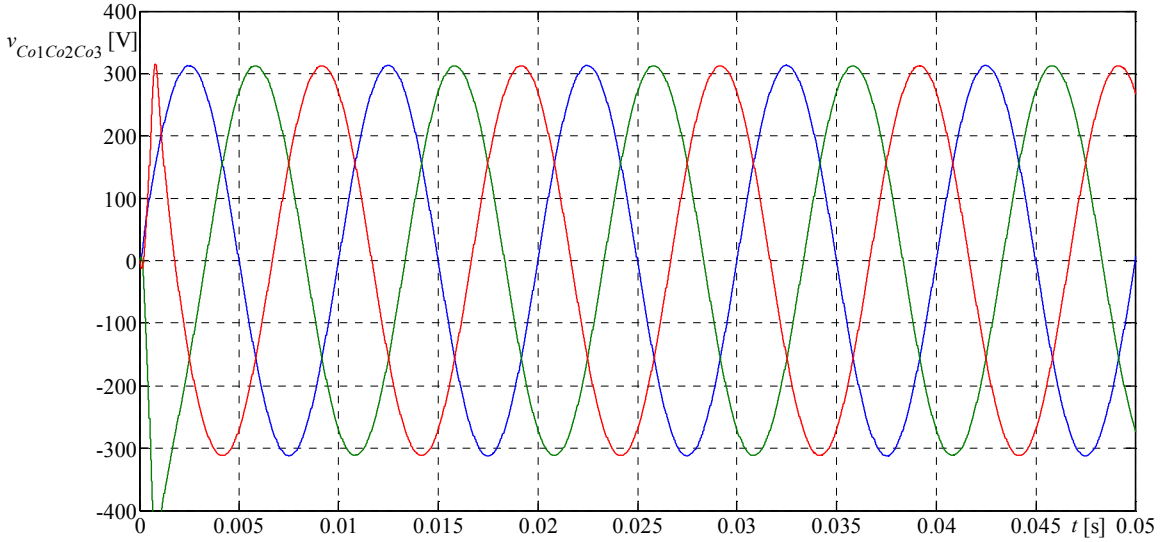

Fig. 4.24. Output capacitor voltages $v_{Co1,Co2,Co3}$

In order to meet the requests mentioned in the introduction the following electric quantities were measured: $v_{a1,a2,a3}$, $i_{a1,a2,a3}$, $v_{La1,La2,La3}$, $i_{ca1,ca2,ca3}$, $v_{b1,b2,b3}$, $i_{b1,b2,b3}$, $v_{Lb1,Lb2,Lb3}$, $i_{cb1,cb2,cb3}$, $v_{s1,s2,s3}$, $i_{s1,s2,s3}$ with a resolution of 2^{17} samples. All CAT values of the simulation are reported in Table 4.6.

Table 4.6. Values of the CAT

CAT	[MVA/s]
H_{MATRIX}	350.86
H_a	-8.8992
H_b	357.94
H_{La}	0.37835
H_{Ca}	-23.376
H_{Lb}	382.63
H_{Cb}	-29.026
$H_{vs1,vs2,vs3}$	13.802
$H_{iL1,iL2,iL3}$	3.5138

As it can be seen from Table 4.6, the CAT generated by the matrix converter H_{MATRIX} calculated by using the (2.44) and (3.75) is about equal to the CAT obtained by summing the two contributions H_a and H_b calculated by (2.15) doing FFT of voltage and current $v_{a1,a2,a3}$, $i_{a1,a2,a3}$, $v_{b1,b2,b3}$, $i_{b1,b2,b3}$,. The same value H_{MATRIX} is also obtained by summing the CATs absorbed by inductors H_{La}, H_{Lb}, capacitors H_{Ca}, H_{Co}, voltage generators $H_{vs1,vs2,vs3}$ and current load $H_{iL1,iL2,iL3}$.

Fig. 4.25, Fig. 4.26 and Fig. 4.27 show the closed areas on the *v-i* plane related to H_a which is generated by the matrix converter in the input side. Since the control strategy gives a unitary input power factor the area generated in the input is only due to the ripple.

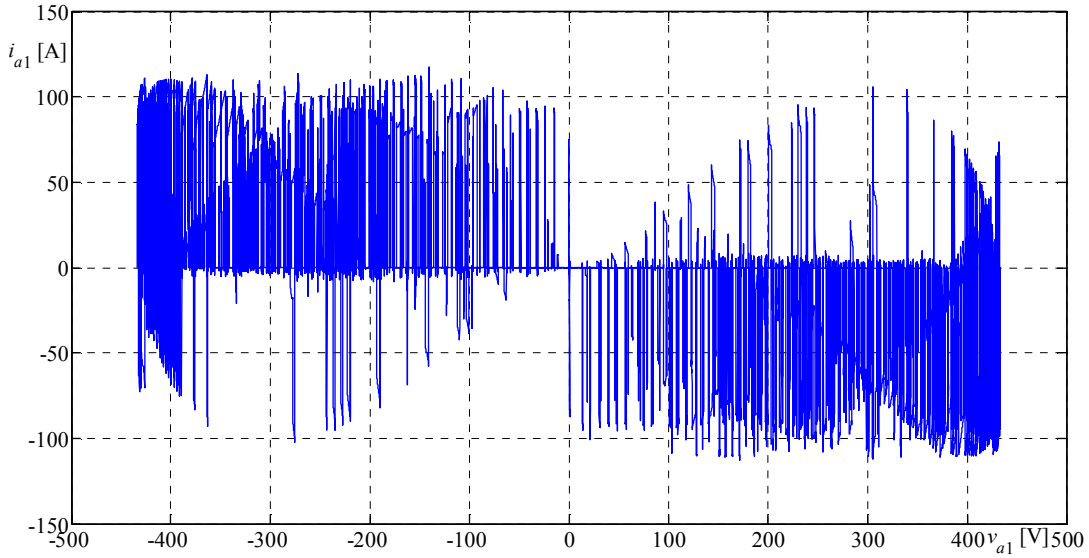

Fig. 4.25. Closed area on the *v-i* plane generated by the matrix converter in the input side − phase 1.

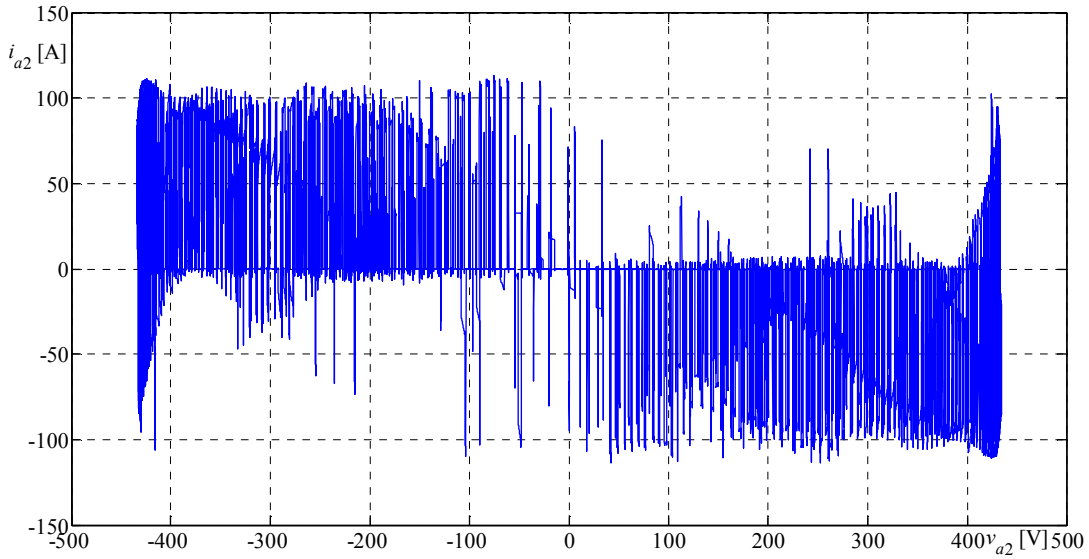

Fig. 4.26. Closed area on the *v-i* plane generated by the matrix converter in the input side − phase 2.

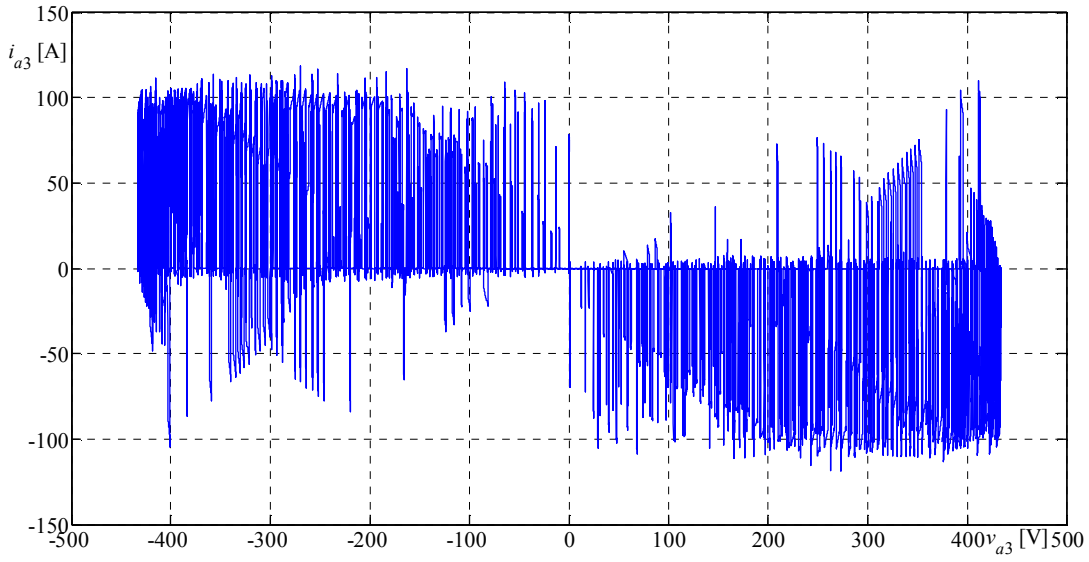

Fig. 4.27. Closed area on the *v*-*i* plane generated by the matrix converter in the input side − phase 3.

Fig. 4.28, Fig. 4.29 and Fig. 4.30 show the closed areas on the *v*-*i* plane related to H_b which is generated by the matrix converter in the output side. Since, in this case, both the output currents and the input voltages are sinusoidal with ripple, the total area is constituted by several distorted elliptic subareas.

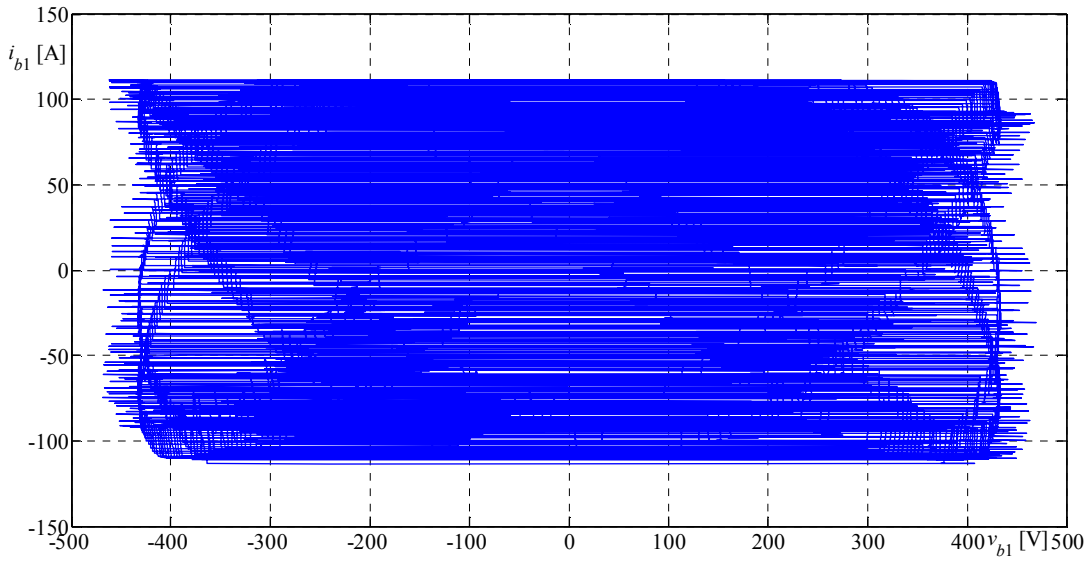

Fig. 4.28. Closed area on the *v*-*i* plane generated by the matrix converter in the output side − phase 1.

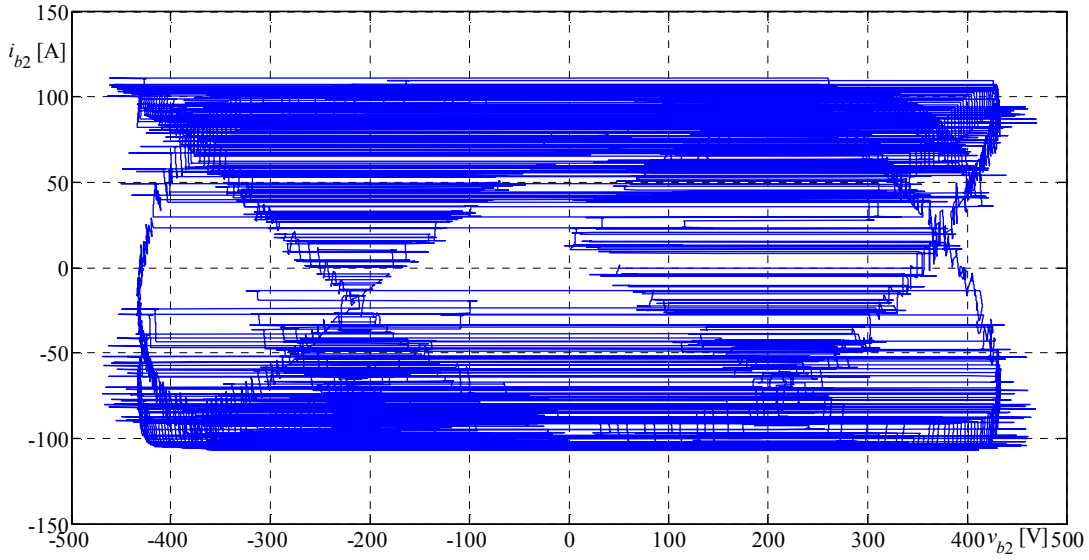

Fig. 4.29. Closed area on the *v*-*i* plane generated by the matrix converter in the output side − phase 2.

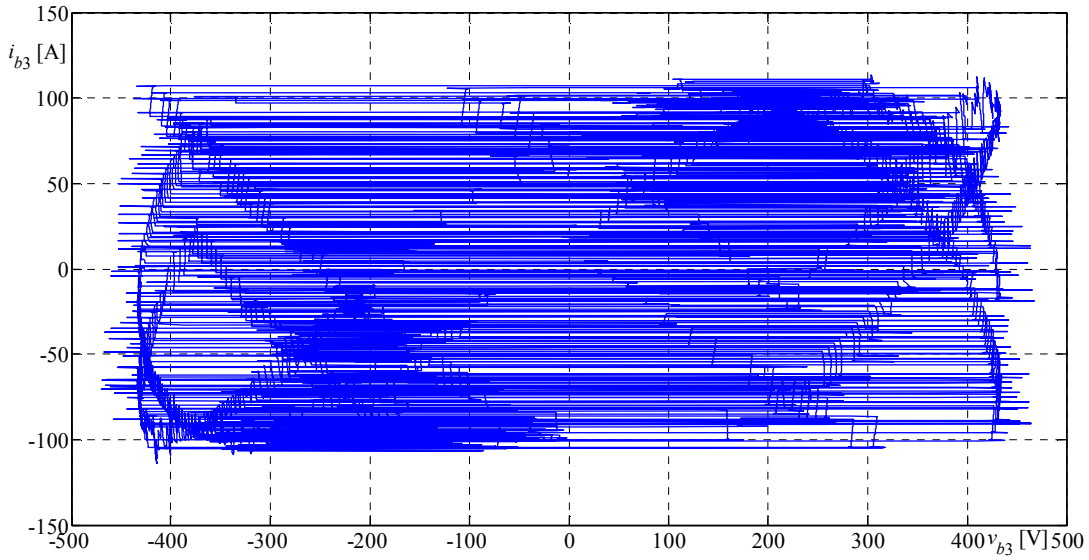

Fig. 4.30. Closed area on the *v*-*i* plane generated by the matrix converter in the output side − phase 3.

5. Jump Power

5.1 Introduction

In this chapter another conservative function, here called *Jump Power* (JP), is developed in order to address some properties and issues of principle regarding one-port elements, in particular ideal diodes and ideal switches. Also in this chapter impulses are explicitly excluded.

5.2 Jump Power

For a two-terminals component, with the reference directions for voltage and current reported in Fig. 2.1 and according to the jump functions (1.64), let us define the *Jump Power* as the following

$$JP(t) = \frac{1}{2} J(v) J(i). \tag{5.1}$$

According to the definition (5.1), the Jump Power is different from zero only when a jump discontinuity both in the voltage and in the current at the same time occurs.

5.2.1 Balance theorem over Jump Power

Since the JP is defined as the product of jump functions of voltage and current which satisfy the Kirchhoff laws, it is possible to state the following:

Theorem 5.I. Given a network constituted by a connection of "p" electric ports and chosen the same reference directions for all ports, the sum of Jump Power extended to the whole network is nil, namely the sum of Jump Power generated is equal to the sum of Jump Power absorbed.

5.2.2 Continuous Generators

For both continuous voltage and continuous current sources, the voltage or the current are imposed to be continuous functions of time, and therefore, the JP absorbed by this kind of generators is always nil.

$$JP_s(t) = 0 \tag{5.2}$$

5.2.3 Resistive one-port

Let us consider a time-invariant nonlinear resistive one-port, with a continuous characteristic on the *v-i* plane, as reported in Fig. 5.1. When a jump discontinuity at the time t^* occurs, the incremental resistance R_Δ (incremental conductance G_Δ) over the interval is considered, as depicted in Fig. 5.1, and according to (1.63), it is possible to write

$$V_\mu \mu(t - t^*) = R_\Delta I_\mu \mu(t - t^*) \quad \left(I_\mu \mu(t - t^*) = G_\Delta V_\mu \mu(t - t^*) \right). \tag{5.3}$$

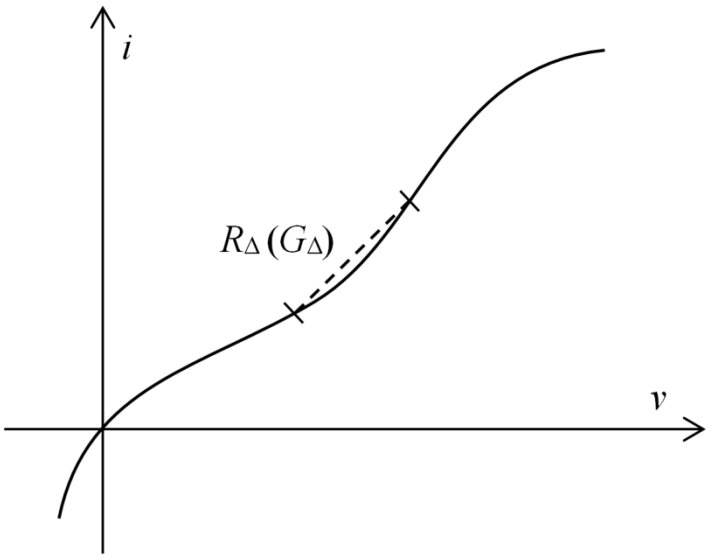

Fig. 5.1. Nonlinear resistor characteristic on the *v-i* plane

By the jump functions (1.64), the (5.3) becomes

$$V_\mu = R_\Delta I_\mu \quad \left(I_\mu = G_\Delta V_\mu\right). \tag{5.4}$$

If the current-voltage characteristic is monotone and nondecreasing, with the constrains $R_\Delta \geq 0$ ($G_\Delta \geq 0$), the JP absorbed by the nonlinear resistor is

$$JP_R = \frac{1}{2} R_\Delta I_\mu^2 \geq 0 \quad \left(JP_R = \frac{1}{2} G_\Delta V_\mu^2 \geq 0\right). \tag{5.5}$$

If the current-voltage characteristic is linear, i.e. $v = Ri$ ($i = Gv$) with the constrains $R \geq 0$ ($G \geq 0$), the (5.5) becomes

$$JP_R = \frac{1}{2} R I_\mu^2 \geq 0 \quad (JP_R(t) = \frac{1}{2} G V_\mu^2 \geq 0). \tag{5.6}$$

By (5.5) and (5.6), it is possible to state that both a linear and a nonlinear resistor, with a monotone nondecreasing characteristic, always absorbs a nonnegative JP.

5.2.4 Inductive one-port

Let us consider a time-invariant nonlinear inductive one-port. Assuming a flux-controlled continuous characteristic $i = i(\psi)$, as shown in Fig. 5.2, at its terminal it holds:

$$v(t) = \frac{d\psi}{dt} \tag{5.7}$$

$$i = \frac{\psi}{L_\Delta} \tag{5.8}$$

where L_Δ is the incremental inductance over the considered interval, as depicted in Fig. 5.2.

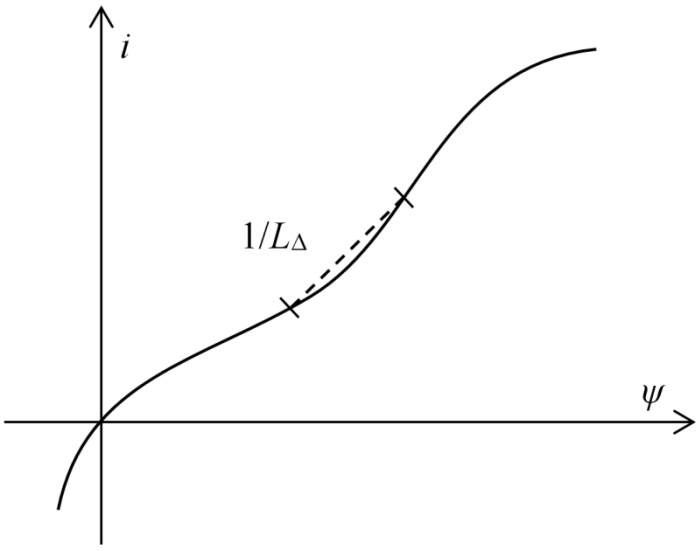

Fig. 5.2. Nonlinear inductor characteristic on the ψ-i plane

From (5.7) and (5.8) the voltage controlled form of the inductor is

$$i(t) = \frac{1}{L_\Delta}\int v dt. \tag{5.9}$$

If the current-flux characteristic is linear, i.e. $i = \psi/L$, the (5.9) becomes

$$i(t) = \frac{1}{L}\int v dt. \tag{5.10}$$

Since the voltage, for hypothesis, does not have impulses, the inductor current is always continuous. Hence, the JP absorbed by both a linear and a nonlinear inductor is always nil.

$$JP_L = 0 \tag{5.11}$$

5.2.5 Capacitive one-port

Let us consider a time-invariant nonlinear capacitive one-port. Assuming a charge-controlled continuous characteristic $v = v(q)$, as shown in Fig. 5.3, at its terminal it holds:

$$i(t) = \frac{dq}{dt} \tag{5.12}$$

$$v = \frac{q}{C_\Delta} \tag{5.13}$$

where C_Δ is the incremental capacitance over the considered interval, as depicted in Fig. 5.3.

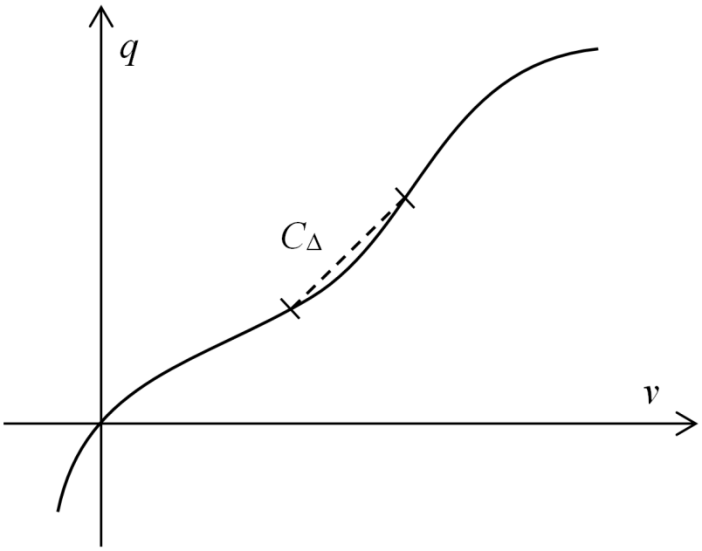

Fig. 5.3. Nonlinear capacitor characteristic on the *v*-*q* plane

From (5.12) and (5.13) the current controlled of the capacitor is

$$v(t) = \frac{1}{C_\Delta}\int i dt. \tag{5.14}$$

If the voltage-charge characteristic is linear, i.e. $v = q/C$, the (5.14) becomes

$$v(t) = \frac{1}{C}\int i dt. \tag{5.15}$$

Since the current, for hypothesis, does not have impulses, the capacitor voltage is always continuous. Hence, the JP absorbed by both a linear and a nonlinear capacitor is always nil.

$$JP_C = 0 \tag{5.16}$$

5.2.6 Ideal Switch one-port

Let us consider the ideal switch depicted in Fig. 2.11.

Closing commutation

When the ideal switch closes at time t^*, the voltage $V_{SW} = v(t^*_-)$ that was applied on the switch becomes nil and the current that was nil becomes $I_{SW} = i(t^*_+)$. Hence, it is possible to write

$$\begin{aligned} v(t) &= V_{SW}(1-\mu(t-t^*)) \\ i(t) &= I_{SW}\mu(t-t^*). \end{aligned} \tag{5.17}$$

According to (5.1) the JP absorbed by the ideal switch is

$$JP_{SWclosed} = -\frac{1}{2}V_{SW}I_{SW}. \tag{5.18}$$

Opening commutation

When the ideal switch opens at time t^*, the current $I_{SW} = i(t^*_-)$ that was flowing is interrupted and the voltage that was nil becomes $V_{SW} = v(t^*_+)$. Hence, it is possible to write

$$\begin{aligned} v(t) &= V_{SW}\,\mu(t-t^*) \\ i(t) &= I_{SW}\,(1-\mu(t-t^*)). \end{aligned} \tag{5.19}$$

According to (5.1) the JP absorbed by the ideal switch is

$$JP_{SWopen} = -\frac{1}{2} V_{SW} I_{SW}. \tag{5.20}$$

Equations (5.18) and (5.20) yield the same result. Hence, the ideal switch involves the same JP both in opening and closing commutations.

If $V_{SW}\, I_{SW} > 0$ (active hard switching) the ideal switch absorbs, both in opening and closing commutations, a negative JP. In other hands, the ideal switch generates JP.

If $V_{SW}\, I_{SW} < 0$ (passive hard switching) the ideal switch absorbs a positive JP. By this fact, it is possible to state that the JP absorbed by the ideal switch depends only on the condition of active or passive hard switching.

According to (2.42) and (2.43) the JP is related to the Switching Power as follows

$$\begin{aligned} JP_{SWclosed} &= -\frac{1}{2} V_{SW} I_{SW} = -A_{SWclosed} \\ JP_{SWopen} &= -\frac{1}{2} V_{SW} I_{SW} = A_{SWopen}. \end{aligned} \tag{5.21}$$

5.2.7 Ideal Diode one-port

Let us consider an ideal diode with its characteristic on the *v-i* plane as reported in Fig. 5.4. It is a particular nonlinear resistor.

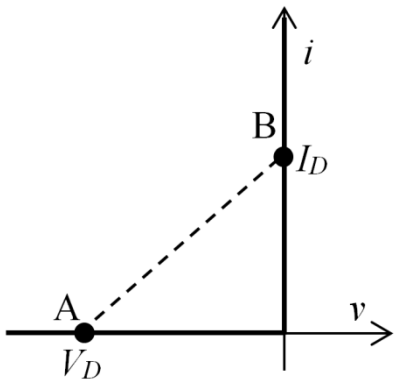

Fig. 5.4. Ideal diode characteristic on the *v-i* plane

Closing commutation

When the ideal diode, due to the remaining part of the network, jumps at time t^* from the point A to the point B on its characteristic, the voltage $V_D = v(t^*_-) \leq 0$ that was applied on the diode becomes nil and the current that was nil becomes $I_D = i(t^*_+) \geq 0$. Hence, it is possible to write

$$\begin{aligned} v(t) &= V_D(1-\mu(t-t^*)) \\ i(t) &= I_D\mu(t-t^*). \end{aligned} \tag{5.22}$$

According to (5.1) the JP absorbed by the ideal diode is

$$JP_{Dclosed} = -\frac{1}{2}V_D I_D \geq 0 \quad (V_D I_D \leq 0). \tag{5.23}$$

Opening commutation

When the ideal diode, due to the remaining part of the network, jumps at time t^* from the point B to the point A on its characteristic, the current $I_D = i(t^*_-) \geq 0$ that was flowing is interrupted and the voltage that was nil becomes $V_D = v(t^*_+) \leq 0$. Hence, it is possible to write

$$\begin{aligned} v(t) &= V_D\mu(t-t^*) \\ i(t) &= I_D(1-\mu(t-t^*)). \end{aligned} \tag{5.24}$$

According to (5.1) the JP absorbed by the ideal switch is

$$JP_{Dopen} = -\frac{1}{2}V_D I_D \geq 0 \quad (V_D I_D \leq 0). \tag{5.25}$$

By (5.23) and (5.25) it is possible to state that the ideal diode can only absorb a nonnegative JP. Indeed, because of its characteristic, only passive hard switching is allowed.

5.3 Some Theorems Based on Jump Power

Table 5.1 shows the Jump Power absorbed by resistors, inductors, capacitors, continuous generators, ideal switches and ideal diodes.

Table 5.1. Jump Power absorbed by one-port elements

Electric Elements	Jump Power
Continuous generators	0
Linear and nonlinear resistor with a monotone nondecreasing characteristic	≥ 0
Linear and nonlinear inductor	0
Linear and nonlinear capacitor	0
Ideal switch	≥ 0 (passive hard switching) ≤ 0 (active hard switching)
Ideal diode	≥ 0 (passive hard switching)

It is shown from Table 5.1 that all dynamic elements, as inductors and capacitors, in addition to continuous generators do not absorb JP. The ideal switch can absorb or generate JP meanwhile the ideal diode can only absorb JP. For this reason it is possible to state the following:

Statement 5.I. Since the JP absorbed by the ideal diode is always nonnegative, it can involve only passive hard switching commutations. This confirms that, as already stated in chapter 2, the ideal diode is a nonlinear resistor which can be seen as an ideal switch, that commutes in soft switching and only in passive hard switching.

Theorem 5.II. Given an electric network composed of continuous generators, resistors, inductors, capacitors, ideal diodes and ideal switches in which Jump Power is involved, then at least one ideal switch that commutes in active hard switching (the only one element able to generate Jump Power) is needed.

Theorem 5.III. If an ideal switch applies an active hard switching commutation generating Jump Power, then in order to obey to the balance theorem over Jump Power, at least another element able to absorb Jump Power, as a resistor, an ideal diode or another ideal switch that commutes in passive hard switching is needed.

Corollary 5.I. Given an electric network composed only of continuous generators, one ideal switch that commutes, and at least one resistor, it is possible to have hard switching commutations.

Corollary 5.II. Given an electric network composed only of continuous generators, inductors, capacitors and only one ideal switch that commutes, only soft switching commutations are possible.

Corollary 5.III. Given an electric network composed only of continuous generators, inductors, capacitors and ideal diodes, only soft switching commutations are possible.

Corollary 5.IV. Given an Ideal Switch Multi Port constituted by different ideal switches and/or ideal diodes where currents or voltages at the external ports are continuous, the total Jump Power absorbed by the Ideal Switch Multi Port is always nil. Hence, the sum of Jump Power into the Ideal Switch Multi Port must be nil, consequently,

- *if only one ideal switch commutes at time, only soft switching commutations are possible;*
- *hard switching commutations can occur only if more than one ideal switch, among which there can be ideal diodes, commutes at the same time;*
- *if the Ideal Switch Multi Port is constituted only by ideal diodes, only soft switching commutations are possible.*

Corollary 5.IV can be extended to any generic network without resistors.

5.4 Some Theorems Based on Jump Power and Switching Power

Table 5.2 shows a comparison between the Jump Power and the Switching Power analyzed in chapter 2 involved by ideal switches and ideal diodes.

Table 5.2. Comparison between SP and JP

	Ideal switch opening	Ideal switch closing	Ideal diode opening	Ideal diode closing
active hard switching	SP < 0 JP < 0	SP > 0 JP < 0	-- --	-- --
passive hard switching	SP > 0 JP > 0	SP < 0 JP > 0	SP > 0 JP > 0	SP < 0 JP > 0

By Table 5.2 it is possible to state the following:

Theorem 5.IV. By considering only commutations of ideal switches and ideal diodes, the Jump Power is involved if, and only if, the Switching Power is involved.

Theorem 5.V. If an Ideal Switch Multi Port generates Switching Power then, at least two ideal switches or one ideal switch and one ideal diode commute at the same time; one of the two element opening in active hard switching (only ideal switch) and the other of the two closing in passive hard switching.

Corollary 5.V. If only two elements of an Ideal Switch Multi Port commute at the same time, each of them generates Switching Power equal to $1/2V_{SW}I_{SW}$ (2.42), (2.43) *and the total Switching Power generated by the Ideal Switch Multi Port is* $V_{SW}I_{SW}$.

Theorem 5.VI. If an Ideal Switch Multi Port absorbs Switching Power then, at least two ideal switches or one ideal switch and one ideal diode commute at the same time; one of the two element closing in active hard switching (only ideal switch) and the other of the two opening in passive hard switching.

Corollary 5.VI. If only two elements of an Ideal Switch Multi Port commute at the same time, each of them absorbs Switching Power equal to $1/2V_{SW}I_{SW}$ (2.42), (2.43) *and the total Switching Power absorbed by the Ideal Switch Multi Port is* $V_{SW}I_{SW}$.

Because of the relationship between the SP and the reactive power, the abovementioned theorems and corollaries state some significant conditions regarding the reactive power that electronic converters can generate or compensate in a power plant.

5.5 Analytical Examples

5.5.1 Ideal Switch

Let us consider the electric circuit depicted in Fig. 5.5. Let us suppose that at the time $t = 0$ the ideal switch closes.

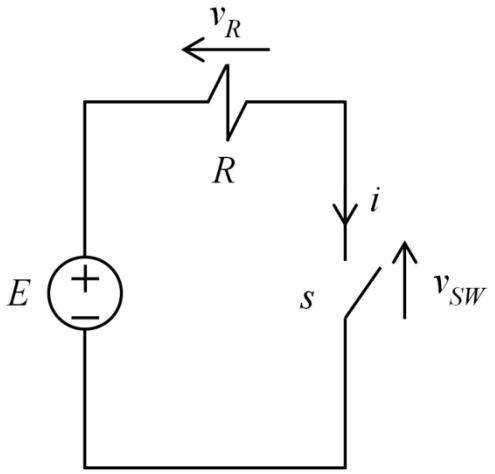

Fig. 5.5. Electric circuit

Before the commutation the electric quantities are as follows

$$\begin{aligned} &i(0\_) = 0 \\ &v_R(0\_) = 0 \\ &v_{SW}(0\_) = E. \end{aligned} \tag{5.26}$$

After the commutation the electric quantities are as follows

$$\begin{aligned} &i(0_+) = \frac{E}{R} \\ &v_R(0_+) = E \\ &v_{SW}(0_+) = 0. \end{aligned} \tag{5.27}$$

In this way, according to (5.1) the JPs absorbed by the voltage generator, resistor and ideal switch are the following

$$\begin{aligned} &JP_E = 0 \\ &JP_R = \frac{1}{2}\frac{E^2}{R} \\ &JP_{SW} = -\frac{1}{2}\frac{E^2}{R}. \end{aligned} \tag{5.28}$$

Indeed, the ideal switch applies an active hard switching commutation generating JP meanwhile the resistor absorbs the same amount of JP.

5.5.2 Voltage Power Electronic Building Block

Let us consider the VPEBB depicted in Fig. 5.6 constituted by GTOs and diodes.

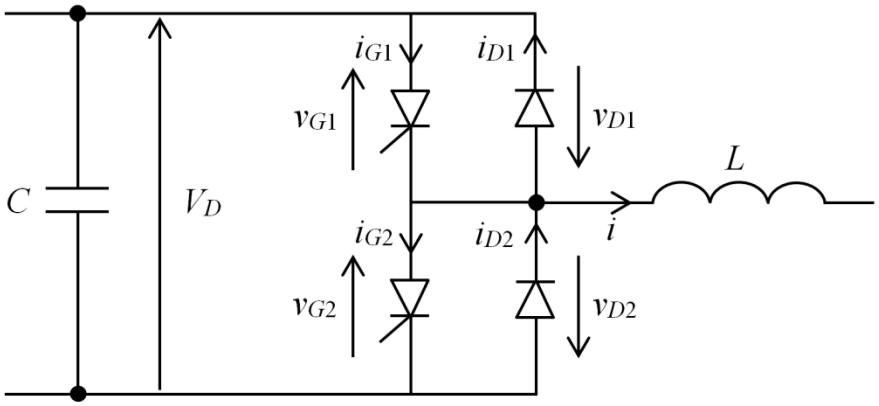

Fig. 5.6. VPEBB

Let us suppose that at the time $t = 0$ the GTO 1 closes while the other opens. Supposed that $V_D > 0$ and $i > 0$, before the commutation the electric quantities are as follows

$$
\begin{aligned}
&i_{G1}(0\_) = 0 \\
&i_{D1}(0\_) = 0 \\
&v_{G1}(0\_) = -v_{D1}(0\_) = V_D \\
&i_{G2}(0\_) = 0 \\
&i_{D2}(0\_) = i \\
&v_{G2}(0\_) = -v_{D2}(0\_) = 0.
\end{aligned}
\tag{5.29}
$$

After the commutation the electric quantities are as follows

$$
\begin{aligned}
&i_{G1}(0\_) = i \\
&i_{D1}(0\_) = 0 \\
&v_{G1}(0\_) = -v_{D1}(0\_) = 0 \\
&i_{G2}(0\_) = 0 \\
&i_{D2}(0\_) = 0 \\
&v_{G2}(0\_) = -v_{D2}(0\_) = V_D.
\end{aligned}
\tag{5.30}
$$

In this way, according to (5.1) the JPs absorbed by the elements are the following

$$
\begin{aligned}
&JP_{G1} = -\frac{1}{2} V_D i \\
&JP_{D1} = 0 \\
&JP_{G2} = 0 \\
&JP_{D2} = \frac{1}{2} V_D i.
\end{aligned}
\tag{5.31}
$$

Indeed, the GTO 1 applies an active hard switching commutation generating JP meanwhile the Diode 2 applies a passive hard switching commutation absorbing the same JP.

5.5.3 Rectifier Bridge

Let us consider the rectifier bridge depicted in Fig. 5.7.

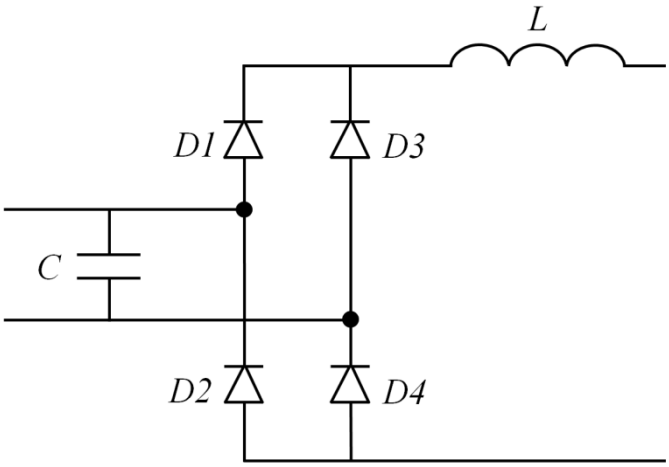

Fig. 5.7. Rectifier bridge

Since diodes can only absorb JP and the total JP must be nil, then the rectifier bridge can only apply soft switching commutations. Indeed, commutations apply only when the voltage over the diodes is zero.

5.5.4 Total Controlled Rectifier Bridge

Let us consider the total controlled rectifier bridge of Fig. 5.8.

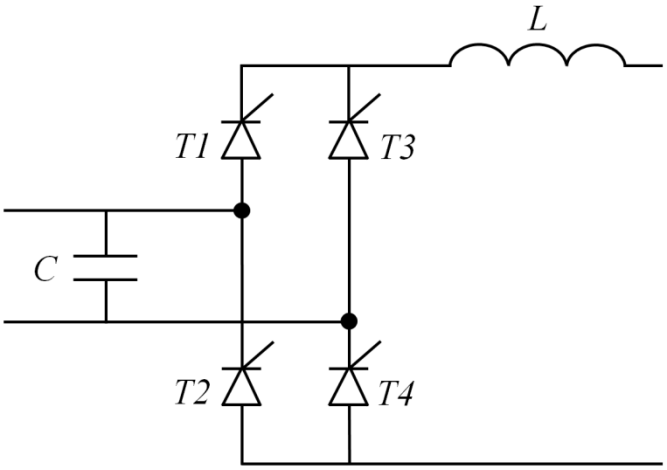

Fig. 5.8. Total controlled rectifier bridge

Since thyristor, like an ideal switch, can also generate JP, then the total controlled rectifier bridge can apply hard switching commutations. Indeed, by means of the firing angle, the thyristor can close when its voltage is different from zero; at the same time the current in the element has a jump discontinuity. The active hard switching at firing causes a passive hard switching commutation in the other thyristor that switches off.

6. Connection Energy and Impulsive Powers

6.1 Introduction

Switched networks are the core of this work. In the past literature, these networks are treated as networks with variant topology following commutations of ideal switches. An interesting aspect, that was much discussed in the past literature, considers the problem regarding the switched networks with inconsistent initial conditions. Generally, this is due to the presence of ideal switches which can yield impulses on the electric qualities. Indeed, they can involve a change in the network topology as for instance, when two capacitors with different initial voltages are connected in parallel to form a new network. The instant when a network forms a new topology will be $t = t^*$. Initial conditions at t^*_- will be called initial conditions simply, while the values immediately after switching are the initial conditions at t^*_+. Voltage and current values at t^*_+ and t^*_- are related by charge conservation in capacitive cutsets and flux conservation in inductive loops. Nevertheless, the application of these laws does not always suffice for obtaining the initial values at t^*_+ from initial values at t^*_-. Indeed in [69], state reinitialization problem has been addressed by utilizing the charge/flux conservation principle. A general formalization of this conservation principle has not been given; it has been explained only through examples. In [70], the principle of charge/flux conservation has been applied to periodically operated switched networks for state reinitialization problem. In [71], the authors proposed a reinitialization method that is based on numerical inversion of Laplace transform. Their method obtains consistent initial states in two steps: one step forward in time to overcome the impulse and one step backward to the switching instant. Reference [72] uses also the Laplace transform method for reinitialization. This line of work has been extended in [73] to periodically switched nonlinear circuits. Other papers that took numerical approaches include [74]−[76]. The distributional framework has been used in [77] where current sources were excluded, in [43] an approach to calculate the energy loss after the discontinuity was developed. Other related work consists of generalizations to nonlinear setting (e.g., [40], [41], [78], [79]) and calculation and interpretation of energy loss in switching instants (e.g., [80]−[82]). For internally controlled switching elements, state reinitialization was considered in [38], [83]−[85]. Also state discontinuities were discussed in the context of switched capacitor circuits in [86], [87], in the context of robust stabilization of complex switched networks in [88], and in the context of steady-state analysis of nonlinear circuits containing ideal switches in [89]. In the literature, switched networks have been almost always treated by fixing a switch configuration and deriving the differential algebraic equations that govern the network. In order to analyze the same circuit for another switch configuration, a typical approach consists of deriving the corresponding circuit equations for the new configuration as in [75].

In this work, the ideal switch is treated as a one-port element with its own constitutive relations and associated conservative functions, and systems constituted by different ideal switches are treated as ISMPs. As a result, it is possible to extend the Kirchhoff laws also to these elements. Consequently, the switched networks can be treated as normal networks with an invariant topology even in the presence of impulses in the electric quantities.

In this chapter, first order Dirac's delta impulses on voltages or currents are allowed, but as previously stated, simultaneous voltage and current impulses on the same port are excluded. Moreover, for simplicity, only linear R, L, C elements are considered in addition to continuous generators, ideal switches and ideal diodes. Other conservative functions, here called Inductive Impulsive Power (IIP), Capacitive Impulsive Power (CIP) and Connection Energy (CE), are developed in order to give a contribution to possible future developments about properties and

issues of principle regarding one-port elements, in particular ideal diodes and ideal switches, in the presence of impulses in the electric quantities.

6.2 Connection Energy, Inductive Impulsive Power and Capacitive Impulsive Power

According to [43] the Connection Energy is the electric energy absorbed by the whole network in a certain time instant as a consequence of the topology change. This change is due to, for example, some ideal switches present in the network, which can yield impulses in the electric quantities. As already stated, ideal switches can be seen as linear time-variant one-port elements that do not involve any change of the network topology. However, they can give rise to impulses in the electric quantities whenever they do switching as suddenly zeroing an inductor current or suddenly zeroing a capacitor voltage. More in general, when two or more capacitors with different initial voltages are connected in parallel or to form a closed loop, dually, when two or more inductors with different initial currents are connected in series or to form a cutset. In [43] the Connection Energy is seen as a function related to the whole network. Instead, in this work the Connection Energy is reformulated as a generalized conservative function related to any electric element.

For a two-terminals component, with the reference directions for voltage and current reported in Fig. 2.1, according to the impulsive functions (1.66), let us define the *Connection Energy* as

$$W^c(t) = \frac{1}{2}\left(V\_Y(i) + I\_Y(v)\right) \tag{6.1}$$

where $V\_$ and $I\_$ are the values of the electric quantities before the discontinuity in a certain time instant; Moreover, according to the jump functions (1.64) and impulsive functions (1.66), let us define the *Inductive Impulsive Power* as

$$Q^{\delta L}(t) = -\frac{1}{2}J(i)Y(v) \tag{6.2}$$

and the *Capacitive Impulsive Power* as

$$Q^{\delta C}(t) = -\frac{1}{2}J(v)Y(i). \tag{6.3}$$

Furthermore, the *Energy* absorbed through the discontinuity is

$$\Delta E(t) = \int_{t\_}^{t_+} vidt. \tag{6.4}$$

6.2.1 Balance Theorem over Connection Energy

Since the Connection Energy is defined as the sum of products of impulses and values before the discontinuity of voltage and current which satisfy, separately, the Kirchhoff laws, it is possible to state the following:

Theorem 6.I. Given a network constituted by a connection of "p" electric ports and chosen the same reference directions for all ports, the sum of Connection Energy extended to the whole network is nil, namely the sum of Connection Energy generated is equal to the sum of Connection Energy absorbed.

6.2.2 Balance Theorem over Impulsive Powers

Since Impulsive Powers are defined as the products of jump functions and impulses of voltage and current which satisfy, separately, the Kirchhoff laws, it is possible to state the following:

Theorem 6.II. Given a network constituted by a connection of "p" electric ports and chosen the same reference directions for all ports, the sum of Inductive Impulsive Power (Capacitive Impulsive Power) extended to the whole network is nil, namely the sum of Inductive Impulsive Power (Capacitive Impulsive Power) generated is equal to the sum of Inductive Impulsive Power (Capacitive Impulsive Power) absorbed.

6.2.3 Continuous Generators

For continuous voltage generators and continuous current generators, the voltage or the current, respectively, are imposed to be continuous functions of time, and therefore, the jump functions are as follows

$$\begin{aligned} &J_g(v(t)) = 0 \quad (\textit{Voltage generators}) \\ &J_g(i(t)) = 0 \quad (\textit{Current generators}). \end{aligned} \tag{6.5}$$

Taking into account (6.5) in (6.2) and (6.3), the IIP and CIP absorbed by continuous generators are always nil.

$$\begin{aligned} &Q_g^{\delta L} = 0 \\ &Q_g^{\delta C} = 0 \end{aligned} \tag{6.6}$$

Instead, the CE and the Energy absorbed by continuous generators may be not nil. Indeed, they depend on both the values of voltage or current of generators before the discontinuity and voltage or current impulses that can be present in the network.

6.2.4 Linear Resistor

Since the characteristic of a linear resistor involves the presence of impulses at the same time in the voltage and current, which are excluded from this work because they would apply infinite energy in the system, then IIP, CIP, CE and the Energy absorbed through the discontinuity are always nil.

$$\begin{aligned} &W_R^c = 0 \\ &Q_R^{\delta L} = 0 \\ &Q_R^{\delta C} = 0 \\ &\Delta E_R = 0 \end{aligned} \tag{6.7}$$

6.2.5 Linear Inductor

Let us consider a linear inductor of inductance L and suppose a jump discontinuity in the inductor current at the instant t^*. According to (1.63) it is possible to write

$$v(t) = L\frac{d}{dt}\left[i_{cont} + I_\mu \mu(t - t^*) \right] \tag{6.8}$$

where $I_\mu = I_+ - I_-$ is the amplitude of the jump discontinuity. Since the term

$$L\frac{d}{dt}\left[I_\mu \mu(t - t^*) \right] = LI_\mu \delta(t - t^*) \tag{6.9}$$

and according to (1.61)

$$I_\mu = \frac{\lambda_\phi}{L} \tag{6.10}$$

then

$$v(t) = L\frac{di_{cont}}{dt} + \lambda_\phi \delta(t - t^*). \tag{6.11}$$

An impulse in the inductor voltage arise. In order to avoid impulses of higher order on the voltage, an impulse on the current is not allowed. In this case

$$\lambda_q = 0. \tag{6.12}$$

Taking into account (6.10) and (6.12) in (6.1), the CE absorbed by the inductor is

$$W_L^c = \frac{1}{2}LI_\mu I_- = \frac{1}{2}L(I_+ - I_-)I_-. \tag{6.13}$$

The increment of the Energy stored in the inductor through the discontinuity is

$$\Delta E_L = E_{L+} - E_{L-} = \frac{1}{2}L(I_+^2 - I_-^2). \tag{6.14}$$

Taking into account (6.10) and (6.11) in (6.2), the IIP absorbed by the inductor is

$$Q_L^{\delta L} = -\frac{1}{2}\frac{\lambda_\phi^2}{L} = -\frac{1}{2}L(I_+ - I_-)^2 \le 0 \tag{6.15}$$

while taking into account (6.12) in (6.3), the CIP is

$$Q_L^{\delta C} = 0. \tag{6.16}$$

When $I_+ = 0$, CE and IIP are equal to the increment of the Energy stored in the inductor. In particular, this increment is negative. Indeed

$$\Delta E_L = Q_L^{\delta L} = W_L^c = -\frac{1}{2} L I_-^2 \le 0. \tag{6.17}$$

6.2.6 Linear Capacitor

Let us consider a linear capacitor of capacitor C and suppose a jump discontinuity in the capacitor voltage at the instant t^*. According to (1.63) it is possible to write

$$i(t) = C \frac{d}{dt}\left[v_{cont} + V_\mu \mu(t - t^*) \right]. \tag{6.18}$$

where $V_\mu = V_+ - V_-$ is the amplitude of the jump discontinuity. Since the term

$$C \frac{d}{dt}\left[V_\mu \mu(t - t^*) \right] = C V_\mu \delta(t - t^*) \tag{6.19}$$

and according to (1.61)

$$V_\mu = \frac{\lambda_q}{C} \tag{6.20}$$

then

$$i(t) = C \frac{dv_{cont}}{dt} + \lambda_q \delta(t - t^*). \tag{6.21}$$

An impulse in the capacitor current arise. In order to avoid impulses of higher order on the current, an impulse on the voltage is not allowed. In this case

$$\lambda_\phi = 0. \tag{6.22}$$

Taking into account (6.20) and (6.22) in (6.1), the CE absorbed by the capacitor is

$$W_C^c = \frac{1}{2} C V_\mu V_- = \frac{1}{2} C (V_+ - V_-) V_-. \tag{6.23}$$

The increment of the Energy stored in the capacitor through the discontinuity is

$$\Delta E_C = E_{C+} - E_{C-} = \frac{1}{2} C (V_+^2 - V_-^2). \tag{6.24}$$

Taking into account (6.22) in (6.2), the IIP absorbed by the capacitor is

$$Q_C^{\delta L} = 0 \tag{6.25}$$

while taking into account (6.20) and (6.21) in (6.3), the CIP is

$$Q_C^{\delta C} = -\frac{1}{2}\frac{\lambda_q^2}{C} = -\frac{1}{2}C(V_+ - V_-)^2 \le 0. \tag{6.26}$$

When $V_+ = 0$, CE and CIP are equal to the increment of the Energy stored in the capacitor. In particular, this increment is negative. Indeed

$$\Delta E_C = Q_C^{\delta C} = W_C^c = -\frac{1}{2}CV_-^2 \le 0. \tag{6.27}$$

6.2.7 Ideal Switch

Let us consider the ideal switch and only one impulse in one of the two electric quantities.

Closing commutation

When the ideal switch closes at time t^*, the voltage $V_{SW} = v(t^*_-)$ that was applied on the ideal switch becomes nil and the current that was nil becomes $I_{SW} = i(t^*_+)$. Since the closing process forces the voltage to zero, no voltage impulse is possible. Therefore, let us suppose an impulse in the current at the switching instant t^*. Hence, it is possible to write

$$\begin{aligned} v(t) &= V_{SW}(1-\mu(t-t^*)) \\ i(t) &= I_{SW}\mu(t-t^*) + \lambda_q\delta(t-t^*). \end{aligned} \tag{6.28}$$

Taking into account (6.28) in (6.1), the CE absorbed by the ideal switch is

$$W_{SWclosed}^c = \frac{1}{2}V_{SW}\lambda_q. \tag{6.29}$$

According to (6.2) the IIP absorbed by the ideal switch is

$$Q_{SWclosed}^{\delta L} = 0 \tag{6.30}$$

while according to (6.3) the CIP absorbed by the ideal switch is

$$Q_{SWclosed}^{\delta C} = \frac{1}{2}V_{SW}\lambda_q. \tag{6.31}$$

The CIP is equal to the CE. The Energy absorbed by the ideal switch is normally zero. In fact, without impulses, one of the two electric quantities is always nil. Instead, when an impulse occurs, according to Colombeau [90], if $a < 0 < b$ and if $f(t)$ is a continuous function in $]-\varepsilon, 0[$ and $]0, \varepsilon[$ and the limits $f(0_-)$ and $f(0_+)$ exist, then

$$\int_a^b f(t)\delta(t)dt = \frac{f(0_-) + f(0_+)}{2}. \tag{6.32}$$

Taking into account (6.28) in (6.32), the Energy absorbed by the ideal switch through the discontinuity is

$$\Delta E_{SWclosed} = \int_{t_-^*}^{t_+^*} vidt = \frac{1}{2} V_{SW} \lambda_q . \tag{6.33}$$

Also the Energy absorbed by the ideal switch, in the closing commutation, is equal to the CE and CIP.

Opening commutation

Dually, when the ideal switch opens at time t^*, the current $I_{SW} = i(t^*_-)$ that was flowing is interrupted and the voltage that was nil becomes $V_{SW} = v(t^*_+)$. Since the opening process forces the current to zero, no current impulse is possible. Therefore, let us suppose an impulse in the voltage at the switching instant t^*. Hence, it is possible to write

$$\begin{aligned} v(t) &= V_{SW} \mu(t - t^*) + \lambda_\phi \delta(t - t^*) \\ i(t) &= I_{SW} (1 - \mu(t - t^*)). \end{aligned} \tag{6.34}$$

Taking into account (6.34) in (6.1), the CE absorbed by the ideal switch is

$$W^c_{SWopen} = \frac{1}{2} I_{SW} \lambda_\phi . \tag{6.35}$$

According to (6.2) the IIP absorbed by the ideal switch is

$$Q^{\delta L}_{SWopen} = \frac{1}{2} I_{SW} \lambda_\phi \tag{6.36}$$

while according to (6.3) the CIP absorbed by the ideal switch is

$$Q^{\delta C}_{SWopen} = 0. \tag{6.37}$$

The IIP is equal to the CE. According to (6.32) and (6.34) the Energy absorbed by the ideal switch through the discontinuity is

$$\Delta E_{SWopen} = \int_{t_-^*}^{t_+^*} vidt = \frac{1}{2} I_{SW} \lambda_\phi . \tag{6.38}$$

Also the Energy absorbed by the ideal switch, in the opening commutation, is equal to the CE and IIP.

6.2.8 Ideal Diode

Let us consider an ideal diode, with its characteristic on the *v*-*i* plane as reported in Fig. 5.4, and only one impulse in one of the two electric quantities.

Closing commutation

When the ideal diode, due to the remaining part of the network, jumps at the time t^* from the point A to the point B on its characteristic, the voltage $V_D = v(t^*_-) \leq 0$ that was applied on the ideal diode becomes nil and the current that was nil becomes $I_D = i(t^*_+) \geq 0$. Moreover, let us suppose an impulse in the current at the switching instant t^*. Hence, it is possible to write

$$\begin{aligned} v(t) &= V_D(1-\mu(t-t^*)) \\ i(t) &= I_D\mu(t-t^*)+\lambda_q\delta(t-t^*). \end{aligned} \tag{6.39}$$

Taking into account (6.39) in (6.1), the CE absorbed by the ideal diode is

$$W^c_{Dclosed} = \frac{1}{2}V_D\lambda_q. \tag{6.40}$$

According to (6.2) the IIP absorbed by the ideal diode is

$$Q^{\delta L}_{Dclosed} = 0 \tag{6.41}$$

while according to (6.3) the CIP absorbed by the ideal diode is

$$Q^{\delta C}_{Dclosed} = \frac{1}{2}V_D\lambda_q. \tag{6.42}$$

Taking into account (6.39) in (6.32), the Energy absorbed by the ideal diode through the discontinuity is

$$\Delta E_{Dclosed} = \int_{t^*_-}^{t^*_+} vidt = \frac{1}{2}V_D\lambda_q. \tag{6.43}$$

The Energy absorbed by the ideal diode, in the closing commutation, is equal to the CE and CIP. By the characteristic reported in Fig. 5.4

$$V_D\lambda_q \leq 0 \tag{6.44}$$

and hence, the Energy, CE and CIP absorbed by the ideal diode are nonpositive, i.e. generated.

Opening commutation

Dually, in the opening commutation, when the ideal diode, due to the remaining part of the network, jumps at the time t^* from the point B to the point A on its characteristic, the current $I_D = i(t^*_-) \geq 0$ that was flowing through the ideal diode becomes nil and the voltage that was nil becomes $V_D = v(t^*_+) \leq 0$. Moreover, let us suppose an impulse in the voltage at the switching instant t^*. Hence, it is possible to write

$$\begin{aligned} v(t) &= V_D(1-\mu(t-t^*)) + \lambda_\phi \delta(t-t^*) \\ i(t) &= I_D \mu(t-t^*). \end{aligned} \tag{6.45}$$

Taking into account (6.45) in (6.1), the CE absorbed by the ideal diode is

$$W^c_{Dopen} = \frac{1}{2} I_D \lambda_\phi. \tag{6.46}$$

According to (6.2) the IIP absorbed by the ideal diode is

$$Q^{\delta L}_{Dopen} = \frac{1}{2} I_D \lambda_\phi \tag{6.47}$$

while according to (6.3) the CIP absorbed by the ideal diode is

$$Q^{\delta C}_{Dopen} = 0. \tag{6.48}$$

Taking into account (6.39) in (6.32), the Energy absorbed by the ideal diode through the discontinuity is

$$\Delta E_{Dopen} = \int_{t^*_-}^{t^*_+} vidt = \frac{1}{2} I_D \lambda_\phi. \tag{6.49}$$

Also in this case, the Energy absorbed by the ideal diode, in the opening commutation, is equal to the CE and CIP. By the characteristic reported in Fig. 5.4

$$I_D \lambda_\phi \le 0 \tag{6.50}$$

and hence, the Energy, CE and IIP absorbed by the ideal diode are nonpositive, i.e. generated.

6.3 Active and Passive Impulsive Hard Switching

In order to get more stringent results, similarly to section 2.5, let us define *active impulsive hard switching* the ideal switch commutations so that one of the followings strict inequalities is valid

$$\begin{aligned} V_{SW} \lambda_q &> 0 \\ I_{SW} \lambda_\phi &> 0. \end{aligned}$$

Let us define *passive impulsive hard switching* the opposite case

$$\begin{aligned} V_{SW} \lambda_q &< 0 \\ I_{SW} \lambda_\phi &< 0. \end{aligned}$$

According to (6.44) and (6.50) it is possible to state that the ideal diode can only apply *passive impulsive hard switching* commutations.

Moreover, by (6.33), (6.38), (6.43) and (6.49), it is possible to recognize a strange result: the ideal switch can absorb or generate energy meanwhile the ideal diode can only generate when an impulsive hard switching commutation occurs. In particular, the fact regarding the generation of energy by these elements is an interesting mathematical aspect that will be discussed later.

6.4 Some Theorems

Table 6.1 shows a summary of the generalized conservative functions, as Connection Energy, Impulsive Powers and Energy, absorbed by continuous generators, linear resistors, linear inductors, linear capacitors, ideal switches and ideal diodes.

Table 6.1. Summary of Connection Energy, Impulsive Powers and Energy absorbed by one-port elements

Electric Elements	Inductive Imp. Power	Capacitive Imp. Power	Connection Energy	Energy through the discontinuity
Continuous generators	0	0	≤ 0 ≥ 0	≤ 0 ≥ 0
Linear resistor	0	0	0	0
Linear inductor	≤ 0	0	≤ 0 ≥ 0	≤ 0 ≥ 0
Linear capacitor	0	≤ 0	≤ 0 ≥ 0	≤ 0 ≥ 0
Ideal switch (closing passive impulsive h. s.) Ideal switch (closing active impulsive h. s.)	0	≤ 0 ≥ 0	≤ 0 ≥ 0	≤ 0 ≥ 0
Ideal switch (opening passive impulsive h. s.) Ideal switch (opening active impulsive h. s.)	≤ 0 ≥ 0	0	≤ 0 ≥ 0	≤ 0 ≥ 0
Ideal diode (closing passive impulsive h. s.)	0	≤ 0	≤ 0	≤ 0
Ideal diode (opening passive impulsive h. s.)	≤ 0	0	≤ 0	≤ 0

According to Table 6.1 it is possible to recognize that the Inductive Impulsive Power is always nil on linear resistors, continuous generators, linear capacitors and ideal diodes and ideal switches in closing commutations; the Capacitive Impulsive Power is always nil on linear resistors, continuous generators, linear inductors and ideal diodes and ideal switches in opening commutations; only ideal switches can, also, absorb Inductive Impulsive Power in opening commutations and Capacitive Impulsive Power in closing commutations.

Assumption 6.I. Given an electric network composed only of elements which are reported in Table 6.1, impulses in the electric quantities can arise only if a jump discontinuity occurs in a inductor current and/or in a capacitor voltage. In fact, the constitutive relations of inductors and capacitors have derivative terms, and therefore, impulses can only rise as derivatives of the jump discontinuities in these constitutive relations.

6.4.1 Theorems based on Inductive Impulsive Power

Since IIP are nil on continuous generators and linear resistors, for the balance theorem over IIP, it is possible to write the following

$$\sum_j Q^{\delta L}_{SWopen(j)} = -\sum_r Q^{\delta L}_{L(r)} - \sum_p Q^{\delta L}_{Dopen(p)} \tag{6.51}$$

where $Q^{\delta L}_{SWopen(j)}$ is the IIP absorbed by the j-th ideal switch, $Q^{\delta L}_{Dopen(p)}$ is the IIP absorbed by the p-th ideal diode and $Q^{\delta L}_{L(r)}$ is the IIP absorbed by the r-th inductor. By equations (6.51) it is possible to state the following:

Theorem 6.III. The sum of Inductive Impulsive Powers absorbed by ideal switches opening in active impulsive hard switching is equal to the sum of Inductive Impulsive Powers generated by linear inductors and ideal diodes and ideal switches opening in passive impulsive hard switching.

Theorem 6.IV. Given an electric network composed of continuous generators, linear resistors, linear inductors, linear capacitors, ideal diodes and ideal switches in which Inductive Impulsive Power is involved, then at least one ideal switch that opens with a voltage impulse is needed.

Theorem 6.V. When an ideal switch opens, with a voltage impulse, in order to obey to the balance theorem over Impulsive Powers and according to the Assumption 6.I, at least one linear inductor must be present.

Theorem 6.VI. According to Theorems 6.III and 6.V, the sum of Inductive Impulsive Powers absorbed by ideal switches opening in active impulsive hard switching is always major of the sum of Inductive Impulsive Powers absorbed by ideal switches and ideal diodes opening in passive impulsive hard switching because of the presence of at least one linear inductor. Since for ideal switches and ideal diodes the Inductive Impulsive Power is always equal to the energy involved by them, then the total energy absorbed by the whole set of ideal switches and ideal diodes is always positive.

6.4.2 Theorems based on Capacitive Impulsive Power

Since CIP are nil on continuous generators and linear resistors, for the balance theorem over CIP, it is possible to write the following

$$\sum_{j} Q^{\delta C}_{SWclosed(j)} = -\sum_{k} Q^{\delta C}_{C(k)} - \sum_{p} Q^{\delta C}_{Dclosed(p)} \tag{6.52}$$

where $Q^{\delta C}_{SWclosed(j)}$ is the CIP absorbed by the *j*-th ideal switch, $Q^{\delta C}_{Dclosed(p)}$ is the CIP absorbed by the *p*-th ideal diode and $Q^{\delta C}_{C(k)}$ is the CIP absorbed by the *k*-th capacitor. By equations (6.52) it is possible to state the following:

Theorem 6.VII. The sum of Capacitive Impulsive Powers absorbed by ideal switches closing in active impulsive hard switching is equal to the sum of Capacitive Impulsive Powers generated by linear capacitors and ideal diodes and ideal switches closing in passive impulsive hard switching.

Theorem 6.VIII. Given an electric network composed of continuous generators, linear resistors, linear inductors, linear capacitors, ideal diodes and ideal switches in which Capacitive Impulsive Power is involved, then at least one ideal switch that closes with a current impulse is needed.

Theorem 6.IX. When an ideal switch closes, with a current impulse, in order to obey to the balance theorem over Impulsive Powers and according to the Assumption 6.I, at least one linear capacitor must be present.

Theorem 6.X. According to Theorem 6.VII and 6.IX, the sum of Capacitive Impulsive Powers absorbed by ideal switches closing in active impulsive hard switching is always major of the sum of Capacitive Impulsive Powers absorbed by ideal switches and ideal diodes closing in passive impulsive hard switching because of the presence of at least one linear capacitor. Since for ideal switches and ideal diodes the Capacitive Impulsive Power is always equal to the energy involved by

them, then the total energy absorbed by the whole set of ideal switches and ideal diodes is always positive.

6.4.3 Theorems based on Connection Energy

Since the CE is nil on linear resistors, for the balance theorem over CE, it is possible to write

$$\sum_j W^c_{SW(j)} + \sum_p W^c_{D(p)} = -\sum_k W^c_{C(k)} - \sum_r W^c_{L(r)} - \sum_l W^c_{g(l)} \tag{6.53}$$

where $W^c_{SW(j)}$ is the CE absorbed by the *j*-th ideal switch, $W^c_{D(p)}$ is the CE absorbed by the *p*-th ideal diode, $W^c_{C(k)}$ is the CE absorbed by the *k*-th capacitor, $W^c_{L(r)}$ is the CE absorbed by the *r*-th inductor and $W^c_{g(l)}$ is the CE absorbed by the *l*-th continuous generator. By equation (6.53), it is possible to state the following:

Theorem 6.XI. The sum of Connection Energy generated by the whole set of linear inductors, linear capacitors and continuous generators is equal to the sum of Connection Energy absorbed by the whole set of ideal switches and ideal diodes.

Since the Energy through the discontinuity due to impulses is always nil on resistors, it is possible to write the following

$$\sum_j \Delta E_{SW(j)} + \sum_p \Delta E_{D(p)} = -\sum_k \Delta E_{C(k)} - \sum_r \Delta E_{L(r)} - \sum_l \Delta E_{g(l)} \tag{6.54}$$

where $\Delta E_{SW(j)}$ is the Energy absorbed by the *j*-th ideal switch, $\Delta E_{D(p)}$ is the Energy absorbed by the *p*-th ideal diode, $\Delta E_{C(k)}$ is the Energy absorbed by the *k*-th capacitor, $\Delta E_{L(r)}$ is the Energy absorbed by the *r*-th inductor and $\Delta E_{g(l)}$ is the Energy absorbed by the *l*-th continuous generator. By equation (6.54), it is possible to state the following:

Theorem 6.XII. The sum of decrement of Energy stored into the whole set of linear inductors, linear capacitors and generated by continuous generators is equal to the sum of Energy absorbed by the whole set of ideal switches and ideal diodes.

Since, according to (6.29), (6.33), (6.35), (6.38), (6.40), (6.43), (6.46) and (6.49) the CE is equal to the Energy absorbed by the ideal switch and ideal diode, it is possible to write

$$\sum_j W^c_{SW(j)} + \sum_p W^c_{D(p)} = \sum_j \Delta E_{SW(j)} + \sum_p \Delta E_{D(p)}. \tag{6.55}$$

Taking into account (6.55) in (6.53), it is possible to write

$$\sum_j \Delta E_{SW(j)} + \sum_p \Delta E_{D(p)} = -\sum_k W^c_{C(k)} - \sum_r W^c_{L(r)} - \sum_l W^c_{g(l)} \tag{6.56}$$

which means that:

Theorem 6.XIII. The sum of Connection Energy generated by the whole set of linear inductors, linear capacitors and continuous generators is equal to the Energy absorbed by the whole set of ideal switches and ideal diodes. According to theorems 6.VI and 6.X this energy is always positive.

Moreover, taking into account (6.54) in (6.56), it is possible to write

$$\sum_k W^c_{C(k)} + \sum_r W^c_{L(r)} + \sum_l W^c_{g(l)} = \sum_k \Delta E_{C(k)} + \sum_r \Delta E_{L(r)} + \sum_l \Delta E_{g(l)} \tag{6.57}$$

which means that:

Theorem 6.XIV. The sum of Connection Energy generated by the whole set of linear inductors, linear capacitors and continuous generators is equal to the decrement of Energy stored into the whole set of linear inductors, linear capacitors and absorbed by continuous generators.

This last theorem confirms what is stated in [43].

6.5 Analytical Examples

The following are analytical examples regarding how to deal with the ideal switch in electric network as invariant topology and how the ideal switch and ideal diode can involve electric energy.

6.5.1 Voltage Impulse

Let us consider the electric circuit reported in Fig. 6.1 constituted by a constant voltage generator E, a linear resistor R, a linear inductor L and an ideal switch s.

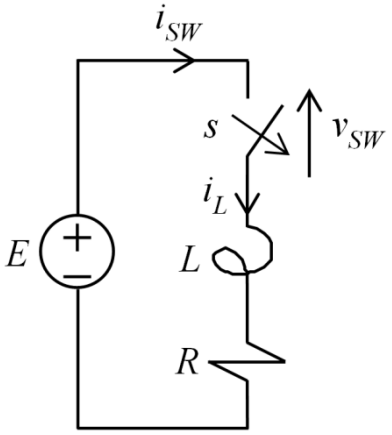

Fig. 6.1. Electric circuit. Voltage impulse

Supposing that the ideal switch is closed since a long time, as the electric circuit is in steady state, at the time $t = 0$ the ideal switch opens, an impulse of voltage arise. The current i_{SW} that flows in the ideal switch is

$$i_{SW}(t) = \frac{E}{R}\left[1 - \mu(t)\right]. \tag{6.58}$$

According to the Current Kirchhoff Law, the current flowing in the inductor is

$$i_L(t) = i_{SW} \tag{6.59}$$

while according to the Voltage Kirchhoff Law, the voltage over the ideal switch is

$$v_{SW}(t) = E - Ri_{SW} - L\frac{di_{SW}}{dt}. \tag{6.60}$$

Taking into account (6.58) the (6.60) becomes

$$v_{SW}(t) = E\mu(t) + \frac{EL}{R}\delta(t). \tag{6.61}$$

From (6.61) it is possible to see that the voltage over the ideal switch is composed of a jump discontinuity and an impulse. In particular, from (6.58) and (6.61) it is possible to recognize

$$\begin{aligned} I_{SW} &= I_{L-} = \frac{E}{R} \\ \lambda_{\phi} &= \frac{EL}{R}. \end{aligned} \tag{6.62}$$

Taking into account (6.62) in (6.13), (6.14) and (6.15) the CE, IIP and the increment of the Energy stored in the inductor are the following

$$\Delta E_L = W_L^c = Q_L^{\delta L} = -\frac{1}{2}LI_{L-}^2 = -\frac{1}{2}L\frac{E^2}{R^2} < 0. \tag{6.63}$$

Taking into account (6.35), (6.36) and (6.38) the CE, IIP and the Energy absorbed by the ideal switch through the discontinuity are the following

$$\Delta E_{SWopen} = W_{SWopen}^c = Q_{SWopen}^{\delta L} = \frac{1}{2}I_{SW}\lambda_{\phi} = \frac{1}{2}L\frac{E^2}{R^2} > 0. \tag{6.64}$$

From (6.63) and (6.64) it is possible to state that the energy stored into the inductor before the commutation is instantaneously dissipated by the ideal switch when it opens. This fact can have a physical meaning because the energy dissipate by the ideal switch is the same energy physically stored into the inductor.

6.5.2 Current Impulse

Let us consider the electric circuit reported in Fig. 6.2 constituted by a constant voltage generator *E*, a linear resistor *R*, a linear capacitor *C* and an ideal switch *s*. Supposing that the ideal switch is opened since a long time, as the electric circuit is in steady state, at the time $t = 0$ the ideal switch closes, an impulse of current arise. The voltage over ideal switch is

$$v_{SW}(t) = E\left[1 - \mu(t)\right]. \tag{6.65}$$

According to the Voltage Kirchhoff Law, the voltage over the capacitor is

$$v_C(t) = v_{SW} \tag{6.66}$$

while according to the Current Kirchhoff Law, the current flowing in the ideal switch is

$$i_{SW}(t)=\frac{E-v_C}{R}-C\frac{dv_C}{dt}. \tag{6.67}$$

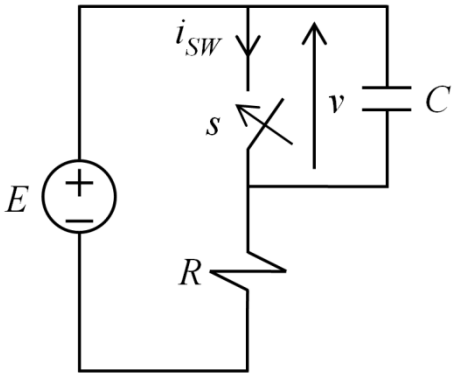

Fig. 6.2. Electric circuit. Current impulse

Taking into account (6.65) the (6.67) becomes

$$i_{SW}(t)=\frac{E}{R}-\frac{E}{R}\left[1-\mu(t)\right]+CE\delta(t). \tag{6.68}$$

From (6.68) it is possible to see that the current flowing in the ideal switch is composed of a constant term, a jump discontinuity and an impulse. In particular, from (6.65) and (6.68) it is possible to recognize

$$\begin{aligned} &V_{SW}=V_{C-}=E \\ &\lambda_q=CE. \end{aligned} \tag{6.69}$$

Taking into account (6.69) in (6.23), (6.24) and (6.26), the CE, CIP and the increment of the Energy stored in the capacitor are the following

$$\Delta E_C=W_C^c=Q_C^{\delta C}=-\frac{1}{2}CV_{C-}^2=-\frac{1}{2}CE^2<0. \tag{6.70}$$

Taking into account (6.29), (6.31) and (6.33) the CE, CIP and the Energy absorbed by the ideal switch through the discontinuity are the following

$$\Delta E_{SWclosed}=W_{SWclosed}^c=Q_{SWclosed}^{\delta C}=\frac{1}{2}V_{SW}\lambda_q=\frac{1}{2}CE^2>0. \tag{6.71}$$

From (6.70) and (6.71) it is possible to state that the energy stored into the capacitor before the commutation is instantaneously dissipated by the ideal switch when it closes. This fact can have a physical meaning because the energy dissipate by the ideal switch is the same energy physically stored into the capacitor.

6.5.3 Two Parallel Capacitors

Let us consider the electric circuit reported in Fig. 6.3 constituted by two linear capacitors C and an ideal switch s.

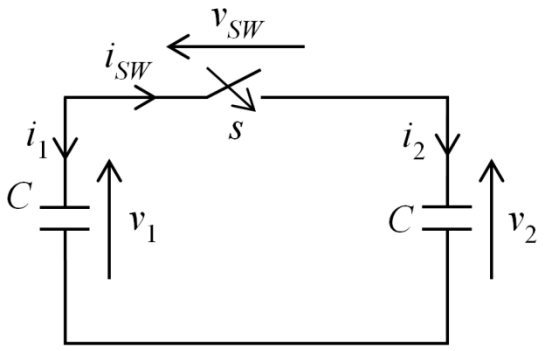

Fig. 6.3. Electric circuit. Two parallel capacitors

Supposing that the two capacitors have two different initial conditions and the ideal switch is open, at the time $t = 0$ the ideal switch closes, an impulse of current arise. The initial conditions are the following

$$\begin{aligned} v_1(0_-) &= V_{1-} \\ v_2(0_-) &= V_{2-}. \end{aligned} \tag{6.72}$$

The differential equation of the electric circuit are

$$\begin{aligned} i_1(t) &= C\frac{dv_1}{dt} \\ i_2(t) &= C\frac{dv_2}{dt} \end{aligned} \tag{6.73}$$

and the Kirchhoff laws are

$$\begin{aligned} v_{SW}(t) &= v_1 - v_2 \\ i_1(t) &= -i_{SW} = i_2. \end{aligned} \tag{6.74}$$

The voltage over the ideal switch is

$$v_{SW}(t) = (V_{1-} - V_{2-})(1 - \mu(t)). \tag{6.75}$$

Taking into account (6.74) and (6.75) in (6.73), the currents are

$$\begin{aligned} i_1(t) &= -\frac{1}{2}C(V_{1-} - V_{2-})\delta(t) \\ i_2(t) &= i_{SW} = \frac{1}{2}C(V_{1-} - V_{2-})\delta(t). \end{aligned} \tag{6.76}$$

Integrating the (6.73) and taking into account (6.76), the capacitor voltages are

$$\begin{aligned} v_1(t) &= \frac{1}{2}(V_{1-} - V_{2-})\mu(t) + V_{1-} \\ v_2(t) &= \frac{1}{2}(V_{2-} - V_{1-})\mu(t) + V_{2-}. \end{aligned} \tag{6.77}$$

From (6.75) and (6.76) it is possible to recognize

$$\begin{aligned} V_{SW} &= (V_{1-} - V_{2-}) \\ \lambda_q &= \frac{1}{2}C(V_{1-} - V_{2-}). \end{aligned} \tag{6.78}$$

According to (6.77) the capacitor voltages after the switching are

$$V_{1+} = V_{2+} = \frac{1}{2}(V_{2-} + V_{1-}). \tag{6.79}$$

Taking into account (6.79) in (6.23), (6.24) and (6.26), the CE, CIP and the increment of the Energy stored in the capacitors are the following

$$\begin{aligned} \Delta E_{C1} &= \frac{1}{8}C\left[(V_{2-} + V_{1-})^2 - 4V_{1-}^2\right] \\ \Delta E_{C2} &= \frac{1}{8}C\left[(V_{2-} + V_{1-})^2 - 4V_{2-}^2\right] \\ W_{C1}^c &= \frac{1}{4}C(V_{2-} - V_{1-})V_{1-} \\ W_{C2}^c &= \frac{1}{4}C(V_{1-} - V_{2-})V_{2-} \\ Q_{C1}^{\delta C} &= -\frac{1}{8}C(V_{2-} - V_{1-})^2 \\ Q_{C2}^{\delta C} &= -\frac{1}{8}C(V_{1-} - V_{2-})^2. \end{aligned} \tag{6.80}$$

Taking into account (6.78) in (6.29), (6.31) and (6.33), the CE, CIP and the Energy absorbed by the ideal switch through the discontinuity are the following

$$\Delta E_{SWclosed} = W_{SWclosed}^c = Q_{SWclosed}^{\delta C} = \frac{1}{4}C(V_{1-} - V_{2-}). \tag{6.81}$$

From (6.80) and (6.81) it is possible to state that the Energy stored into the capacitors before the commutation is dissipated by the ideal switch when it closes. Indeed

$$\Delta E_{C1} + \Delta E_{C2} = W_{C1}^c + W_{C2}^c = Q_{C1}^{\delta C} + Q_{C2}^{\delta C} = E_{SWclosed}. \tag{6.82}$$

Also in this case the dissipation of energy by means of the ideal switch can have a physical meaning because the energy dissipated corresponds to the decrement of energy stored into the two capacitors after the commutation.

6.5.4 Ideal Switch: Energy Generation

Let us consider the circuit depicted in Fig. 6.4, composed of two capacitors C, with two different initial conditions, and one ideal switches and one ideal diode, initially, open. The initial conditions are the following

$$\begin{aligned} v_1(0^-) &= V_{1-} = 2V_0 \\ v_2(0^-) &= V_{2-} = -V_0. \end{aligned} \tag{6.83}$$

At the time $t = 0$ the ideal switch closes. Two possible hypothesis can be made for the state of the diode after the switching. If the ideal diode remained open the circuit becomes like the previous case in which the two capacitors would be in parallel and the voltage over the capacitors after the commutation, according to (6.79), would be $1{,}5V_0$. This is impossible because the ideal diode cannot have a positive voltage. Hence, the correct hypothesis is one that the ideal diode closes at the same time in which also the ideal switch closes. In this way, the two capacitors are in parallel with the constrains that the ideal diode imposes a nil voltage after the commutation.

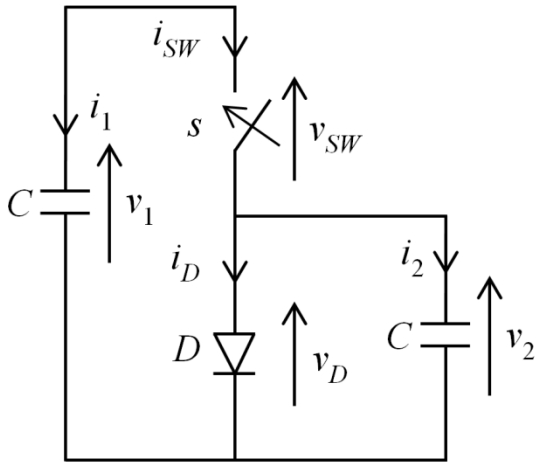

Fig. 6.4. Electric circuit. Ideal switch with energy generation

Let us resolve the circuit in the time domain where the two ideal switches impose the following voltages

$$\begin{aligned} v_{SW}(t) &= 3V_0\left[1-\mu(t)\right] \\ v_D(t) &= -V_0\left[1-\mu(t)\right]. \end{aligned} \tag{6.84}$$

By Voltage Kirchhoff Laws, it is possible to write

$$\begin{aligned} v_1(t) &= v_{SW} + v_D \\ v_2(t) &= v_D. \end{aligned} \tag{6.85}$$

The two current i_1, i_2 flowing in the capacitors are

$$\begin{aligned} i_1(t) &= C\frac{dv_1}{dt} \\ i_2(t) &= C\frac{dv_2}{dt}. \end{aligned} \tag{6.86}$$

Taking into account (6.84) and (6.85) the (6.86) becomes

$$\begin{aligned} i_1(t) &= C(-3V_0 + V_0)\delta(t) = -2CV_0\delta(t) \\ i_2(t) &= CV_0\delta(t). \end{aligned} \tag{6.87}$$

By Current Kirchhoff Laws, currents flowing through the ideal switches i_{SW} and the ideal diode i_D are

$$\begin{aligned} i_{SW}(t) &= -i_1 = -\lambda_{q1}\delta(t) \\ i_D(t) &= -i_1 - i_2 = (-\lambda_{q1} - \lambda_{q2})\delta(t). \end{aligned} \tag{6.88}$$

From (6.83), (6.84), (6.85) and (6.87), it is possible to recognize the values of the electric quantities before the discontinuity and the impulses of current as follows

$$\begin{aligned} V_{SW} &= 3V_0 \\ V_D &= -V_0 \\ V_{1-} &= 2V_0 \\ V_{2-} &= -V_0 \\ \lambda_{q1} &= -2CV_0 \\ \lambda_{q2} &= CV_0. \end{aligned} \tag{6.89}$$

Taking into account (6.89) in (6.33), Energies absorbed by the ideal switch and diode through the discontinuity are the following

$$\begin{aligned} \Delta E_{SWclosed} &= 3CV_0^2 \\ \Delta E_D &= -\frac{1}{2}CV_0^2. \end{aligned} \tag{6.90}$$

Taking into account (6.89) in (6.24), the increment of Energy stored in the two capacitors are

$$\begin{aligned} \Delta E_{C1} &= -2CV_0^2 \\ \Delta E_{C2} &= -\frac{1}{2}CV_0^2. \end{aligned} \tag{6.91}$$

Finally, the balance property over the Energy applies, indeed

$$\Delta E_{C1} + \Delta E_{C2} = \Delta E_{SWclosed} + \Delta E_D. \tag{6.92}$$

In this case the ideal diode generates energy which is absorbed by the ideal switch. In fact, the total decrement of energy stored into the two capacitors is equal to $2{,}5CV_0^2$ while the ideal switch dissipates $3CV_0^2$. The remaining energy, in order to obey the balance principle, is generated by the

ideal diode. This amount of energy has not a physical meaning because it does not correspond to any physical energy stored in some elements. Only the part of this energy stored into the two capacitors has a physical meaning.

6.6 Discussion

Based on (6.33), (6.38), (6.49) confirmed by the previous analytical examples, the ideal switch can absorb electric energy when an impulse is involved both in opening and closing commutations meanwhile the ideal diode can only generate energy in these switching processes. In case this energy is absorbed, it is instantaneously dissipated by means of impulse. However, this dissipation in the real switch occurs in the finite resistance of the switch itself. On the contrary, if this energy is generated, its occurrence is not a physical phenomenon but an interesting mathematical aspect of the ideal model. As a result, the formulas of the ideal model allow also to generate energy by switching when an impulse is involved.

Results presented in this chapter confirmed by case studies give rise to an outstanding, and in a sense unexpected, result. The connection energy [43] is the quantitative evaluation of the variation of the total energy in reactive elements of the network caused by a change of topology. The connection energy theory demonstrates that such energy gap is always in decrement in an autonomous network. In a model featured by lumped parameters and instantaneous variations, such energy is conveyed by Dirac impulses. From the physical point of view, such gap of energy is expected to be dissipated into the elements that perform the change in topology.

The presented approach considers the switching elements as a part of the network. Therefore, the network is not yet under variant topology but time-variant, due to the presence of time-variant elements (ideal switching). According to the presented approach, the Connection Energy is demonstrated to be totally dissipated in the ideal switches at the moment of switching. This obvious result is a consequence of Tellegen's theorem.

The total energy absorbed by switching has a clear physical significance, as it is related to the variation of stored energy in the set of reactive elements or generated energy by electric sources. In case of more the one element, the partition of this energy among the different switching elements has no physical correspondence with the loss of energy into the single element. This fact is evident by the formulas that allow a negative energy (i.e. generated) in some elements, a fact confirmed in case study section 6.5.4.

Therefore, the present discussion confirms the theory of Connection Energy [43]. Moreover, it confirms that the Connection Energy has to be considered a quantity associated to the whole circuit, in a complete agreement with the approach in [43]. On the contrary, it is not meaningful to associate the Connection Energy to a single element, this aspect is remarkable and worthy of further future investigation.

Despite the Inductive Impulsive Power and Capacitive Impulsive Power functions have similar properties to the Connection Energy, they are more powerful and meaningful. In fact, by these functions it is possible to separate the effect of capacitors from inductors, reaching to the Theorems 6.V and 6.IX. Moreover, equations (6.15) and (6.26) show that IIP and CIP are always negative (generated) in response to any nonnil change in inductor or capacitor energy, irrespective of the sign of the change, contrary to (6.13), (6.23). In such a way, the outstanding result is achieved, i.e. whatever step change in inductor or capacitor energy implies dissipation in switching.

Conclusion

In this work a new theory based on the *v-i* plane, called *Swept Area Theory*, in addition to definitions of two conservative functions, *Area Velocity* and *Closed Area over Time*, are proposed and analyzed. This work gives a contribution to improve the theory of nonlinear and time-variant circuits under both continuous and discontinuous conditions. Some results presented in the literature are found and extended; in particular some past proposals are fully validated.

A balance rule concerning harmonic reactive powers over nonlinear resistor under continuous conditions is obtained and discussed as a novel interesting result. This aspect impacts on possible extended definition of reactive power under distorted conditions. Indeed, the CAT is always nil over nonlinear resistors, nonnegative over nonlinear inductors and nonpositive over nonlinear capacitors.

Another interesting result is that nonlinear resistor can absorb or generate harmonic reactive power under discontinuous conditions.

A significant contribution is achieved to enhance understanding of the periodic switching. Thanks to the *Switching Power*, a novel quantitative relation between hard switching commutations and CAT is obtained, with both theoretical and applicative relevance. More in detail, a demonstration is given in order to show how ideal switch and power converters can become sources of reactive power.

From a theoretical point of view, the SAT explains the equivalence, on some aspects, between a nonlinear element and a time-variant element, as the ideal diode. In fact, the ideal diode, which is a particular nonlinear resistor, can be treated as an ideal switch that commutes only in soft switching and passive hard switching.

Issues of principle regarding the ideal switch model with respect to the real one is another important result of this work.

Such results are embedded into an overall theory with straightforward graphical support. This propose can also be viewed as a tool for specific results, some of them are shown in case studies, others are still to be explored.

Moreover, a unified theory regarding the power converters are proposed. Definitions of Ideal Switch Multi Port in a matrix form, multilevel voltage element (VPEEB) and multilevel current element (CPEBB) are given. In this way, it is possible to give a general structure to most of the power converters existing and recognize some constrains on the possible switching combinations based on the type of converter itself. Furthermore, the SAT is extended to the ISMP in order to find relations between SP and commutations of power converters. Through these relations, the possibility of a power converter to generate or absorb reactive power is proved. This work gives a contribution to develop new control strategies of power converters based on SAT theory.

Another conservative function, *Jump Power*, is proposed. By this function, it is possible to state some theorems regarding nonlinear elements, in particular ideal switches and ideal diodes, in the presence of jump discontinuities. Possible conditions in networks are addressed whereby soft switching, passive or active hard switching commutations occur.

Furthermore, networks in the presence of impulses in electric quantities are analyzed. In this case the *Connection Energy*, a function already appeared in the past literature regarding the whole network, is here reformulated as a conservative function on each electric component. Another two novel conservative functions, *Inductive Impulsive Power* and *Capacitive Impulsive Power* are defined, by means of which it is possible to state other theorems regarding nonlinear elements, in particular ideal switches and ideal diodes in the presence of impulses. These latter conservative functions IIP and CIP, despite having similar properties to the CE, are still more powerful and meaningful. In fact through IIP and CIP, it is possible to separate the effect of capacitors from inductors.

Additionally, an interesting result is found: the ideal switch can absorb or generate electric energy when an impulse of current or voltage occurs meanwhile the ideal diode can only generate. These facts are important mathematical aspects regarding the ideal model of switches and diodes. In some cases, these facts cannot have a physical meaning, as it is shown in the analytical examples. In any case, the total energy absorbed by switching has a clear physical significance, as it is related to the variation of energy stored in the set of reactive elements or generated by electric sources. On the other hand, in the presence of more the one element, the partition of this energy among the different switching elements still has no physical correspondence with the loss of energy into the single element.

Finally, an important consideration of principle is worth to be expressed. In the present work, jump discontinuities and impulses are widely considered as basis of analysis of ideal switches and ideal diodes. Moreover, they are used in the definitions of Jump Power and Impulsive Powers. On the other hand, discontinuities are only useful schematizations of the actual behavior of voltages and currents. Indeed, voltages and currents are continuous functions in real systems. Nevertheless, the results of this thesis have to be considered in models constituted by lumped elements, that are considered as usual models used in the analysis, design and control of systems, for instance electronic power converters. Moreover, the definition of different conservative functions does not always need to have a corresponding physical meaning. Instead, what is important for these functions is to have properties whereby it is possible to understand the real essence of a phenomena.

In the deep human minds, souls create models to be a conceptual schematization of what humans have to achieve and what are independent values necessary to reach their targets and achieve their goals. However, the utilization of these models varies. Scientists use models to represent real physical systems or specific phenomena but engineers, on the contrary, use them to create or modify these current physical systems or phenomena. In other words, the model for scientists is an approximation of the real system, meanwhile the real system for engineers is an approximation of the model.

This aspect makes the value of this work meaningful and fruitful. It is useful for the analysis and design of switching systems. Moreover, it gives a contribution to the deep understanding of the behavior of such systems.

References

[1] P. Penfield, R. Spence, and S. Duinker: "Tellegen's theorem and electrical networks," M.I.T. Press, USA: Cambridge, 1970.

[2] N. LaWhite and M. D. Ilic, "Vector space decomposition of reactive power for periodic nonsinusoidal signals," *IEEE Trans. Circuits Syst. I, Fundam. Theory Appl.*, vol. 44, no. 4, pp. 338−346, Apr. 1997.

[3] W. Shepherd and P. Zakikhani: "Suggested definition of reactive power for nonsinusoidal systems," *Proc. Inst. Elec. Eng.*, vol. 119, pp.1361−1362, Sept. 1972.

[4] N. L. Kusters and W. J. M. Moore, "On the definition of reactive power under non-sinusoidal conditions," *IEEE Trans. on Power Apparatus and System*, vol. PAS-99, no. 5, pp. 1845−1854, Sep.−Oct. 1980.

[5] C.H. Page: "Reactive Power in Non-Sinusoidal Situations," *IEEE Trans. of Instrumentation and Measuremen*, Vol IM-29, no.4, pp 420−423, Dec 1990.

[6] L.S. Czarnecki: "Power factor improvement of three-phase unbalanced loads with nonsinusoidal supply voltages," *European Trans. on Electrical Power Engineering (ETEP)*, Vol. 3, no. 1, pp. 67−72, Jan.−Feb. 1993.

[7] L.S. Czarnecki: "Minimization of Reactive Power under Nonsinusoidal Conditions," *IEEE Trans. on Instrumentation and Measurements*, vol.IM-36, no.1, pp. 18−22, 1987.

[8] J.L. Willems: "Power factor correction for distorted bus voltages," *Electr. Mach. a. Power Syst,* 13, pp.207−218, 1987.

[9] H. Akagi and A. Nabae: "The p-q Theory in Three-Phase Systems under Non-Sinusoidal Conditions," *European Trans. on Electrical Power Engineering (ETEP)*, Vol. 3, no. 1, pp. 27−31, Jan. −Feb. 1993.

[10] M. Depenbrock, D. A. Marshall, and J. D. van Wyk: "Formulating Requirements for a Universally Applicable Power Theory as Control Algorithm in Power Compensators," *European Trans. On Electrical Power Engineering (ETEP)*, Vol. 4, no. 6, pp. 445-455, Nov−Dec 1994.

[11] M. Depenbrock: "The FBD-method, a generally applicable tool for analysing power relations," *IEEE Trans. on Power Systems*, vol.8, no.2, pp 381−386, May 1993.

[12] P. H. Swart, M. J, Case, and J. D. van Wyk: "On Techniques for Localization of Sources Producing Distortion in Electric Power Networks," *European Trans. on Electrical Power Engineering (ETEP)*, Vol. 4, no. 6, pp. 485−490, Nov−Dec 1994.

[13] A. Ferrero, A. Menchetti, and R. Sasdelli: "The measurement of the electric power quality and related problems," *European Trans. On Electrical Power Engineering (ETEP)*, Vol. 6, no. 6, pp. 401−406, 1996,

[14] A. Ferrero: "Definitions of Electrical Quantities Commonly Used in Non- Sinusoidal Conditions," *European Trans. on Electrical Power Engineering (ETEP)*, Vol. 8, no. 4, pp. 235−240, 1998.

[15] L.S. Czarnecki: "Orthogonal Decomposition of the Currents in a 3-Phase Nonlinear Asymmetrical Circuit with a Nonsinusoidal Voltage Source," *IEEE Trans. on Instrumentation and Measurements*, vol.IM-37, no.1, pp.30−34, March 1988.

[16] L.S. Czarnecki: "Reactive and unbalanced currents compensation in three-phase asymmetrical circuits under non-sinusoidal conditions," *IEEE Trans. on Instrumentation and Measurements*, vol.IM-38, 1989.

[17] L.S. Czarnecki: "Scattered and reactive current, voltage, and Power in Circuits with nonsinusoidal waveforms and their compensation," *IEEE Trans. on Instrumentation and Measurements*, vol.IM-40, no.3, pp. 56−567, 1991.

[18] P. Mattavelli and P. Tenti: “Third-order load identification under nonsinusoidal conditions,” *European Trans. on Electrical Power Engineering (ETEP)*, Vol. 12, no. 2, pp. 93−100, March−April 2002.
[19] S. Leszek Czarnecki: “Considerations on the reactive power in nonsinusoidal situations,” *IEEE Trans. Instrumentation and Measurement*, vol. IM-34, no. 3, pp. 399−404, Sep. 1985.
[20] S. Leszek Czarnecki, “What is Wrong with the Budeanu Concept of Reactive and Distortion power and Why It Should be Abandoned,” *IEEE Trans. Instrumentation and Measurement*, vol. IM-36, no. 3, pp. 834−837, Sep. 1987.
[21] A. E. Emanuel, "Powers in nonsinusoidal situations-a review of definitions and physical meaning," *IEEE Trans. Power Delivery,* vol. 5, no. 3, pp. 1377−1389, Jul. 1990.
[22] P. Tenti, H. K M Paredes, and P. Mattavelli, "Conservative Power Theory, a Framework to Approach Control and Accountability Issues in Smart Microgrids," *IEEE Trans. On Power Electronics*, vol. 26, no. 3, pp. 664−673, Mar. 2011.
[23] J. L. Willems, “Budeanu’s Reactive power and Related Concepts Revisited,” *IEEE Trans. Instrumentation and Measurement*, vol. 60, no. 4, pp. 1182−1186, Apr. 2011.
[24] M. Castro-Nunez and R. Castro-Puche, "The IEEE Standard 1459, the CPC Power Theory, and Geometric Algebra in Circuits With Nonsinusoidal Sources and Linear Loads," *IEEE Trans. Circuits Syst. I, Reg. Papers*, vol. 59, no. 12, pp. 2980−2990, Dec. 2012.
[25] A. M. Sommariva, "Power Analysis of One-Ports Under Periodic Multi-Sinusoidal Linear Operation," *IEEE Trans. Circuits Syst. I, Reg. Papers*, vol. 53, no. 9, pp. 2068−2074, Sep. 2006.
[26] A. Menti, T. Zacharias, and J. Milias-Argitis, "Geometric algebra: A powerful tool for representing power under nonsinusoidal conditions," *IEEE Trans. Circuits Syst. I, Reg. Papers*, vol. 54, no. 3, pp. 601−609, Mar. 2007.
[27] M. Castro-Nunez and R. Castro-Puche, "Advantages of Geometric Algebra Over Complex Numbers in the Analysis of Networks With Nonsinusoidal Sources and Linear Loads," *IEEE Trans. Circuits Syst. I, Reg. Papers*, vol. 59, no. 9, pp. 2056−2064, Sep. 2012.
[28] M. Castilla, J. C. Bravo, M. Ordonez, and J. C. Montano, "Clifford Theory: A Geometrical Interpretation of Multivectorial Apparent Power," *IEEE Trans. Circuits Syst. I, Reg. Papers*, vol. 55, no. 10, pp. 3358−3367, Nov. 2008.
[29] W. Millar, “Some general theorems for non-linear systems possessing resistance,” Phil. Mag. 42, Ser. 7, pp. 1150−1160, 1951.
[30] R. K. Brayton and J. K. Moser, “A theory of non-linear networks - I and II,” Quart. of Appl. Math. 22, pp. 1−33 and 81−104, 1964.
[31] L. O. Chua and N.N. Wang, “Complete stability of autonomous reciprocal nonlinear networks,” *IEEE Trans Circuit Theory and appl.*, vol. 6, pp. 211−241, 1978.
[32] L. Weiss, W. Mathis, and L. Trajkovic, “A generalization of Brayton-Moser's mixed potential function,” *IEEE Trans. Circuits Syst. I, Fundam. Theory Appl.*, vol. 45, no. 4, pp. 423−427, Apr. 1998.
[33] D. Jeltsema, R. Ortega, and J. M. A. Scherpen, “On passivity and power-balance inequalities of nonlinear RLC circuits,” *IEEE Trans. Circuits Syst. I, Fundam. Theory Appl.*, vol. 50, no. 9, pp. 1174−1179, Sep. 2003.
[34] G. Blankenstein, “Geometric modeling of nonlinear RLC circuits,” *IEEE Trans. Circuits Syst. I, Reg. Papers*, vol. 52, no. 2, pp. 396−404, Feb. 2005.
[35] J. P. Fortney, “Dirac Structures in Pseudo-Gradient Systems With an Emphasis on Electrical Networks,” *IEEE Trans. Circuits Syst. I, Reg. Papers*, vol. 57, no. 7, pp. 1732−1745, Jul. 2010.
[36] N. Mohan, W. P. Robbins, T. M. Undeland, R. Nilssen, and O. Mo, “Simulation of power electronic and motion control systems—An overview,” *Proc. IEEE*, vol. 82, pp. 1287−1302, Aug. 1994.
[37] Fei Yuan and A. Opal, "Computer methods for switched circuits," *IEEE Trans. Circuits Syst. I, Fundam. Theory Appl.*, vol. 50, no. 8, pp. 1013−1024, Aug. 2003.

[38] M. K. Camlibel, W. P. M. H. Heemels, A. J. van der Schaft, and J. M. Schumacher, "Switched networks and complementarity," *IEEE Trans. Circuits Syst. I, Fundam. Theory Appl.*, vol. 50, no. 8, pp. 1036−1046, Aug. 2003.
[39] L. Iannelli, F. Vasca, and G. Angelone, "Computation of Steady-State Oscillations in Power Converters Through Complementarity," *IEEE Trans. Circuits Syst. I, Reg. Papers*, vol. 58, no. 6, pp. 1421−1432, Jun. 2011.
[40] A. Opal and J. Vlach, "Consistent initial conditions of nonlinear networks with switches," *IEEE Trans. Circuits Syst.*, vol. 38, no. 7, pp. 698−710, Jul. 1991.
[41] J. Vlach, J. M. Wojciechowski, and A. Opal, "Analysis of nonlinear networks with inconsistent initial conditions," *IEEE Trans. Circuits Syst. I, Fundam. Theory Appl.*, vol. 42, no. 4, pp. 195−200, Apr. 1995.
[42] R. Frasca, M. K. Camlibel, I. C. Goknar, L. Iannelli, and F. Vasca, "Linear Passive Networks With Ideal Switches: Consistent Initial Conditions and State Discontinuities *IEEE Trans. Circuits Syst. I, Reg. Papers*, vol. 57, no. 12, pp. 3138−3151, Dec. 2010.
[43] J. Tolsa and M. Salichs, "Analysis of linear-networks with inconsistent initial conditions," *IEEE Trans. Circuits Syst. I, Fundam. Theory Appl.*, vol. 40, no. 12, pp. 885−894, Dec. 1993.
[44] G. Superti-Furga and L. Pinola, "The Mean Generalized Content: A Conservative Quantity in Periodically-Forced Non-Linear Networks," ETEP, vol. 4, no. 3, pp. 205−212, May-June 1994.
[45] G. Superti-Furga, "Searching for a Generalization of the Reactive Power − a Proposal," ETEP, vol. 4, no. 5, pp. 411−420, Sept-Oct 1994.
[46] A. Monti, M. Riva and G. Superti-Furga, "An Approach to the Analysis of Power Flow with Time-Variant Components: The Switching Power," ETEP, vol. 6, no. 6, pp. 407−412, Nov. −Dec. 1996.
[47] B. D. H. Tellegen, "A general network theorem, with applications," *Philips Res. Rept.*, vol. 7, pp. 259−269, August 1952.
[48] B. D. H. Tellegen, "A general network theorem, with applications," *Proc. Inst. Radio Engrs. ,(Australia)*, vol. 14, pp. 266−270, November 1953.
[49] P. Penfield, JR. R. Spence, and S. Duinker: "A Generalized Form of Tellegen's Theorem," *IEEE Trans. Circuit Theory,* vol. CT-17, n. 3, pp. 302−305, August 1970.
[50] ANSI/IEEE, "Standard dictionary for power of electrical & electronics terms," USA: ANSI/IEEE, 1977.
[51] C. Budeanu, "Reactive and fictitious powers," *Rumanian National Institute*, no. 2, 1927.
[52] S. Fryze: "Wirk-Blind-und Scheinleistung in elektrischen Stromkreisen mit nichtsinusförmigem Verlauf von Strom und Spannung," *Elektrotechnishce Zeitschrift*, no. 25, pp 596−599, 625−627, 700−702, 1932.
[53] D. Sharon: "Reactive power definition and power factor improvement in non-linear systems," *Proc IEE*, Vol 120, no 6, pp. 704−706, July 1973.
[54] P. Tenti, P. Mattavelli, and H. K. Morales Paredes: "Conservative power theory, sequence components and accounting in smart grids," *Przeglad Elektrotechniczny (Elect. Rev.)*, vol. 86, no. 6, pp. 30−37, Jun. 2010.
[55] M. A. Iliovici: "Definition et mesure de la puissance et de l'ènergie reactives," Bull. de la Soc. Franc. des Electriciens, vol. 5, pp. 931−954, 1925.
[56] A. E. Emanuel: "Power Definitions and the Physical Mechanism of Power Flow," *IEEE Press*, Wiley, 2010.
[57] IEEE Std 1459-2010, "IEEE Standard Definitions for the Measurement of Electric Power Quantities Under Sinusoidal, Nonsinusoidal, Balanced, or Unbalanced Conditions," New York, 19 March 2010.

[58] J. L. Wyatt and M. D. Ilic, "Time-domain reactive power concepts for nonlinear, nonsinusoidal or nonperiodic networks," *Proc. IEEE Int. Symp. Circuits Syst.*, vol. 1, pp. 387−390, 1990.

[59] P. Tenti, P. Mattavelli, and E. Tedeschi, "Compensations Techniques based on reactive Power Conservation," *Seventh International Workshop on power Definitions and Measurements under Non-Sinusoidal Conditions*, Cagliari, Jul. 2006.

[60] M. S. Erlicki and A. Emanuel-Eigeles, "New Aspects of Power Factor Improvement. Part I − Theoretical Basis. Part II − Practical Circuits," *IEEE Transactions on Industry and General Applications*, vol. IGA-4, no. 4, pp. 441−455, Jul. −Aug. 1968.

[61] M. T. Hartman: "The integral method to calculate the power states in electrical circuits," *Compatibility and Power Electronics, 2009. CPE '09*, pp. 180−185, 20−22 May 2009.

[62] M. T. Hartman and D. Wojciechowski: "Emanuel's method versus Iliovici's method for reactive power compensation in passive-active power conditioning scheme," *Compatibility and Power Electronics (CPE), 2013 8th International Conference on*, pp. 92−96, 5−7 Jun. 2013.

[63] J. M. Manley and H. E. Rowe: "Some general properties of nonlinear elements-Pt I. General energy relations," *Proc. IRE,* vol. 44, pp. 901−913, July 1956.

[64] L. Gyugyi: "Power electronics in electric utilities: static var compensators," *Proc. of IEEE*, vol. 76, no.4, pp.483-493, Apr. 1988.

[65] Murray R Spiegel, Schaum's Outline of Fourier Analysis with Applications to Boundary Value Problems, pp. 175, B-25.

[66] Murray R Spiegel, Schaum's Outline of Fourier Analysis with Applications to Boundary Value Problems, pp. 171, B-12.

[67] M. S. Carmeli, F. Castelli-Dezza, L. Piegari, and G. Superti-Furga, "Digital synchronous current control of power electronic building block in modular converters," in *Proc. IEEE ISIE*, pp. 2909−2914, 4−7 Jul. 2010.

[68] A. Monti and F. Ponci, "PEBB Standardization for High-Level Control: A Proposal," *Industrial Electronics, IEEE Transactions on* , vol. 59, no. 10, pp. 3700−3709, Oct. 2012.

[69] Mingyan Wang and Kai TianS: "A Nine-Switch Three-Level Inverter for Electric Vehicle Applications," *IEEE Vehicle Power and Propulsion Conference (VPPC)*, September 3-5, 2008, Harbin, China.

[70] M. Liou: "Exact analysis of linear circuits containing periodically operated switches with applications," *IEEE Trans. Circuit Theory*, vol. 19, no. CT-2, pp. 146−154, 1972.

[71] A. Opal and J. Vlach, "Consistent initial conditions of linear switched networks," *IEEE Trans. Circuits Syst.*, vol. 37, no. 3, pp. 364−372, Mar. 1990.

[72] A. Opal: "The transition matrix for linear circuits," *IEEE Trans. Comput.-Aided Design Integr. Circuits Syst.*, vol. 16, no. 5, pp. 427−436, May 1997.

[73] Q. Li and F. Yuan, "Time-domain response and sensitivity of periodically switched nonlinear circuits," *IEEE Trans. Circuits Syst. I, Fundam. Theory Appl.*, vol. 50, no. 11, pp. 1436−1446, Nov. 2003.

[74] Z. Zuhao: "ZZ model method for initial condition analysis of dynamics networks," *IEEE Trans. Circuits Syst.*, vol. 38, no. 8, pp. 937−941, Aug. 1991.

[75] A. Massarini, U. Reggiani, and M. K. Kazimierczuk, "Analysis of networks with ideal switches by state equations," *IEEE Trans. Circuits Syst. I, Fundam. Theory Appl.*, vol. 44, no. 8, pp. 692−697, Aug. 1997.

[76] B. De Kelper, L. A. Dessaint, K. Al-Haddad, and H. Nakra, "A comprehensive approach to fixed-step simulation of switched circuits," *IEEE Trans. Power Electron.*, vol. 17, no. 2, pp. 216−224, Mar. 2002.

[77] Y. Murakami: "A method for the formulation and solution of circuits composed of switches and linear RLC elements," *IEEE Trans. Circuits Syst.*, vol. 34, no. 5, pp. 496−509, May 1987.

[78] A. Opal: "Sampled data simulation of linear and nonlinear circuits, "*IEEE Trans. Comput.-Aided Design Integr. Circuits Syst.*, vol. 15, no. 3, pp. 295−307, Mar. 1996.

[79] F. Del Aguila Lopez, P. Schonwilder, J. Dalmau, and R. Mas: "A discrete-time technique for the steady state analysis of nonlinear switched circuits with inconsistent initial conditions," in *IEEE Int. Symp. Circuits Syst.*, vol. 3, pp. 357−360, 2001.

[80] I. C. Goknar: "Conservation of energy at initial time for passive RLCM network," *IEEE Trans. Circuit Theory*, vol. CT-19, no. 4, pp. 365−367, Jul. 1972.

[81] P. Mayer, J. Jeffries, and G. Paulik: "The two-capacitor problem reconsidered," *IEEE Trans. Educ.*, vol. 36, no. 3, pp. 307−309, Aug. 1993.

[82] A. M. Sommariva: "Solving the two capacitor paradox through a new asymptotic approach," *IEE Proc. Circuits Devices Syst.*, vol. 150, no. 3, pp. 227−231, 2003.

[83] D. G. Bedrosian and J. Vlach: "Time-domain analysis of networks with internally controlled switches," *IEEE Trans. Circuits Syst. I, Fundam. Theory Appl.*, vol. 39, no. 3, pp. 199−212, Mar. 1992.

[84] M. K. Camlibel, W. P. M. H. Heemels, and J. M. Schumacher: "On the dynamic analysis of piecewise-linear networks," *IEEE Trans. Circuits Syst. I, Fundam. Theory Appl.*, vol. 49, no. 3, pp. 315−327, Mar. 2002.

[85] F. Vasca, L. Iannelli, M. K. Camlibel, and R. Frasca: "A new perspective for modeling power electronics converters: Complementarity framework," *IEEE Trans. Power Electron.*, vol. 24, no. 2, pp. 465−468, Feb. 2009.

[86] S.-C. Tan, S. Bronstein, M. Nur, Y. Lai, A. Ioinovici, and C. Tse, "Variable structure modeling and design of switched-capacitor converters, "*IEEE Trans. Circuits Syst. I, Reg. Papers*, vol. 56, no. 9, pp. 2132−2142, Sep. 2009.

[87] J. Ruiz-Amaya, M. Delgado-Restituto, and A. Rodriguez-Vazquez, "Accurate settling-time modeling and design procedures for two-stage miller-compensated amplifiers for switched-capacitor circuits," *IEEE Trans. Circuits Syst. I, Reg. Papers*, vol. 56, no. 6, pp. 1077−1087, Jun. 2009.

[88] Y. Wang, M. Yang, H. Wang, and Z. Guan: "Robust stabilization of complex switched networks with parametric uncertainties and delays via impulsive control," *IEEE Trans. Circuits Syst. I, Reg. Papers*, vol. 56, no. 6, pp. 2100−2108, Jun. 2009.

[89] F. del-Águila López, P. Palà-Schönwälder, P. Molina-Gaudó, and A. Mediano-Heredia: "A discrete-time technique for the steady-state analysis of nonlinear class-E amplifiers," *IEEE Trans. Circuits.*

[90] J. F. Colombeau: "Elementary Introduction to New Generalized Functions," Amsterdam: North-Holland, 1985.